Towards the Synthesis of the Monoterpene Furanoid Oxides via the Ozonolysis of Bicyclic Bridged 1,2-Dioxines

A thesis presented in fulfilment of the requirements for the degree of

Doctor of Philosophy

Nicole Marie Cain

BTech (Forens&AnalytChem), BSc (Hons)

The University of Adelaide

South Australia

School of Agriculture, Food and Wine

November 2010

Table of Contents

Abstract

1,2-Dioxines, also known as endoperoxides are a specific type of cyclic peroxide, characterised by an unsaturated six-membered peroxide ring. They are abundant in nature and have been isolated from many natural products and have been shown to exhibit a wide spectrum of biological roles. Ozonolysis is a well established method for the oxidative cleavage of alkenes, although examples involving 1,2-dioxines are extremely rare.

The furanoid and anhydrofuran linalool oxides have been established as common compounds in wine and as natural products from other sources. Previous methods of synthesis have followed a variety of different routes although many experimental details are unclear and of limited value. It was therefore felt that a gap exists in the literature with regard to an effective synthesis for these compounds and the development of a new synthetic pathway to afford both compounds, and analogues thereof, from a common starting material would be of value.

The aim of this project was therefore to combine these areas and utilise 1,2-dioxine chemistry for the synthesis of the furanoid and anhydrofuran linalool oxides, with a key step in the synthesis being the ozonolysis of a bicyclic bridged 1,2-dioxine to yield the necessary keto-aldehyde precursor.

Since little attention has been focussed on exploring the ozonolysis reaction of bicyclic alkenes, particularly the alkene moiety of bicyclic 1,2-dioxines, the first part of this thesis is focussed on investigating the scope of this novel reaction. A range of 1,4-disubstituted bicyclic 1,2-dioxines and a steroidal 1,2-dioxine were used for this study, with their synthesis outlined in Chapter 2. Chapter 3 presents the results for this section of work, where it was found that upon reaction with ozone, the nature of substrates at the bridgehead positions of the 1,2-dioxines had a major influence on the outcome of the reaction; with some of the substrates giving the expected dialdehydes, whilst others behaved in an unexpected manner towards ozone. Additional experiments were then conducted to provide further insight into these unusual results. The potential mechanism

involved in these rearrangements is also discussed, with several plausible options presented.

Chapter 4 presents some *Ab-Initio* computational analyses to support the preliminary mechanistic insights into the ozonolysis reaction, with specific regard to bicyclic 1,2-dioxine systems. This was done by examining the relative energy differences for all possible isomers involved in each stage of the proposed mechanism in order to locate the lowest energy pathway, and therefore that which is most likely followed.

The second part of this thesis, presented in Chapter 5, was to utilise this novel transformation as a key step in the synthesis of both the furanoid and anhydrofuran linalool oxides, from a common starting material. The pathway began with the synthesis of a new bicyclic 1,2-dioxine, followed by successful ozonolysis and ring-contraction into the core 2,2,5-trisubstituted THF. It was found that having a hydroxyl α to either the furan or dioxine ring systems could be problematic and led to unwanted ring-opening and further rearrangements. Investigations revealed that this could be overcome upon protection of the hydroxyl, thereby enabling structural manipulation of the other functional groups to proceed smoothly.

Research along the synthetic pathway did reveal a new potential route to dioxabicyclo[3.2.1]octanes, with two new bicyclic compounds formed as a result of selective 1,6-cyclisation of a *cis*-γ-hydroxydione intermediate, a reaction previously unseen within the literature.

Time was a limiting factor in being able to complete the total synthesis of the desired compounds, but the major ground work was achieved. The C_2 functionalisation of the THF ring was successfully completed, and some new and novel chemistry was uncovered, which has further enhanced the understanding of the chemical nature of these types of compounds, along with their potential use in the synthesis of these important wine aroma compounds and other natural products.

Declaration

This thesis contains no material that has been accepted for the award of any other degree or diploma in any university or other tertiary institution. To the best of my knowledge it contains no material published or written by any other person, except where due reference has been made.

I give my consent for this copy of my thesis, when deposited in the University Library being available for loan and photocopying, subject to the provisions of the Copyright Act 1968.

I also give permission for the digital version of my thesis to be made available on the web, via the University's digital research repository, the Library catalogue, the Australasian Digital Theses Program (ADTP) and also through web search engines, unless permission has been granted by the University to restrict access for a period of time.

.....

Nicole Marie Cain

.....

Acknowledgements

Firstly I would like to express my sincere thanks to my principal supervisor, Professor Dennis Taylor for giving me the opportunity to work on this project. Your door was always open, full of chemistry knowledge and expert guidance, but you allowed me to work independently, in order to learn and grow on my own. Your enthusiasm and continual optimism has been an inspiration, especially during my periods of 'pessimism'. Also, a huge thanks to my co-supervisor Dr Gordon Elsey, whose never-ending wisdom, wealth of information and guidance has been of immense benefit.

I wish to also thank Dr Tom Avery for all his help in the beginning and providing me with all the support and guidance that I needed during my first year. Also thanks to Dr Mark Sefton and Dr George Skouroumounis for their helpful advice; Dr Pete Valente for all his assistance, especially with showing me the ropes when I first started; and Dr Ondrej Zvarec for helping me out at North Terrace with lab work and NMR's.

A huge thanks to all members of the Taylor group, which has grown so much over the past few years that there are too many people to name. Thanks for putting up with my whinging and keeping things fun, light hearted and a little crazy. The conversations have certainly been interesting and have broadened my horizons to the ways of the world! Question mark, question mark...

Furthermore, I would like to thank Professor Edward Tiekink for X-ray crystallography and Phil Clements for running all the 600 MHz NMRs.

Most of all I would like to thank my parents. I cannot ever thank you enough for all you have done for me. You have always encouraged me to chase my dreams, and many times you have believed in me more that I have believed in myself. Thanks for your unconditional love and support and for putting up with all my grumpiness. And of course I cannot forget my best four-legged friend Penny, for all those late nights waiting for me to come home...Hut-two!!

Abbreviations

Å	angstroms
Ac	acetyl
AIBN	2,2-azobisisobutyronitrile
apt	apparent
ASTM	American Society for Testing and Materials
Bn	benzyl
br	broad
c	concentration
ca	approximately
COSY	correlation spectroscopy
d	doublet
DCC	dicyclohexylcarbodiimide
DCM	dichloromethane
Δ	heat
DMAP	4-*N*,*N*-dimethylaminopyridine
DMF	*N*,*N*-dimethylformamide
$dmgH_2$	dimethylglyoxime
ds	diastereoselectivity
E_a	activation energy
ee	enantiomeric excess
E_h	Hartree
equiv	equivalent(s)
ESI	electrospray ionisation
Et	ethyl
FTMS	fourier transform mass spectroscopy
GC	gas chromatography
GO-O	gas chromatography-olfactometry
HF	Hartree-Fock
HMBC	heteronuclear Multiple Bond coherence
HMQC	heteronuclear Multiple Quantum Coherence

HRMS	high resolution mass spectroscopy
hrs	hours
hv	light
Hz	hertz
i-Pr	*iso*-propyl
IR	infra red
J	coupling constant
KJ	kilojoules
lit	literature
LPM	litres per minute
LSIMS	liquid secondary ion mass spectrometry
m	multiplet
M	moles per litre
m/z	mass to charge ratio
m-CPBA	*meta*-chloroperbenzoic acid
Me	methyl
Me_2S	dimethyl sulfide
MHz	mega-hertz
min	minutes
MIRC	Michael Initiated Ring Closure
mol	mole(s)
mp	melting point
nm	nanometers
NMR	nuclear magnetic resonance
nOe	nuclear overhauser effect
Ph	phenyl
ppm	parts per million
PTSA	*p*-toluenesulfonic acid
q	quartet
quin	quintet
R_f	retention factor
ROESY	rotational overhauser effect spectroscopy

sept	septet
t	triplet
TBHP	*t*-butyl hydroperoxide
TCNE	tetracyanoethylene
tert	tertiary
THF	tetrahydrofuran
TLC	thin layer chromatography
TMS	tetramethyl silane

CHAPTER 1: Introduction

1.1 The Chemistry of 1,2-Dioxines.

1.1.1 Introduction.

Cyclic peroxides are a useful class of organic compounds classified by their weak O-O linkage. The peroxide bond is the weakest covalent bond found in organic compounds, with an average bond energy of only 34 kcal/mol, less than half of that for a C-C single bond.[1] Cyclic peroxides are abundant in nature and have been isolated from many natural products and have been shown to exhibit a wide spectrum of biological roles including antimalarial,[2] antifungal,[3,4] and cytotoxic activities against cancer cells.[5]

Artemisinin, (**1**) extracted from the plant *Artemesia annua L.* was first isolated in 1972, and its peroxide function proved to be essential for its potent antimalarial activity.[6] Recent studies have also suggested that artemisinin is also effective in treating various forms of cancer such as leukemia and breast cancer.[7,8] Plakortide F (**2**), isolated from the Jamaican sponge *Plakortis,* has been found to exhibit bioactivity towards antimalaria, cardiac SR-Ca^{2+} uptake, HIV and several cancer cell lines.[9,10]

1,2-Dioxines, also known as endoperoxides are a specific type of cyclic peroxide, characterised by an unsaturated six-membered peroxide ring. They are found in a diverse range of compounds ranging from monocyclic, bicyclic, aromatic and even steroidal, with any given number of other functionalities incorporated as part of the structure. The major focus of this body of work lays within the field of bicyclic 1,2-dioxines.

One of the simplest and most widely recognised bicyclic 1,2-dioxines is ascaridole (**3a**), which was first isolated from *Chenopodium* oil, produced by the distillation of the weed *Chenopodium ambrosioides* (L.).[11,12] It has since been isolated from over a dozen other natural sources and has been the subject of much research into its biological activity.[5]

Another popular bicyclic 1,2-dioxine, ergosterol peroxide (**4**) has been isolated from numerous sources, both marine and terrestrial[13] and has a number of important biological roles including antitumour activity against carsinosarcoma and breast cancer cell lines[14] and has shown antiviral activity against influenza A virus strains.[15]

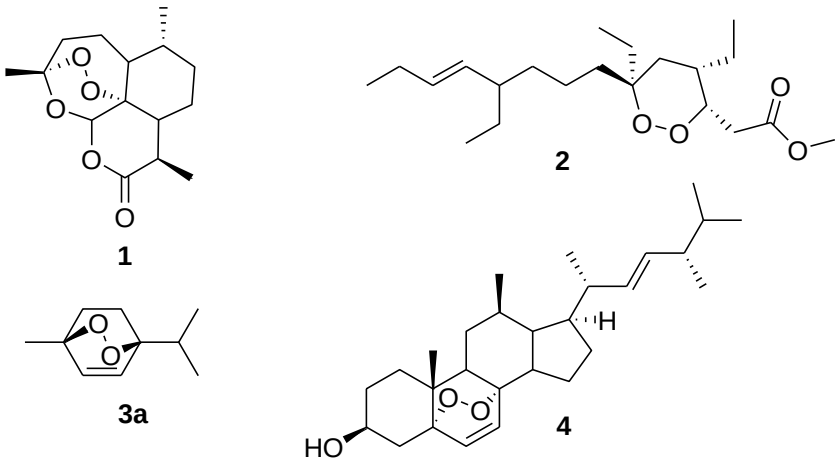

Figure 1: Naturally occurring cyclic peroxides.

1.1.2 Synthesis of 1,2-Dioxines.

The most practical and popular method of 1,2-dioxine synthesis is *via* a thermally allowed [4π +2π] cycloaddition of a 1,3-butadiene with singlet oxygen ($^1O_2$). This sensitised photo-oxygenation of olefins is now widely used in organic synthesis, enabling a diverse range of 1,2-dioxines to be synthesised from a versatile range of acyclic and cyclic 1,3-butadienes.[16]

The mechanistic aspects of this reaction have been well studied.[17,18] As seen in *Scheme 1*, Ground state (triplet) oxygen ($^3O_2$) exists as a diradical and does not have the correct electronic configuration to undergo a Diels-Alder cycloaddition. Singlet oxygen, which lays 93 kJ/mol higher in energy than triplet oxygen, does possess the required configuration, but the transition of ground state to singlet oxygen is forbidden by selection rules.[19] The preferred method for the generation of singlet oxygen is through the dye-sensitised photoexcitation of ground state oxygen. A number of highly conjugated dyes have been reported as effective sensitisers including methylene blue,

tetraphenylporphine and rose bengal. When irradiated with light, these dyes acts as a sensitiser to absorb a photon which excites the ground-state triplet oxygen to singlet state oxygen after collision. Singlet oxygen now possesses the required 'alkene-like' character allowing it to add across conjugated dienes.[17,20-23]

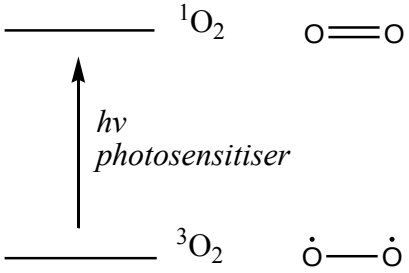

Scheme 1

There are some limitations as to what type of 1,3-butadiene can be used for the synthesis of 1,2-dioxines, as singlet oxygen can undergo several alternative reactions with 1,3-butadienes. Dienes **5a** and **6** are required for the [4π + 2π] cycloaddition to occur, yielding the desired 1,2-dioxines **7** and **3**, respectively**.** For monocyclic 1,2-dioxines consideration must therefore be given to the geometry of the 1,3-butadiene used. Although interconversion of conformer **5b** can occur under photolytic conditions, there is still potential for competing reactions, namely [2π +2π] cycloaddition and the 'ene' reaction, to occur, resulting in the formation of 1,2-dioxetanes **8** and hydroperoxides **9** respectively, *Scheme 2a*.[17,18,20] In cyclic systems there is conformational restriction keeping the diene in a '*s-cisoid'*-geometry thus minimising competing reactions in favour of [4π + 2π] addition, *Scheme 2b*.[19]

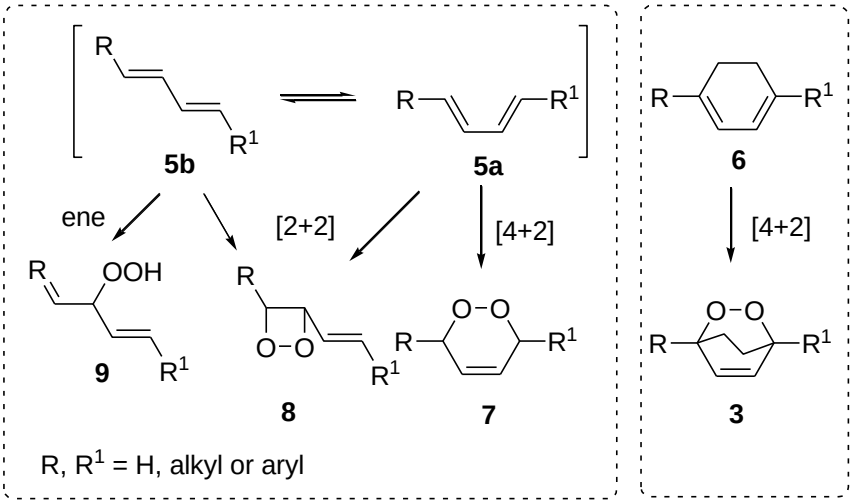

Scheme 2

1.1.3 Versatility of 1,2-Dioxines.

1,2-Dioxines have proven to be extremely versatile starting materials. Synthetically, they provide the organic chemist with a powerful tool for structural modification due to the presence of an easily cleaved O-O bond, which can be used to incorporate oxygen into a wide variety of substrates.

1.1.3.1 Reactions Resulting in Cleavage of the Peroxide Bond of Cyclic Peroxides.

Scheme 3 shows a number of examples developed by the Taylor group where the peroxide bond is cleaved during the course of further reaction. These will each be briefly discussed sequentially.

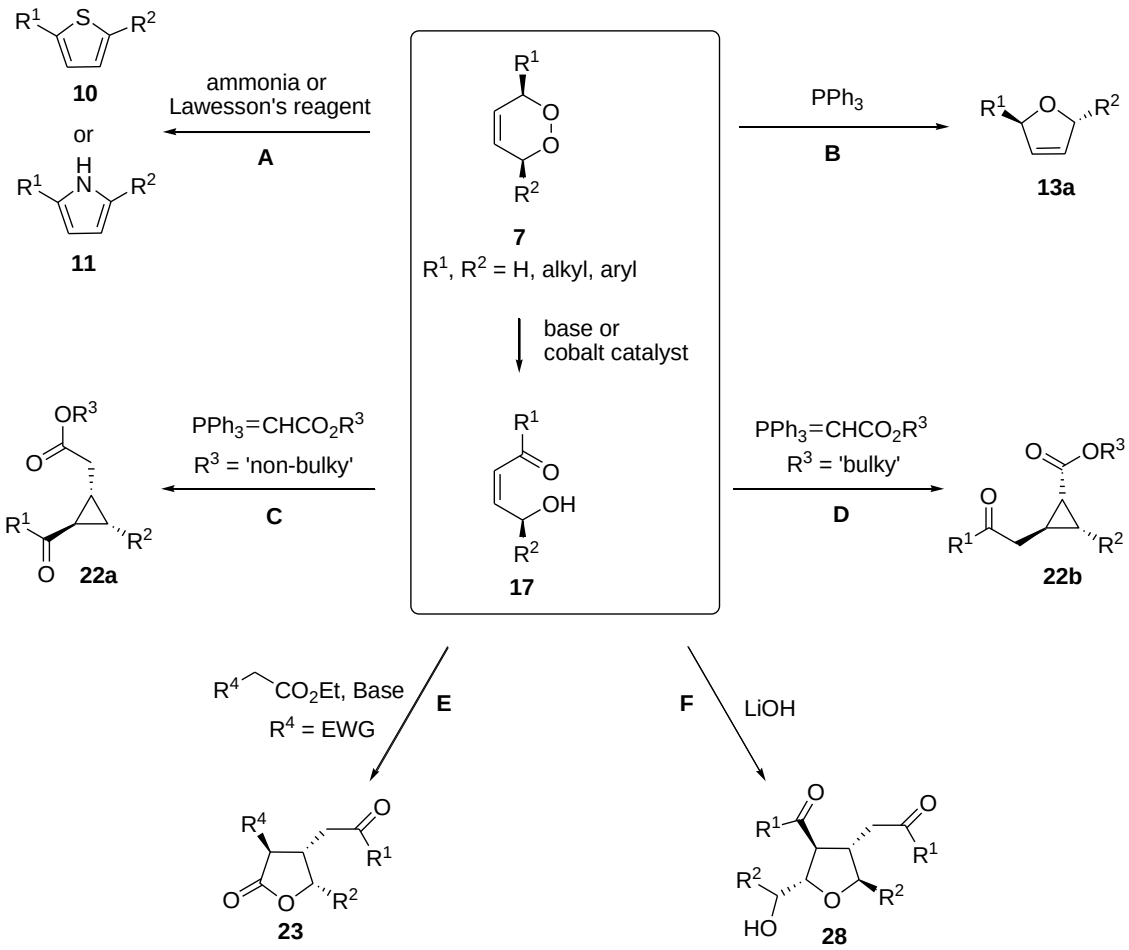

Scheme 3

1,2-Dioxines can easily be converted *via* a one pot synthesis into disubstituted thiophenes **10** or pyrroles **11** using ammonia or Lawesson's reagent respectively, *Pathway A, Scheme 3*.[24] Such thiophenes and pyrroles are useful in the construction of a range of natural products.[25,26]

Numerous examples can be found within the literature whereby furan compounds are synthesised from 1,2-dioxines, using a variety of reagents, *Pathway B, Scheme 3*.[27-31] One paper of particular interest by Greatrex *et al.*[32] discusses the effect of triphenylphosphine on 1,2-dioxine systems. It was found that when a series of disubstituted monocyclic 1,2-dioxines **12** were treated with PPh_3, ring-contraction to the corresponding furan **13b** resulted *via* intramolecular nucleophilic attack of the C-O-P^+Ph_3 centre, *Scheme 4*. It was concluded that ring-contraction is a favourable process when free rotation is possible around the C-O bond.

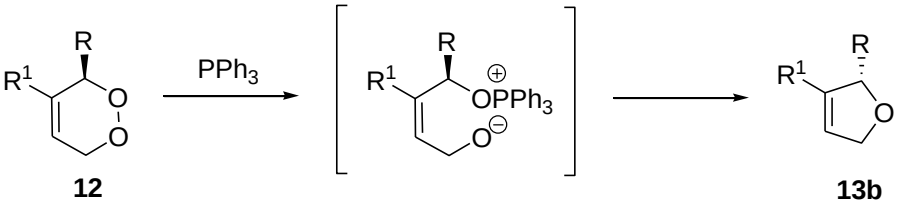

Scheme 4

In contrast to this, when bicyclic 1,2-dioxines are treated with PPh_3 either allylic epoxides **14** or *trans* 1,4-diols **15** are formed depending on whether the starting 1,2-dioxine is unsaturated **3** or saturated **16**, *Scheme 5*. This is due to the inability of the intermediate ionic species to undergo the intramolecular nucleophilic attack at the C-O-P^+Ph_3 centre due to the barrier to rotation within these cyclic systems.[33-35]

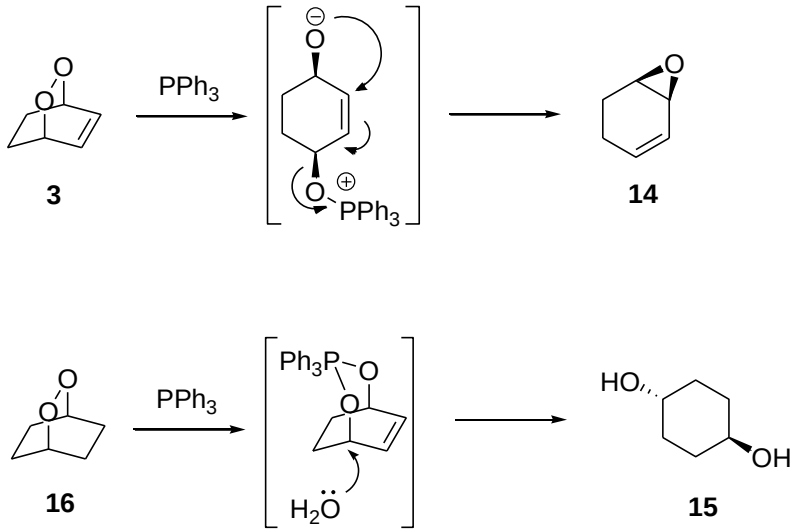

Scheme 5

1.1.3.1a Formation of *cis*-γ-Hydroxyenones from Cyclic Peroxides.

1,2-Dioxines can be viewed effectively as masked *cis*-γ-hydroxyenones **17**, as many of the transformations that they undergo rely upon the initial formation of this ring-opened species. Two efficient methods are commonly employed for the formation of *cis*-γ-hydroxyenones.

1,2-Dioxines that contain an acidic proton on the carbon α to the peroxide linkage are susceptible to undergoing a Kornblum-DeLaMare rearrangement upon treatment with a base, *Scheme 6*.[36] This transformation occurs through deprotonation followed by cleavage of the peroxide linkage in an internal elimination-type reaction to furnish a carbonyl and hydroxyl group within **17**. These moieties also allow the *cis*-γ-hydroxyenones to exist in equilibrium with their furanols **18**. Under acidic conditions the furanols dehydrate to form furans **19**, whilst under basic conditions the furanols generate 1,4-dicarbonyls **20**, although the mechanism of their formation remains unclear. [37,38]

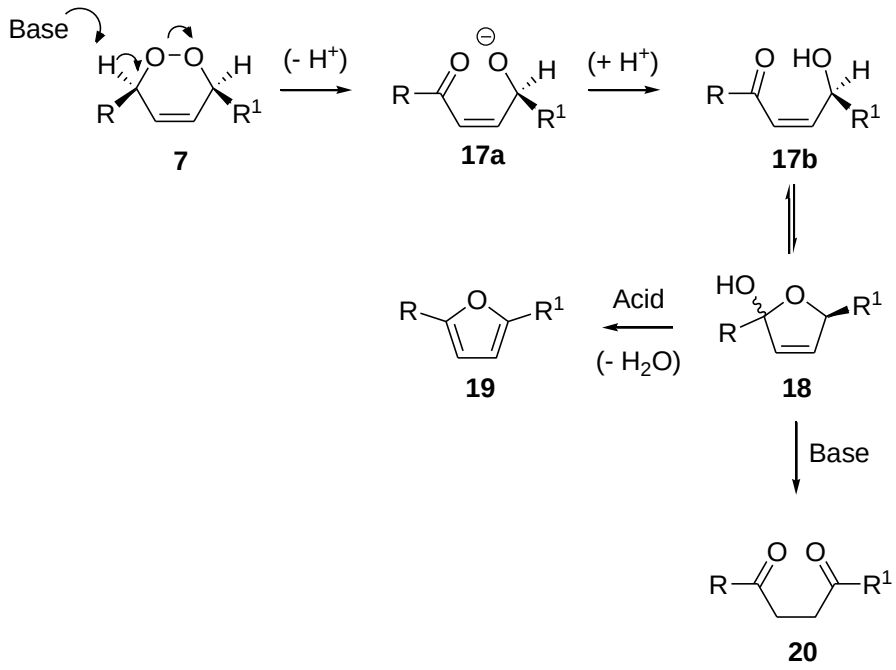

Scheme 6

Alternatively, *cis*-γ-hydroxyenones can also be generated using transition metal complexes such as Co(II),[28,39] Fe(II),[40] Rh(I)[41] and Pd(0)[42]. These complexes induce a single electron oxidative addition to the peroxide bond resulting in the formation of a metal oxygen bond and an oxygen radical species **21**, which then undergoes 1,5-hydrogen atom abstraction to yield the *cis*-γ-hydroxyenones **17**, as depicted in *Scheme 7*.[43]

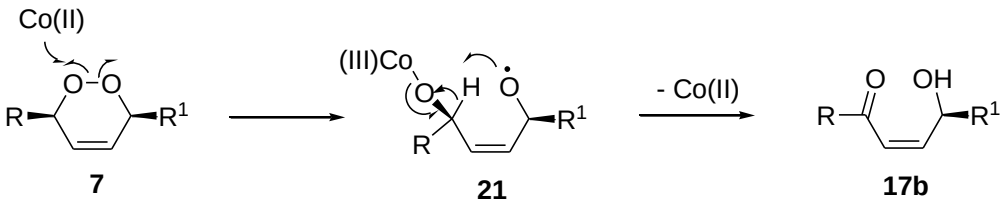

Scheme 7

1.1.3.1b Reactions of *cis*-γ-Hydroxyenones.

cis-γ-Hydroxyenones are a highly reactive species that can rearrange rapidly under either acidic or basic conditions. They can therefore serve as a starting platform for a number of transformations beginning with 1,2-dioxines.

As shown in *Scheme 3* (*Pathways C and D*), allowing 1,2-dioxines to react with an ylide results in regioselective cyclopropanes **22**. The is due to the ylide acting as a mild base inducing a Kornblum-DeLaMare rearrangement to give the *cis*-γ-hydroxyenones which then rapidly undergo a Michael Initiated Ring Closure (MIRC) to yield the appropriate cyclopropane.[37] Conveniently, the regiochemistry of the reaction can be controlled *via* the type of ylide used.[44,45] The Taylor group has previously conducted extensive research into this cyclopropanation reaction, resulting in a significant contribution to the literature within this field.[37,39,44-50]

Highly substituted γ-lactones can be also synthesised from 1,2-dioxines (*Scheme 3, Pathway E*). Greatrex *et al.* showed that the formation of these γ-lactones proceeds *via* their initial conversion into *cis*-γ-hydroxyenones **17** using a strong base and subsequent *anti* 1,4-addition of a malonic ester. Intramolecular cyclisation then yields the γ-lactones **23** in high diastereoselectivity, *Scheme 8*.[51,52]

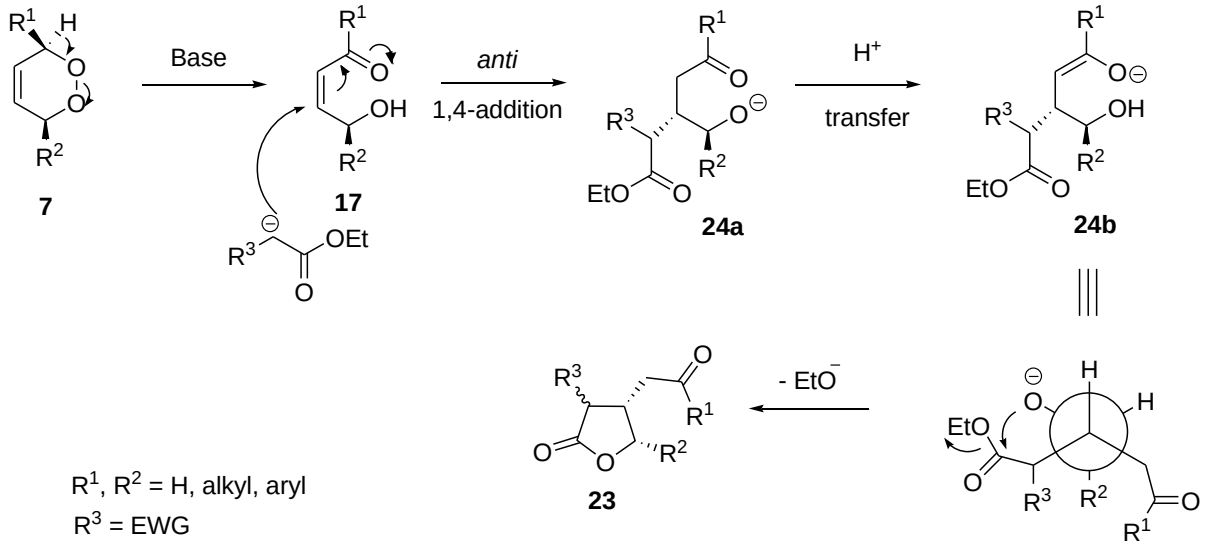

Scheme 8

Recently this synthetic pathway was utilised by Brown *et al.* in the total synthesis of the two naturally occurring stereoisomers of Oak Lactone (**25**), along with their enantiomeric counterparts (*Scheme 9*).[53] The two naturally occurring isomers are extracted from wood into alcoholic beverages during fermentation and/or maturation and make an important sensory contribution to wine. The synthesis of enantiomerically pure isomers of the oak lactones *via* this pathway enabled accurate odour detection thresholds to be determined for all four isomers in both red and white wine.[54]

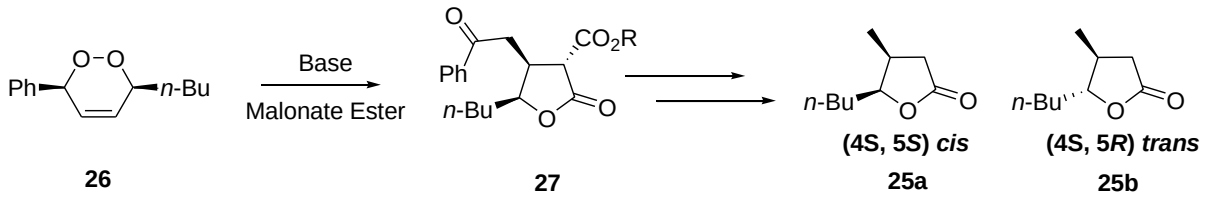

26 **27** **25a** **25b**

Scheme 9

As previously mentioned, treatment of *cis*-γ-hydroxyenones with base typically leads to 1,4-dicarbonyls. Avery *et al.* recently showed that upon treatment with hydroxide or ethoxide bases, tetrahydrofurans with the base structure of **28** (seen in *Pathway F, Scheme 3*) can be obtained with no trace of the 1,4-dicarbonyls. This occurs *via* a self-

condensation of the γ-hydroxyenones *via* an oxa-Michael/Michael ring-closing cascade reaction.[55] With many natural products possessing the tetrahydrofuran ring core, these tetra-substituted tetrahydrofurans can act as useful building blocks towards the synthesis of a multitude of compounds.

1.1.3.2 Reactions Where the Peroxide Bond is Maintained Within Cyclic Peroxides.

As seen above, there are many examples within the literature whereby the peroxide bond is ruptured during the course of reaction. In many cases this is desirable and enables 1,2-dioxines to be versatile starting materials for incorporating oxygen functionality into compounds. However, as mentioned, the peroxide moiety is a useful and necessary component of many natural products and intermediates. Chemists are often deterred from using endoperoxides in synthesis due to the traditional view that the peroxide bond is too weak to be retained during many conventional synthetic transformations. As a result of this, a whole field of chemistry has remained untouched for many years, as there are limited examples in the literature involving the manipulation of peroxide molecules without rupturing the dioxygen linkage. A selection of these examples are given below.

Reduction of the alkene portion of a bicyclic 1,2-dioxine can selectively be achieved, whilst maintaining the peroxide bond with the use of diimide. To date this is the only method established for this process, and is only successful for bicyclic systems.[17] Adam *et al.* illustrated this reaction by reducing the alkene portion of a simple unsaturated bicyclic endoperoxide **29** with diimide in methanol to give the fully saturated endoperoxide **30**, as seen in *Scheme 10*.[56]

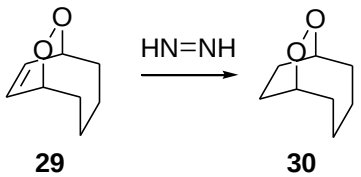

29 **30**

Scheme 10

Addition to the double bond can also be achieved, usually with an electrophilic reagent whilst maintaining the peroxide linkage. Epoxidations can be carried out with peracids such as *m*-CPBA or CF_3CO_3H and halogenations with bromine or chlorine results in the addition of the two halogens *trans*- to each other. Examples of these transformations have been seen in both monocyclic[57] and bicyclic endoperoxides.[58] Foster *et al.* showed that the double bond of endoperoxide **31** could be converted into epoxide **32** by reaction with CF_3CO_3H and to dibromide **33** upon reaction with bromine in chloroform (*Scheme 11*).[58]

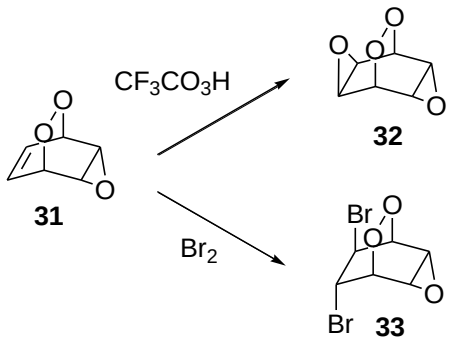

Scheme 11

Recent work by members of the Taylor group has focussed on the osmium catalysed dihydroxylation of 1,2-dioxines. Robinson *et al.* subjected monocyclic 1,2-dioxines to dihydroxylation with osmium tetraoxide to furnish peroxy diols **34** which were stereoselectively reduced to give tetrols **35**. The peroxy diols were also ring-opened using Co(II) salen complexes to give novel hydroxyl ketones **36**, *Scheme 12a*.[59] This work was utilised in the synthesis of the rare sugar psicose **37**, *Scheme 12b*.[59]

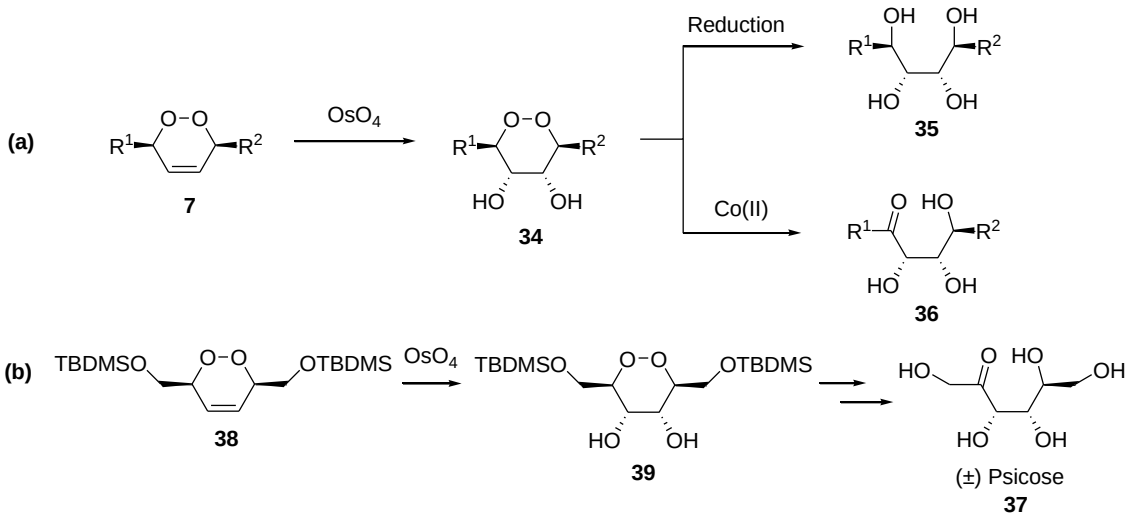

Scheme 12

Valente *et al.* investigated the dihydroxylation of bicyclic dioxines under similar conditions to give bicyclic peroxy diols **40** whilst maintaining the peroxide linkage. Further reduction resulted in the ultimate cleavage of the peroxide bond to furnish their respective tetrols **41**. It was also found in this work that upon treatment with heat or light the diols underwent a previously unknown rearrangement to carbonyls of type **20** and **42**, as seen in *Scheme 13*.[60]

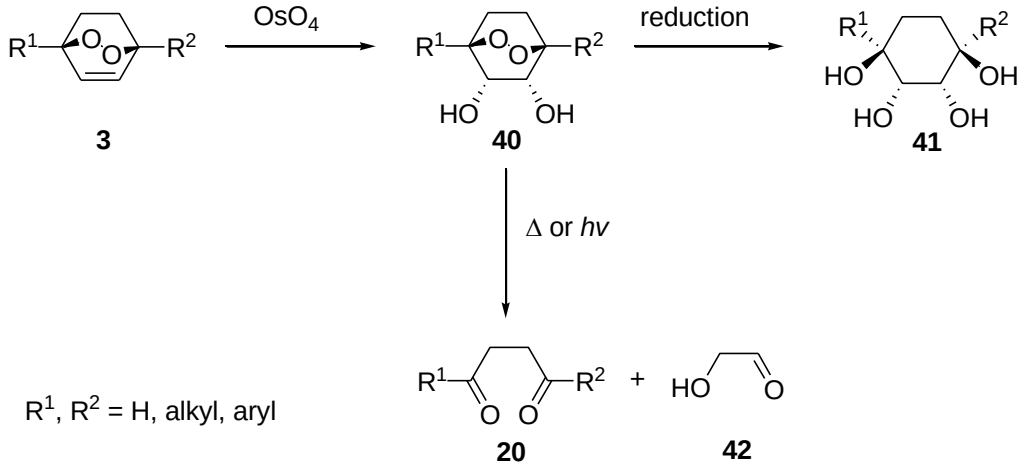

Scheme 13

Further research from the Taylor group (Zvarec *et al.*), has recently investigated the cyclisations of tethered hydroxyl and carboxylic acid moieties onto the olefinic motif of 1,2-dioxines, **43**, to generate tetrahydrofurans **44** and dihydrofuran-2(3*H*)-ones **45**. As depicted in *Scheme 14*, this was done whilst, once again, maintaining the peroxide linkage intact.[61]

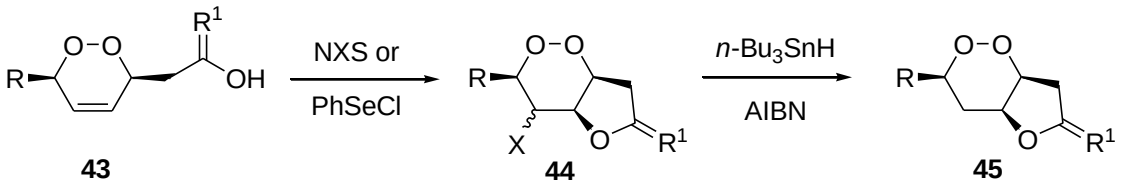

43 **44** **45**

R = alkyl, aryl
R^1 = O, H_2

X = SePh, I, Br

Scheme 14

1.2 Ozonolysis of Alkenes.

1.2.1 An Introduction.

Ozone (**46**) is a symmetrical bent molecule with a central positively charged oxygen atom and two terminal oxygen atoms that share a negative charge. It is a 1,3-dipole resonance-stabilised zwitterion, *Scheme 15*.[62]

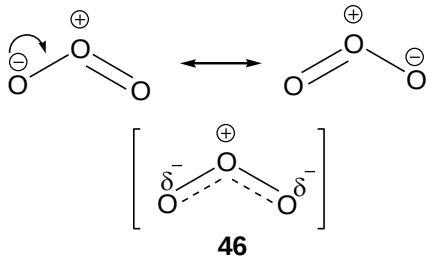

46

Scheme 15

Ozone is an important natural constituent of the atmosphere, being principally concentrated between the altitudes of 15 to 25 km. It is formed by solar UV radiation in the range 240 to 300 nm *via* the following reactions.[63]

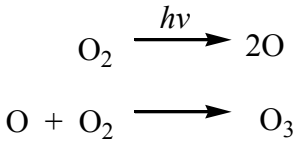

Ozone is a very powerful oxidant which can easily be generated from oxygen *via* electric discharge (corona discharge), whereby the oxygen undergoes partial dissociation *via* the following equations; (where M is any third particle).[64]

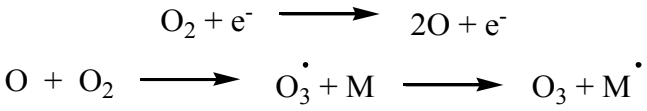

The ozonolysis of alkenes was first reported in 1840, and remains one of the most important and classical methods for oxidative cleavage of alkenes.[65] For example, a *Scifinder*® search for ozone related conversion of alkenes returns thousands of examples.

1.2.2 Mechanism.

The basic mechanism for the ozonolysis reaction was formulated by Criegee in the mid-1950's.[66,67] Since then, a large amount of work has been done on the mechanism, [68,69] although not all details are known or fully understood.[70,71] The Criegee mechanism has become generally accepted, although a great number of exceptions to this mechanism have appeared, prompting numerous 'modified-Criegee' mechanisms to be reported.[72,73] It is beyond the focus of this thesis to give a thorough review of the mechanistic aspects of this reaction; suffice it to say that any deviations or abnormalities from the accepted mechanism will be discussed within forthcoming chapters. The basic principles of the Criegee mechanism are described below.

As can be seen in *Scheme 16,* the first step involves a highly exothermic 1,3-dipolar cycloaddition of ozone with an alkene **47** to generate a highly unstable primary ozonide (1,2,3-trioxolane) **48**. This spontaneously decomposes *via* a cycloreversion to a

carbonyl **49** and carbonyl oxide **50**. A further 1,3-cycloaddition reaction occurs between the two carbonyl compounds to produce an ozonide (1,2,4-trioxolane) **51**.[74]

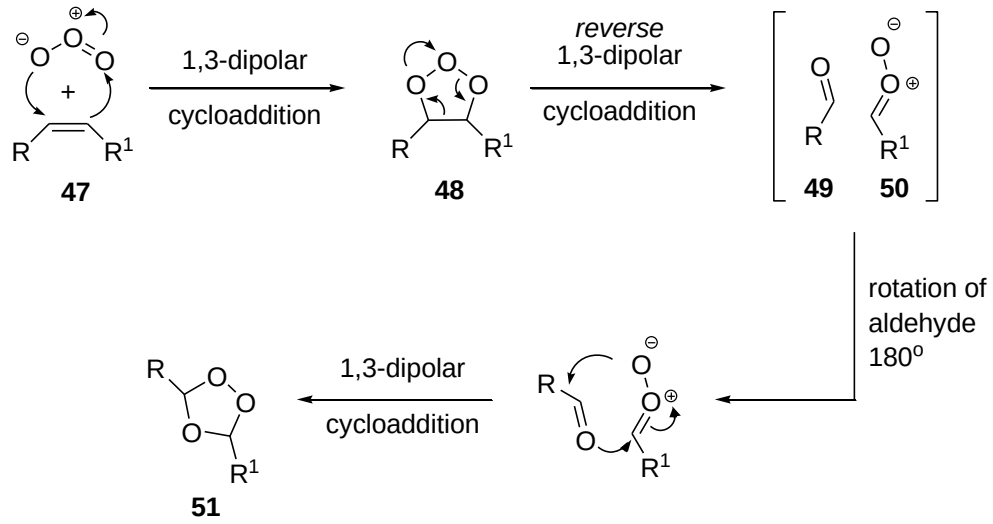

Scheme 16

Ozonides possess a dangerous combination of kinetic stability and thermochemical instability.[65] They can be isolated, yet due to their instability are capable of spontaneous and dangerously exothermic decomposition reactions, particularly upon concentration.[65,75] Many researchers have nevertheless proceeded to isolate these highly unstable intermediates in a bid to study their chemical properties and decomposition or as precursors for compounds other than carbonyl compounds.[76-79] This body of research is focussed on the ozonolysis products after complete reduction of ozonides, therefore ozonide chemistry will not be discussed, aside from one interesting example given below.

The ozonide Arterolane (OZ277) (**52**) is a synthetic peroxide drug development candidate that is now in phase III clinical trials for antimalarial treatment.[80-82] Its identification by Vennerstrom *et al.*[80] was considered a significant breakthrough in the antimalarial drug development efforts of the past decade.[81] The spiroadamantane ring system and peroxide bond are found to be essential for its activity,[83] which is in line with the previously mentioned cyclic peroxide Artemisinin (**1**), whose antimalarial activity was also found to be attributed to the peroxide functionality. The ozonide **52**

was synthesised by Dong *et al.* starting with Griesbauum coozonolysis[84] of *O*-methyl-2-adamantanone oxime (**53**) and methyl 4-oxocyclohexyl acetate (**54**) to form the crystalline ozonide **55** in 78% yield. This was converted into **52** over several subsequent steps, *Scheme 17*.[83]

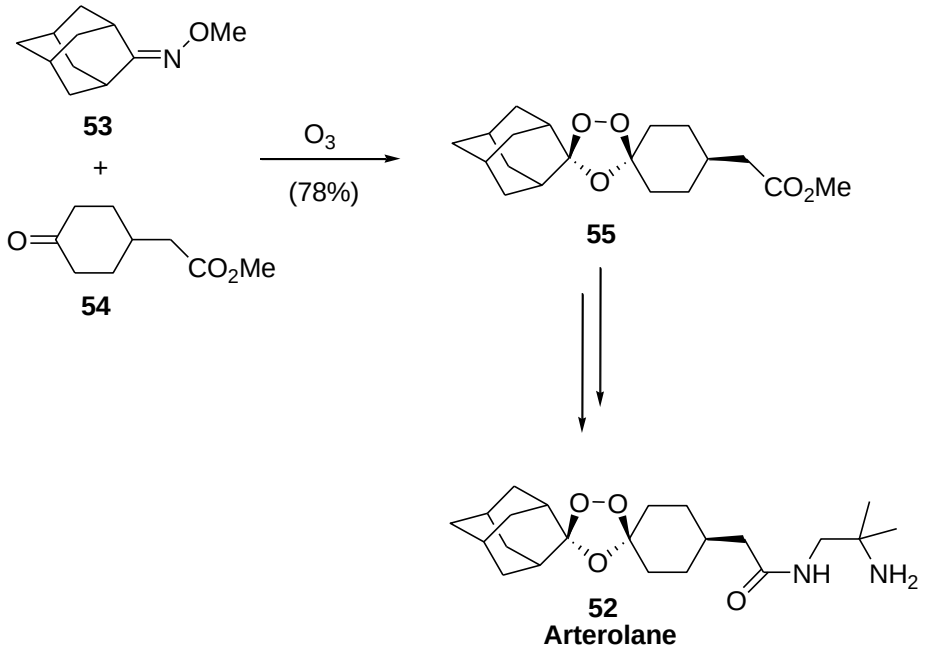

Scheme 17

1.2.3 Decomposition of Ozonides.

The decomposition of ozonides can be carried out using a variety of reagents, to give a number of different functional products. A schematic representation of some transformations of ozonides is given in *Scheme 18*. Commonly, mild reducing agents such as triphenylphosphine, dimethylsulfide,[85] zinc/acetic acid[76] are employed to produce aldehydes (*Pathway A*). Ozonides can also be oxidised with oxygen, peroxyacids or H_2O_2[86] to give carboxylic acids (*Pathway B*), or they can be treated with reducing agents such as $LiAlH_4$,[70] $NaBH_4$[87] or BH_3[88] to give alcohols (*Pathway C*). Treatment with ammonia and hydrogen, together with a catalyst gives the corresponding amines (*Pathway D*),[89] whereas treatment with alcohol (R^2OH) and anhydrous HCl affords the corresponding esters (*Pathway E*).[90]

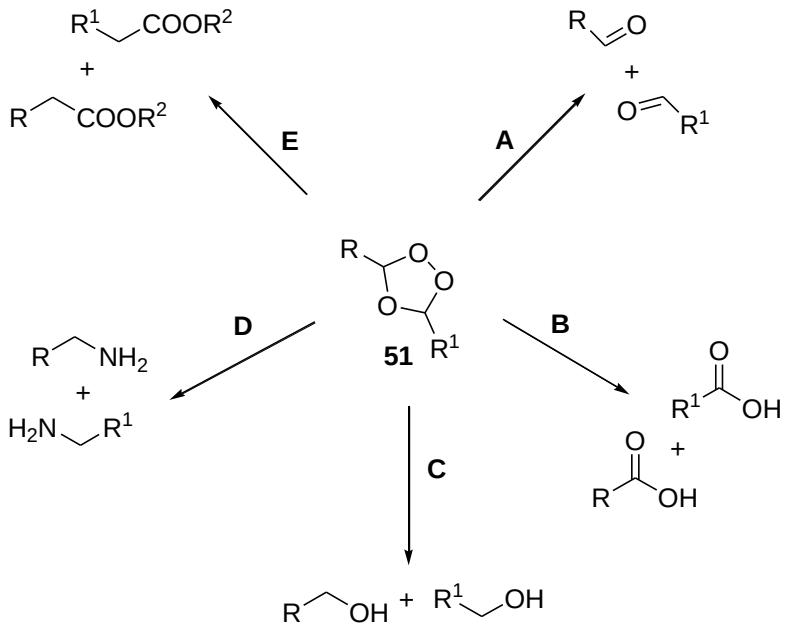

Scheme 18

One of the classical and most widespread methods for reduction of ozonides is with the use of triphenylphoshine (PPh_3) which reduces the ozonide *via* nucleophilic attack.[91,92] PPh_3 reduction of ozonides reportedly proceeds quantitatively, and is best carried out in the absence of oxygen, as this may contribute to the direct oxidation of PPh_3.[93-95] It is also commonly reported that although PPh_3 is an effective reducing agent, it can generate problems with product separation and purification, making it difficult to separate any unreacted PPh_3 and PPh_3O (a reaction byproduct) from the desired products.[65,93] The mechanism for the reduction of ozonides *via* PPh_3 has been evaluated using ^{18}O-labelled ozonides, showing that the reduction occurs by exclusive attack at the peroxide oxygen atoms, *Scheme 19*.[91,96]

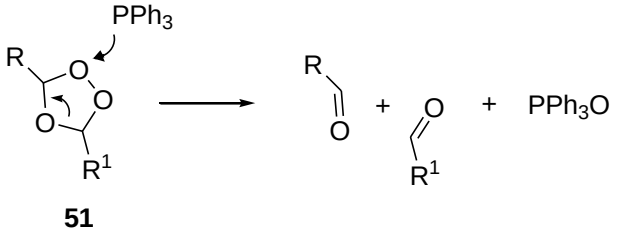

Scheme 19

1.2.4 Examples of Ozonolysis.

A wide variety of alkenes can undergo ozonolysis reactions. Cleavage of acyclic alkenes results in the generation of two molecules, whereas cyclic olefins result in cleavage of the alkene to give one bifunctional product. There is little precedent for the ozonolysis of bicyclic or other polycyclic alkenes, with the few examples found within the literature given below, along with a couple of other examples of interest.

LY235959 (**56**) is a potent NMDA receptor antagonist previously under development for the treatment of neurodegenerative disorders such as Alzheimer's disease.[97,98] Hansen *et al.* reported a novel total synthesis in 17 steps and 13% overall yield from (*R*)-pantolactone (**57**).[99] The synthesis incorporated the ozonolysis of bicyclic alkene **58** followed by addition of solid sodium borohydride to give the expected diol **59** in 92% yield, *Scheme 20*. The authors reported that the yield for this reaction was somewhat variable, with a 'significant' byproduct being characterised as acid **60**.[99] No further discussion of the ozonolysis reaction was presented.

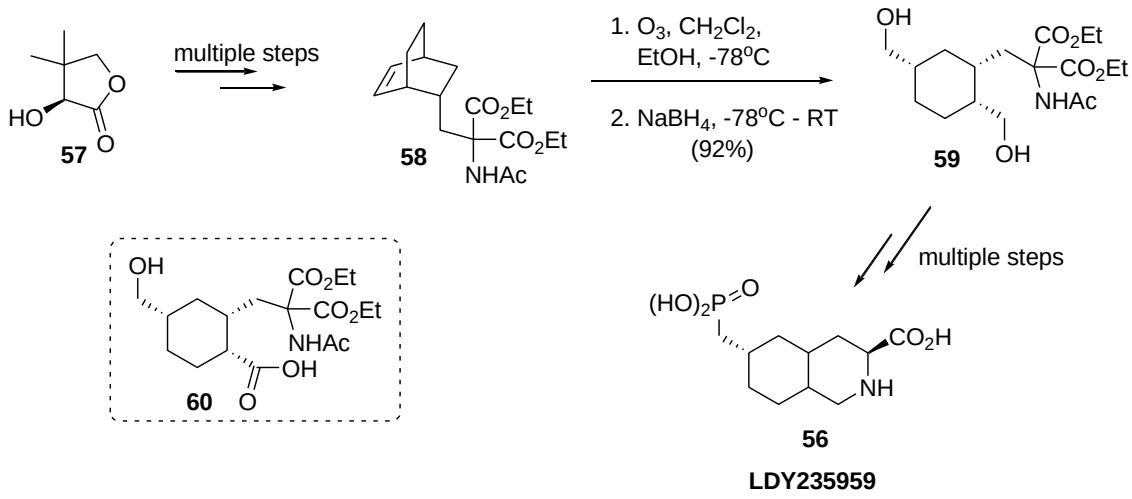

Scheme 20

Another example of a bicyclic olefin undergoing ozonolysis is as part of the total synthesis of (±)-Annuionone B (**61**) and (±)-Tanarifuranonol (**62**). Annuionone B was first isolated from *Helianthus annuus* (sunflower) as an allelopathic agent in 1998[100]

with its structure being revised and corrected in 2004.[101] Tanarifuranonol was first obtained from the plant extracts of *Macaranga tanarius* in 2005.[102] Shiao *et al.* synthesised both these products from bromo-substituted phenol **63**, *Scheme 21*.[103] An important step in the synthesis of these compounds involved the ozonolysis of a tricyclic alkene **64** to the keto-aldehyde **65** which possesses the requisite 6-oxabicyclo[3.2.1]octane skeleton required by these natural products. Unfortunately the reaction is only mentioned in passing, with no discussion presented.

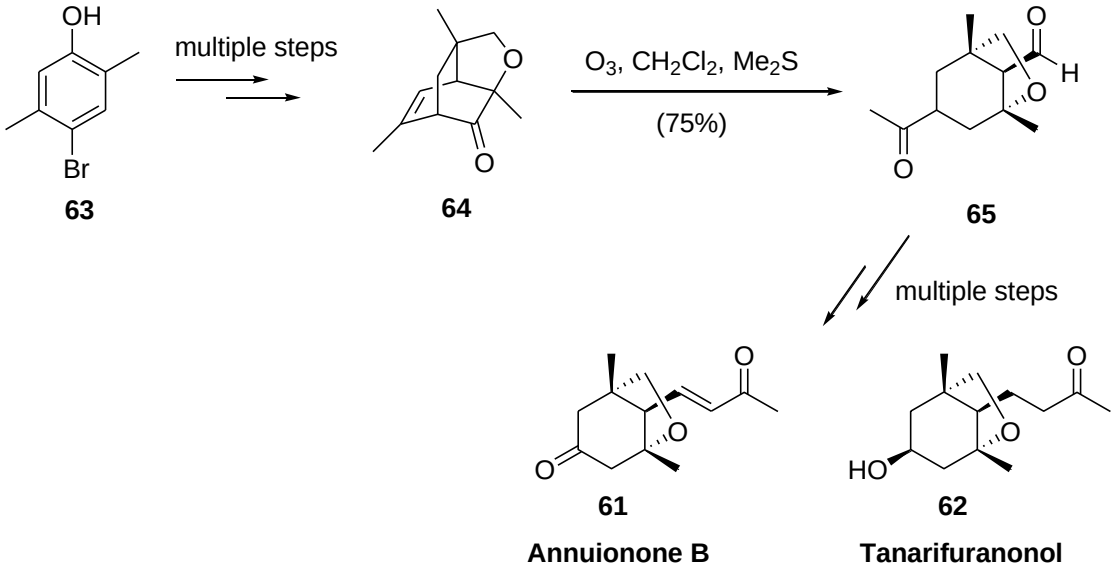

63 **64** **65**

61 **62**

Annuionone B **Tanarifuranonol**

Scheme 21

Mehta and Vidya have reported on the ozonolysis of polycyclic alkene compounds in the synthesis of novel oxa-bowls.[104] The authors provide three examples of polycyclic dienes **66**, **67**, and **68**, which underwent ozonolysis followed by dimethyl sulphide reduction to yield tetra-aldehydes **69**, **70**, and **71** which were not isolated, but immediately treated with acid catalyst Amberlyst-15 to promote cyclisation to tetraoxa-cages **72**, **73** and **74** respectively in 30-50% yields, *Scheme 22*.

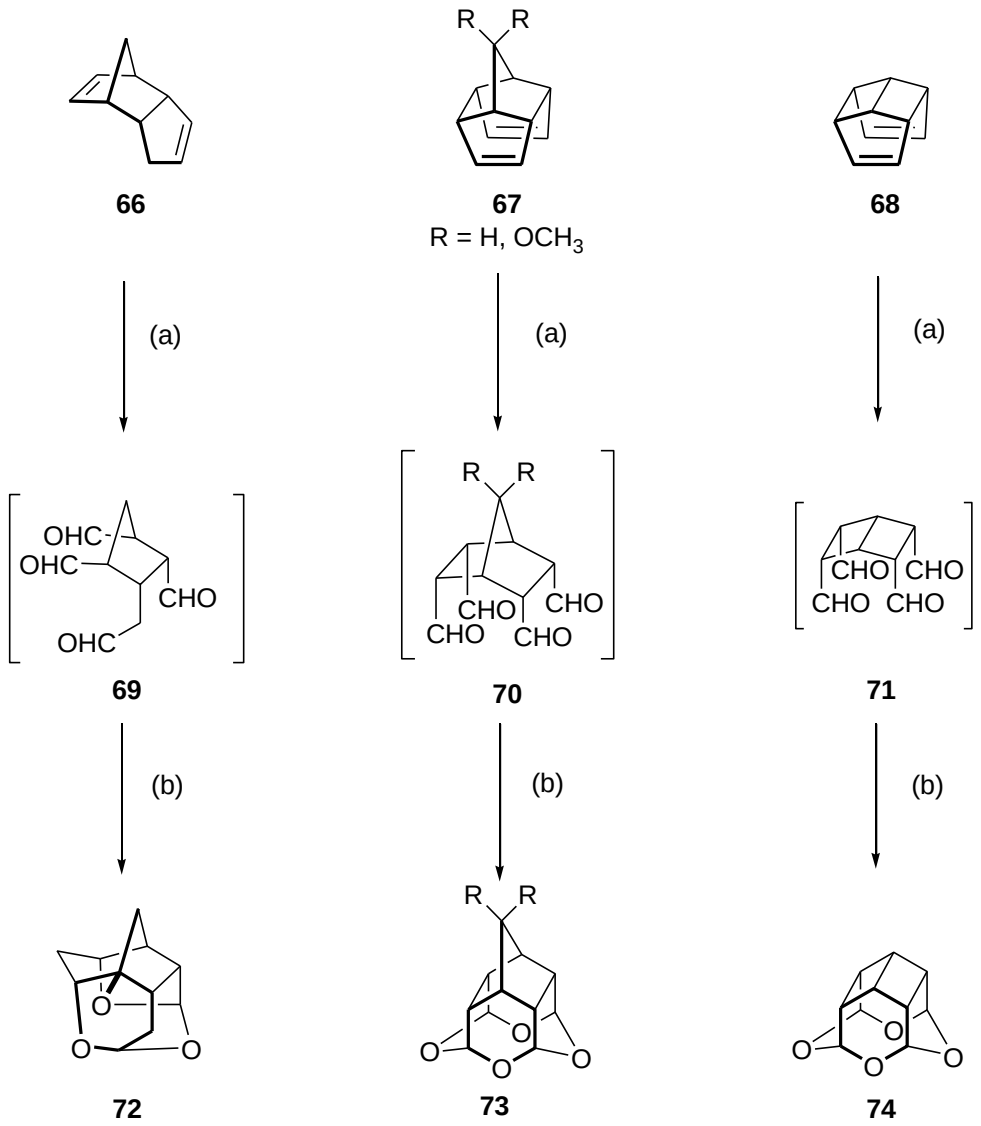

(a) O_3, DCM, -78 ^oC; Me_2S (b) Amberlyst-15, rt, 3-5 hrs

Scheme 22

Ozonolysis reactions are typically limited to small-scale reactions within an academic/research setting,[75] although several chemical and pharmaceutical companies have been able to safely execute large-scale ozonolysis processes.[105-107]

For example, chemists at Pfizer used ozonolysis to prepare a bisulfite adduct **75** required as a 'surrogate' aldehyde in a reductive amination reaction to give a pharmaceutical intermediate.[105] 2-Indanone (**76**) underwent Grignard addition with vinylmagnesium bromide to give the alkene **77**. Firstly, ozonolysis of **77** in dichloromethane at -78 ^oC followed by reductive workup with dimethyl sulfide was

trialled, although this resulted in a complex mixture of products due to the aldehyde **78** forming dimers and higher oligomers, *Scheme 23A*. An alternative method was trialled using ozone in methanol at -60 ^{o}C. Methanol traps the carbonyl oxide as the methoxyhydroperoxide **79** (rather than forming an ozonide); which was then reduced with sodium bisulfite to give the desired bisulfite adduct **75** (*Scheme 23B*). After careful assessment of the safety and calorimetry data, this reaction was safely scaled up to a 3 kg scale.[105]

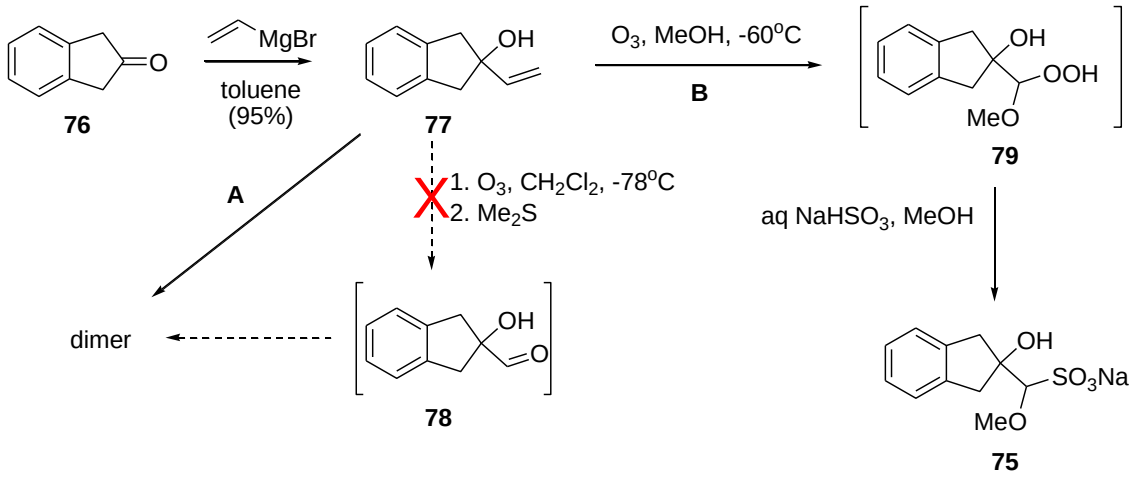

Scheme 23

As mentioned earlier, Artemisinin, (**1**) is a potent antimalarial peroxide extracted from the plant *Artemesia annua L.* Interestingly, Avery *et al*. used a 10-step sequence in the total synthesis of Artemisinin, incorporating an abnormal ozonolysis combined with cyclisation as part of a final one-pot reaction to yield the cyclic peroxide **1**.[108] As seen in *Scheme 24*, starting with (*R*)-(+)-pulegone (**80**) nine sequential steps were undertaken to furnish the ofelin **81**. Ozonolysis of **81** in dichloromethane was followed by successive addition of aqueous sulphuric acid and silica gel to effect a complex process of dioxetane formation, ketal deprotection, and multiple cyclisations to furnish Artemisinin (**1**) in 35% yield.

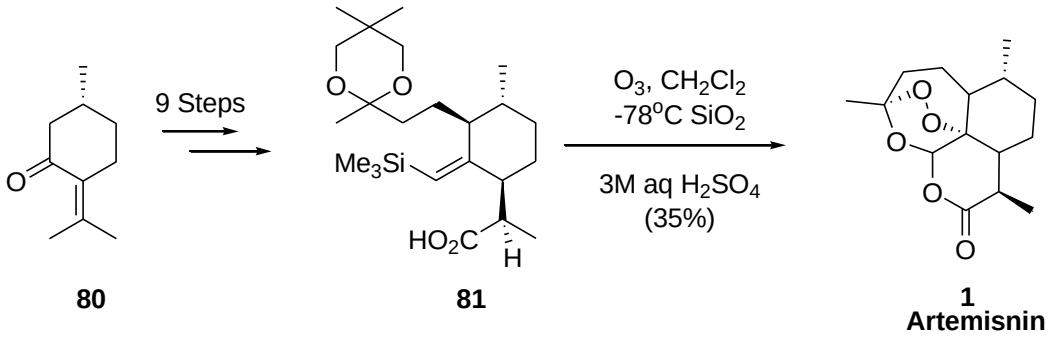

80 **81** **1**
Artemisnin

Scheme 24

1.3 Ozonolysis of the Alkene Moiety of 1,2-Dioxines.

Although the literature contains many examples of the ozonolysis of alkenes and of other reactions involving 1,2-dioxines, very few exist that incorporate dioxines undergoing an ozonolysis reaction.

Two papers of interest, both published by Gumulka *et al.*[109,110] investigate the ozonolysis of 7-dehydrocholesterol acetate endoperoxide (**82**). The authors performed an ozonolysis on the named steroid in a bid to understand the reaction mechanism and pathway undertaken to the final products, *Scheme 25*. The resulting ozonide was allowed to decompose over time (a number of weeks to months), with various decomposition products being isolated and characterised along the way. The final products were said to be secodione **83** and hemiacetal **84**. A full transformation of the ozonolysis products into compounds **83** and **84** reportedly lasted approximately eight weeks (at room temperature), with dialdehyde **85** being isolated as an unstable intermediate.

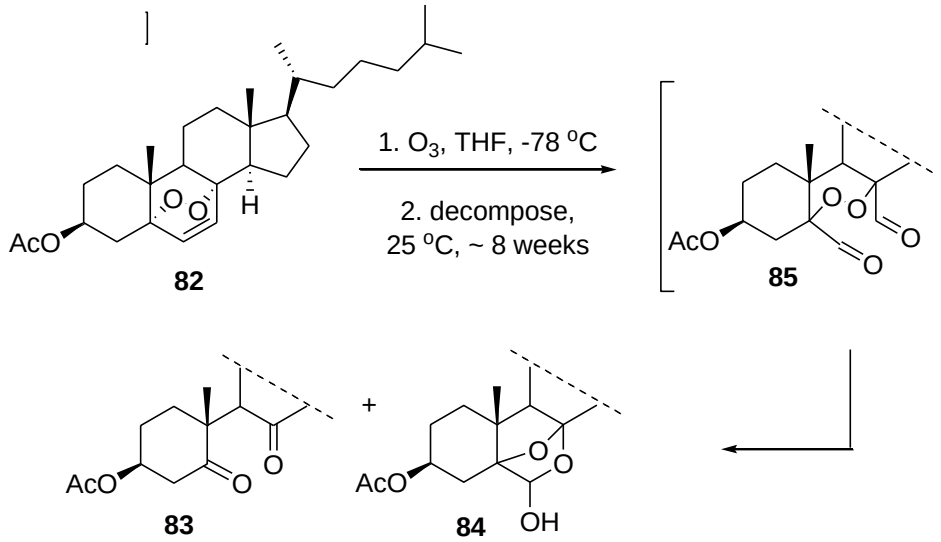

Scheme 25

Ordinarily, as discussed earlier, ozonolysis reactions typically proceed *via* the formation of the ozonide, followed by prompt reduction to the desired product. The authors in this instance did not reduce the ozonide, but rather studied its decomposition products. Their approach towards this study had several questionable shortcomings especially with regard to their vague experimental details (making their work somewhat unreproducible) and the lack of detail given in the characterisation of the products.

In addition to the two papers mentioned above, a thorough search of the literature found only a handful of examples of ozonolysis reactions being conducted on compounds containing the endoperoxide functionality. These examples are typically part of a 'total synthesis', with ozonolysis incorporated into the synthetic pathway, but not as a key reaction, therefore little to no emphasis was placed on the reaction, but rather it is mentioned only in passing. Details of these reactions are described below.

In 2003 del Sol Jimenez *et al.* reported the isolation, structural elucidation and biological activities of polyketide endoperoxide Plakortide M (**86**) isolated from the Caribbean marine sponge *Plakortis halichondrioides*.[111] Bioactive cyclic peroxides are quite commonly found in the organic extracts of marine sponges, with numerous analogues of **86** previously identified.[112-115] To determine the absolute stereocentre at

the remote chiral centre C-10, del Sol Jimenez *et al.* employed a procedure based on the ^{1}H NMR chemical shift difference on derivatives of **86**. The details of this derivatisation and subsequent stereochemistry determinations are unimportant here, the relevance to this body of work lies with the first step of this structural modification, which involved the ozonolysis of **86**, followed by reduction with $NaBH_4$, as shown in *Scheme 26*. The ozonolysis proceeded without disruption of the peroxide bond, and gave two products **87** and **88**. The major product selectively cleaved only the C-11 alkene (this product then underwent further derivatisation in a bid to confirm the C-10 stereochemistry), whereas the minor product had both alkenes cleaved.[111]

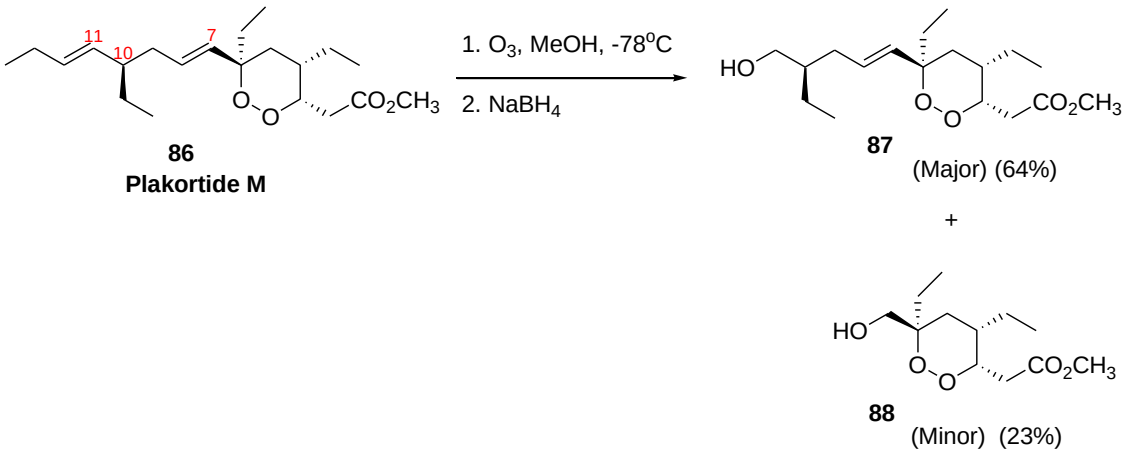

86
Plakortide M

87
(Major) (64%)

+

88
(Minor) (23%)

Scheme 26

The above authors refer to an earlier paper with similar work published by Stierle *et al.* in 1980, whereby they identified two precursor endoperoxide analogues of Plakortide M, namely 3-epiplakortin (**89**) and 9,10-dyhydro-3-epipakortin (**90**) isolated from the same marine sponge, *Plakortis halichondrioides*.[112] Structural modifications were again undertaken to confirm the stereochemistry of these compounds, involving ozonolysis reactions on two separate endoperoxide derivatives. Dialkene **91** underwent ozonolysis followed by reduction of the ozonide with Me_2S to afford the aldehyde **92**, *Scheme 27a*. The authors suggest that the trisubstituted olefin was too sterically hindered to react with ozone. The second endoperoxide-dialkene **93** was ozonised followed by oxidation with Jones' reagent resulting in the expected double cleavage of the olefin product **94**, *Scheme 27b*.

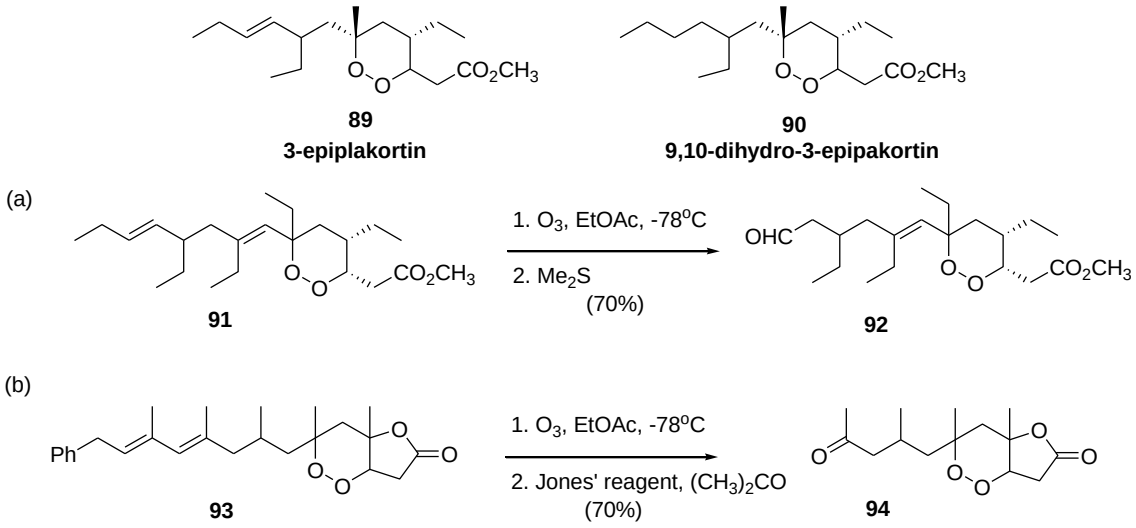

Scheme 27

Ayer *et al.*[116] synthesised (-) Warburganal (**95**) from levopimaric acid (isolated from pine oleoresin). This synthesis involved photolysing methyl levopimarate to give the endoperoxide **96**, which was then ozonised to give the keto-aldehyde **97**, as seen in *Scheme 28*. This ozonolysis was not a key reaction in the paper, but rather a minor constituent in a 15-step total synthesis. In the paper's discussion little emphasis was again placed on this reaction, or on the stability or characterisation of the resulting dicarbonyl product.

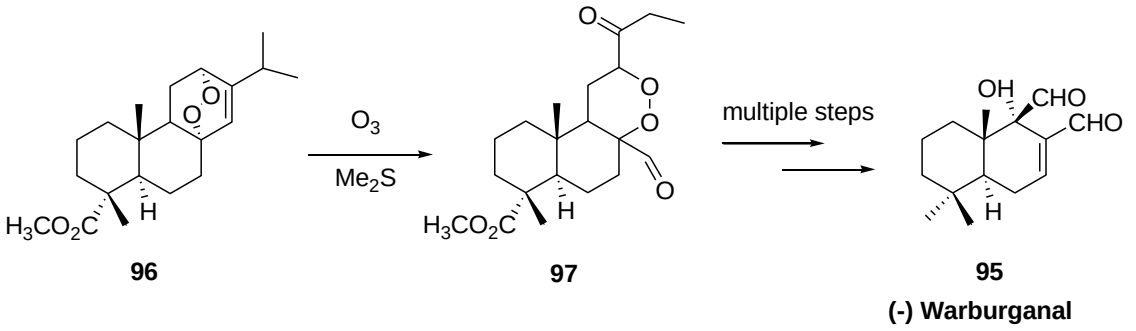

Scheme 28

In 1978 Adam *et al.*[117] published a short report on the trapping of unstable fulvene/singlet oxygen adducts by reduction with diazene. As shown in *Scheme 29*, this work included the cyclic peroxide **98** being ozonised in the presence of

tetracyanoethylene (TCNE) to give the ketone **99**, which was unstable and readily decarbonylated at -10 ^{o}C to give succinaldehyde (**100**). As with the report published by Ayer[116] above, limited detail of the ozonolysis reaction was provided in this paper.

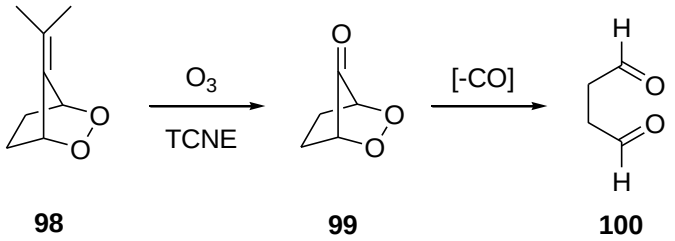

98 **99** **100**

Scheme 29

As can be seen from the above highlights, only a few examples have been reported whereby ozonolysis has been performed on alkene systems incorporating 1,2-dioxine functionality, and researchers in these instances have paid little attention to the significance of this reaction. As a result, no real scientific studies have been performed within this field, leaving a gap in the literature towards the knowledge of the reactivity of bicyclic 1,2-dioxines towards ozone, which will form the emphasis of this thesis.

1.4 Aims.

The work presented within this chapter summarises the importance and versatility of both 1,2-dioxine and ozonolysis chemistry.

Since comparatively little work has been done on maintaining the peroxide linkage of 1,2-dioxines during synthesis, it was thought that further examples of this would prove useful towards understanding the synthetic versatility of 1,2-dioxines. In addition to this, a thorough search of the literature revealed that little attention has been paid to exploring the ozonolysis reaction on bicyclic alkenes, particularly the alkene moiety of bicyclic 1,2-dioxines.

The aim of this project was therefore to combine these two areas, and perform the ozonolysis reaction on a range of simple 1,4-disubstituted bicyclic 1,2-dioxines, **3** in order to explore the products formed. It was seen as worthwhile to also conduct some theoretical computational studies into the ozonolysis of the parent bicyclic 1,2-dioxine system in order to provide further mechanistic insight into the reaction. The second aim of this project was to utilise this novel transformation to synthesise important wine compounds, namely the furanoid linalool oxides (**101**) and anhydrofuran linalool oxides (**102**). These two compounds are commonly found in wine, and an efficient method for their synthesis was seen as a worthwhile pursuit. An introduction to **101** and **102** will be given in chapter 5, while the overall aims of this project are summarised in *Scheme 30*.

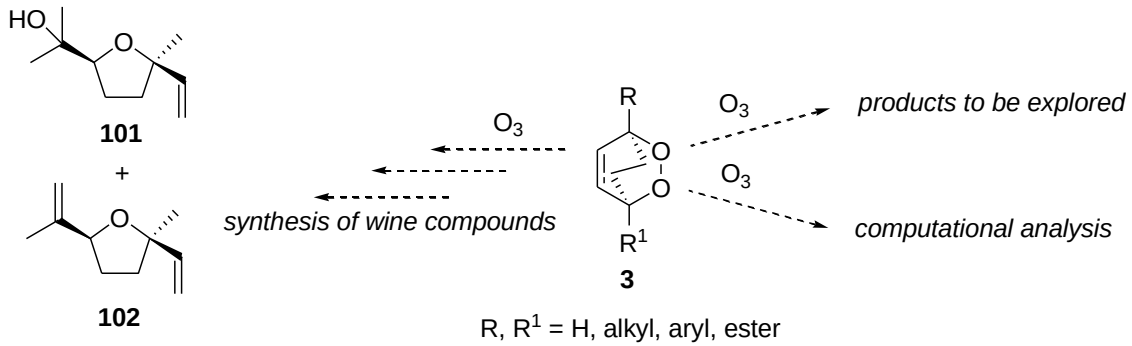

Scheme 30

CHAPTER 2: Synthesis of Bicyclic 1,2-Dioxines.

A range of 1,4-disubstituted bicyclic 1,2-dioxines were needed in order to investigate the scope of reaction for the ozonolysis of bicyclic bridged 1,2-dioxines. As discussed within Chapter 1, the synthesis of these requisite 1,2-dioxines requires the use of cyclic 1,3-hexadienes along with singlet oxygen in a [4π + 2π] cycloaddition reaction. Two core types of 1,2-dioxines were targeted for these studies, namely a set of simple 1,4-disubstituted 1,2-dioxines along with an example of a more complex steroidal endoperoxide. The synthesis of both sets of compounds is presented within this chapter.

2.1 Synthesis of Simple 1,4-Disubstituted 1,3-Cyclohexadienes (6a-e).

Table 1 shows the various substrates chosen for this study, including both *meso* and asymmetrical derivatives with varying substituents located at the 1- and 4-positions. Such substitution would allow us to explore the effects of sterics and electronics on the proposed ozonolysis reactions.

Table 1: 1,4-Cyclohexa-1,3-dienes Used in This Study.

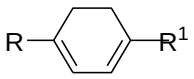

	R	**R^1**
6a	Me	*i*-Pr
6b	H	Ph
6c	Ph	Ph
6d	CH_2CO_2Me	CH_2CO_2Me
6e	CO_2Me	CO_2Me

α-Terpinene (**6a**) was commercially available, and therefore did not require synthesis. Cyclohexa-1,3-dien-1-yl-benzene (**6b**) was prepared by a standard Grignard addition of phenylmagnesium bromide (**104**) to 2-cyclohexenone (**105**) to furnish the allyl alcohol **106**, which was subsequently dehydrated to the 1,3-diene *via* a sequential sulfenate-

sulfoxide [2,3]-sigmatropic rearrangement and *syn*-elimination using 2,4-dinitrobenzenesulfenyl chloride (**107**) and triethylamine,[118] *Scheme 31*.

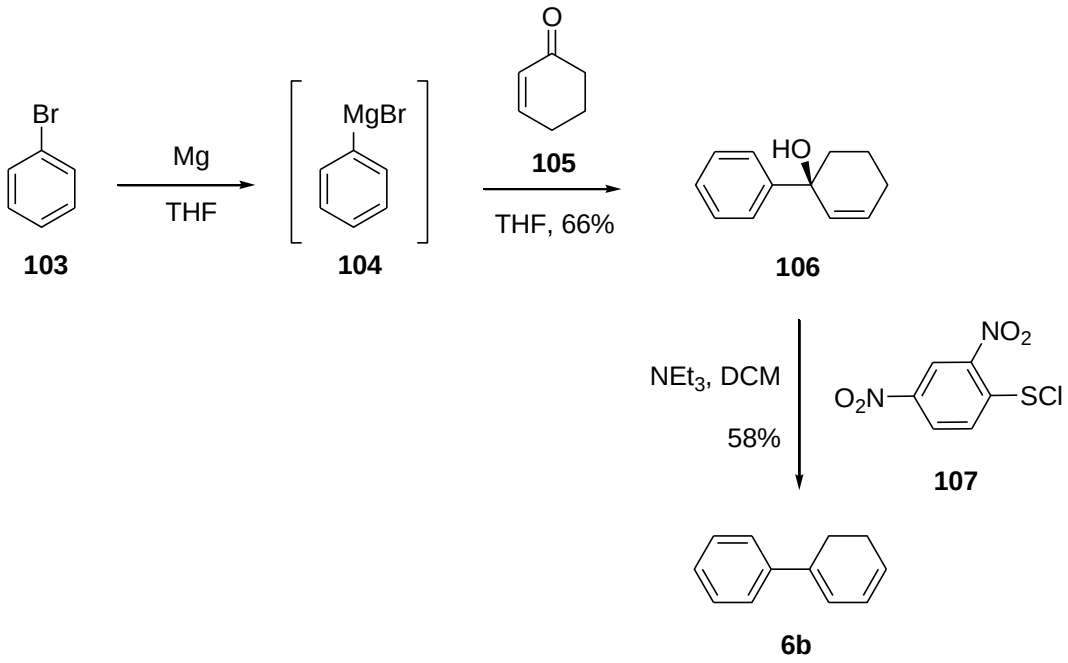

Scheme 31

The diphenyl substituted 1,3-diene **6c** was prepared *via* the pathway outlined in *Scheme 32*. Phenyl lithium (**108**) was prepared from bromobenzene (**103**) and *n*-butyllithium and allowed to react *in situ* with 1,4-cyclohexadione (**109**) to give tertiary diol **110**. This was then dehydrated *in situ* with 50% H_2SO_4 to afford a 60 : 40 mixture of the 1,3- and 1,4-dienes **6c** and **111**, respectively. The product ratio was determined by integrating the ^{1}H NMR alkene peaks for each isomer, specifically a singlet at δ = 6.53 ppm for the 1,3-diene and a multiplet at δ = 6.28 ppm for the 1,4-diene. Investigation into this reaction by Dale *et al.*[119] found that the initial dehydration product was the nonconjugated 1,4-diene **111**, while isomerisation to the conjugated 1,3-diene **6c** took place over time. The authors also found that by heating the mixture at reflux in *t*-butanol containing potassium *t*-butoxide resulted in complete conversion to the conjugated diene, suggesting that this is the thermodynamic product, with the nonconjugated diene therefore being the kinetic product. Upon replicating this method complete conversion to the 1,3-diene **6c** was found in 91% isolated yield.

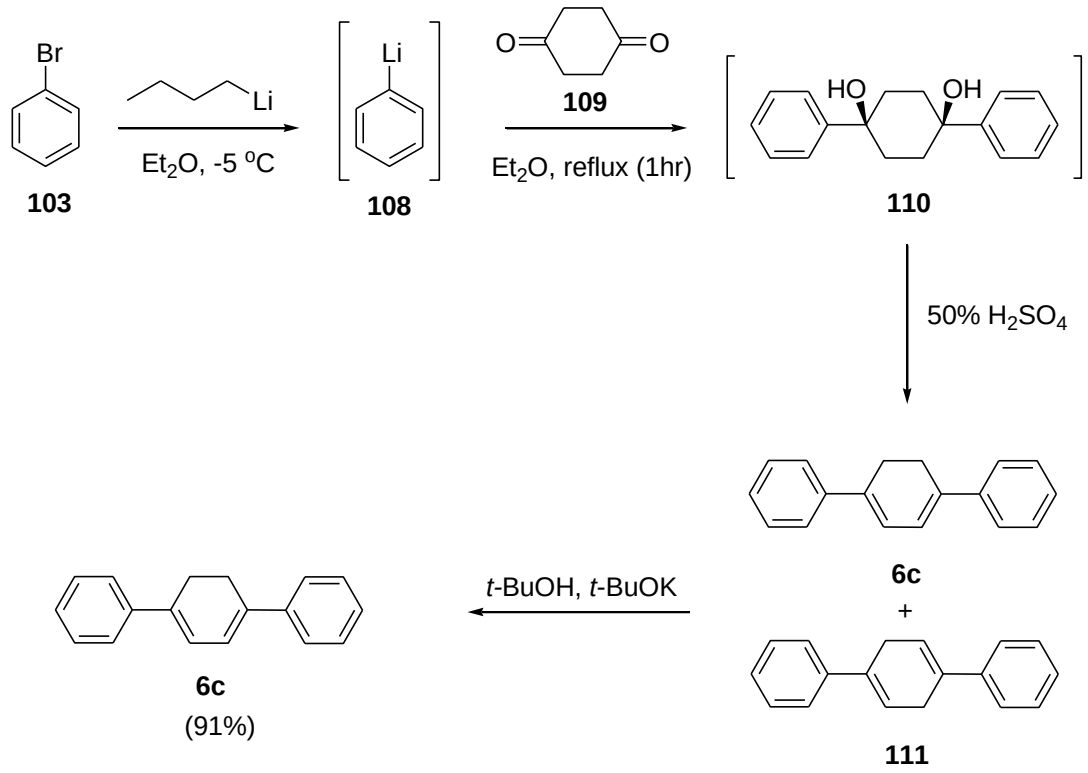

Scheme 32

Diester **6d** was prepared in a three-step synthesis beginning with a Horner-Wadsworth-Emmons olefination as previously reported by Engel *et al.*[120] This involved the nucleophilic addition of triethyl phosphonate (**112**) to both carbonyl moieties within 1,4-cyclohexadione (**109**) to yield a 60 : 20 : 20 mixture of 1,3-diene **113** and the related (*E*) and (*Z*) diesters **114a** and **114b**, respectively. The isomeric mixture subsequently underwent hydrolysis and isomerisation under basic alcoholic conditions to afford the 1,4-diene diacid **115** in good yield (76%). Finally, acid **115** was esterified *via* acid catalysis to furnish the desired methyl diester **6d** in good yield (71%), as depicted in *Scheme 33*.

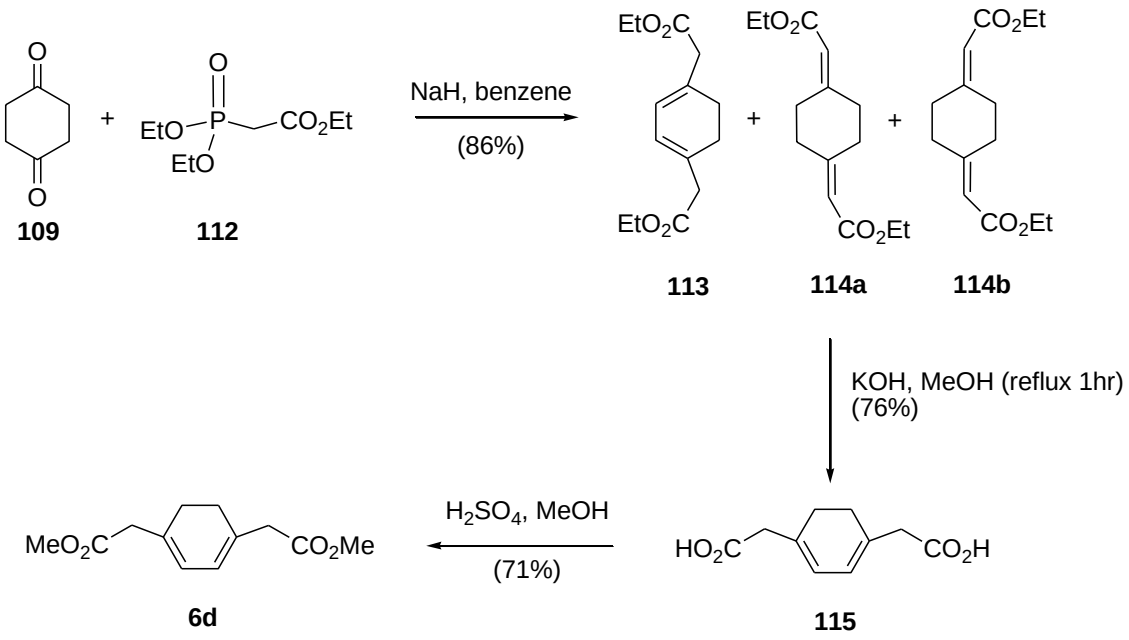

Scheme 33

A second diester substituted diene **6e** was also synthesised with the aim of comparing their relative reactivities. Unlike the previously synthesised diester **6d**, diester **6e** has the carbonyl group directly attached to the bridgehead carbon, thus placing the carbonyls in conjugation with the alkene moieties. Diester **6e** was prepared using a multistep sequence that was carried out as a 'one-pot' reaction, adapted from work published by Chapman *et al.,*[121] *Scheme 34*. Thionyl chloride was used to convert 1,4-cyclohexanedicarboxylic acid (**116**) to the acid chloride **117**, followed by subsequent bromination to give a mixture of *cis*- and *trans*-α-bromo-acyl chlorides **118**. Esterification in methanol afforded the *cis*- and *trans*-bromoesters **119**, which were readily separable due to the *trans* isomer being an isolable solid, easily filtered off from the methanol solution, leaving behind the *cis* isomer as an oil. Together the *cis*- and *trans*-dibromoesters underwent dehydrobromination in pyridine to furnish the desired diester **6e** in a pleasing 80% overall yield.

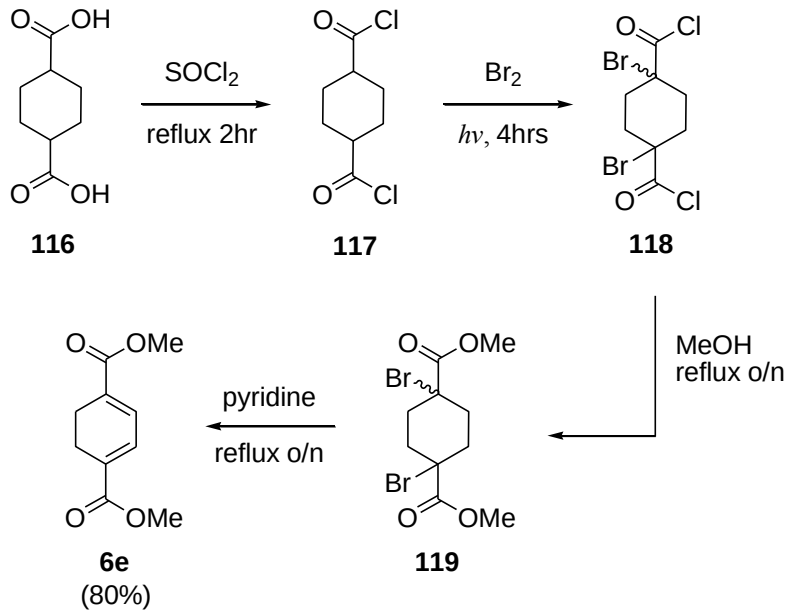

Scheme 34

2.2 Synthesis of Simple 1,4-Disubstituted Bicyclic 1,2-Dioxines (3a-e).

With the reqisite 1,3-butadienes in hand, the 1,2-dioxines were to be prepared by a photo-oxidative [4π + 2π] cycloaddition with singlet oxygen. The photolysis of all dienes was conducted in dichloromethane employing a catalytic amount of rose bengal *bis* (triethylammonium) salt as the photosensitiser. Reactions were followed to completion *via* TLC and purified by flash chromatography, which allowed separation from the rose bengal and any more polar by-products. Yields were variable, depending on the substitution of the 1,3-diene, *Table 2*.

The known 1,2-dioxines **3a**,[22] **3b**,[60] **3c**[122] and **3d**[60] gave physical and chemical data consistent with the literature. The previously unknown diester 1,2-dioxine **3e** showed the expected ^{1}H NMR resonances, with the characteristic vinylic proton seen as a singlet at δ = 6.88 ppm.

Table 2: Photolysis of Dienes **6** with Singlet Oxygen.

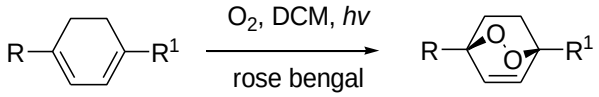

Diene	R	R^1	Dioxine	Yield (%)
6a	Me	*i*-Pr	**3a**	94
6b	H	Ph	**3b**	36
6c	Ph	Ph	**3c**	83
6d	CH_2CO_2Me	CH_2CO_2Me	**3d**	63
6e	CO_2Me	CO_2Me	**3e**	46

2.3 Synthesis of Steroid Endoperoxide 86.

Aside from the synthesis of 1,4-disubstituted bicyclic dioxines, it was also seen as important to synthesise the steroid dioxine **82** in order to validate and expand upon the ozonolysis work done by Gumulka *et al.*[109,110] Commercially available 7-dehydrocholersterol (**120**) was acetylated in excellent yield to give the acetate **121**, which was then subjected to the standard photolysis conditions outlined above to afford the endoperoxide **82** in good yield, *Scheme 35*. The physical and spectral properties were consistent with previously published literature data.[123,124]

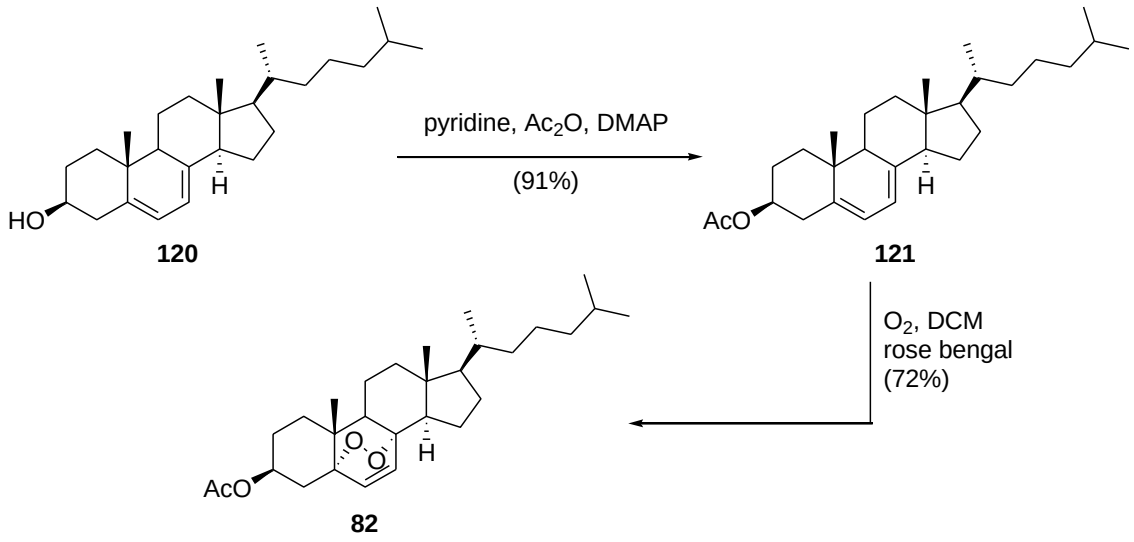

Scheme 35

Previous NMR and computational studies on these types of steroids have confirmed that the peroxide bridge is formed with α-π-facial selectivity to afford the 5α,8α-steroid. This is due to the fact that the C-19 methyl group is β (axial) to the ring system,[125] This can be clearly seen in *Scheme 34*, which shows the AM1-optimised structures of the steroid diene **121** and subsequent dioxine **82**. In addition to this, the crystal structure of dioxine **82** has been previously published by Takahashi *et al.* upon isolation from the egg of the sea hare *Aplysia Juliana*.[126]

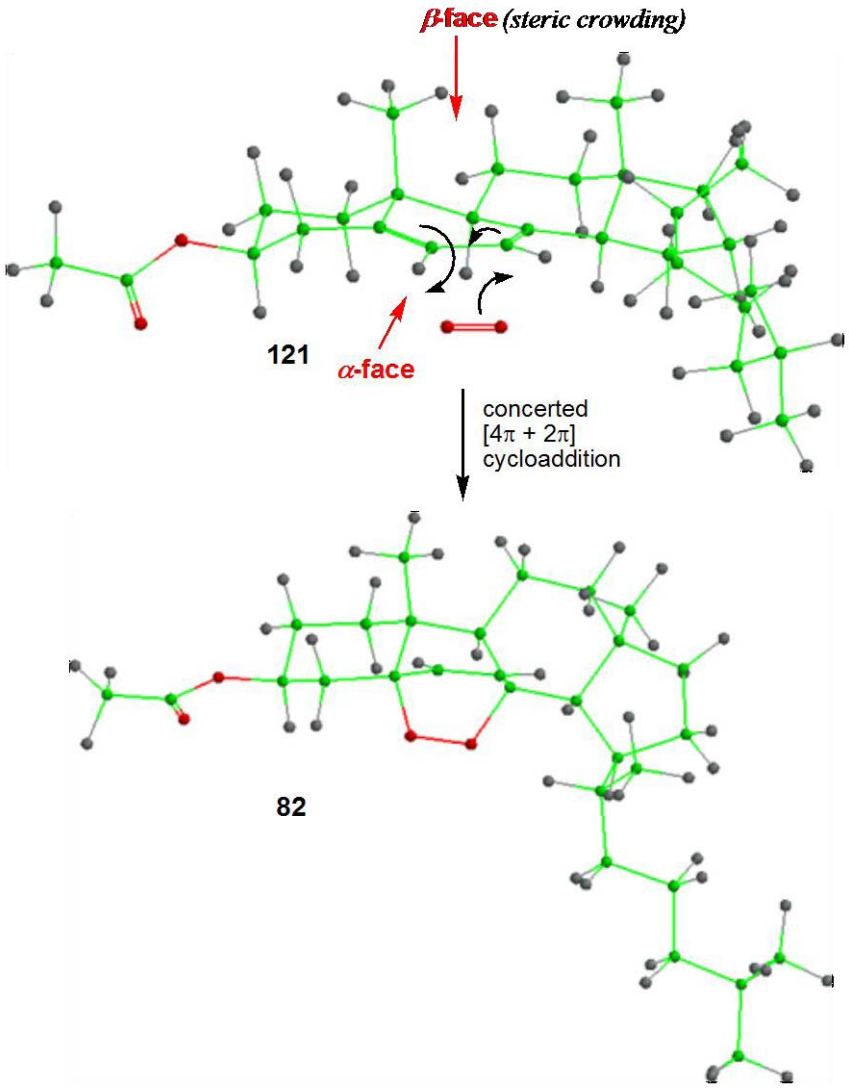

Scheme 36

This chapter has described the efficient synthesis of the bicyclic bridged 1,2-dioxines **3a**-**e** and the steroidal 1,2-dioxine **82** that are to be utilised for an investigation into the ozonolysis of bicyclic 1,2-dioxines, which will be the topic of the following chapter.

CHAPTER 3: Ozonolysis of Bicyclic Bridged 1,2-Dioxines

With the synthesis of the requisite 1,2-dioxines complete, investigations into the individual ozonolysis of each dioxine could begin. As mentioned, the aims of this study were to perform ozonolysis on each dioxine substrate to verify that the alkene bond could be cleaved without disrupting the peroxide moiety.

All ozonolysis reactions, unless otherwise stated, were carried out in dichloromethane at -78 ^{o}C under an atmosphere of argon. Ozone was generated from oxygen using Corona discharge *via* an ozone generator, and pumped through the solution as a gaseous mixture of O_2/O_3. Reactions were continued until the solution turned pale blue, indicating saturation with ozone and cessation of reaction. After completion, the mixture was raised to room temperature, and reduced with triphenyl phosphine (PPh_3), typically 1.1 eq, unless otherwise stated. All products were purified *via* flash chromatography. The polar triphenyl phosphine oxide (PPh_3O) by-product remained on the base line, with any unreacted PPh_3 eluting with the solvent front. Since aldehydes are notoriously unstable it was predicted that the products might need to be protected in order to allow for the full characterisation necessary to facilitate product analysis. This could be easily achieved *via* a Wittig reaction, using a stabilised phosphorous ylide to create more stable alkene products.

The results of these experiments are presented within this chapter. For ease of discussion, the results for the ozonolysis of 1,2-dioxines have been divided into two categories; firstly the substrates that behaved as ‘expected’ or ‘anticipated’ towards ozone, and secondly the substrates that behaved in an ‘unexpected’ manner towards ozone. This will be followed by some further investigative experiments that were conducted in order to shed some light into the unusual results, along with a discussion into structural and mechanistic considerations including some theoretical computational investigations. Firstly, it is necessary to revisit the ozonolysis mechanism, paying particular attention to bicyclic alkene systems.

3.1 Mechanism for the Ozonolysis of Bicylic 1,2-Dioxines.

The generally accepted Criegee mechanism for the ozonolysis of alkenes was discussed in Chapter 1,[66,67] with a general example given for a typical acyclic system (*Scheme 16*). As mentioned, there is little precedent for the ozonolysis of bicyclic (or other polycyclic) alkenes, and even fewer examples for the ozonolysis of bicyclic 1,2-dioxines (along with monocyclic 1,2-dioxines, although our focus in this study is on bicyclic systems). It is therefore of interest to examine this mechanism in more detail, with specific regard to bicyclic 1,2-dioxines.

Our proposed general mechanism for the ozonolysis of an alkene moiety incorporated into a bicyclic 1,2-dioxine system is shown in *Scheme 37*. Ozone can potentially approach the alkene moiety of **3** from two directions, namely the *exo* face (from above) or from the *endo* face (from below). The term '*endo*' is used here to indicate that ozone approaches from opposite the peroxide linkage, whereas in the case of '*exo*' the ozone approaches from the same side. Intuitively, one would postulate that the direction of 'attack' would be *via* the *endo* face, resulting in molozonide **123**. If 'attack' were to occur *via* the *exo* face, steric and especially electronic repulsions would occur between the oxygen atoms of the peroxide bridge and the ozone molecule, represented by dashed red lines in *Scheme 37*. These interactions would clearly be minimised upon approach from the *endo* face. This 'intuitive' theory will be further supported by theoretical calculations in Chapter 4. Once the molozonide **123** is formed, it would be expected to promptly undergo a retro 1,3-dipolar cycloaddition to afford the aldehyde-carbonyl oxide **124.** At this point there are two potential pathways that could be undertaken to give one of two possible ozonides, **125a** or **125b**, (*Scheme 37, Pathways A* and *B* respectively). Once again, intuition would have one propose that ozonide **125a** would be favoured over **125b**, due to a minimising of the electronic interference between oxygen atoms. Theoretical calculations supporting this argument will be presented in Chapter 4.

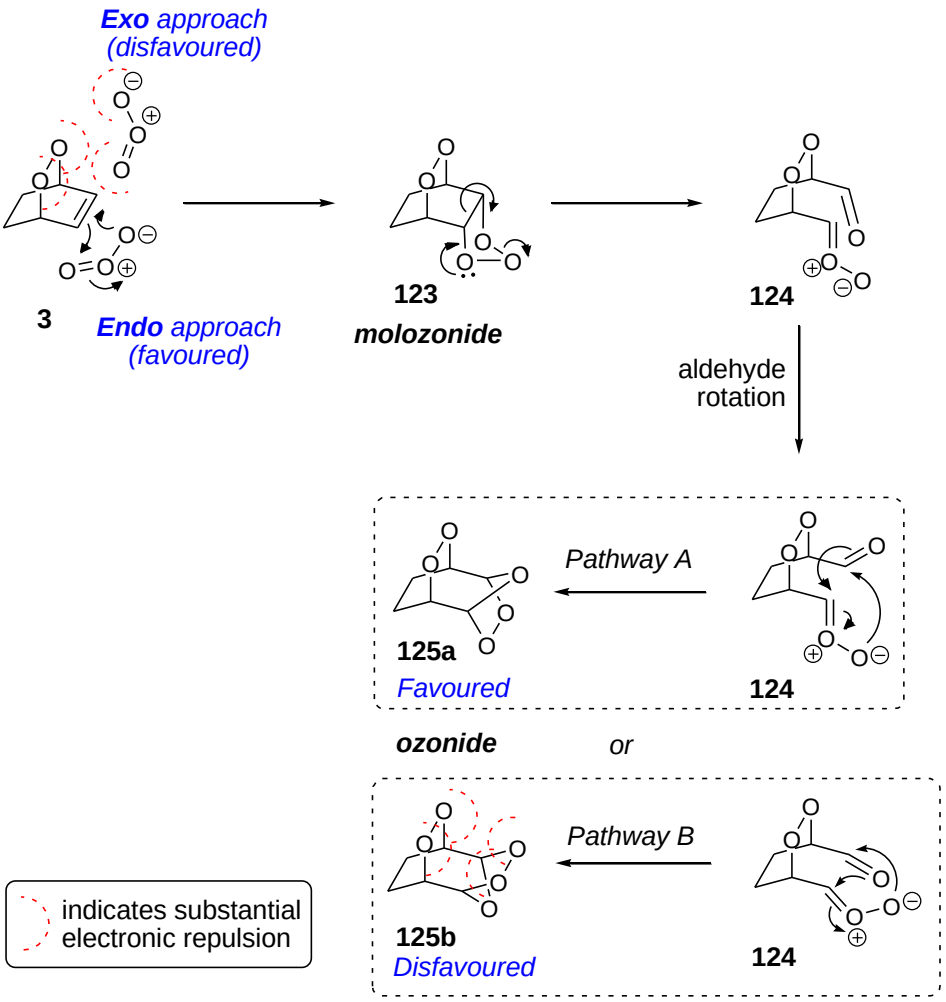

Scheme 37

3.2 Ozonolysis of Steroid 1,2-Dioxine 82.

Before commencing work on the ozonolysis of the 1,4-disubstituted dioxines, ozonolysis was initially performed on the steroid dioxine **82** to expand upon the sketchy work previously published by Gumulka *et al.*[109,110] some 30 years ago. As discussed in Chapter 1, the focus of their study was the investigation of steroid ozonide decomposition with a view to understanding the reaction mechanism and pathway undertaken to the final products (*Scheme 25,* Chapter 1). Rather than reducing the ozonide formed from the reaction, they allowed it to decompose over time, with dialdehyde **85** reportedly being found as an unstable intermediate. In our opinion this paper had several shortcomings, specifically, the use of vague reaction conditions along with insufficient characterisation of any of the products formed, leading one to question

whether they were indeed formed at all, and in what quantities. Our aim here was not to reproduce the final products that the authors found, but rather expand upon their work by applying a rigorous scientific approach towards the ozonolysis of steroid **82**. This was to be done by immediately reducing the ozonide upon formation in order to validate that the expected dialdehyde was indeed formed, and to confirm that the peroxide bond was not broken during the process, *Scheme 38*.

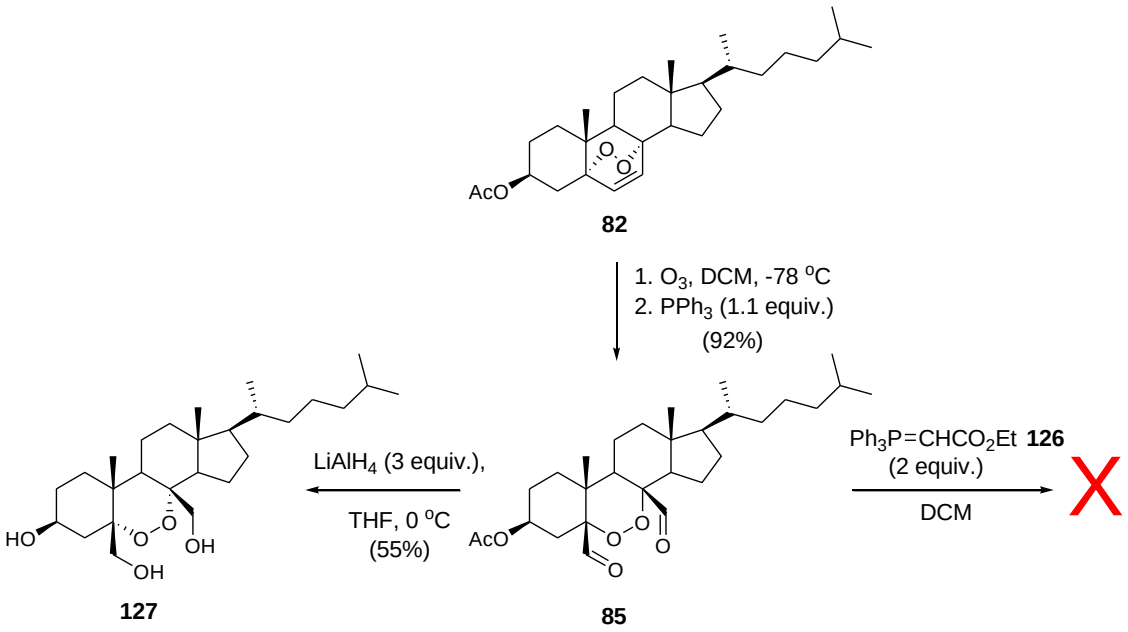

Scheme 38

Crude ^{1}H NMR of the ozonolysis products clearly showed that aldehyde **85** had formed. Flash chromatography furnished pure dialdehyde **85** in excellent yield (92%), although product instability meant that only ^{1}H and ^{13}C NMR could be obtained. The expected aldehyde peaks could clearly be seen in the ^{1}H NMR spectrum resonating as singlets at δ = 10.01 and 9.62 ppm, and δ = 202.5 and 196.8 ppm for the ^{13}C NMR spectrum, along with the absence of any alkene peaks in both spectra. The bridgehead carbons α to the peroxide linkage showed characteristic ^{13}C NMR peaks at δ = 88.5 and 87.7 ppm, indicating that the peroxide bond was still intact.

A Wittig reaction was trialled using stabilised phosphorous ylide **126** to trap dialdehyde **85** and thereby enable full characterisation. Upon adding two equivalents of ylide **126** to the dialdehyde **85** in dichloromethane, no reaction occurred, even upon heating the

solution to reflux. This was likely due to the steroid being too hindered to allow for nucleophilic 'attack' of the bulky ylide, *Scheme 38*. Another method of stabilising the aldehydes was therefore sought. It is worth noting that although the purified dialdehyde is unstable, once placed in solution, the addition of either ylide or PPh_3/PPh_3O appears to stabilise the aldehydes, even upon heating, and prevent them from decomposing.

In Chapter 1, the versatility of 1,2-dioxines and the fragility of the peroxide bond was discussed, with a number of examples provided that either cleaved or maintained the peroxide bond. One important reaction that was not discussed was reduction, in particular the use of $LiAlH_4$ in the presence of peroxides, due to contradicting reports of its outcome in dioxine chemistry. It is known that the peroxide bond can be readily broken upon treatment with an excess of $LiAlH_4$, to give the respective diol.[19,127] In contrast to this, there are also literature reports detailing the successful use of $LiAlH_4$ to reduce carbonyl functionalities in the presence of peroxide bonds without their rupture. One paper of interest, published by Jin *et al.* focuses on the susceptibility of peroxide bonds to hydride reduction.[1] The authors used a variety of 1,2-dioxines with various ester groups and subjected each of them to a number of common hydride reducing agents under various conditions to investigate the peroxy bond survival rate along with completeness of the reduction reaction. They found that in most cases the peroxide bond remained untouched, particularly at low temperatures. $LiAlH_4$ was found be an excellent candidate when used at 0 ^oC, due to the cleanliness of the reaction along with complete reduction of ester groups whilst maintaining the peroxide linkage.

Using this work as a precedent, dialdehyde **85** was successfully reduced to triol **127** in moderate yield, *Scheme 38*. Upon using an excess of reducing agent (3 equiv.), it was anticipated that the acetate would also succumb to reduction, which was evident through the lack of a distinct acetate peak in the ^1H NMR spectra. Triol **127** was the only product isolated, with NMR resonances for both ^{13}C and ^1H spectra showing the absence of aldehyde peaks. The bridgehead carbons were seen in the ^{13}C NMR at δ = 85.8 and 85.2 ppm, consistent with the quaternary carbons α to the peroxide linkage, whilst the two CH_2OH carbons resonated at δ = 67.3 and 64.6 ppm. The IR showed a large hydroxyl absorption peak at 3313 cm^{-1} and an absence of any carbonyl peaks, as

expected. This reduction is in itself an interesting reaction, providing another example of the peroxide bond remaining intact upon being exposed to quite harsh reducing conditions.

The AM1 optimised structures of dioxine **82**, and the resulting dialdehyde **85** are shown in *Figure 2*. Since we know that the peroxide bond is facing in a fixed downwards position (Chapter 2, *Scheme 36*), then upon cleavage of the alkene bond by ozone, the resulting dialdehyde must assume the stereochemistry as shown in *Figure 2*. This relative and absolute stereochemistry must also be that for the triol **127**.

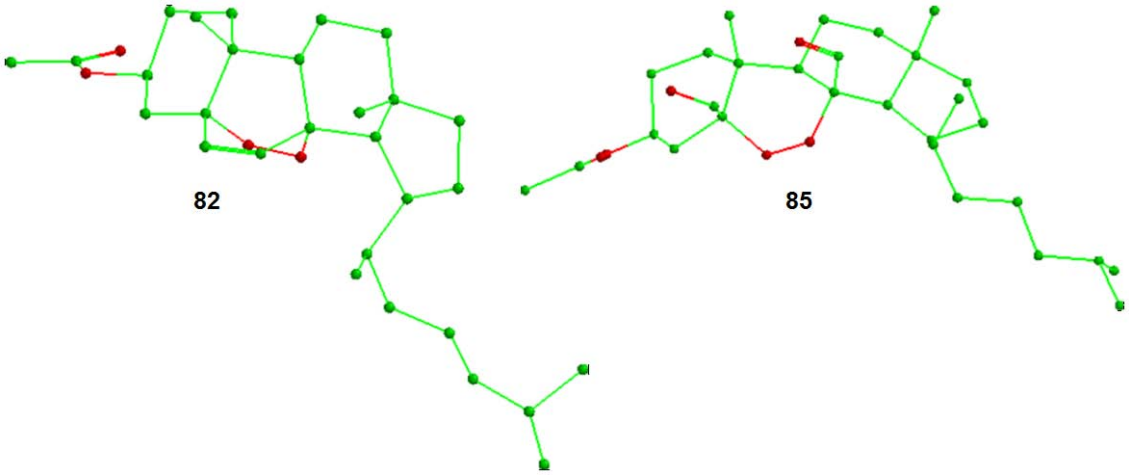

Figure 2: AM1 optimised structures for steroid dioxine **82** and dialdehyde **85**.

3.3 Ozonolysis and Protection of 1,2-Dioxines 3a, 3b and 3d.

3.3.1 Ozonolysis of 1,2-Dioxines 3a, 3b and 3d.

Dioxines **3a, b** and **d** gave the expected dialdehydes **128a, b** and **d** upon reaction with ozone followed by reduction with triphenylphosphine. Tedious column chromatography provided enough pure sample to characterise the dialdehydes by ^{1}H and ^{13}C NMR. *Table 3* shows the characteristic aldehyde peaks seen in both the ^{1}H and ^{13}C NMR spectra, along with the ^{13}C NMR signals seen for the carbons α to peroxide linkage, which provide evidence that the peroxide bond remained intact during the reaction.

Table 3: Crude Yield Estimates and Characteristic ^{1}H and ^{13}C NMR Peaks for Dialdehydes **128a**,**b**,**d**.

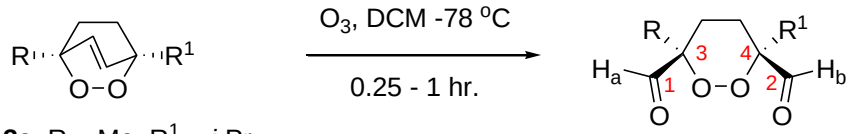

3a R = Me, R^1 = *i*-Pr
3b R = H, R^1 = Ph
3d R = R^1 = CH_2CO_2Me

128a,b,d

Dialdehyde	Yield (%)	δ H_a/H_b (ppm)	δ C_1/C_2 (ppm)	δ C_3/C_4 (ppm)
128a	77#	9.69 (s), 9.42 (s)	202.7, 199.1	89.1, 84.4
128b	33^	9.69 (d, *J* = 1.5 Hz), 9.61 (s)	197.7, 197.0	89.0, 84.7
128d*	64#	9.93 (s), 9.71 (s)	-	-

Crude estimates only.

^Isolated yield.

* Aldehyde signals for diester **128d** were taken from crude ^{1}H NMR spectra; ^{13}C NMR data was not obtained for this compound.

The crude yield estimates (seen in *Table 3*) for dialdehydes **128a** and **128d** are based on the crude reaction material after column chromatography in order to remove the PPh_3O by-product, although the dialdehyde products were still somewhat impure. Accurate yield determination proved difficult due to difficulties encountered in purification of the dialdehydes, along with their inherent instability. Several separations using different solvent systems were required to adequately separate the aldehydes from other byproducts. This process was tedious and resulted in further decomposition of the aldehydes along with loss of product and concomitantly lower yields. Almost immediately after the fractions were isolated by column chromatography, the products began to decompose, allowing only NMR spectra to be obtained from a small sample of pure product.

Separation by flash chromatography provided a small pure sample of dialdehyde **128a** which gave clean NMR spectra showing two distinctive aldehyde peaks. The ^{1}H NMR spectrum for **128a** is shown in *Figure 3* below.

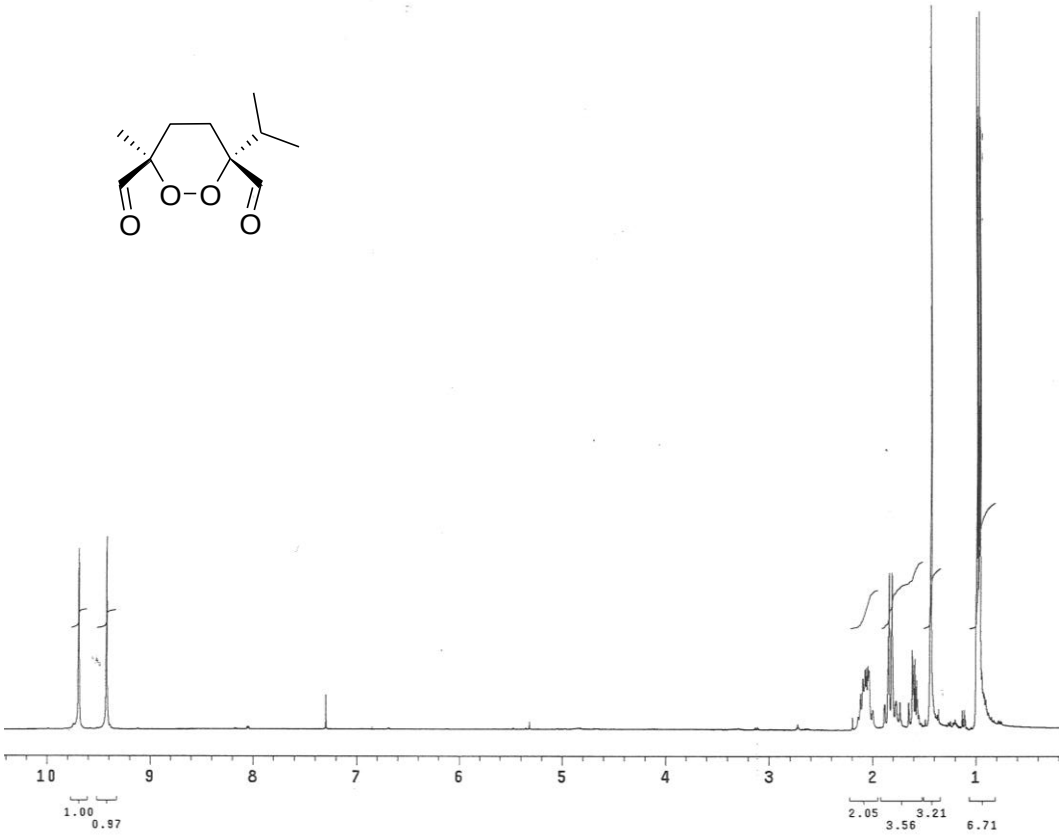

Figure 3: 300MHz ^{1}H NMR Spectra for dialdehyde **128a**.

It is also interesting to note the formation of diketone **20a**, which appeared in small quantities as a byproduct in all reaction mixtures for the ozonolysis of 1,2-dioxine **3a**. Accurate yield determination of **20a** proved difficult due to the product 'smearing' throughout the column upon attempted purification, making it difficult to quantify the amount formed, although based on recovered pure and impure fractions yields can be estimated to be between 2 – 15 %. The formation of diketone **20a** will be discussed in more detail later in this chapter.

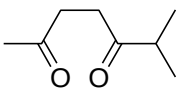

20a

Fairly pure ^{1}H and ^{13}C NMR spectra were obtained for phenyl-substituted dialdehyde **128b** from a sample isolated in 33% yield, with further purification efforts proving ineffective. However, this yield is not complete, as other impure fractions were obtained from the column as well, making the total yield higher. The ^{1}H NMR spectrum of **128b** showed splitting of J = 1.5 Hz on one of the aldehydes, which is likely due to long range coupling of H_b with its β-methylene protons.

Attempts to purify diester dialdehyde **128d** were unsuccessful, with the product appearing to decompose on the silica column. The crude ^{1}H NMR spectra showed the presence of two downfield aldehyde peaks, indicating that the ozonolysis reaction had been successful. The crude mixture was allowed to react immediately upon preparation with ylide **126** and purified as the stable Wittig product.

3.3.2 Protection of Dialdehydes 128a, 128b and 128d in Order to Improve Stability for Full Characterisation.

The Wittig reaction on the crude dialdehyde products **128a, b** and **d** was utilised in all three instances to furnish protected products **129a, b** and **d** (*Scheme 39*), in order to aid characterisation. The reactions were performed in dichloromethane, using 2 equivalents of ethyl 2-(triphenylphosphanylidene) acetate (**126**) (based upon the molar amount of dioxine initially used).

In the cases of the alkyl and phenyl substituted dioxines, **3a** and **3b** respectively, the ylide only added to one aldehyde moiety which was determined by 2D NMR to be the least hindered side of the molecule. Even though this left one aldehyde unprotected, both compounds were sufficiently stable to allow characterisation, confirming the structures (**129a** and **129b**) which in turn confirmed the preceding dialdehyde structures (**128a** and **128b**). The ylide added to both aldehydes of the diester dialdehyde **128d**, as expected since both aldehydes have equivalent steric congestion, giving the tetra-ester **129d**. *Table 4* shows the reaction yields over the three steps from dioxine **3a, b** and **d** to alkenes **129a, b** and **d**. It is worthy to note that within this thesis, the ozonolysis reaction is considered as a two-step reaction, even though it occurs as a 'one-pot' procedure. Two chemical processes are involved, ie formation of the ozonide and

subsequent reduction, both occurring *in-situ*, thus defining the reaction as a two-step process. Therefore, although the yields obtained for the formation of alkenes **129a**, **b** and **d** were low to moderate one must bear in mind that this is the total yield for a three-step process (ozonolysis, reduction and Wittig).

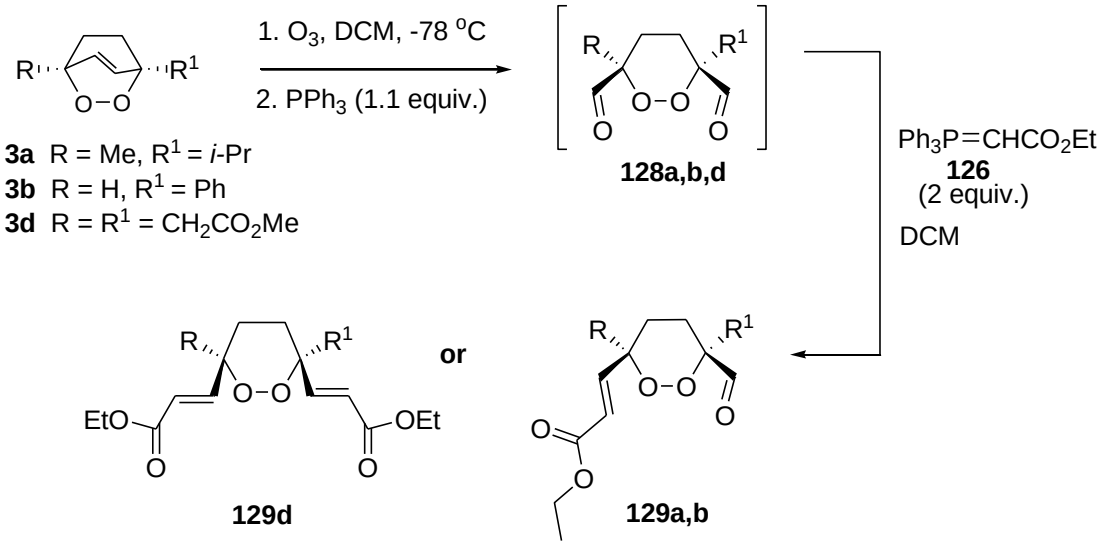

Scheme 39

Table 4: Yields for Ozonolysis and Wittig Addition Reactions on 1,2-Dioxines **3a**,**b**,**d**.

Dioxine	Alkene	Yield (%)
3a	**129a**	44
3b	**129b**	10
3d	**129d**	21

The alkene peaks of **129a** show coupling of J = 16.2 Hz, indicative of the expected E geometry. NoE correlations were seen between the aldehyde and *iso*-propyl methyl protons, along with HMBC correlations between the alkene carbon and methyl protons, as depicted in *Figure 4*. This coupling confirms that the ylide did indeed attack the least hindered side of molecule, as could be predicted.

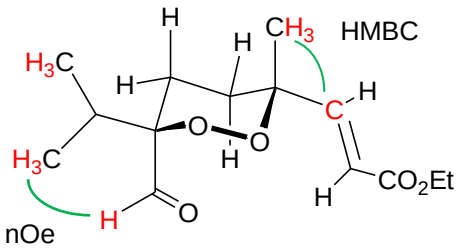

Figure 4: Chair conformation for aldehyde **129a**.

As mentioned above, the ^{1}H NMR spectra for dialdehyde **128b** showed long-range coupling for one of the aldehyde peaks. The ^{1}H NMR spectrum for the protected adduct **129b** also showed similar splitting (doublet at δ = 9.71 ppm, J = 2.1 Hz), indicative of long-range coupling between the aldehyde and methylene protons. The alkene peaks also show the expected *trans* coupling of J = 16.2 Hz. The yield for this reaction was low (10%), although crude TLC showed a complex mixture consisting of at least 8 spots, with the only isolable product being **129b**. The mass spectrum for **129b** showed the base peak at *m/z* = 261, which equates to a loss of 29 mass units. This is a strong indication of decarbonylation (- CHO) occurring immediately upon subjecting **129b** to the 'bombardment' of electrons in the mass spectrometer.

Standard proton and carbon NMR spectra of the tetra-ester **129d** acquired at ambient temperature showed broadened peaks for the alkene and methylene protons (shown in red, *Figure 5*). The ^{1}H NMR spectra at ambient temperature is shown in *Figure 6a* (page 47). This broadening is likely due to the two bulky methyl and ethyl ester groups fluctuating between the two chair conformations causing broadening of NMR signals. Upon raising the temperature to + 50 ^{o}C, the peaks in both the ^{1}H and ^{13}C NMR spectra sharpened, due to the increased energy applied to the system. *Figure 6b* (page 48) shows the ^{1}H NMR spectrum upon raising the tempetature to +50 ^{o}C, sharpened methylene protons can be seen along with the alkene peaks giving a coupling constant of J = 16.2 Hz, indicating the expected *trans*-geometry.

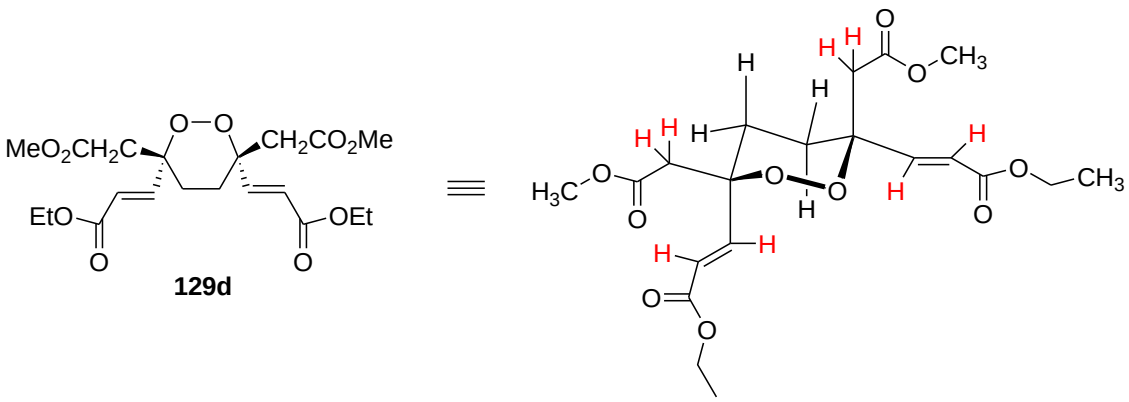

Figure 5: Chair conformation for tetra-ester **129d**

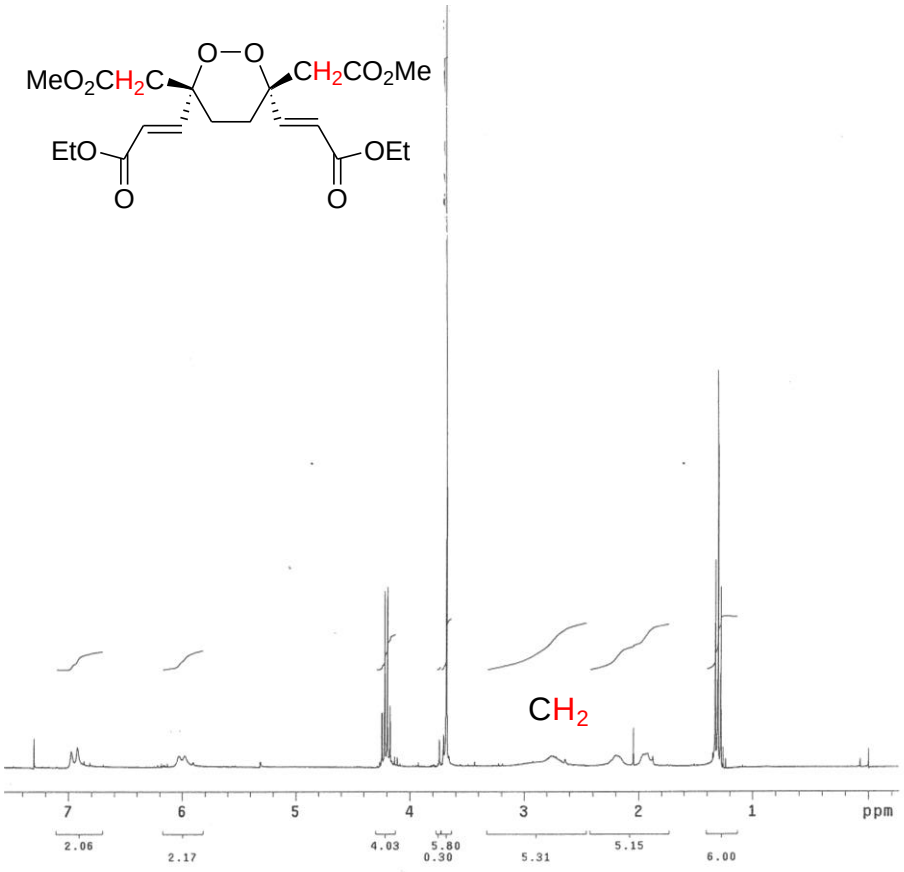

Figure 6a: 300 MHz ^{1}H NMR Spectrum of **129d** at ambient temperature.

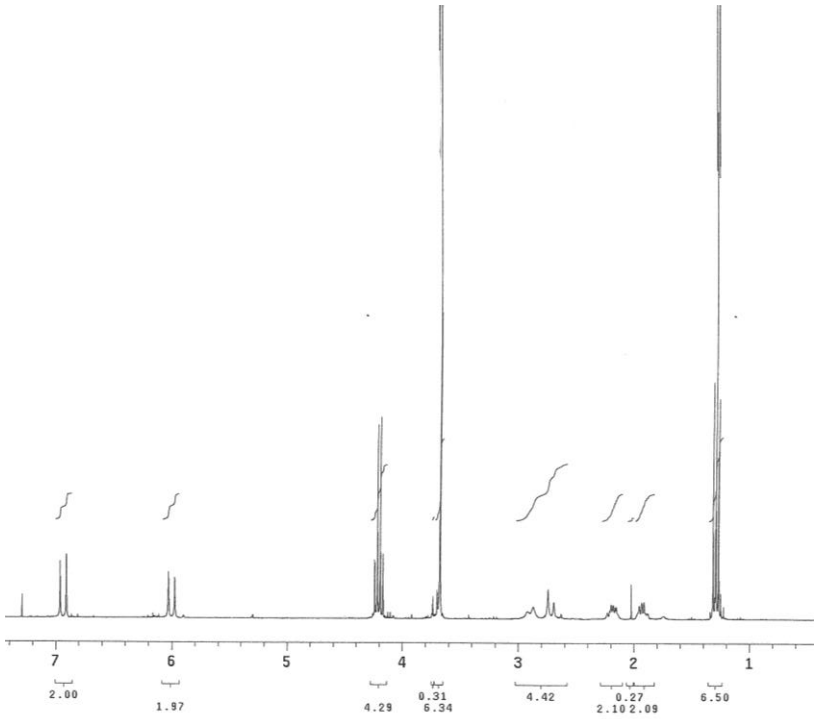

Figure 6b: 300 MHz ^{1}H NMR Spectrum of **129d** at + 50 ^{o}C.

A quick note on yields: As previously mentioned, yields were not fully optimised due to time restraints, and therefore were predominantly in the low to moderate range. Reacting the ozonolysis products crude resulted in large amounts of PPh_3O needing to be removed from the reaction mixture, which was formed as a by-product of both the ozonolysis reduction and Wittig reactions, along with any unreacted PPh_3. These products are notoriously difficult to remove from reaction mixtures, and are prone to streaking through the column,[65,93] contributing to the lowered isolated yields seen. Triturating the crude mixture with hexane, did partially alleviate the problem by separating out some of the desired products from the by-products, but it also left behind some of the desired product in amongst the crude by-product mixture, thereby lowering the yield obtained. It is also worth bearing in mind the complexity of this procedure and the highly reactive intermediates formed upon reacting 1,2-dioxines with ozone. The highly oxygenated intermediate species present ample opportunity for side reactions to occur, thereby contributing to a lowered yield. With these constraints in hand, we therefore consider the overall yields obtained within this work to be reasonable to excellent in retrospect.

In addition to protecting dialdehyde **128a** with an ylide to form alkene-ester **129a**, it was decided to also attempt a hydride reduction (with $LiAlH_4$) as an alternative 'trapping' technique for the aldehydes, as this proved successful for the steroid dialdehyde **85**. Ozonolysis was performed on dioxine **3a** to afford the crude dialdehyde **128a**, which was triturated with hexane to remove most of the PPh_3O by-product. The dialdehyde was treated with 3 equivalents of $LiAlH_4$, with crude TLC showing a complex mixture of products, which proved difficult to separate. Numerous solvent systems were trialled, although the products continuously coeluted off the column. Despite crude ^1H NMR spectra showing a mixture of products, it importantly showed the absence of any aldehyde peaks. It was decided to acetylate the crude mixture containing diol **130**, and isolate the subsequent products for characterisation. Diacetate **131** was subsequently isolated in moderate yield (32% over four steps from the dioxine), *Scheme 40*.

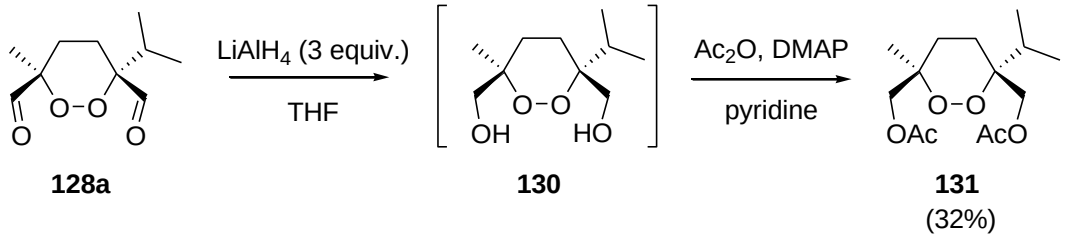

128a **130** **131** (32%)

Scheme 40

Broadened peaks were observed in the ^1H and ^{13}C NMR spectra of the diacetate **131** when acquired at ambient temperature. Upon lowering the temperature to - 50 ^oC the signals separated out into multiple peaks, likely due to 'freezing' out the conformers by lowering the interconversion rate. Increasing the temperature to + 50 ^oC saw a single set of sharp peaks. Distinctive acetate resonances were seen as singlets within the proton NMR sprectum at δ = 2.08 and 2.07 ppm, while the carbon NMR spectra showed the characteristic quaternary carbons α to the peroxide bond at δ = 82.74 and 78.8 ppm. It is worth noting that at both room temperature and refrigerator temperature (~ 4-5 ^oC), diacetate **131** existed as an oil, although upon freezing the sample crystallised out into a white crystalline solid. Multiple attempts were made to recrystallise the sample, although it continuously melted into an oil upon raising the temperature a few degrees above zero. The product therefore appears to be a low-melting crystalline solid.

Even though the desired diol was unable to be isolated in its own right, this sequence did show that the peroxide linkage remained untouched during the reduction, providing a further example of the peroxide bond remaining intact during the somewhat 'harsh' reducing conditions of $LiAlH_4$. These examples show chemoselectivity of the aldehydes, along with illustrating an alternative method for the protection of ozonolysis products, particularly if the aldehyde groupings are too hindered for reaction with a bulky ylide.

3.4 Ozonolysis of 1,2-Dioxines 3c and 3e.

As demonstrated from the above section, dioxines **3a**, **b** and **d** gave the expected dialdehydes upon treatment with ozone and subsequent reduction with triphenylphosphine. As anticipated, it was necessary to protect the resulting aldehydes in all three cases, to enable full structural elucidation. The ozonolysis of 1,2-dioxines **3c** and **3d** did not follow the same pathway as the other dioxines mentioned. The outcomes of these two reactions are discussed below.

Ozonolysis of the diphenyl substituted dioxine **3c** resulted in keto-aldehyde **132a** being formed. It was clearly evident from both ^{1}H and ^{13}C NMR spectra along with IR spectra that the expected symmetrical dialdehyde **128c** had not been formed, but rather a compound containing a ketone, aldehyde and alcohol functionalities. This indicated that the peroxide bond must have been fragmented to furnish **132a**, *Scheme 41*. Furthermore, since **132a** was a crystalline solid (Mp 82 - 84 ^{o}C), single crystal X-ray analysis was obtained, unambiguously confirming the structure and stereochemistry to be that of keto-aldehyde **132a**, *Figure 7*. Mass spectral data revealed a base peak at *m/z* 239, which is 29 units lower than the M^{+} peak. As seen previously, this is strong evidence that the aldehyde is decarbonylated readily upon being subjected to mass spectrometer conditions. A discussion of the mechanistic and theoretical aspects of how keto-aldehyde **132a** may have been formed will be presented later in this chapter.

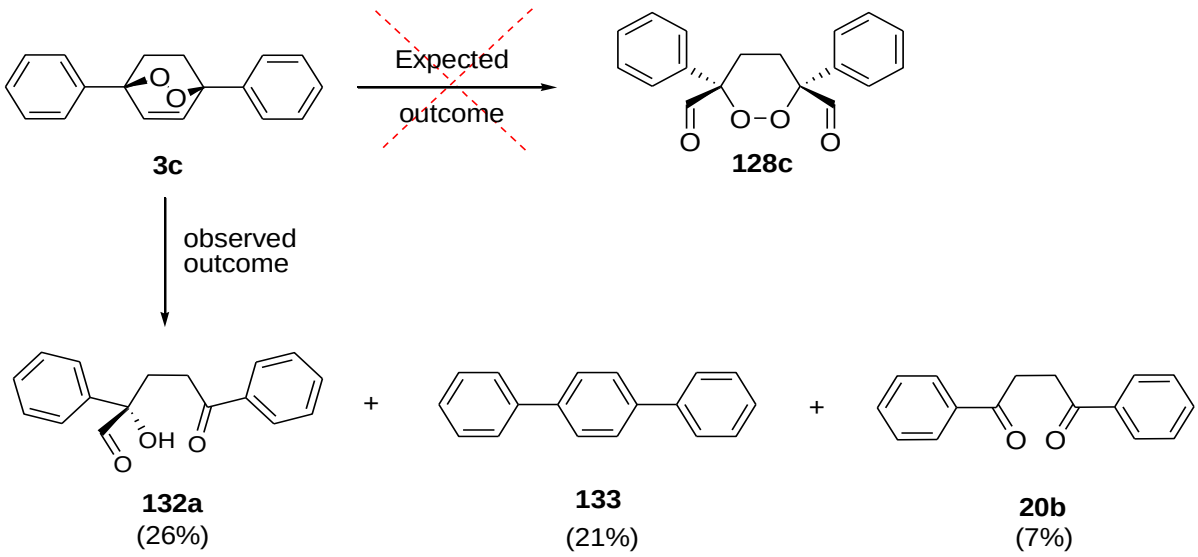

Scheme 41

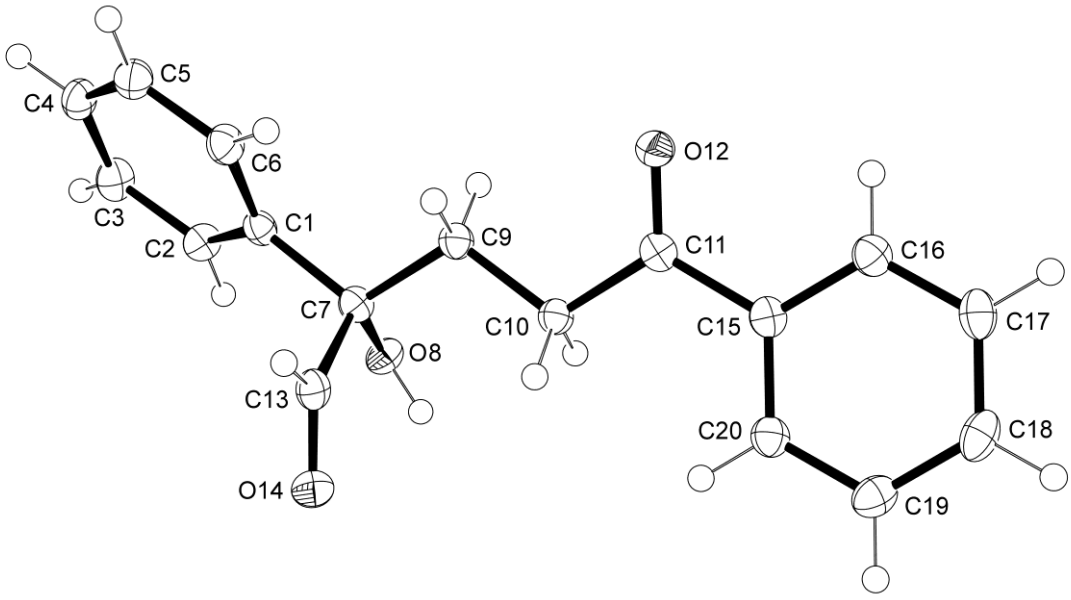

Figure 7: Crystal structure of keto-aldehyde **132a** showing the crystallographic numbering scheme employed.

Along with the keto-aldehyde **132a** (formed in 26% yield), two other products were isolated, namely terphenyl (**133**) (21%) and the diphenyl diketone **20b** (7%). Previously (page 43), we saw that the ozonolysis of ascaridole (**3a**) resulted in the formation of a similar diketone by-product, **20a**. The formation of these two dicarbonyl compounds

will be discussed later in this chapter. There is no precedence for the formation of terphenyl (**133**) under these circumstances, which raises the question of how was **133** formed? Does ozone on interaction with the alkene moiety of **3c** lower the transition state for the loss of singlet oxygen (to yield diene **6c**) followed by aerial oxidation (*Scheme 42, Pathway A*), or perhaps ozone assists in the deoxygenation of the dioxine by removal of the proton β to the peroxide linkage (*Scheme 42, Pathway B*), or was **133** formed *via* another intermediate species that ruptured the peroxide linkage causing a loss of oxygen along with concomitant rearomatisation, (*Scheme 42, Pathway C*). Whilst the formation of **133** is of interest, further investigation into the mechanisms involved in its formation is beyond the scope of this thesis.

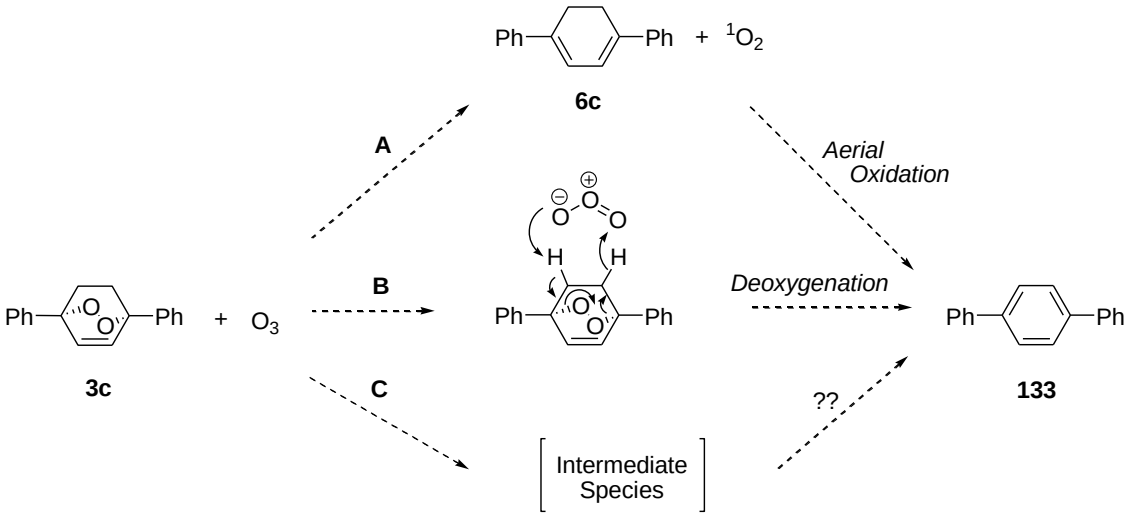

Scheme 42

It was a considered that dialdehyde **128c** may not have formed due to the presence of two bulky phenyl groups α to the alkene thereby inhibiting the triphenylphosphine from being able to reduce the subsequent ozonide, thereby leading the ozonide to decompose directly into keto-aldehyde **132a**. This theory was tested by reducing the ozonolysis products with dimethyl sulphide (1.1 equiv.) in order to see whether the same products were formed upon using a smaller reducing agent. Indeed, the same products did form in similar yields and ratios, eliminating the possibility that the bulkiness of the triphenylphosphine and phenyl groups of the 1,2-dioxines may have caused these unexpected results.

Purification of the products formed *via* the ozonolysis and subsequent triphenylphosphine reduction of diester dioxine **3e** proved difficult, with multiple attempts being made to separate and purify the crude products, with little success. Numerous solvent systems were trialled, but separation of the products failed, with products continuously coeluting off the column and/or decomposing. As discussed previously, this same problem occurred upon attempted purification of the ozonolysis products of diester dioxine **3d**. The crude ^{1}H NMR spectrum of the products formed from the ozonolysis of **3e** showed two distinct aldehyde peaks as singlets at δ = 9.60 and 9.58 ppm, integrating in a 1 : 1 ratio. This indicates that the dialdehydes were likely present within the crude mixture. It was decided to react the crude mixture with ylide **126** to attempt isolation and identification of the stabilised products, *Scheme 43*.

Upon adding 2 equivalents of ylide **126**, three products were formed, which were readily separable *via* flash chromatography. The purified products were initially named 'Products A, B and C', in relation to the order in which they eluted off the column. It was immediately recognisable from NMR spectra that product C was symmetrical, and the other two were not. 2D NMR spectra along with accurate mass and IR spectra determined the structures to be that of **134**, **135**, and **136**, for products A, B and C, respectively, totalling 53% yield over three steps (ozonolysis, reduction and subsequent Wittig protection), *Scheme 43*. The individual characterisation of the three products will be discussed below.

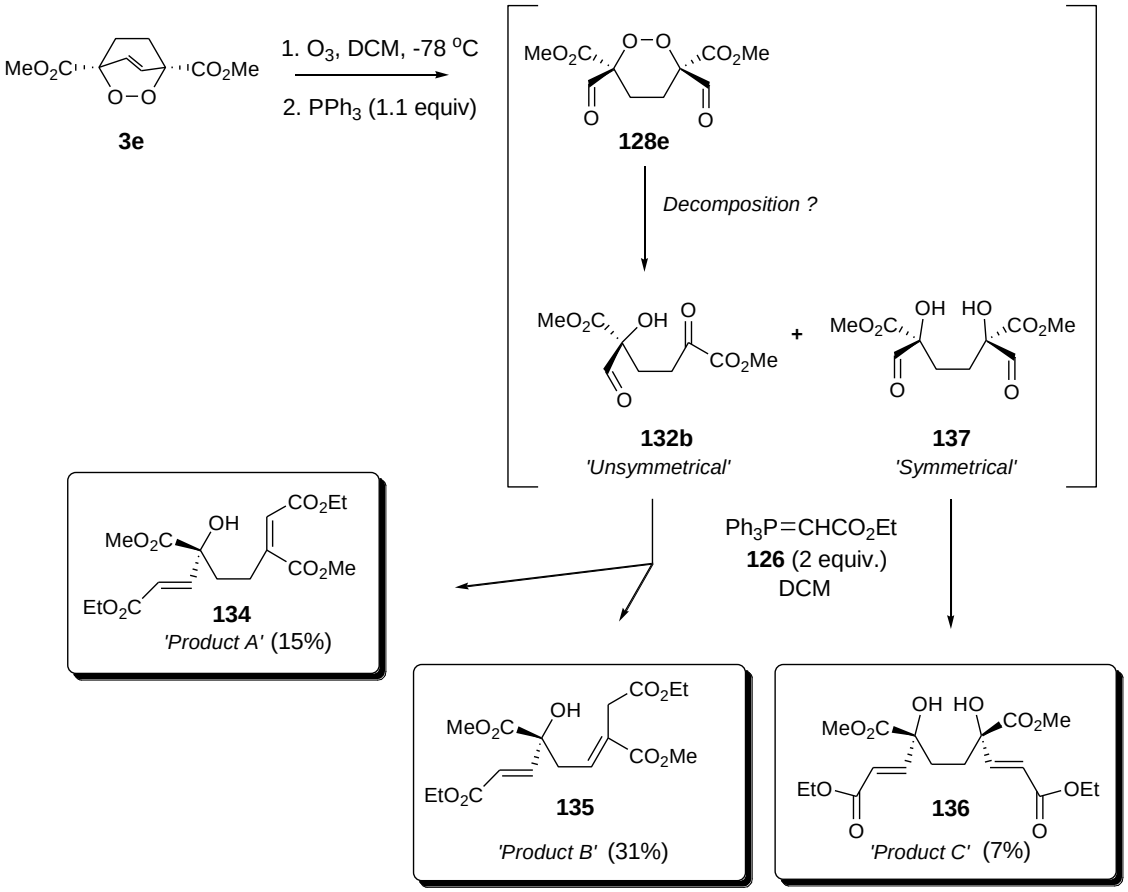

Scheme 43

Product A, determined to be **134**, showed a large hydroxyl absorption in the IR spectrum, although the hydroxyl proton was not visible in the ^{1}H NMR spectrum. The disubstituted alkene protons showed coupling of J = 15.3 Hz in the ^{1}H NMR, indicative of *E* geometry. COSY correlations (along with proton NMR coupling) showed that structurally, the two CH_2 groups sat next to each other (unlike product B, where they were separated by an alkene moiety). The single alkene proton from the trisubstituted alkene resonated as a singlet at δ = 6.77 ppm in the ^{1}H NMR sprctrum. This proton could potentially sit as either *E* or *Z* relative to the main backbone. *Figure 8* shows an nOe correlation between this alkene proton and the γ-CH_2 protons indicating that the geometry must be *Z*, as this γ-coupling would not be seen if the proton was sitting in *E* geometry.

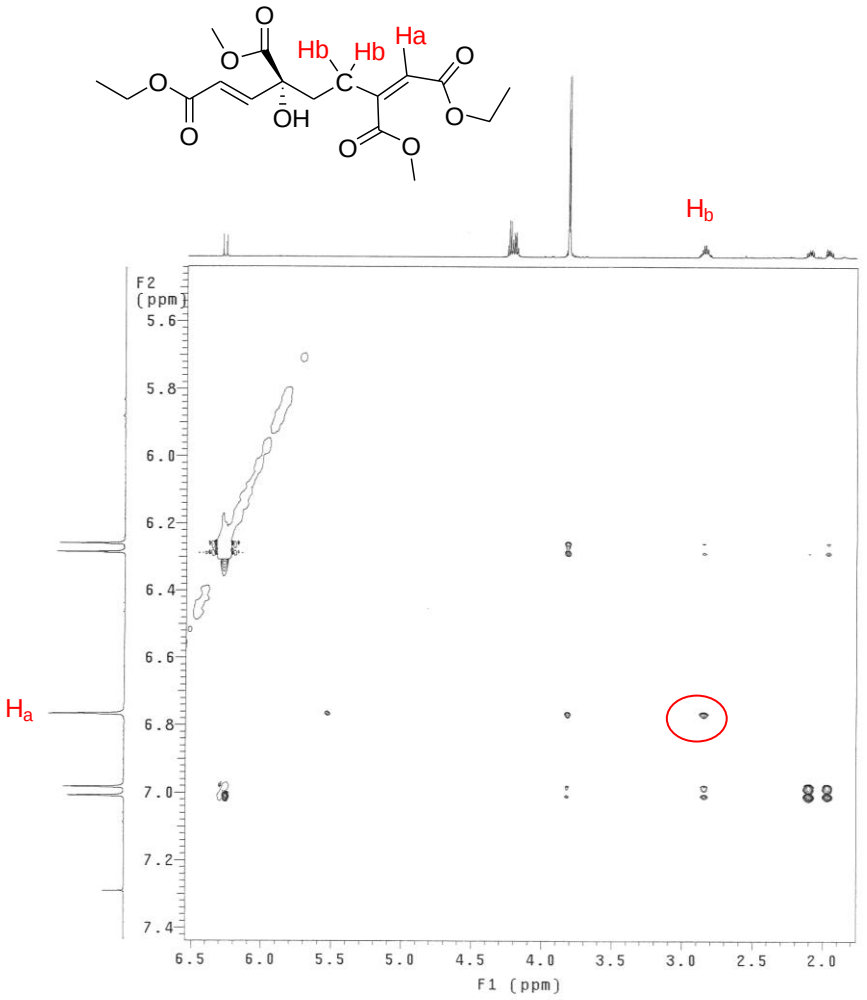

Figure 8: ROESY spectrum of **134** ('Product A').

The two potential geometries of **134** can be seen in *Figure 9*, showing how the nOe correlation could only be seen in the *E*, *Z* geometry.

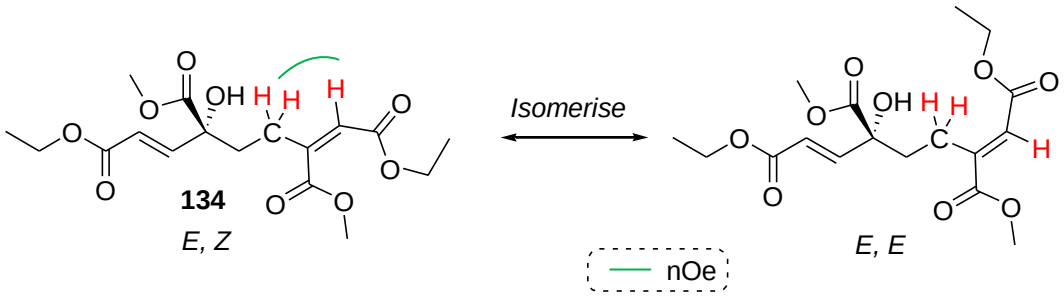

Figure 9: nOe correlations for **134** (Product 'A').

Product B was determined to be **135**. The ^{1}H NMR spectrum, as seen in *Figure 10*, shows proton coupling of J = 15.6 Hz on the disubstituted alkene, indicating *E* geometry. The proton on the trisubstituted alkene appeares as a triplet at δ = 5.83 ppm with coupling of J = 1.5 Hz, indicating that it is coupled to a CH_2 group. The singlet seen at δ = 3.51 ppm was identified as being the hydroxyl proton due to disappearance upon addition of a drop of D_2O into the NMR tube.

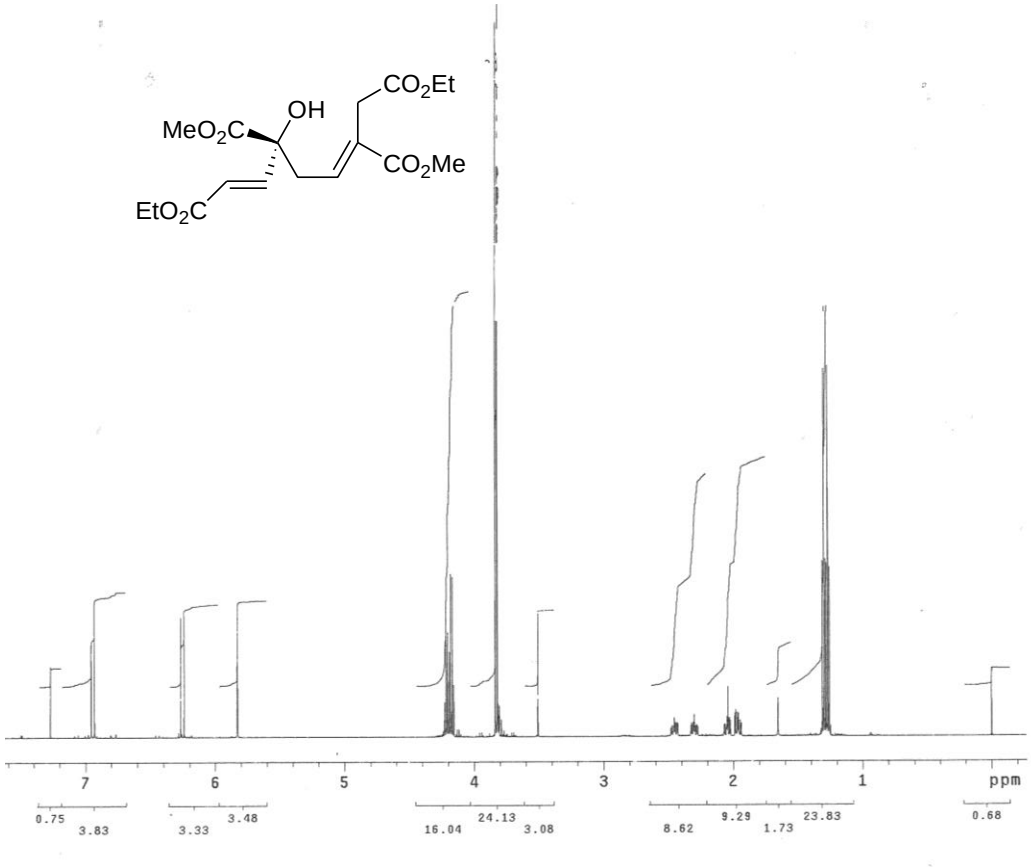

Figure 10: 600 MHz ^{1}H NMR spectrum of **135** ('Product B').

As can be seen in *Figure 11*, products A and B are structural isomers, occurring in an approximately 1 : 2 ratio (A : B). Product A, **134**, is the expected product upon aldehyde protection of the 'unsymmetrical' keto-aldehyde **132b** with ylide **126**, whereas in product B, **135**, the alkene has migrated so that it is no longer in conjugation with both ester groups. Products A and B were both subjected to heat and acidic conditions in order to facilitate isomerisation between the two products, but no change

was seen (*Table 5*), indicating that the two isomers are stable but are not easily interconvertible under conventional conditions.

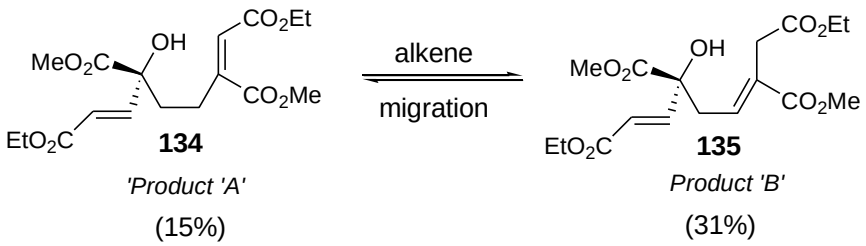

Figure 11: Migration of product A, **134**, to product B, **135**.

Table 5: Conditions used for Isomerisation of **134** and **135**.

Product		Conditions	Result
'A'	**134**	Heat[1]	No Reaction
		PTSA[2] + Heat[1]	No Reaction
'B'	**135**	Heat[1]	No Reaction
		PTSA[2] + Heat[1]	No Reaction

[1] temperature maintained at 60 °C.

[2] Catalytic amount of PTSA added.

The symmetrical product 'C' was identified as **136**. Both ^{1}H and ^{13}C NMR spectra show a symmetrical product, with half the number of peaks confirmed to be within the structure, as can be seen for the ^{13}C spectrum in *Figure 12*. The peroxide bond was directly cleaved during the course of reaction, although no further fragmentation or rearrangements were seen, indicating that the two aldehydes were likely to have been subsequently trapped to give the symmetrical tetra-ester **136**. The reaction yield for **136**, was quite low (7%) making this only a minor byproduct compared to Products A and B (**134** and **135**), which were formed in 15% and 31% yields respectively. *Table 6* shows the characteristic nOe and HMBC correlations for **136** (shown for half the molecule only).

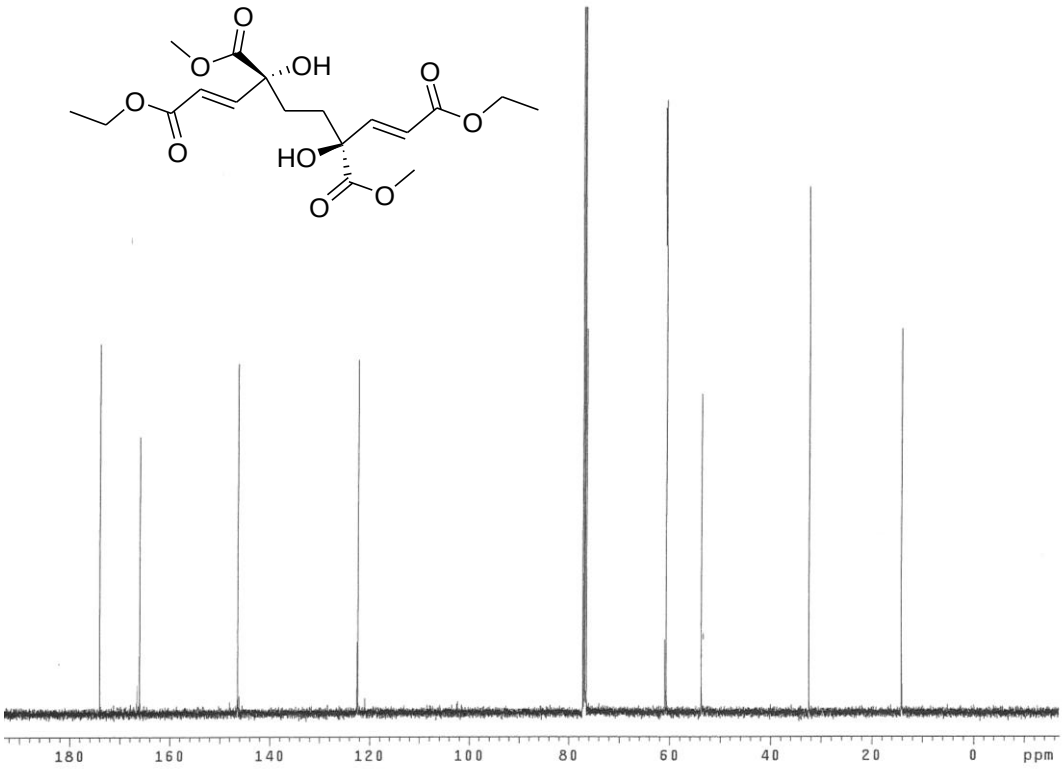

Figure 12: 600 MHz ^{13}C NMR spectrum for **136** ('Product C').

Table 6: nOe and HMBC Correlations for **136** (Product 'C').

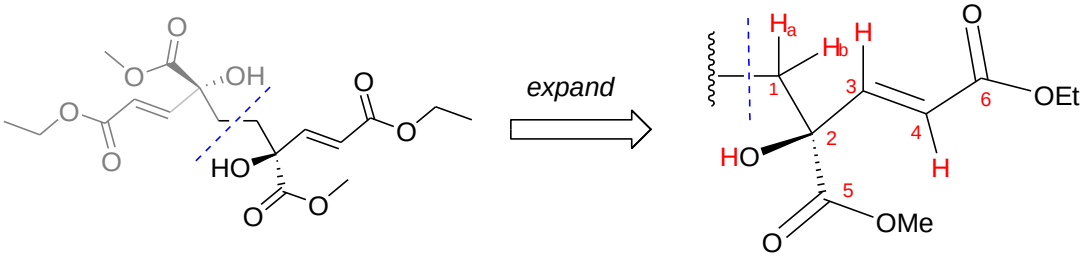

600 MHz ^{1}H NMR δ(ppm) = H_a 1.95 (dd, 2H, *J* = 13.8, 4.8 Hz)
H_b 1.72 (dd, 2H, *J* = 13.8, 4.8 Hz)

nOe	OH	↔	$H_{1(a)}$ & $H_{1(b)}$
	H_3	↔	$H_{1(a)}$ & $H_{1(b)}$
HMBC	C_2	↔	$H_{1(a)}$, $H_{1(b)}$ & H_4
	C_3	↔	$H_{1(a)}$
	C_5	↔	$H_{1(b)}$
	C_6	↔	H_3 & H_4

As mentioned, the direct ozonolysis products of the diester dioxine **3e** were unable to be isolated, although the three products resulting from the Wittig reaction appear to have come from the 'unsymmetrical' keto-aldehyde **132b** and 'symmetrical' dialdehyde **137**, as seen in *Scheme 43*, in a ratio of approximately 6.5 : 1 respectively, (ie (31 + 15) : 7).

The results discussed so far raise the question of why some of the dioxines behaved as expected (**3a**, **d** and **e**), and others deviated from this (**3e** and **c**), and how mechanistically these rearrangements occurred. A short investigation to extend upon the ozonolysis work already conducted was undertaken, in a bid to further understand these different outcomes. It was decided to subject one dioxine that underwent rearrangement upon standard ozonolysis (diester dioxine **3e**) and one dioxine that gave the expected results (ascaridole **3a**) to an ozonolysis reaction utilising different conditions. It was hoped that by performing this additional set of experiments it would provide some additional insight into the mechanics of these rearrangements, particularly as to whether or not incomplete reduction of the ozonides was responsible for these rearrangements, and whether similar rearrangements would be observed when only one aldehyde is produced.

3.5 Unsymmetrical Ozonolysis of Dioxines 3a and 3e.

One way to test the mechanistic question of whether these rearrangements were occurring *via* direct decomposition of the ozonide (and therefore not actually forming the dialdehydes at all) or *via* another method, and also to address the idea that the rearrangements may be occurring due to the nature of the bridgehead substitution was to investigate the ozonolysis reaction under a different set of conditions commonly known as, and referred to within this thesis as 'unsymmetrical ozonolysis'.

The readily accepted Criegee mechanism was discussed in Chapter 1, and again at the beginning of this chapter with its mechanism involving the formation of a primary ozonide **48**, and decomposition into carbonyl **49** and carbonyl oxide **50**, which then recombine to produce ozonide **51** (*Scheme 16*). This ozonide can then decompose into a variety of functional products (*Scheme 18*), usually resulting in both functional groups being the same (eg dialdehyde).

Unsymmetrical ozonolysis was first reported by Schreiber *et al.* in 1982,[128] and as its name suggests results in two different functional groups being produced from the oxidative cleavage of the alkene, in this case, namely an aldehyde and an ester. This is done by using a protic solvent (unhindered alcohol) which results in cleavage of the molozonide **139** in an unsymmetrical fashion to produce a carbonyl and carbonyl oxide **140**, *Scheme 44*. The alcohol then traps the carbonyl oxide to produce the hydroperoxy acetal **141**, which is subsequently dehydrated to form an ester, **142**.[128,129] As can be seen in *Scheme 44*, when two different substituents are present, cleavage of the primary ozonide **139** can occur in two different directions, resulting in the formation of two regioisomers **140a** and **140b**. The direction of cleavage favoured is often dependent on the nature of the substituents, with electronic and steric effects known to play a part,[129-131] although it is beyond the scope of this research to detail this. A key aspect of this reaction worth noting is that no ozonide is formed (in contrast to 'standard' ozonolysis), making this reaction a good way to investigate whether similar results are observed for dioxines **3a** and **e** under conditions where no ozonide is formed, thus eliminating the ozonide as a possible cause of the rearrangements seen.

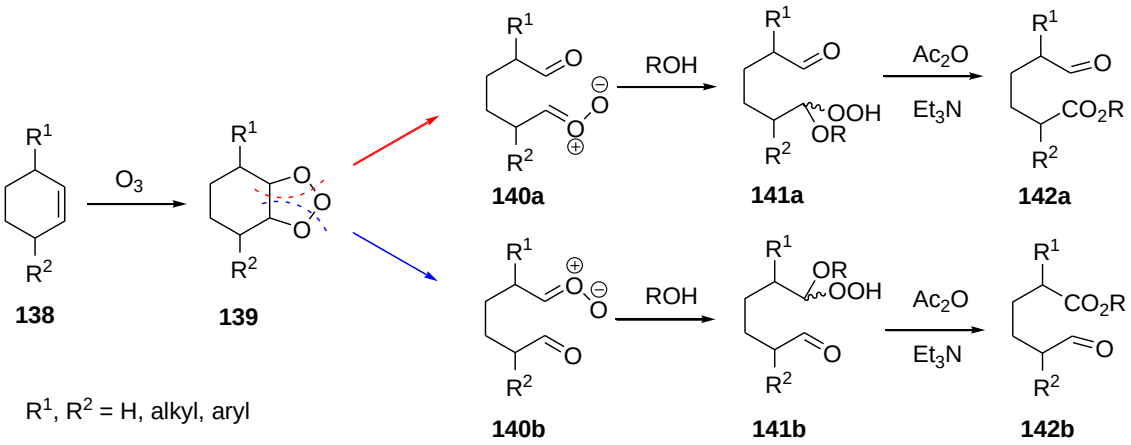

Scheme 44

As discussed in Chapter 1, there are only a handful of examples within the literature whereby ozonolysis has been performed on alkene systems incorporating a dioxine functionality. To the best of our knowledge, this unsymmetrical ozonolysis reaction has not been previously reported on a dioxine (either monocyclic or bicylic) before, making

the reactions reported below the first reported examples of unsymmetrical ozonolysis being performed on alkene systems within 1,2-dioxines.

Scheme 45 below depicts what we expect to occur for the unsymmetrical ozonolysis of bicyclic 1,2-dioxines of type **3**. The final product is expected to be a dioxine incorporating aldehyde-ester functionalities, **144**. If the two substituents (R and R^1) are different, two regioisomers will be possible.

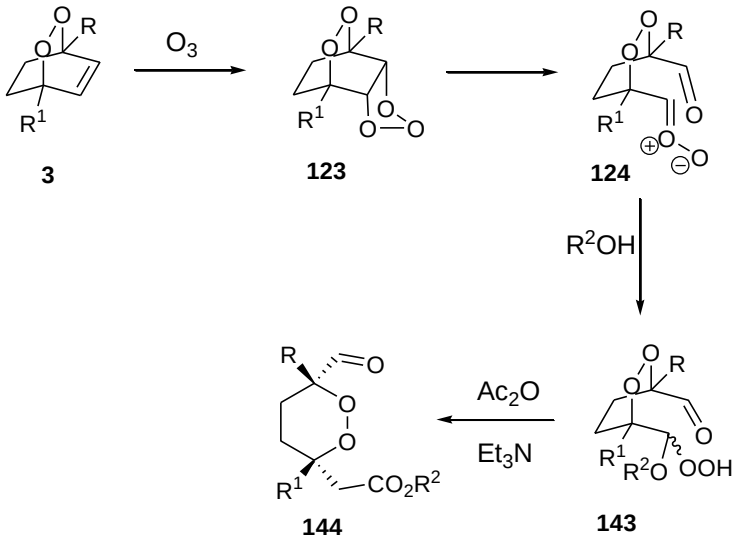

Scheme 45

Ascaridole (**3a**) gave the 'expected' dialdehyde **128a** under standard ozonolysis conditions. Upon being exposed to unsymmetrical ozonolysis conditions, **3a** yielded the 'expected' ester-aldehydes. Being an unsymmetrical dioxine, there was the potential for two possible regioisomers to be formed, **145a** and **145b**, and as can be seen in *Scheme 46*, little selectivity was seen. The two isomers were easily separable *via* flash chromatography and were initially labelled as 'Isomer 1' and 'Isomer 2' in reference to their elution order off the column. 2D NMR was utilised to aid in identification of each isomer. Diketone **20a**, which was seen as a byproduct in the standard ozonolysis of ascaridole (**3a**), was also observed under these unsymmetrical conditions, in 21% yield. A discussion on the formation of this product is reserved for later in this chapter.

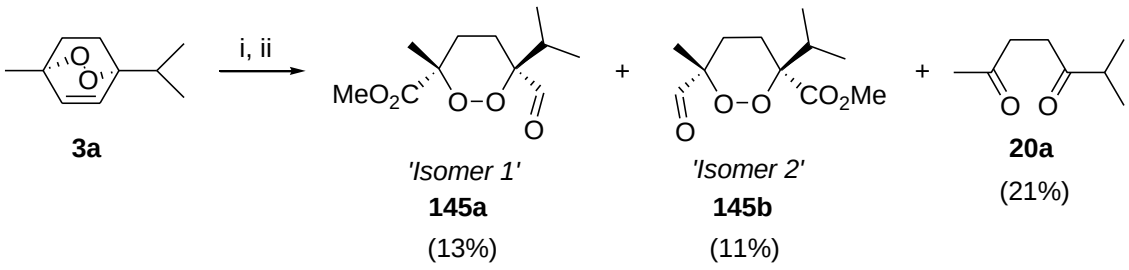

'Isomer 1' **145a** (13%) + *'Isomer 2'* **145b** (11%) +

(i) O_3, DCM : MeOH (5 : 1), -78 ^{o}C; (ii) NEt_3, Ac_2O

Scheme 46

HMBC correlations were used to aid in the identification of Isomers 1 and 2. Clear correlations were seen for Isomer 1, between the carbonyl carbon and the methyl protons α to the peroxide bond, thereby identifying this isomer as product **145a**, *Figure 13a*. In contrast, Isomer 2 showed a HMBC correlation between the aldehyde carbon and methyl protons, confirming its structure as being **146b**, *Figure 13b*.

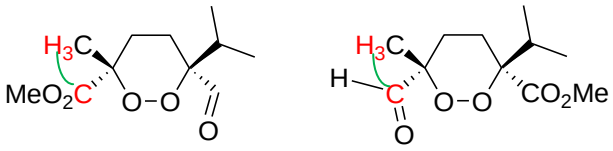

(a) (b)

Figure 13: HMBC correlations for (a) **145a** ('Isomer 1') and (b) **145b** ('Isomer 2').

In addition to this, Isomer 1 was crystalline, which allowed single crystal X-ray analysis to be obtained, with unambiguous confirmation of the structure and stereochemistry of **145a**, *Figure 14*. It can be seen from the crystal structure of **145a** that the ester and *iso*-propyl groups are both sitting equatorial, as expected. In contrast to the crystalline isomer **145a**, Isomer 2, **145b**, was an oil, which showed early signs of decomposition thereby making its purification difficult. The reason for this may be due to the *iso*-propyl flanking the aldehyde in Isomer 1, thereby creating a shielding effect aiding in the protection and hinderance of its decomposition, whereas Isomer 2's aldehyde is adjacent to the small methyl group, which would have no such effect, thereby leaving the aldehyde open to premature decomposition.

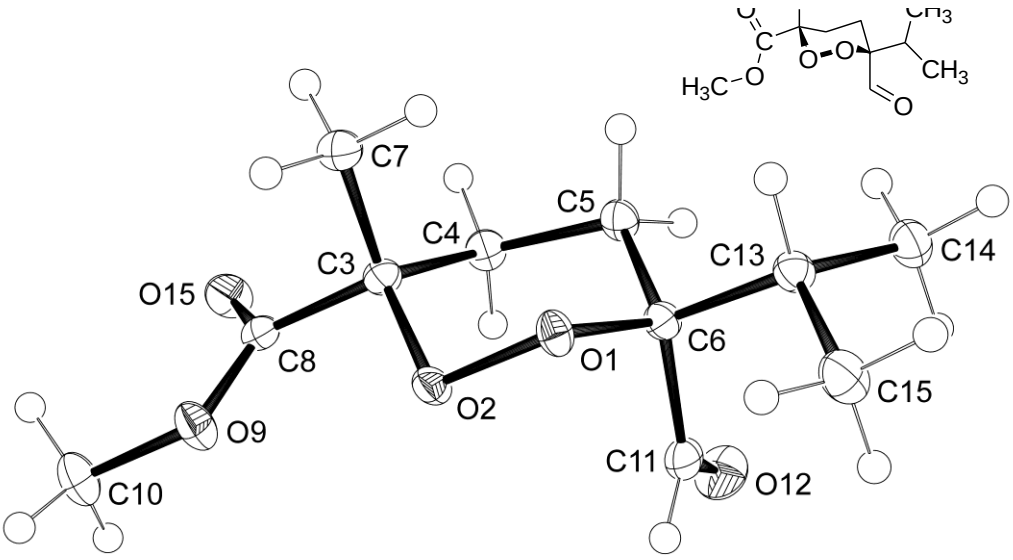

Figure 14: Crystal structure of 'Isomer 1' aldehyde-ester **145a** showing the crystallographic numbering scheme employed.

The meso-diester dioxine **3e** which underwent standard ozonolysis and reduction with triphenylphosphine followed by Wittig protection to give three ring-opened products **134**, **135** and **136** (*Scheme 43*) was subjected to the unsymmetrical ozonolysis to see if it would undergo a similar rearrangement to yield tri-ester aldehyde **146**, *Scheme 47*.

Only one major product was isolated upon treating **3e** to the unsymmetrical ozonolysis conditions. ^{1}H and NMR data from the purified product clearly shows three singlet peaks at δ = 3.84, 3.82 and 3.80 ppm indicating three methyl ester protons, likewise the ^{13}C showed three carbonyl peaks at δ = 169.4, 169.4 and 168.4 ppm indicating the three carbonyls from the esters. This showed the three expected esters were present, but it was immediately evident through the lack of an aldehyde peak in the NMR spectra that the theoretically expected tri-ester aldehyde **146** had not been formed. It was anticipated that a similar ring-opening rearrangement previously seen for the diester dioxine may have occurred, giving structure **147**, although the absence of a further downfield ketone peak needed in the ^{13}C NMR dismissed the product being that of **147**. Two carbon peaks seen at 104.1 and 87.3 ppm suggested two quaternary carbons of a furan α to an alcohol and diester, respectively, suggesting furan **148**. It is likely that the furan **148** is in equilibrium with the ketol **147** (*Scheme 47*). 2D NMR experiments support structure

148, which is a racemic mixture, due to the ring-opened alcohol attacking the ketone in **147** to give furan **148** equally from both faces.

.

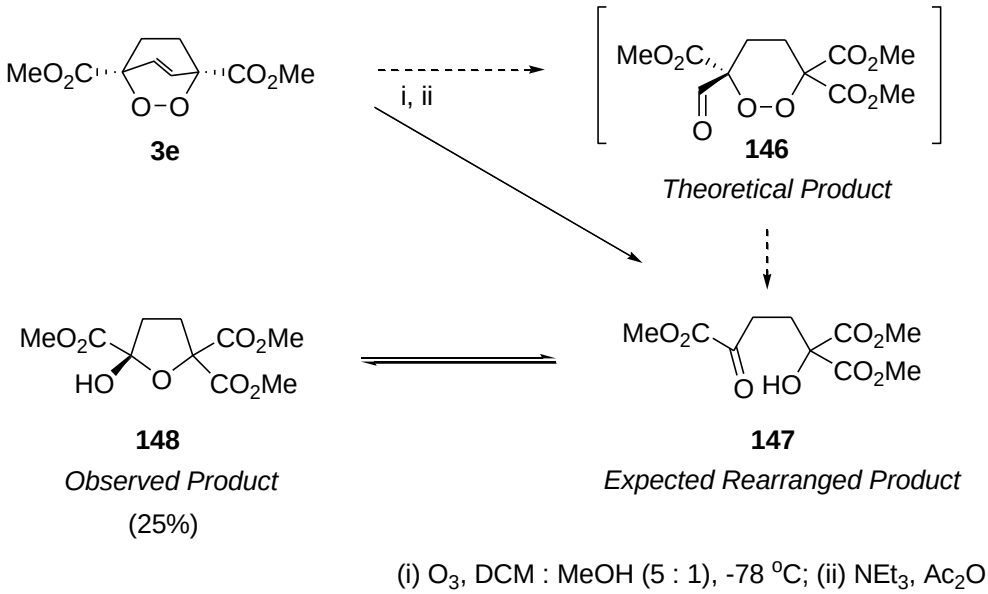

Scheme 47

The hydroxyl peak is seen as a singlet resonating at 4.26 ppm in the ^{1}H spectrum, and is also seen as a large band within the IR spectrum at 3471 cm^{-1}. The molecular ion of **148** was not detected in the high resolution mass spectromertry, but a mass of 245.2066 was identified, with a molecular formula equating to M – OH; this is likely due to the hydroxyl group being immediately lost in the mass spectrometer, leaving behind the daughter fragment.

3.6 Formation of Diketone Products 20a and 20b.

The formation of two different diketone products was observed within this body of work. **20a** was seen in both the standard and unsymmetrical ozonolysis of ascaridole (**3a**), whilst **20b** was formed during the standard ozonolysis of diphenyl-1,2-dioxine **3c**, *Table 7*. The respective 1,4-dicarbonyls of this nature were not observed in the ozonolysis of the other 1,2-dioxines (**3c**, **d** or **e**) used within this study, although this is not to say that they were not indeed formed in small quantities, as the ozonolysis products typically involved a complex mixture of unidentifiable products.

Table 7: Formation of 1,4-Dicarbonyls **20a** and **20b**.

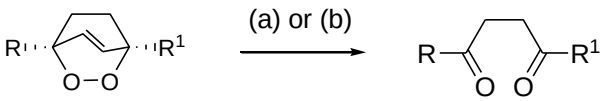

3a R = Me, R^1 = *i*-Pr
3c R = R^1 = Ph

20a R = Me, R^1 = *i*-Pr
20b R = R^1 = Ph

(a) 1. O_3, DCM, -78 ^oC 2. PPh_3 (1.1 equiv.)
(b) 1. O_3, DCM : MeOH (5 : 1), -78 ^oC 2. NEt_3, Ac_2O

	Yield (%)	
Diketone	**Symmetrical (a)**	**Unsymmetrical (b)**
20a	~2-15*	21
20b	7	-

* approximate, based on impure fractions, see discussion.

1,4-Dicarbonyls of this type have recently been reported by the Taylor group, and were found to be the result of thermal decomposition of diols **149a-g**, *Scheme 48*.[60] This radical process involved the homolytic cleavage of the peroxide followed by subsequent double *β*-scission to afford dicarbonyls **20a-g**.

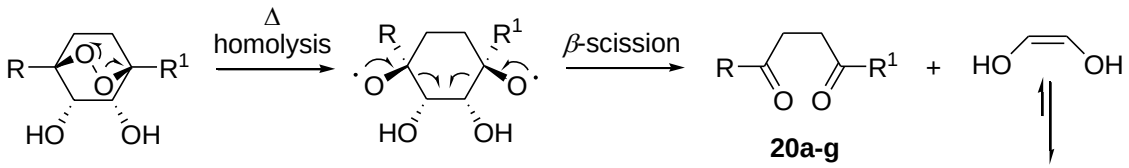

149a R = Me R^1 = *i*-Pr
149b R = R^1 = Ph
149c R = Ph, R^1 = H
149d R= R^1 = Me
149e R = Me, R^1 = $CH_2CH_2CO_2Me$
149f R = R^1 = CH_2CO_2Me
149g R = R^1 = *p*-F-Ph

Scheme 48

It is not clear how diketones **20a** and **b** were formed in this instance, although it is unlikely that their formation resulted from this same mechanistic process, due to the absence of either heat or light, thereby limiting the ability for a radical process to occur.

As mentioned in Chapter 1, Adam *et al.*[117] reported on the ozonolysis of endoperoxide **98** in the presence of tetracyanoethylene to give ketone **99**, which was unstable and readily decarbonylated at -10 ^{o}C to give succinaldehyde (**100**) (*Scheme 29*). Limited details of the decarbonylation were given aside from the authors reporting that **99** decarbonylates with 'emission of light' therefore implying that it can be regarded as an 'energy reservoir'. The formation of 1,4-dicarbonyls resulting from the Kornblum-DeLaMare rearrangement was also discussed in Chapter 1, and have previously been reported by the Taylor group as cyclopropanation by-products formed under basic conditions.[37]

As it can be seen, 1,4-dicarbonyls of this nature have previously been seen as by-products in 1,2-dioxine chemistry.[37,60,117] Reaction conditions common to both symmetrical and unsymmetrical ozonolysis was the use of base, namely triphenyl phosphine or triethylamine, respectively. It is difficult to postulate how by-products, **20a** and **b** were formed in this instance, as there are several potential mechanistic pathways possible, including breakdown of either dioxine-dialdehyde **128a** or **128c** or dioxine-ester **145**, or alternatively and probably more likely, *via* the decomposition of molozonide intermediate **123**, as summarised in *Scheme 49*. Whilst their formation is of synthetic and mechanistic interest, a more detailed investigation was beyond the scope of this work.

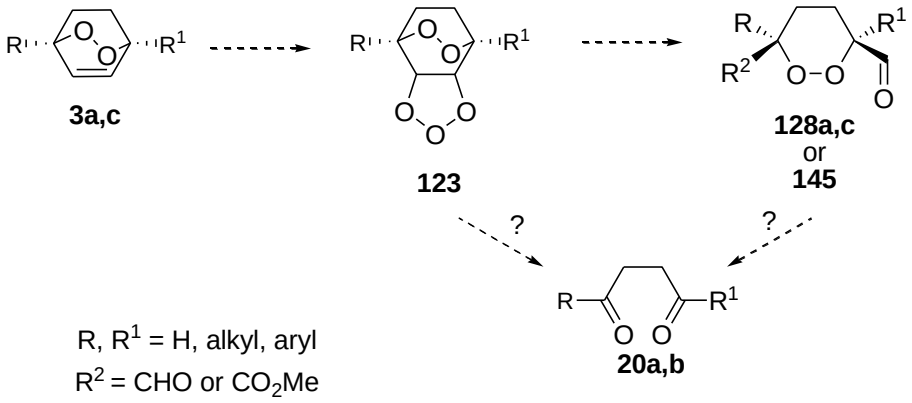

Scheme 49

3.7 Mechanistic Considerations.

As we have seen, two different pathways were observed upon the ozonolysis of the disubstituted 1,2-dioxines, one pathway saw the 'expected' results, whilst the other saw the unexpected cleavage of the peroxide linkage along with loss of either CO or CO_2 (depending on the proposed mechanism). A second set of experiments performed in order to try and shed light into these rearrangements, saw the same two pathways observed. A general summary of these outcomes is shown in *Scheme 50* and *Table 8*.

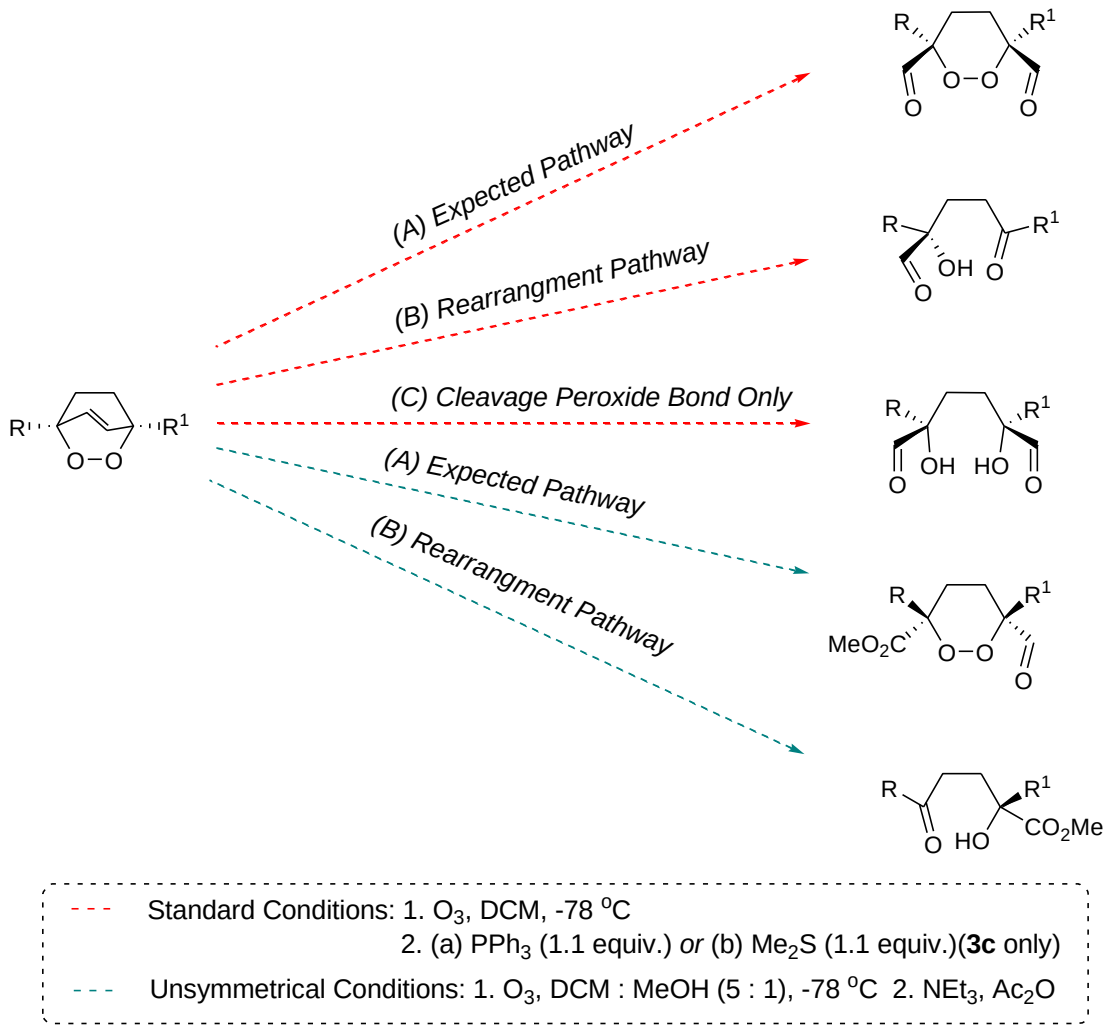

Scheme 50

Table 8: Summary of Ozonolysis Reactions on Dioxines **3a-e**.

Dioxine	R	R^1	Conditions*	Rearranged
3a	Me	*i*-Pr	i(a)	No
3a	Me	*i*-Pr	ii	No
3b	H	Ph	i(a)	No
3c	Ph	Ph	i(a)	Yes
3c	Ph	Ph	i(b)	Yes
3d	CH_2CO_2Me	CH_2CO_2Me	i(a)	No
3e	CO_2Me	CO_2Me	i(a)	Yes
3e	CO_2Me	CO_2Me	ii	Yes

* (i) = standard, (a) = PPh_3 reduction, (b) = Me_2S reduction; (ii) = unsymmetrical

Two important questions arise from these results; firstly why did some of the 1,2-dioxines behave in a manner that yielded the expected results, whilst others rearranged under the same conditions, and secondly how, mechanistically, did these rearrangements occur?

It is apparent that the nature of the substituents must be influencing the reaction outcome, due to experiments conducted showing that the alkyl substituted 1,2-dioxine (ascaridole, **3a**) did not rearrange under either standard or unsymmetrical conditions, whereas the diester dioxine **3e** rearranged in both cases. It is premature to speculate about the factors influencing the rearrangements, as a more in depth study taking into account electronic and kinetic effects would be required. It seems reasonable to postulate that perhaps electronics plays a part, with electron donating groups producing the expected dialdehyde, whereas upon removing electron density from the peroxide *via* electron withdrawing groups, rearrangements are then seen. Phenyl groups have the ability to respond to the demands placed upon it in terms of donating or withdrawing electron density from a system. It could be proposed that in the case of these ozonolysis experiments, one phenyl group (seen in dioxine **3b**) has little effect on altering the reaction outcome, whereas adding an additional phenyl moiety to the system (seen in dioxine **3c**) removes enough electron density to weaken the peroxide bonds and enable rearrangements to readily occur. Previous research has shown that reactions of alkenes with ozone are sensitive to electronic effects, with electron deficient alkenes having

much lower rate constants than those alkenes with greater electron density.[132-134] This is believed to be due to the electrophilic nature of ozone, which adds to the nucleophilic π-bond of the alkene, which is enriched by lone pair donation of the electron donating group, thereby assisting in the lowering of the activation energy barrier, and thus enhancing the reaction rate.[132,134] When the rate is increased, there is less chance for rearrangements to occur, making it reasonable to suggest that using electron withdrawing groups in the bridgehead positions may assist in slowing the rate of reaction and thereby raising the likelihood of rearrangements occurring.

All rearranged products show a loss of CO or CO_2 (depending on the proposed mechanism, see discussion below), along with cleavage of the peroxide bond, with a similar mechanism appearing to be at play for both symmetrical and unsymmetrical ozonolysis conditions. In attempting to answer the question of how did these rearrangements occur, a careful analysis of all available data is required. Did these rearrangements proceed *via* ozonide **125** decomposing into the expected dialdehydes **128** followed by spontaneous rearrangement into **132** or **146**, (*Scheme 51*, *Pathway A*) or alternatively did ozonide **125** directly decompose into **132** or **146**, *Scheme 51*, *Pathway B*. Moreover, does the addition of PPh_3 assist in these rearrangements?

Since reduction of the phenyl-phenyl substituted 1,2-dioxine **3c** rearranged upon reduction with both PPh_3 and Me_2S, it is unlikely that the PPh_3 was solely responsible for the rearrangement seen under the standard ozonolysis conditions. We know that the unsymmetrical ozonolysis mechanism does not involve the formation of an ozonide, and since the same rearrangement was seen under these unsymmetrical conditions, it is likely that the rearranged products did not come directly from ozonide **125** in the standard conditions, thereby ruling out *Pathway B* in *Scheme 51*. *Pathway A* is further supported by the two aldehyde peaks, with 1 : 1 integrations, that were seen in the crude ^{1}H NMR spectra from the ozonolysis of diester dioxine **3e**.

If the dialdehyde **128** (or aldehyde ester **144** for unsymmetrical ozonolysis) is indeed forming, and spontaneously decomposing to give the rearranged products, how is this happening? *Scheme 51* outlines a couple of potential pathways involving both concerted

and stepwise mechanisms for *Pathway A*, both involving decarbonylation (- CO) of the aldehyde moiety.

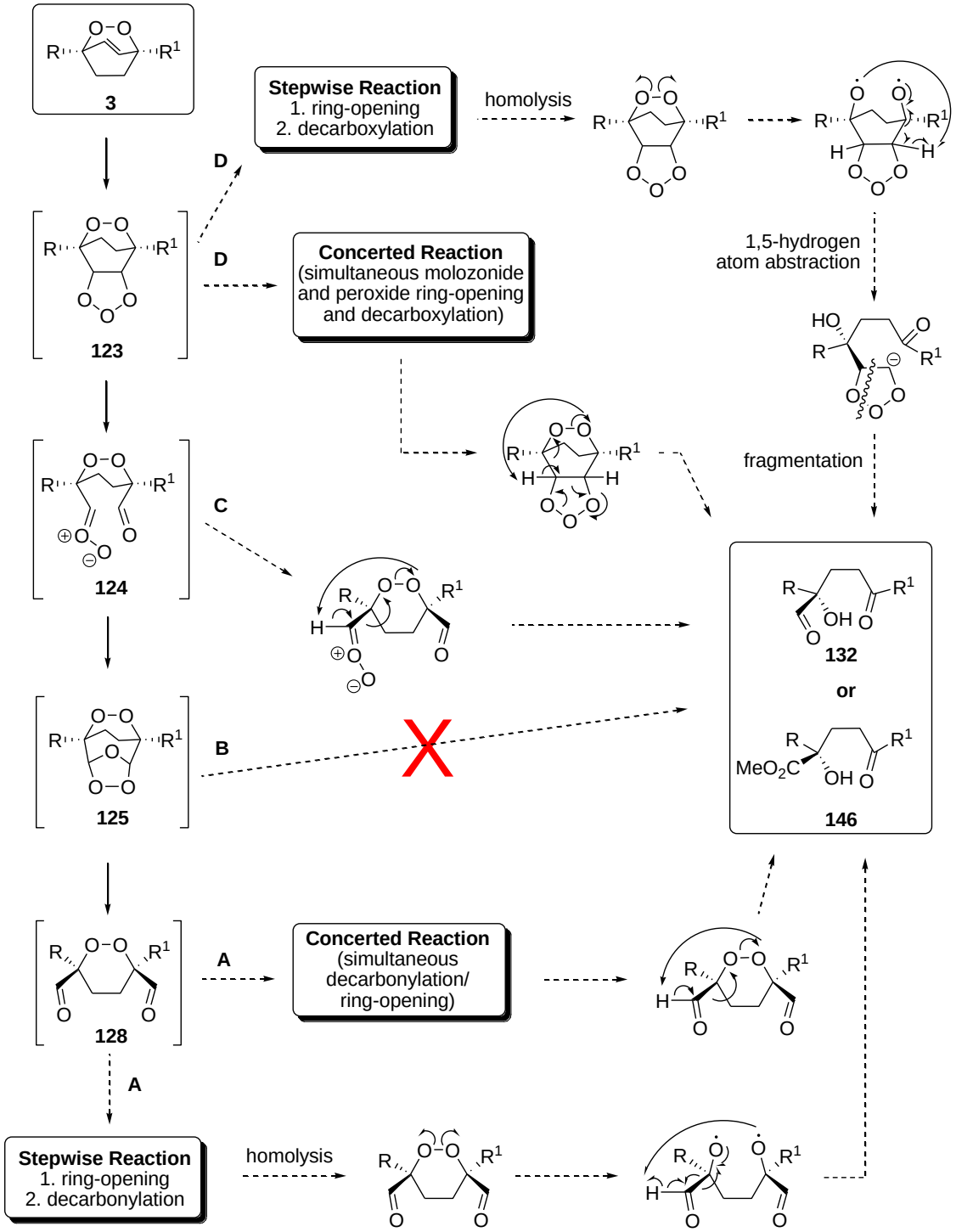

Scheme 51

Decarbonylation of aldehydes is usually seen in the presence of transition metal catalysts,[135-137] or radical initiators.[138,139] A thorough search of the literature found no precedent for the loss of a carbonyl group α to a peroxide bond, making this type of rearrangement quite unique.

Another mechanistic possibility is that either the aldehyde-carbonyl-oxide species **124** or the molozonide **123** are directly rearranging into products **132** or **146**, *Scheme 51*, *Pathways C* and *D* respectively. These intermediates are common to both the symmetrical and unsymmetrical ozonolysis reactions, and again, there are numerous plausible mechanisms *via* which these two species could form the rearranged products, involving a total loss of CO_2. If the aldehyde-carbonyl oxide moieties, **124**, are indeed formed, then decarboxylation is likely to occur *via* loss of the carbonyl oxide group, rather than decarbonylation from the aldehyde moiety, *Scheme 51*, *Pathway C*.

Breakdown of the molozonide **123** into **132** or **146** could occur *via* a concerted mechanism (*Scheme 51 Pathway D*), although a series of stepwise reactions involving breakdown of the molozonide, decarboxylation, ring opening and proton abstraction are possible. If a multiple step process from the molozonide is involved, then the question arises as to in what order do these reactions occur?

The ozonolysis of bicyclic 1,2-dioxines is an unusual reaction, with the mechanism involving many oxygen atoms with lone pairs of electrons creating a high potential for the expulsion of oxygen *via* decarbonylation or decarboxylation in an entropically favoured bid to lower the energy of the system. These unique rearrangements are of synthetic interest, with preliminary experiments laying the foundation for further research to be carried out in order for a clear mechanistic picture to be obtained. With optimised conditions and the correct functional groups present, the ozonolysis of bicyclic 1,2-dioxines could be controlled in a predictable manner and provide a useful pathway to many synthetic and naturally occurring organics.

CHAPTER 4: An *Ab Initio* Investigation into the Ozonolysis Mechanism of Bicyclic 1,2-Dioxines

The Criegee mechanism for the ozonolysis of simple acyclic alkenes was discussed in Chapter 1 (*Scheme 16*, pg 15), whilst Chapter 3 saw our proposed mechanism for the ozonolysis of an alkene moiety incorporated into a bicyclic bridged 1,2-dioxine (*Scheme 37*, pg 38). This chapter will focus on supporting the theory proposed in Chapter 3 that ozone approaches the 1,2-dioxine *via* the 'endo' face to yield molozonide **123a** and ultimately ozonide **125a**. This will be done by examining the relative differences in energies for all possible isomers at each stage of the reaction in order to locate the lowest energy pathway, and therefore that which is most likely followed.

Appreciable theoretical work has already been conducted on alkene ozonolysis,[140-143] with a recent paper published by Kharbuli and Lyngdoh[134] providing a good review of previous theoretical work done on the mechanism. This previous work has ranged from semi-empirical to high-level sophisticated theories, with some qualitative agreements found between the semi-empirical and higher level calculations.[134] As previously mentioned, there is little precedent for the ozonolysis of bicyclic alkenes, and even fewer incorporating 1,2-dioxine moieties, thus making the theoretical work outlined here a first of its kind.

All calculations were performed using the *Spartan '08* program.[144] Taking into account the delicate balance between time and accuracy of data, Hartree-Fock (HF) was seen as an adequate level of theory for this application, as previous work at this level has yielded realistic energy profiles for the ozonolysis mechanism,[145] with the 6-31G* basis set able to provide a reliable set of data for both gas and solvent (dichloromethane) phases. To obtain more accurate data, all calculations were firstly performed at the semi-empirical AM1 level to provide initial starting geometries. These were then utilised for the HF/3-21G* basis set, with these results then used as input for the 6-31G* basis set. Frequency calculations were performed at each level to confirm whether the

obtained species were intermediates (with all real frequencies) or transition states (with one imaginary frequency).

Calculations were undertaken using a simple parent bicyclic 1,2-dioxine system **3**, with no substituent effects taken into account. Only the HF/6-31G* data set will be discussed within this chapter. Full sets of raw energy data for the AM1 and HF/3-21G* calculations are provided in appendices 1 and 2, pages 179 and 180 respectively.

Before commencing discussion of the theoretical results obtained, it is necessary to firstly outline the proposed mechanistic pathway in more detail, incorporating transition states and intermediates for all conformers possible at each stage.

4.1 Mechanism for the Ozonolysis of Bicyclic 1,2-Dioxines (Revisited).

Scheme 52 shows a detailed outline of the transition states and intermediate products involved in the proposed mechanistic pathway, shown for both an *exo* and *endo* approach of ozone (**46**) onto the parent 1,2-dioxine system **3**. Four configurational possibilities exist for the formation of the molozonide transition state (TS1, **150a-d**), the intermediate molozonide (IM1, **123a-d**) and the second transition state involving the molozonide ring-opening (TS2, **151a-d**). These depend on firstly whether ozone 'attacks' the alkene from either the top (*exo*) or bottom (*endo*) face, and secondly whether the central oxygen within the molozonide is pointed outwards (labelled here as *exo*) or inwards (*endo*). The term '*endo*' is used here to indicate that the ozone approaches from opposite the peroxide linkage, whilst ozone approaches from the same face for the '*exo*' case. Once the molozonide ring-opens the aldehyde and carbonyl oxide intermediate products (IM2, **124a-d**) are formed, which upon rotation into the correct conformer react *via* an intramolecular 1,3-dipolar cycloaddition (TS3, **152a-b**) to give one of two potential ozonides (P, **125a** or **125b**). As illustrated in *Scheme 52*, it is plausible that crossover from the *endo* isomers of IM2 (**124a-b**) into the *exo* isomer of TS3 (**152b**), and *vice-versa* is possible, as this is dependent on finding the most favourable conformation of **124** for the cycloaddition to occur. Our aim here is to determine *via* theoretical calculations which of these pathways is energetically the most feasible.

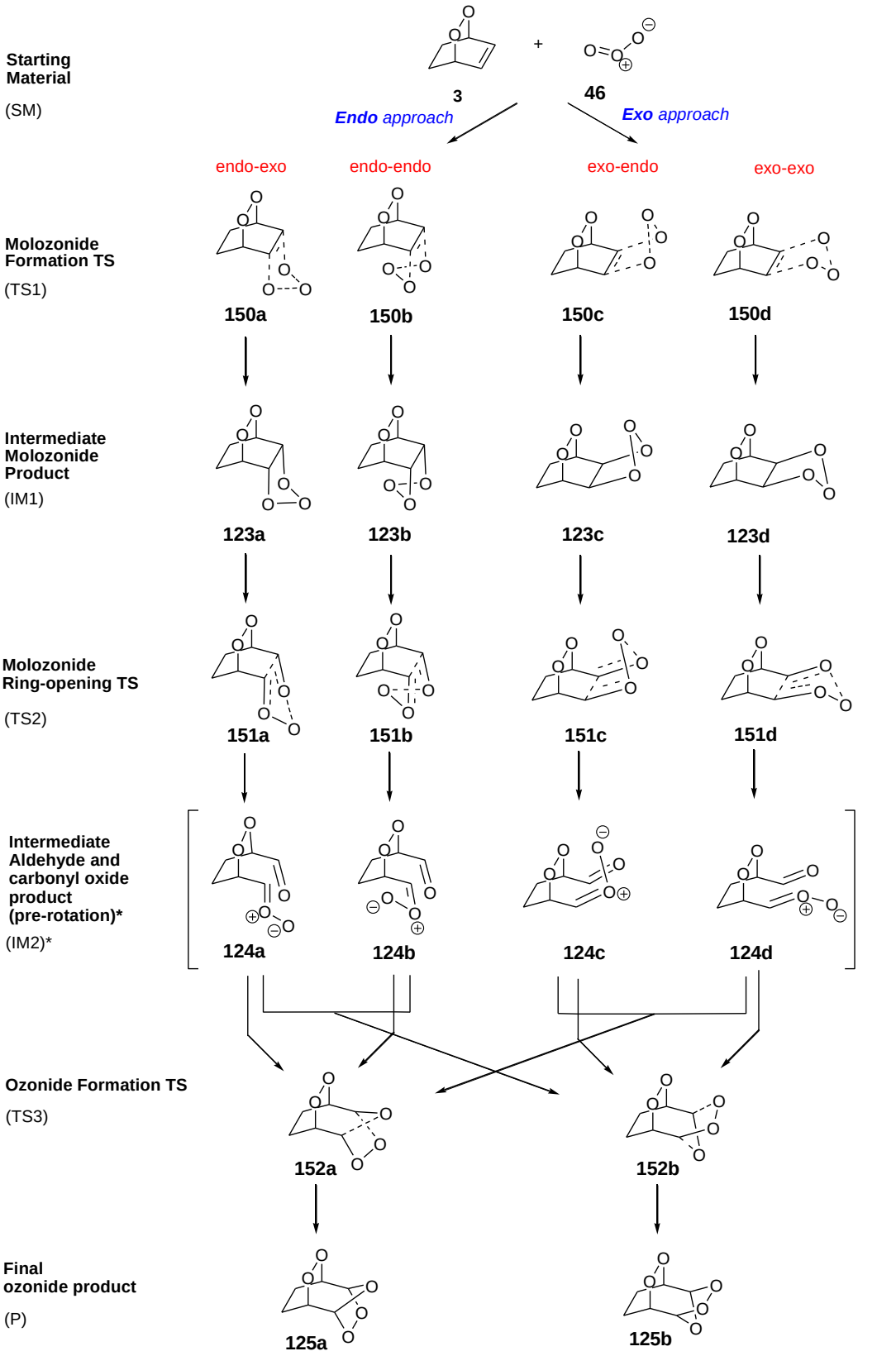

* representation only - see discussion and *Scheme 53*

Scheme 52

According to the traditional Criegee mechanism, once molozonide **123** has ring-opened to yield the aldehyde and carbonyl oxide intermediate product (IM2, **124a-c**) the aldehyde moiety proceeds to rotate 180^{o} in order to undergo a 1,3-dipolar cycloaddition to yield the final ozonide **125**. Due to rotational restrictions imparted by the bicyclic system, this may not be possible in this case, however either species could undergo a semi-rotation in order to find a configuration suitable for formation of either ozonides **125a** or **125b**. The dipolar products **124a-d** are illustrated as intermediates (IM2) in *Scheme 52*, and are tentatively shown in their pre-rotational forms. Conformational analysis was performed in order to find what may be considered the most likely conformation(s) favoured by the system that could lead to the formation of either ozonide **125a** and **125b**, as depicted in *Scheme 53*. The results of this will be discussed below.

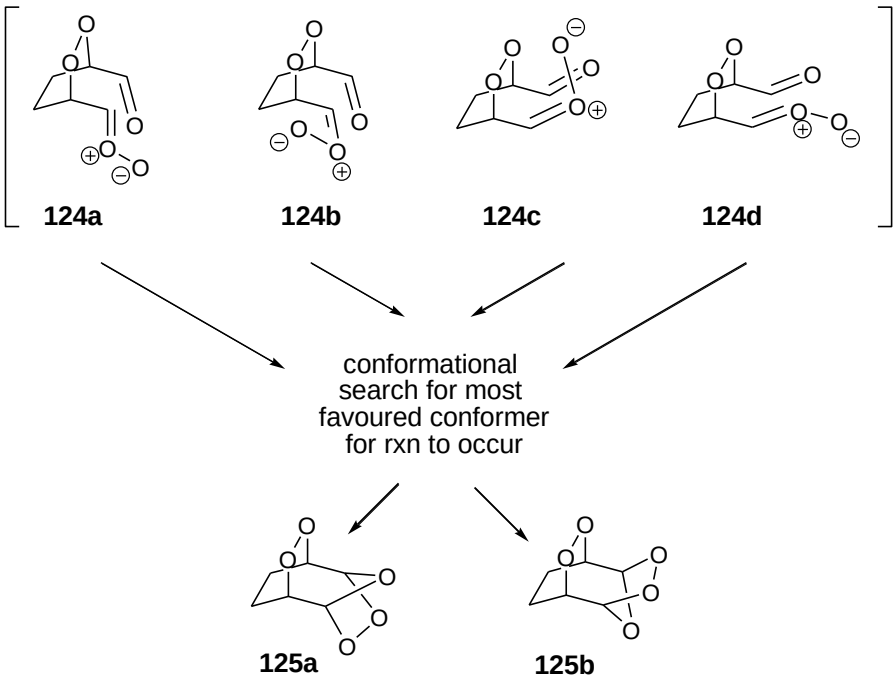

Scheme 53

4.2 Energy Profiles for *Ab Initio* Calculations.

4.2.1 HF/6-31G* (Gas Phase).

The calculated raw data for each stage of the proposed reaction mechanism is given in *Table 9*, for gas (vacuum) phase analysis. The layout for *Table 9* follows that of *Scheme 52*, whereby only one set of data is needed for the starting materials, four isomers are possible for TS1, IM1 and TS2, whilst TS3 and P have only two possible conformers. Energies are given in Hartree (E_h), the atomic unity of energy, equivalent to the approximate value of the electrical potential energy of the hydrogen atom in its ground state.

Table 9: HF/6-31G* (Gas) Energy Values for the Ozonolysis Mechanism (Hartree, E_h).

	exo-endo	***exo-exo***	***endo-endo***	***endo-exo***
SM (Ozone)*		-224.261436		
SM (Dioxine)*		-381.444974		
SM (Total)*		-605.706410		
TS1	-605.681908	-605.679206	-605.681621	-605.683171
IM1	-605.850569	-605.850958	-605.855833	-605.856015
TS2	-605.762592	-605.765741	-605.772264	-605.773567
IM2^		-605.875129		
TS3[#]	-605.832959		-605.839105	
P[#]	-605.930266		-605.928714	

* Single set of values (*endo*/*exo* does not apply for SM).
^ Representation only, see discussion.
[#] Only two conformations for TS3 and P (*exo* and *endo*).

As mentioned above, a conformer search was performed on the second intermediate product (IM2, **124**) in a bid to find the conformer(s) most likely to correspond to the formation of the *endo* and *exo* ozonides **125a** and **125b** respectively. The results proved unsuccessful, with no conformers found to have the right configuration that would be required to enable the 1,3-dipolar cycloaddition reaction to occur between the aldehyde and carbonyl oxide moieties. Despite the inability to find a suitable conformer on a theoretical level, this by no means raises any doubt as to the mechanism proposed, as we have experimentally seen the successful outcome of this reaction in the laboratory. For the purposes of this work calculations for IM2 were performed on the optimised

'*endo-exo*' structure, **124a** and used for all pathways within the HF/6-31G* energy profile (hence why only one value is reported for IM2). As will be seen, irrespective of this outcome, the final transition state (TS3) is clearly lower in energy for the *endo* pathway by approximately 16 kJ/mol.

Table 10 shows the relative energy differences (in kJ/mol) for each stage of the reaction, with the sum of the two starting materials set to zero. This data was used to map an energy profile of the mechanism (*Figure 15*), in order to evaluate which isomers presented the lowest energy pathway.

Table 10: HF/6-31G* (Gas) Relative Energy Differences (kJ/mol).

	exo-endo	***exo-exo***	***endo-endo***	***endo-exo***
SM (Total)*		0.00		
TS1	64.33	71.42	65.08	61.01
IM1	-378.49	-379.51	-392.31	-392.79
TS2	-147.51	-155.77	-172.90	-176.32
IM2^		-442.97		
TS3#	-332.25		-348.39	
P#	-587.73		-583.66	

* Single set of values (*endo*/*exo* does not apply for SM).
^ Representation only, see discussion.
# Only two conformations for TS3 and P (*exo* and *endo*).

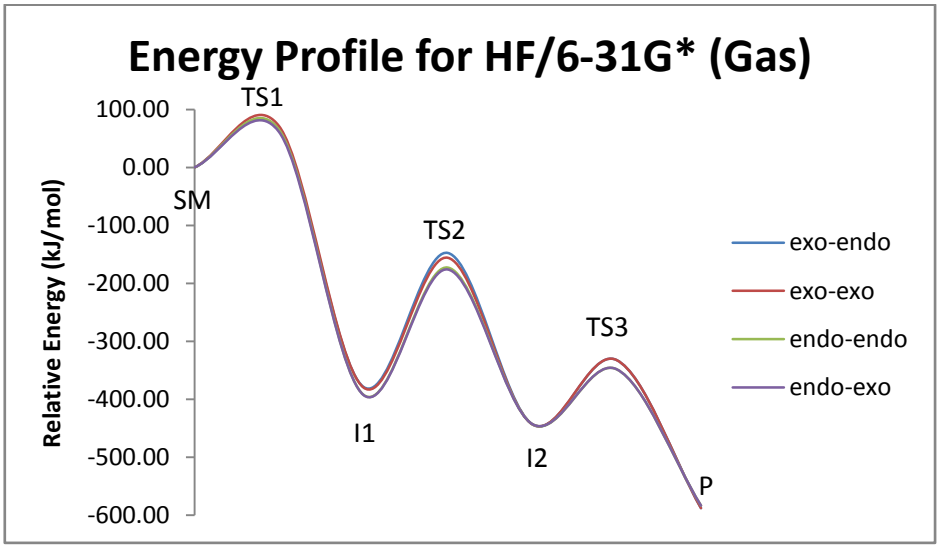

Figure 15: HF/6-31G* (Gas) Energy profile for ozonolysis mechanism.

As can be seen in *Figure 15*, the ozonolysis mechanism is highly exothermic with each transition state decreasing with energy, as expected. Except for the final product, the endo-exo pathway is globally the lowest in energy, supporting the theory proposed in Chapter 3, that endo 'attack' of ozone would be favoured due to the minimisation of electronic (ie lone pair repulsions) and steric effects. The calculated energy difference between the final ozonide products is 4.07 kJ/mol, with the *exo* sitting lower in energy than the *endo*, although analysis of the activation energies for each transition state (*Table 11*) clearly shows that *endo-exo* pathway is globally the lowest in overall energy.

Table 11: HF/6-31G* (Gas) Activation Energy Barriers (Ea, kJ/mol).

E_a (KJ/mol)	*exo-endo*	*exo-exo*	*endo-endo*	*endo-exo*
***via* TS1**	64.33	71.42	65.08	61.01
***via* TS2**	230.98	223.74	219.41	216.47
via* TS3	110.72		94.58	

* Only two conformations for TS3 (*exo* and *endo*).

4.2.2 HF/6-31G* (Dichloromethane).

Since all standard ozonolysis reactions performed experimentally within this thesis used dichloromethane as the solvent, it was deemed appropriate to investigate the mechanistic pathway (*Scheme 52*) whilst taking the solvent into account, in order to see what effect this had on the theoretical outcome of the reaction. The results obtained are tabulated in the same manner as the gas phase results, with the raw data shown in *Table 12*, the relative energy differences in *Table 13* and the energy profile in *Figure 16*.

Table 12: HF/6-31G* (DCM) Energy Values for the Ozonolysis Mechanism (Hartree, E_h).

	exo-endo	***exo-exo***	***endo-endo***	***endo-exo***
SM (Ozone)*		-224.264221		
SM (Dioxine)*		-381.455531		
SM (Total)*		-605.719752		
TS1	-605.693246	-605.691227	-605.692239	-605.705372
IM1	-605.864726	-605.864987	-605.866501	-605.866663
TS2	-605.778803	-605.781287	-605.784075	-605.786333
IM2^		-605.897908		
TS3#	-605.850515		-605.853846	
P#	-605.942619		-605.939597	

* Single set of values (*endo*/*exo* does not apply for SM).
^ Representation only, see discussion.
# Only two conformations for TS3 and P (*exo* and *endo*).

Table 13: HF/6-31G* (DCM) Relative Energy Differences (kJ/mol).

	exo-endo	***exo-exo***	***endo-endo***	***endo-exo***
SM (Total)*		0.00		
TS1	69.59	74.89	72.24	37.75
IM1	-380.63	-381.31	-385.29	-385.71
TS2	-155.04	-161.56	-168.88	-174.81
IM2^		-467.75		
TS3#	-343.32		-352.06	
P#	-585.14		-577.20	

* Single set of values (*endo*/*exo* does not apply for SM).
^ Representation only, see discussion.
# Only two conformations for TS3 and P (*exo* and *endo*).

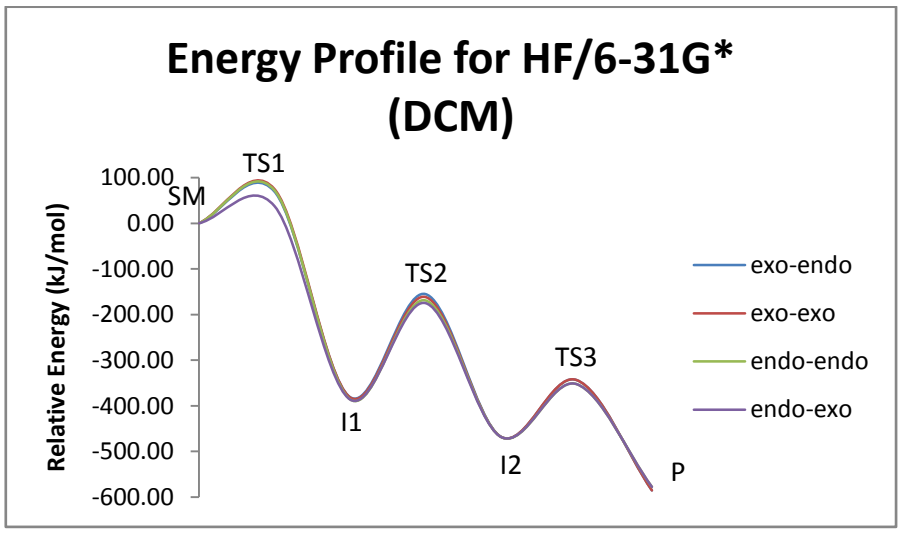

Figure 16: HF/6-31G* (DCM) Energy profile for ozonolysis mechanism.

The energy profile that takes into account the effects of dichloromethane (*Figure 16*) follows the same trend as seen for the gas phase (*Figure 15*), with the *endo-exo* pathway being the global minimum in energy (once again apart from the final product). In dichloromethane, the *exo* product sits almost 8 kJ/mol lower in energy than its *endo* counterpart (approximately double the energy difference as that seen for the gas phase), although overall this is not important, as analysis of the activation energy barriers (*Table 14*) shows that the final transition state (TS3) for the *endo* isomer is almost 9 kJ/mol lower than the *exo* isomer, indicating that the *endo* pathway is clearly favoured. Interestingly, the activation energy (E_a) for the initial transition state (TS1) for the *endo-exo* isomer is around 23 kJ/mol lower in dichloromethane than in the gas phase. The E_a for the other three isomers in TS1 and both isomers in TS3 sit higher in the solvent than in a gas phase, whilst all the activation barriers for TS2 are lower in dichloromethane than calculated for the gas phase. Clearly this indicates that the solvent does indeed have an effect on the reaction energies, although it is beyond the objectives of this work to examine these solvent-induced differences in detail. Importantly, the overall trends and favourable pathways remain the same in both cases.

Table 14: HF/6-31G* (DCM) Activation Barriers (Ea, kJ/mol).

E_a (KJ/mol)	*exo-endo*	*exo-exo*	*endo-endo*	*endo-exo*
***via* TS1**	69.59	74.89	72.24	37.75
***via* TS2**	225.59	219.75	216.41	210.91
via* TS3	124.43		115.68	

* Only two conformations for TS3 (*exo* and *endo*).

Optimised structures for all isomers of the HF/6-31G* (DCM) calculations (except for the IM2, since no suitable conformer was found) can be seen in *Figures 17 – 22*. Bond distances are given in angstroms (blue) and angles in degrees (black). The optimised structures for SM, TS1, IM1 and P are all symmetrical, whilst TS2 and TS3 are unsymmetrical molecules. Interestingly, the peroxide bond length differed only slightly between all isomers at each stage of the mechanism.

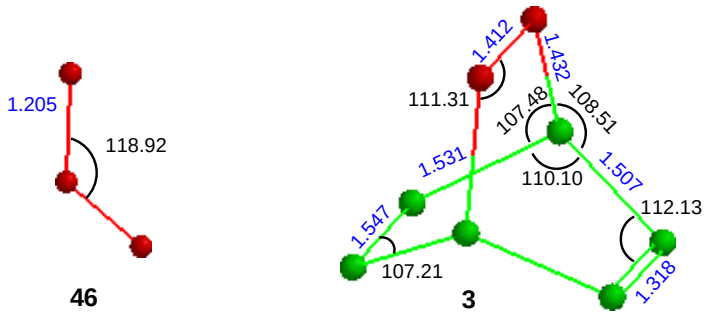

Figure 17: HF/6-31G* (DCM) optimised geometries for the starting materials (SM, **3** and **46**).

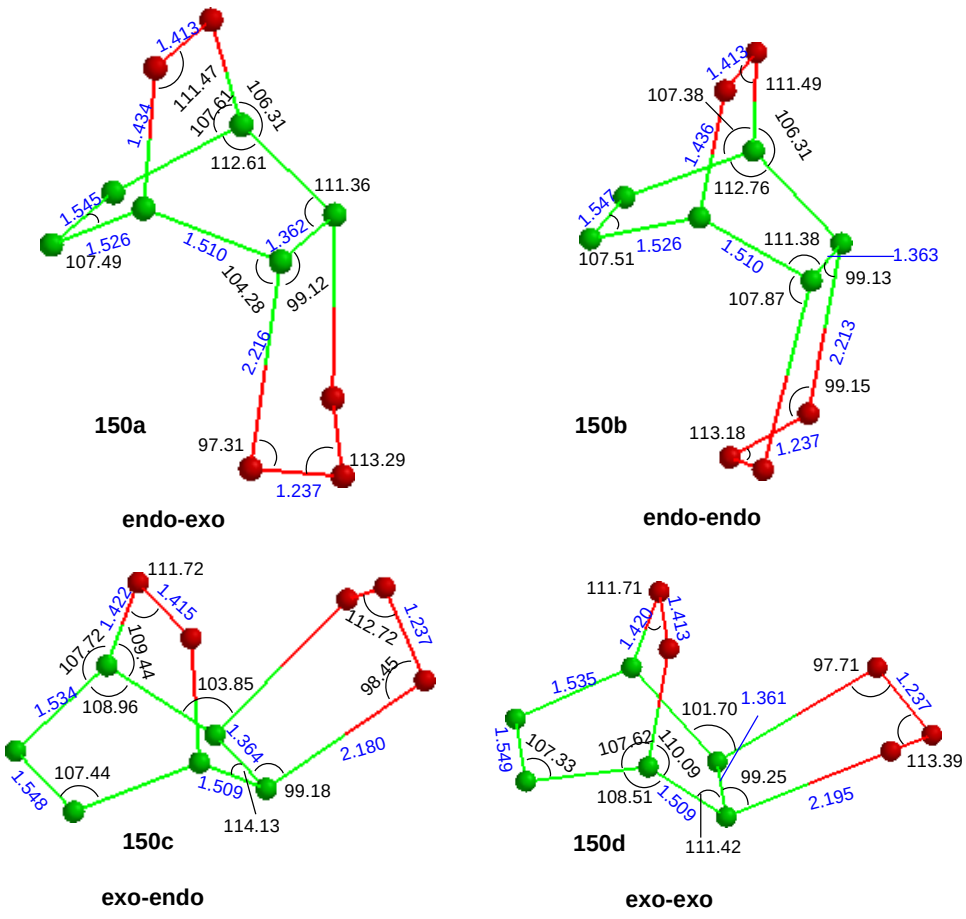

Figure 18: HF/6-31G* (DCM) optimised geometries for the molozonide formation (TS1, **150a-d**).

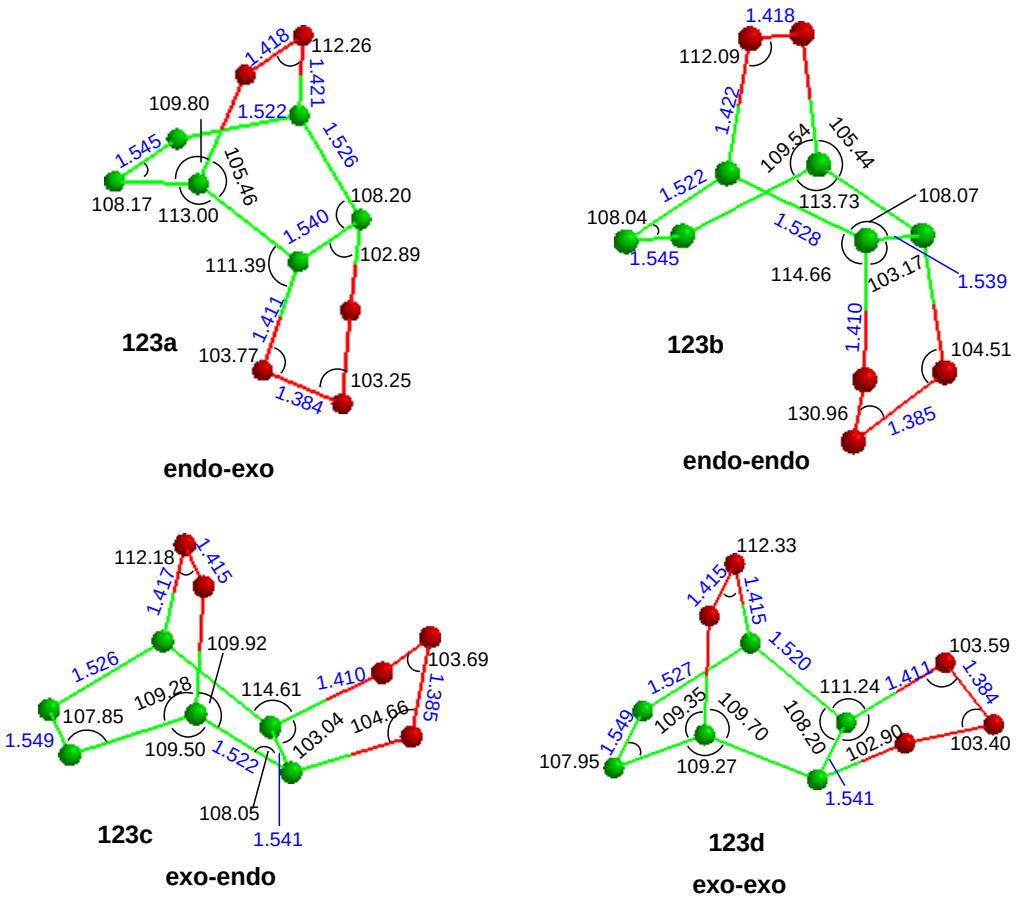

Figure 19: HF/6-31G* (DCM) optimised geometries for the intermediate molozonide product (IM1, **123a-d**).

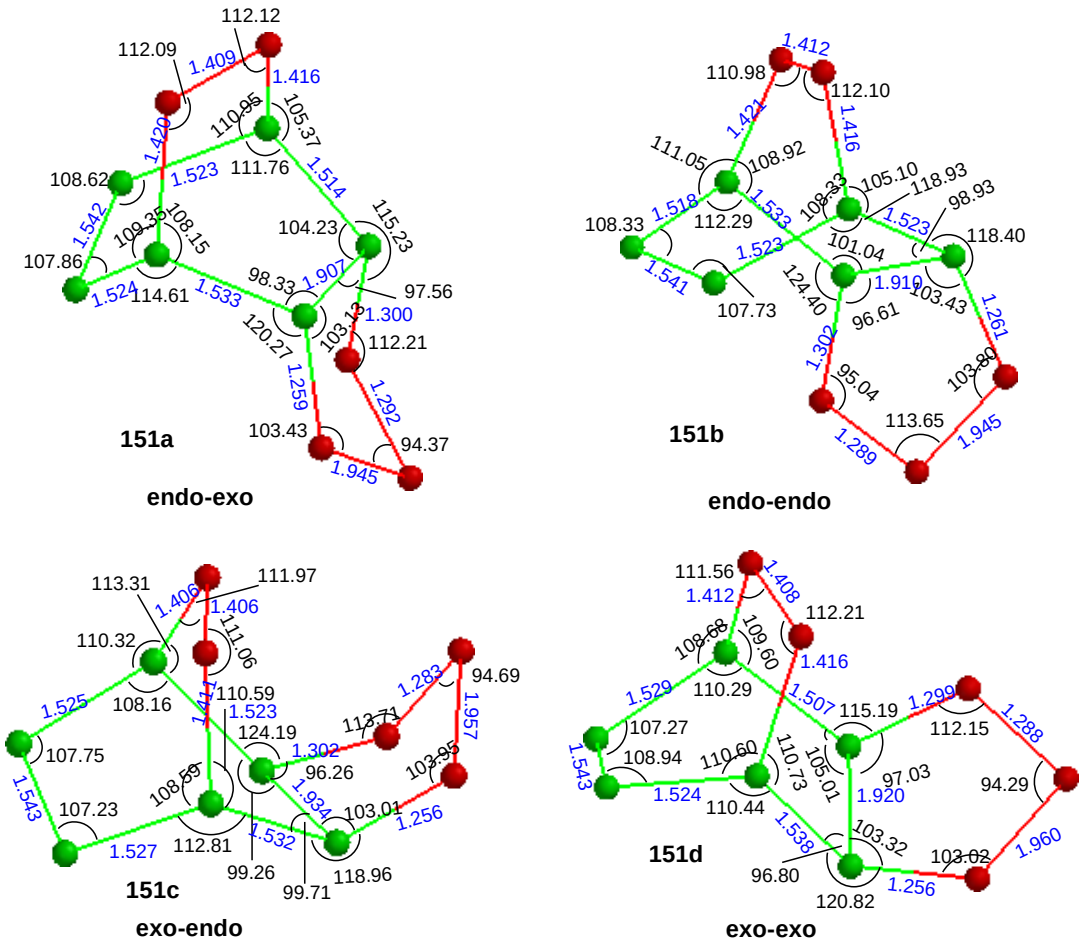

Figure 20: HF/6-31G* (DCM) optimised geometries for the molozonide ring-opening (TS2, **151a-d**).

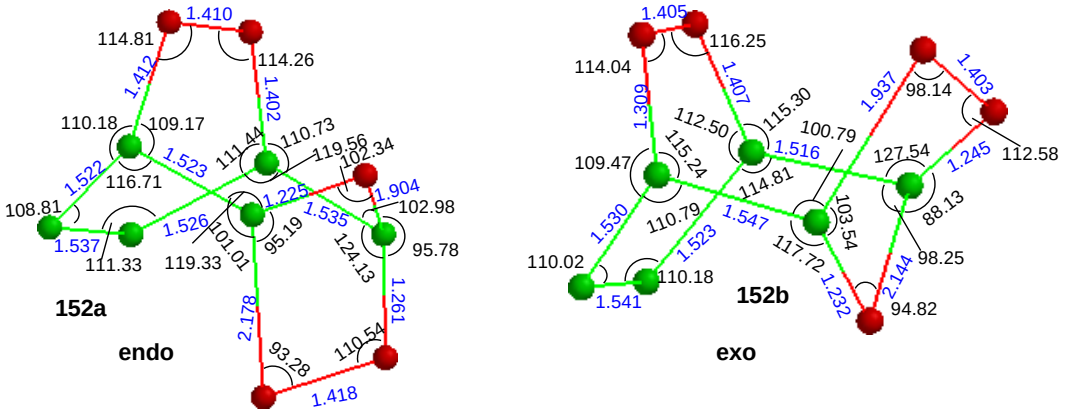

Figure 21: HF/6-31G* (DCM) optimised geometries for the ozonide formation (TS3, **152a,b**).

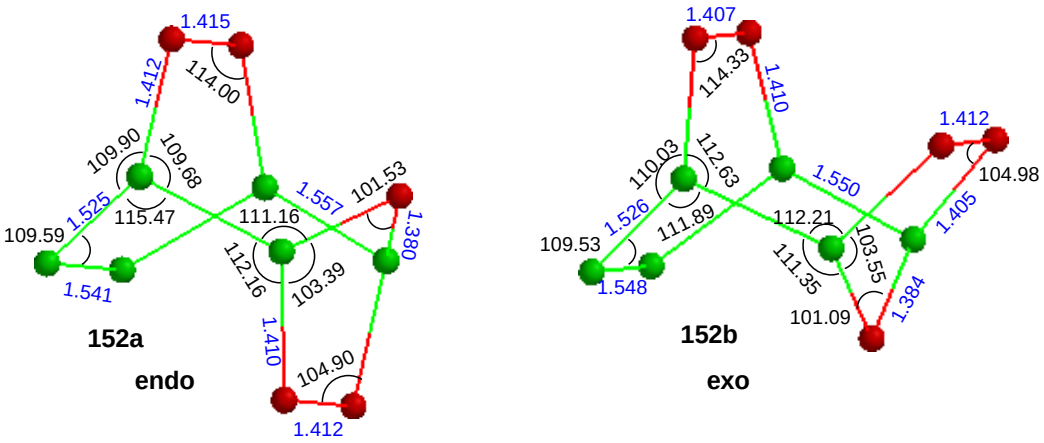

Figure 22: HF/6-31G* (DCM) optimised geometries for the final ozonide product (P, **125a,b**).

4.3 Conclusion.

This was by no means meant to be a thorough, in-depth theoretical study into the ozonolysis mechanism, but rather serve as a useful tool for evaluating the relative energy differences between the possible isomers involved in our proposed mechanism, and shed light onto the pathway these 1,2-dioxines undertake upon reaction with ozone. The data obtained in this theoretical analysis supports our originally proposed mechanism in Chapter 3 whereby an '*endo*' approach of ozone is favoured and is likely due to electronic and steric repulsions. These results help to bridge the gap between the experimental observations seen in the laboratory and a theoretical understanding of the chemistry at play.

CHAPTER 5: Towards the Synthesis of the Monoterpene Furanoid Oxides

The furanoid and anhydrofuran linalool oxides (**101** and **102**, respectively) have been established as common compounds in wine and as natural products from other sources.[146-150] Previous methods of synthesis have followed a variety of different routes, although as will be demonstrated, many experimental details are unclear and of limited value. It was therefore felt that a gap exists in the literature with regard to an effective synthesis of **101** and **102**, and the development of a new synthetic pathway to afford both compounds, and analogues thereof, from a common starting material would be of value.

The first part of this thesis focussed on the ozonolysis of bicyclic 1,2-dioxines, and it was envisioned that a synthetic pathway towards the synthesis of **101** and **102** incorporating the ozonolysis of a 1,2-dioxine precursor would provide a novel route to the requisite furan precursor **153**. The aim of this section of research therefore was to explore the synthesis of the wine compounds **101** and **102** from a common starting material, with a key step involving the ozonolysis of a 1,2-dioxine precursor.

The retro-synthetic pathway, shown in *Scheme 54* illustrates the key steps involving the formation of bicyclic 1,2-dioxine **154** from its precursor 1,3-diene **155**. This dioxine may then undergo ozonolysis to afford keto-aldehyde **156**, and subsequent Kornblum DeLaMare rearrangement under basic conditions to yield the necessary furan precursor **153**. With the core furan structure in place, many synthetic options exist to structurally manipulate the C_2 and C_5 substituted furans into the desired compounds **101** and **102**.

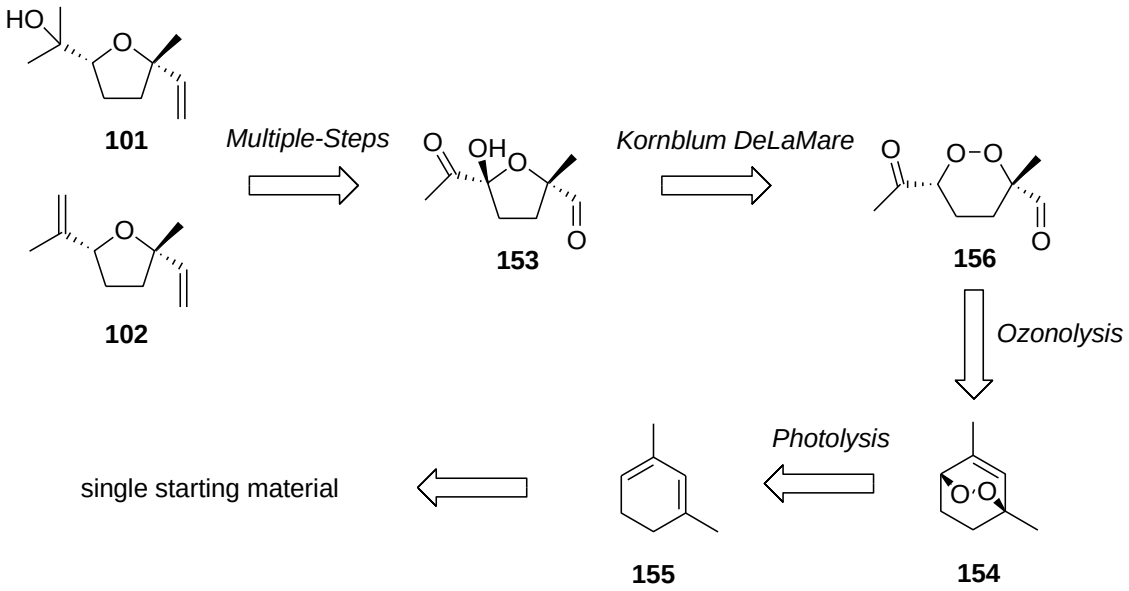

Scheme 54

Before presenting the results of this body of work, it is pertinent to firstly provide an introduction to the furanoid and anhydrofuran linalool oxides (**101** and **102**), and summarise their history and importance to wine aroma.

5.1 Introduction to Wine Aroma, Flavour and Terpenes.

Over 6,000 volatile compounds have been detected in food and beverages, with over 1,300 of these having been specifically identified in wine. These include alcohols, esters, organic acids, aldehydes, ketones and monoterpenes as well as nitrogen and sulfur containing compounds.[151,152]

Early investigations into volatile constituents of wine date back to the year 1942, when Hennig and Villforth used classical chemical methods to identify a few compounds in wine.[146,153] In the late 1950s Bayer *et al.*[154] were the first to apply gas chromatography to the field of wine aroma, where they identified some higher alcohols and a few esters.

Terpenes are a class of natural hydrocarbons derived from isoprene (2-methyl-1,3-butadiene) (**157**), *Figure 23*. They are widespread in nature, found mainly in plants, and are considered to be the most important constituents of essential oils. Monoterpenes are

the simplest class of terpenes and contain two isoprene units, they are commonly used as flavourings and fragrances, and have more recently been used as intermediates in the pharmaceutical industry.[155,156] At present over three hundred monoterpene compounds are known, of which about fifty are found in grapes and wine.[153,157-161]

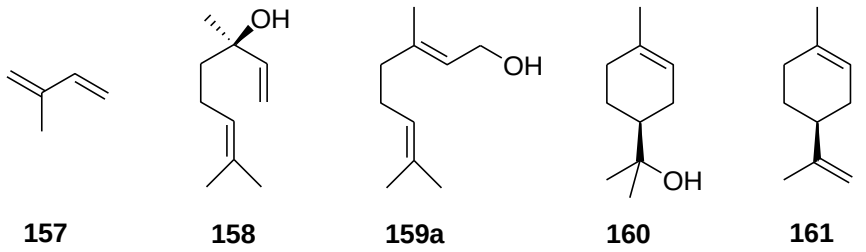

Figure 23: Isoprene (**157**) and common monoterpenes found in wine (**158-161**).

Monoterpenes were first recognised in muscat grapes over 50 years ago, when Cordonnier[162] tentatively identified linalool (**158**), geraniol (**159a**), α-terpineol (**160**) and limonene (**161**) by means of TLC. Linalool (**158**) and geraniol (**159a**) are considered to be the most significant monoterpenes in grapes, together representing about 80% of the total monoterpene concentration in Muscat grapes.[160,161]

Monoterpenes show considerable changes during grape ripening and development along with the aging process of wine. Rearrangements and release of volatiles within the grape result in substantial changes in monoterpene concentration, with some compounds showing an increase in concentration and others a decrease, as well as new compounds being formed that are not present in young wine. This can have an affect on the flavour and aroma of wine over time.[146,153]

Besides volatile aromatic components, monoterpenes exist in grapes as non-volatile odourless glycosides.[160,163] A significant portion (~90%) of the terpenes are present as non-volatile glycoside precursors, which constitute potential flavourants that generally remain odourless. These bound glycosides can be hydrolysed to the sugar moiety and corresponding free terpene during fermentation or aging.[152] Hydrolytic reactions usually proceed *via* a series of complex equilibria and may involve several intermediates.[163] This hydrolysis may be either acid[164,165] or enzyme[158,166] catalysed.

5.2 The Linalool Oxides.

5.2.1 Introduction.

The linalool oxides have been identified, and widely reported in the literature as being found in many essential oils, fruits and plants, and are recognised as being common compounds of grape and wine aroma.[146-150]

The linalool oxides exist in two isomeric forms, furanoid (five-membered ring, **101**) and pyranoid (six-membered ring, **162**), *Figure 24*. Each of the pyranoid and furanoid forms of the linalool oxides contain two stereocentres, and therefore each exist as two diastereomeric pairs of enantiomers. In this body of work we are only concerned with the furanoid linalool oxides, so no further reference will be made to the pyranoid linalool oxides.

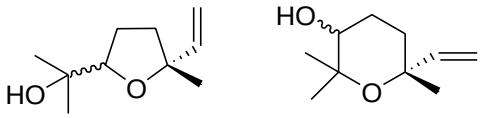

101 **162**

Figure 24: Furanoid (**101**) and Pyranoid (**162**) Linalool Oxides.

The diastereomers of the furanoid linalool oxides, shown in *Figure 25*, consist of two *cis* (2*S*,5*R*) (**101a**), (2*R*,5*S*) (**101b**) and two *trans* (2*R*,5*R*) (**101c**), (2*S*,5*S*) (**101d**) enantiomeric pairs. The literature commonly groups the furanoid linalool oxides into the *cis*- and *trans*- forms, but rarely differentiates between the two enantiomers within each isomer set. The furanoid linalool oxides were first isolated from Mexican linaloe oil (*Bursera* spp.) and Bois de rose cayenne (*Aniba rosaeodora*) in 1908,[167] however, their correct configurations were not elucidated until 1963.[168]

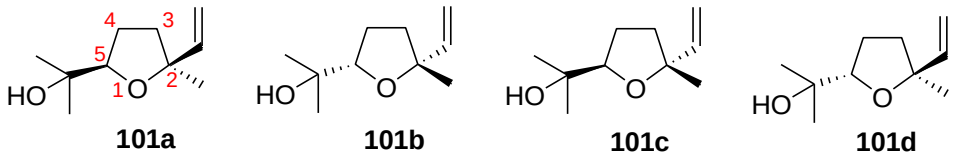

101a **101b** **101c** **101d**

Figure 25: Isomers of Furanoid Linalool Oxides.

Another set of isomeric compounds found in wine are the anhydrofuran linalool oxides (**102**), *Figure 26*. Structurally related to the furanoid linalool oxides, they also exist as two *cis* (2*S*,5*R*) (**102a**), (2*R*,5*S*) (**102b**) and two *trans* (2*R*,5*R*) (**102c**), (2*S*,5*S*) (**102d**) enantiomeric pairs. They have been identified as being formed during wine aging,[146,169] likely to be due to slow dehydration of **101a-d** over time.

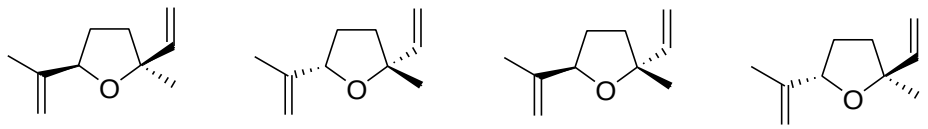

102a **102b** **102c** **102d**

Figure 26: Isomers of Anhydrofuran Linalool Oxides.

Both **101** and **102** are classified as free aroma compounds, found in both grapes and wine and have been identified as metabolic products of linalool.[159,161] The systematic numbering system used for all isomers of both **101** and **102** is shown for **101a** in *Scheme 25*.

5.2.2 Formation of 101 and 102 in Wine and Changes with Aging.

In 1980, Williams *et al.*[169] first reported the identification of four hydroxylated linalool derivatives (polyols) in chloroform extracts of Muscat grapes. These polyols were reportedly derived from either linalool (**158**) or geraniol (**159a**) by oxidation, reduction or hydrolysis and are now widely recognised in the literature as being precursors to a range of monoterpenes *via* acid hydrolysis at wine pH.[161,169,170] Two of these polyols, triol **163** and diol **164** gave isomeric mixtures of **101** and **102** respectively, *Scheme 55*.

This was the first time the anhydrofuran linalool oxides had been identified in grape or wine products.[169]

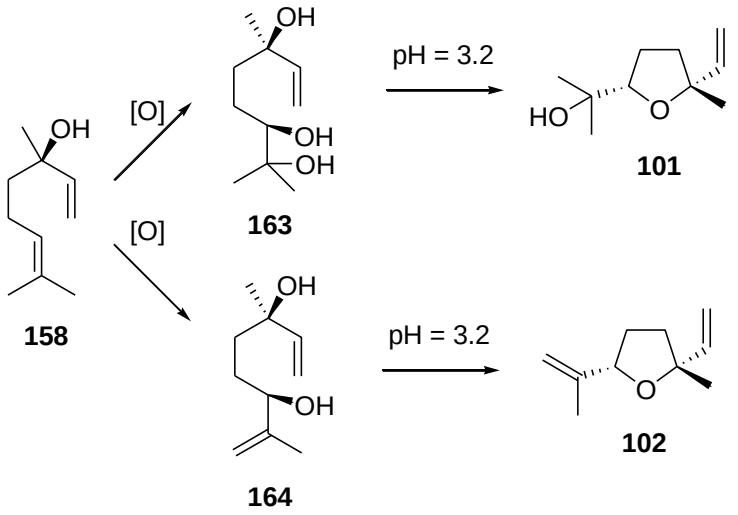

Scheme 55

It has been suggested by several authors that triol **163** might arise from epoxide **165** being itself derived from linalool (**158**), *Scheme 56*,[150,169,171,172] although other authors have dismissed this claim, reporting that there is no evidence for it.[161,173]

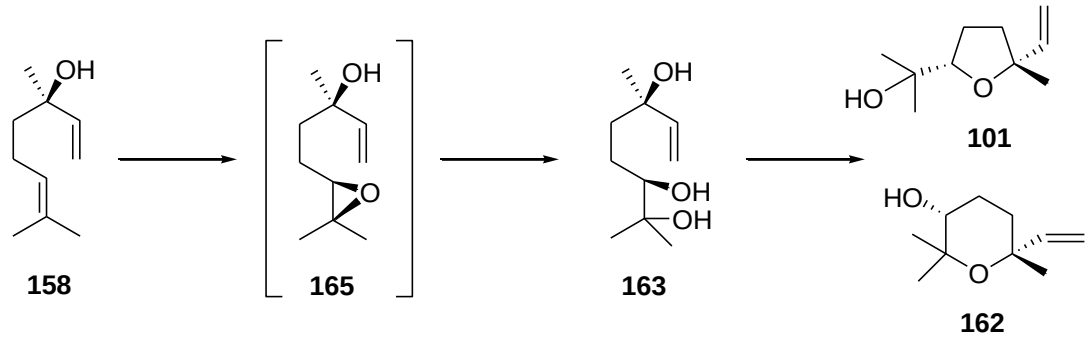

Scheme 56

It has been widely reported that heat-treatment of grape juice gives rise to many changes in terpene composition and concentrations.[159-161,165] For example, Williams *et al.*[165] reported that **101** and **102** are major components in extracts of Muscat d'Alexandrie grape juice that was heated at both pH 3 and pH 1. Heating the Muscat

d'Alexandrie grape juice for 15 minutes at 70 ^{o}C resulted in an increase in the concentrations of *cis*- and *trans*-furan linalool oxides.[161]

Anhydrofuran linalool oxides (**102**) have been reported to be formed during the aging of white wines.[146,168] A thorough search of the literature reveals little other information on these oxides.

Conflict appears within the literature as to whether the concentrations of **101** increase or decrease during wine aging. In two studies by Simpson *et al*., higher concentrations of **101** were found in older wines, as compared to younger wines.[174,175] Wilson *et al.* also found that the concentration of **101** increased with veraison (berry ripening),[176] whereas reviews published by Rapp[153] and Maicas[164] reported that they decreased in concentration during the course of aging.

It appears that grape variety and climatic conditions could play a role in the concentration of these, and many other terpenes. It has been suggested that an increase in grape maturity can cause increases, followed by decreases in the concentration of certain terpenes.[177] It is beyond the scope of this study to elaborate further on this issue. This constitutes a complex area in need of constant research, as there are many factors that affect the wine making and maturation processes.

5.2.3 Sensory Impact of 101 and 102.

The sensory properties of aroma compounds often depend on their absolute stereochemistry. Enantiomers can differ in their odour quality and are also known to show tremendous differences in their odour thresholds. For example, as mentioned in Chapter 1 (*Scheme 9*), Brown *et al.* synthesised all four isomers of the oak lactones (**25**) in order to determine their individual odour detection thresholds in wine.[54] It was found that the natural *cis*-isomer **25a** had an odour detection threshold of 24 μg/L in white wine. This is approximately seven times lower than the natural *trans*-isomer **25b**, which was found to have a threshold of 172 μg/L in white wine. One stereoisomer may therefore be many times more potent than its mirror image.[167,178] In natural systems one enantiomer may pre-dominate because enzymes are often enantiospecific, and during

the process of odour perception, the receptor site, which is optically active, can distinguish between stereoisomeric stimuli.[157,167,178] As a result, the analysis of chiral compounds in natural flavours has grown in importance over recent years, with a major focus on understanding the sensory impact of individual enantiomers.

Little is known about the sensory impact of either **101** or **102** in wine or any other medium. It has been reported that the furan linalool oxides have flavour thresholds of 3000-5000 μg/L.[146,158] This range is based on a study done by Ribereau-Gayon *et al.*[179] in 1975, whereby the flavour thresholds for the *cis*- and *trans*-furanoid linalool oxides (**101**) were determined *via* the percentage of panel members who were able to detect the aroma of the isomers at the given concentration in a 'synthetic medium' (consisting of a mixture of sugar, water and various concentrations of other monoterpenes). A table of their finding is given below, *Table 15*.

Table 15: Percentage of Panellists able to Detect **101** in a Synthetic Medium.[179]

Isomer	**Thresholds**		
	4000 μg/L	5000 μg/L	6000 μg/L
trans-(**101a,b**)	6%	17%	34%
cis-(**101c,d**)	6%	17%	45%

Although these results provide a preliminary implication that the isomers have high aroma thresholds, very little else can be inferred from this data. The results are quite vague and inconclusive and were determined under inaccurate and unreproducible conditions. As mentioned, it is known that individual enantiomers can exhibit different odour qualities and thresholds and therefore it is important to establish the sensory impact of each individual enantiomer. This was not done in this case, as the enantiomers were examined together.

In commercially concentrated blackberry juice, Georgilopoulos *et al.*[180] reported that the *trans*-isomers of the furanoid linalool oxides, **101a** and **101b** exhibited a 'strong odour' by GC-O, whereas the *cis*-isomers **101c** and **101d** had 'medium-intense odour', although no odour descriptions were given.

Wang *et al*.[181] reported that the odour character of the furanoid linalool oxides **101** was regulated by the absolute configuration of the C2 stereocentre: Both (2*R*)-isomers had leafy, earthy notes (*cis*-isomer stronger than the *trans*-), and the (2*S*)-isomers, both had sweet floral creamy notes, however it needs to be recognised that these authors mislabelled the stereocentres in their structures for the furanoid linalool oxides, with the 2*R* stereocentre being labelled as 2*S*, and *vice versa*. They then refer to the *cis*-isomers as the *trans*-, and *vice versa*. This makes their results rather speculative, as one cannot be certain as to whereabouts the error lies and therefore which compounds are being referred to with regard to their elution order of the GC column, or their sensory impact reported.

Both the *cis*- and *trans*-isomers of **101** were identified by Ito *et al*.[182] as potent odorants in Chinese Jasmine tea scented with flowers of *Jasminum sambac*. Their sensory profiles were evaluated, and both isomers were found to have odour descriptions of 'leafy and citrus'. It was also found that the furanoid linalool oxides showed optical activity for the (2*R*)-isomer in jasmine tea. In a study published by Wüst *et al.*[167] it was found that in lavender oil the (2*R*)-configured linalool oxides clearly dominated, whereas in *Osmanthus* oil the (2*R*)-configured linalool oxides were only slightly enriched.

Studies have been performed to investigate the enantiomeric ratios of the isomers of the linalool furanoid oxides. The *trans*-isomers of **101** have been reported by several authors in higher concentration in wine and juice extracts than the *cis*-isomers.[159,165,174,176] Although, in contradiction to this, a report by Askari[147] identified racemic mixtures of **101** in various wines, although no quantification was carried out. As can be seen, there is limited previous work relating to the sensory impact of these compounds, of which many contain inaccuracies and contradictions. This further highlights the need for proper sensory assessment of the furanoid linalool oxides (**101**),

and their structurally related counterparts the anhydrofuran linalool oxides, (**102**). Consequently, and as mentioned earlier we planned to explore possible new synthetic routes to such compounds.

5.2.4 Previous Methods for the Synthesis of 101 and 102.

A search of the literature reveals numerous methods trialled for the synthesis of the furanoid linalool oxides (**101**), and all four isomers have been fully characterised. However, as will be demonstrated below, many of the experimental details published for these methods are sketchy with little information given regarding conditions, yields and stereochemistry. Few previous examples exist for the synthesis of the anhydrofuran linalool oxides (**102**).

Transformations of linalool (**158**) *via* fungal, enzymatic or acidic means, replicating the bio- and hydrolytic transformations that occur during the wine making and aging processes have been reported.[173,183-186] In most cases, the *cis*- and *trans*- enantiomeric pairs have been synthesised together, although importantly they are reportedly separable *via* column chromatography.[187,188] Several other methods have also been reported for the synthesis of these oxides from linalool. These are outlined in *Scheme 57*, with conditions and yields given in *Table 16*.

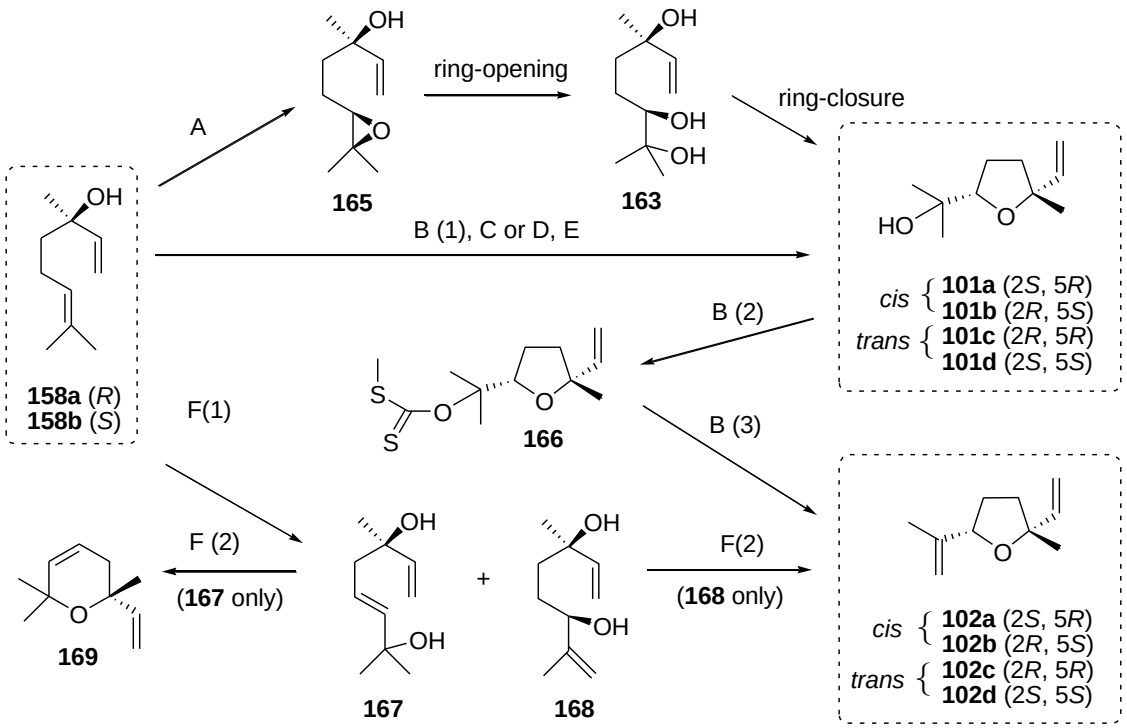

Scheme 57

Table 16: Previous Methods of Synthesis for **101** and **102**.

Pathway	SM	Conditions	Products	Yield (%)
A	**158a**	*m*-CPBA, DCM	**101a**, **101c**	[a]
A	**158b**	*as above*	**101b**, **101d**	[a]
B(1)	**158**[b]	*m*-CPBA, DCM, r.t, 22 hrs	**101**[b]	[a]
B(2)	**101**[b]	NaH, CS_2, MeI, THF, 0 ^oC	**166**[b]	[a]
B(3)	**166**[b]	200 ^oC	**102**[b]	[a]
C	**158**[b]	Cp_2TiCl_2, TBHP, ms, 40 ^oC, 46 hrs, DCM	**101**[c]	55
D	**158a**	VOL(OEt), TBHP, $CHCl_3$, 20 ^oC, 48 hrs	**101**[d]	65
E	**158a**	HCO_2H, H_2O_2	**101b**, **101c**	[a]
F(1)	**158**[b]	Na Lamp, 10 ^oC, O_2, MeOH	**167, 168**[b,e]	39
F(2)	**167**	5% H_2SO_4, 10 hrs	**159**[b]	[a]
F(2)	**18**	5% H_2SO_4, 10 hrs	**102**[b]	[a]

[a] limited or no details given; [b] no indication of stereochemistry given; [c] *cis*:*trans* 53:47; [d] *cis*:*trans* 61:39; [e] **167**:**168** 42.2:56.8% *via* GC analysis.

Borg-Karlson *et al.*[189] separately treated each enantiomer of **158** with *m*-CPBA to initially form epoxide **165**, which subsequently underwent ring-opening to give triol **163**, followed by ring-closure to furnish furanoid oxides **101** (*Scheme 57, Pathway A*) The configuration at the original stereocentre was reportedly retained during the ring-closing step, with (*S*)-linalool yielding a mixture of the (2*S*, 5*S*) and (2*R*, 5*S*) furans, whilst (*R*)-linalool gives the (2*R*, 5*R*) and (2*S*, 5*R*) isomers. Yields and further experimental conditions were not given within this paper, or references cited therein. Several other authors have also used similar procedures to follow the same pathway to give the furans **101**, although many of the experimental details are limited. [172,184,190]

The furanoid and anhydrofuranoid linalool oxides (**101** and **102**, respectively) were both synthesised by Konstantinovic *et al.*[191] as part of a synthetic route to the natural product Karahanaenone, starting from linalool (**158**). **158** was converted into **101** *via m*-CPBA epoxidation and subsequently transformed into **102** *via* formation of xanthate **166** followed by thermolysis (*Scheme 57*, *Pathway B*). The procedures within the paper are poorly reported with no details of yields obtained or control of stereochemistry.

A titanocene-catalysed oxidative cyclisation of **158** using *t*-butyl hydroperoxide (TBHP) and activated 4Å molecular sieves was performed by Lattanzi *et al.*[192] to yield an approximately 1 : 1 ratio of *cis* : *trans* isomers of **101** in 55% yield (*Scheme 57*, *Pathway C*), whereas Hartung et al.[187,193] utilised a Vanadium (V) complex catalysed cyclisation with TBHP to give a 65% yield of **101** (3 : 2 *cis* : *trans*) (*Scheme 57*, *Pathway D*).

Askari and Mosandl[194] converted (*R*)-linalool (**158**) into the (2*R*)-configured *cis*- and *trans*-diastereomers (**1b** and **1c**) *via* treatment with formic acid and hydrogen peroxide, although they reported a partial racemisation (~15%) of the resulting oxides (*Scheme 4*, *Pathway E*). Wu *et al.*[195] report that photooxidation of **8** resulted in a mixture of diols **167** and **168**, which upon heating with 5% H_2SO_4 for 10 hours yielding cyclisation products **169** and **101**, respectively (*Scheme 57*, *Pathway F*) Further details from this paper are limited, with some experimental details unclear and no indication of stereochemistry or regioselectivity given. It is also not clear whether the reported yields

are isolated or determined *via* GC analysis. *Scheme 58* illustrates previous methods for synthesis of **101** from a range of compounds other that linalool.

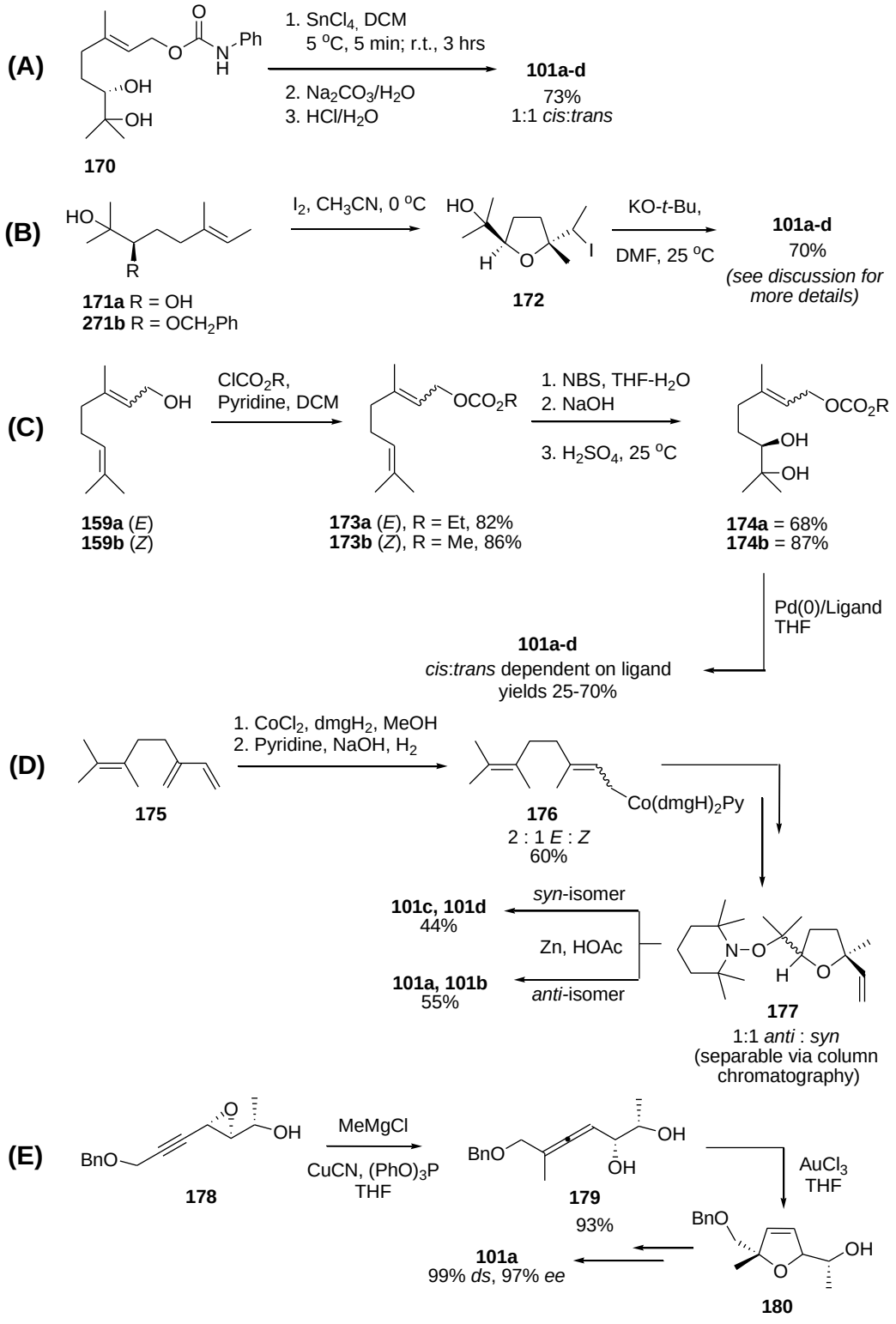

Scheme 58

Meou *et al.*[188] treated dihydroxygeranyl phenylcarbamate (**170**) with tin (IV) chloride in dichloromethane to give an equal mixture of *cis*- and *trans*-isomers of **101** with no way to control the stereochemical outcome (*Scheme 58*, *Pathway A*).

Upon investigating the stereocontrolled construction of substituted tetrahydrofuran structures, Rychnovsky *et al.*[196] individually synthesised the *cis*- and *trans*-isomers of **101** in high stereoselectivity using two different starting materials as depicted in *Scheme 58*, *Pathway B*. The tertiary alcohol **171a** afforded the *trans*-isomers as the major products (20:1 *trans*:*cis*) in 70% yield, whereas the benzylether-acetate **171b** furnished predominantly *cis*-furans (13:1 *cis*:*trans*), again in 70% yield.

Fournier-Nguefack *et al.*[197] synthesised the oxides from either geraniol (**159a**, *E*-isomer) or nerol (**159b**, *Z*-isomer) *via* the initial formation of dihydroxylesters 1**73a** and 1**73b**, which underwent palladium(0)-catalysed ring-closure to form **101** (*Scheme 58*, *Pathway C*). The ratio of *cis*:*trans* isomers was dependent on the nature of the ligand used and yields varied from 25-70%. They also found that the geometry of the double bond in the starting material (*Z* or *E*) was independent of the stereochemical outcome of the reaction.

In 1990 Howell and Pattenden[198,199] synthesised **101** as part of a demonstration of hydrocobaltation reactions of 1,3-dienes and the subsequent uses of the resulting allylcobalt complexes in the synthesis of terpenols. A four-step synthetic route starting with the terpene myrcene (**175**) gave either the *cis*- or *trans*-isomers of **101**, depending on whether the *syn* or *anti* precursor **177** was used, as outlined in *Scheme 58*, *Pathway D*. The yields however were only average.

Volz *et al.*[200] utilised gold catalysis in the synthesis of the (2*S*,5*R*) enantiomer **101a** from propargyl oxirane (**178**), in a five-step synthesis. The key steps were the *anti*-selective copper-mediated S_N2'-substitution of **178** followed by the gold-catalysed cycloisomerisation of the resulting dihydroxyallene **179** to give the core THF structure **180**. Two further steps ultimately yielded **101a** in 97% enantiopurity (*Scheme 58*, *Pathway E*).

As we have seen, the furanoid and anhydrofuranoid linalool oxides (**101** and **102**, respectively) have been established as important aroma compounds, particularly within wine. Much literature exists whereby these compounds have been identified in wine (and other natural products), but accurate quantification of their sensory importance is yet to be established. Previous methods of synthesis have followed a variety of different routes, although as demonstrated, many of the yields were average (or unreported) and control of stereochemistry was either difficult or not possible therefore making much of this work of limited value. It was therefore felt that there is a gap in the literature with regard to an effective synthesis of **101** and **102**, and the development of a new synthetic pathway to give both compounds from a common starting material would be of some value. As mentioned at the start of this chapter, it was therefore envisioned that the incorporation of the ozonolysis of a 1,2-dioxine precursor into a synthetic pathway towards the synthesis of **101** and **102** would provide a novel way to produce the requisite THF structure needed for these wine compounds whilst further exploring some interesting synthetic chemistry.

5.3 Synthesis of Wine Compounds 101 and 102.

Referring back to the retrosynthesis highlighted within *Scheme 54*, it was envisioned that the wine compounds **101** and **102** could be made *via* ozonolysis of 1,2-dioxine **154**. Chapter 1 introduced the methodology of 1,2-dioxine synthesis involving the [4π +2π] cycloaddition reaction with singlet oxygen, and Chapter 2 saw the synthesis of dioxines **3a**-**e** and steroid dioxine **82**. The same methodology for the synthesis of dioxine **154** was utilised from its 1,3-diene precursor **155**. A notable difference was that the methyl substituents are not in the 1,4-bridgehead positions, as per 1,2-dioxines **3a**-**e** but rather in the 1,3-positions as required for the synthesis of the wine compounds **101** and **102**. This also allowed us to further explore the ozonolysis reactions of 1,2-dioxines with varying substitution patterns.

5.3.1 Synthesis of 1,3-Disubstituted Bicyclic 1,2-Dioxine 154.

A simple and practical way to make the required 1,3-cyclohexadiene **155** precursor would be *via* a Birch (dissolving metal) reduction[201,202] of *m*-xylene (**181**) followed by isomerisation of the resulting 1,4-diene into its 1,3-analogue, *Scheme 59*.

Upon treating **181** with liquid ammonia and lithium only the symmetrical 1,4-diene **182** was isolated, in 59% yield. Multiple attempts were made to isomerise **182** into its conjugated 1,3-analogue **155** utilising both acidic and basic conditions but little success was achieved, with the product appearing to polymerise with each attempt. This polymerisation problem has previously been reported by several authors,[203,204] so an alternative method of directly synthesising **155** was investigated.

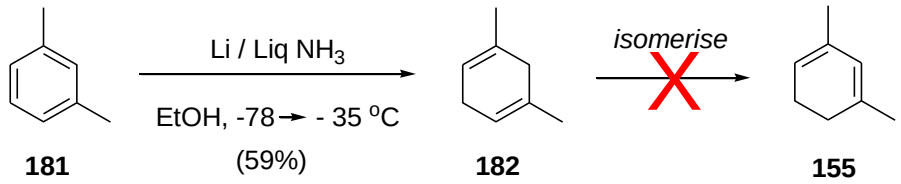

Scheme 59

It has been reported that in an attempt to synthesise diene **155** from alcohol **183**, Mirrington *et al*.[205] found that an inseparable 1 : 1 mixture of dienes (**184** and **155**) was formed when mild acidic conditions were used, *Scheme 60*. Stronger acidic conditions resulted in a reduced amount of **184**, although this was in favour of large amounts of polymeric material (along with reduced amounts of **155**). The diene mixture was also found to decompose upon standing, with the authors suggesting that upon formation, the mixture should be used without delay. In order to trial this method for the synthesis of **155**, it was firstly necessary to synthesise the tertiary alcohol **183**. Commercially available 3-methyl-2-cyclohexen-1-one (**185**) was subjected to a Grignard reaction with methylmagnesium bromide to furnish **183** in a good yield of 88%, *Scheme 60*.[205,206]

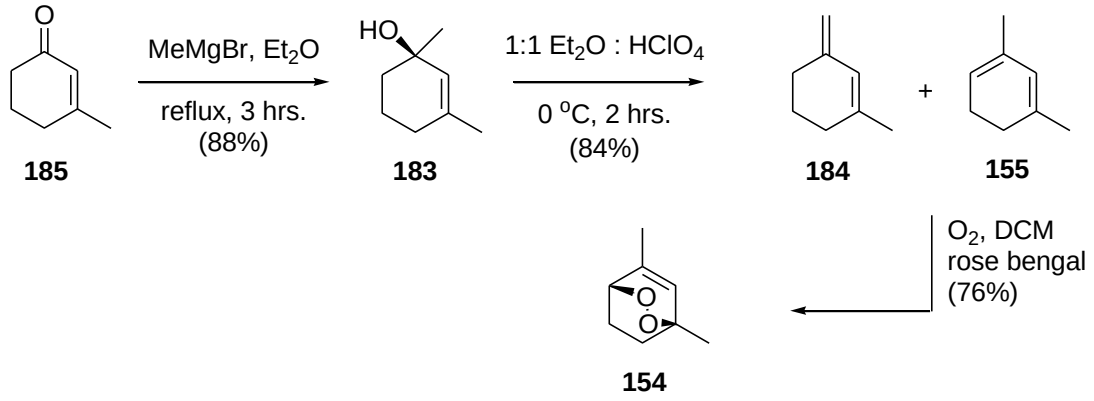

Scheme 60

With enone **185** in hand and upon repeating the best conditions reported by Mirrington (using a 1:1 mixture of diethyl ether and 5% perchloric acid solution at room temperature), a mixture of dienes **184** and **155** was formed. Crude NMR spectra showed minimal impurities, with no further purification needed. Integration of the olefinic ^{1}H NMR peaks confirmed a 1:1 mixture of the dienes, with the ^{1}H NMR data matching that previously reported within the literature, *Figure 27*.[205,206]

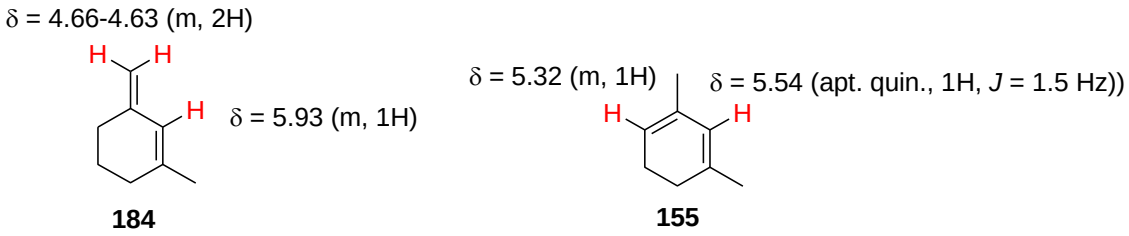

Figure 27: ^{1}H NMR signals used to determine ratio of dienes **184** and **155**.

The diene mixture was photolysed to afford the desired 1,2-dioxine **154**. A complex mixture of products was formed during the photolysis, although the major isolable product was **154** in 76% yield, *Scheme 60*. This yield was based upon the molar amount of 1,3-diene **155** within the reaction mixture. It was predicted that diene **184** could potentially form hazardous hydroperoxides along with other byproducts during its reaction with singlet oxygen, but none of these products were isolated upon purification.

The previously unknown 1,2-dioxine was formed as a racemic mixture, **154a** and **154b**, due to singlet oxygen 'attacking' the achiral diene equally from both faces, *Figure 28a*. The expected ^{1}H NMR signals were seen for the olefinic proton (δ = 6.03 ppm) and the proton α to the peroxide linkage (δ = 4.42 ppm), *Figure 28b*.

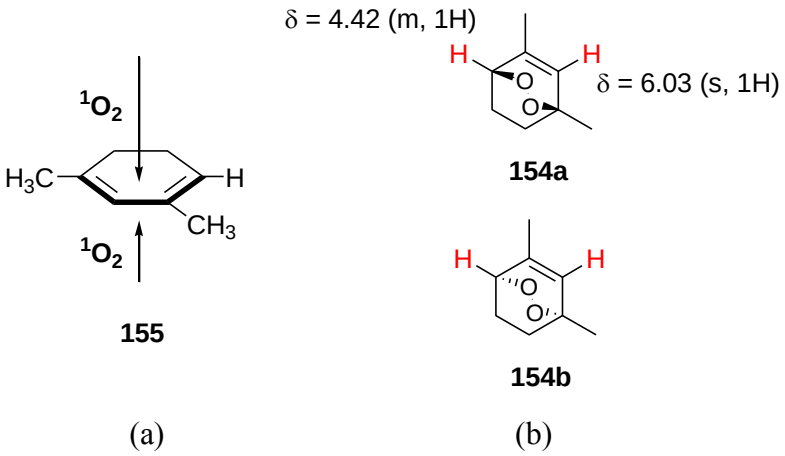

Figure 28: Details for (a) formation of and (b) characterisation of 1,2-Dioxine **154**.

5.3.2 Ozonolysis and Ring-Contractions of 1,2-Dioxine 154.

With the precursor 1,2-dioxine **154** in hand, referring back to *Scheme 54*, the next step was to perform ozonolysis on **154** in the same manner as described for 1,2-dioxines **3a-e** in Chapter 3. Triphenylphosphine was once again employed to reduce the ozonide, and it is worthy to note that the expected dicarbonyl product in this case is keto-aldehyde **156** (rather than dialdehydes as previously seen), due to having a methyl group attached to one of the alkene carbons.

The ozonolysis of **154** proceeded smoothly, resulting in the desired keto-aldehyde **156** in 45% yield, *Scheme 61*. The product was stable upon purification enabling full characterisation, and fortunately no rearrangements were seen. The ^{1}H NMR spectrum showed an aldehyde peak at δ = 9.75 ppm, appearing as a doublet with a small coupling constant of J = 1.8 Hz. The ROESY spectrum showed a correlation between the aldehyde proton and its peri-methyl protons, which would account for this long-range splitting. Singlets were seen for the methyl and methyl ketone peaks at δ = 1.19 and

2.14 ppm respectively. The ^{13}C NMR spectrum (*Figure 29*) showed the expected aldehyde and ketone peaks at δ = 204.0 and 202.2 ppm respectively, along with the bridgehead carbons α to the peroxide linkage at δ = 85.8 and 85.3 ppm indicative of the peroxide linkage remaining intact.

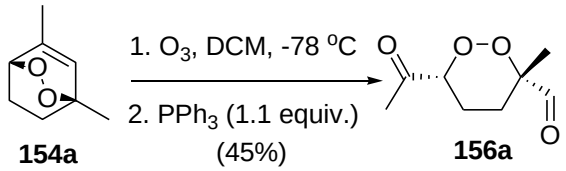

Scheme 61

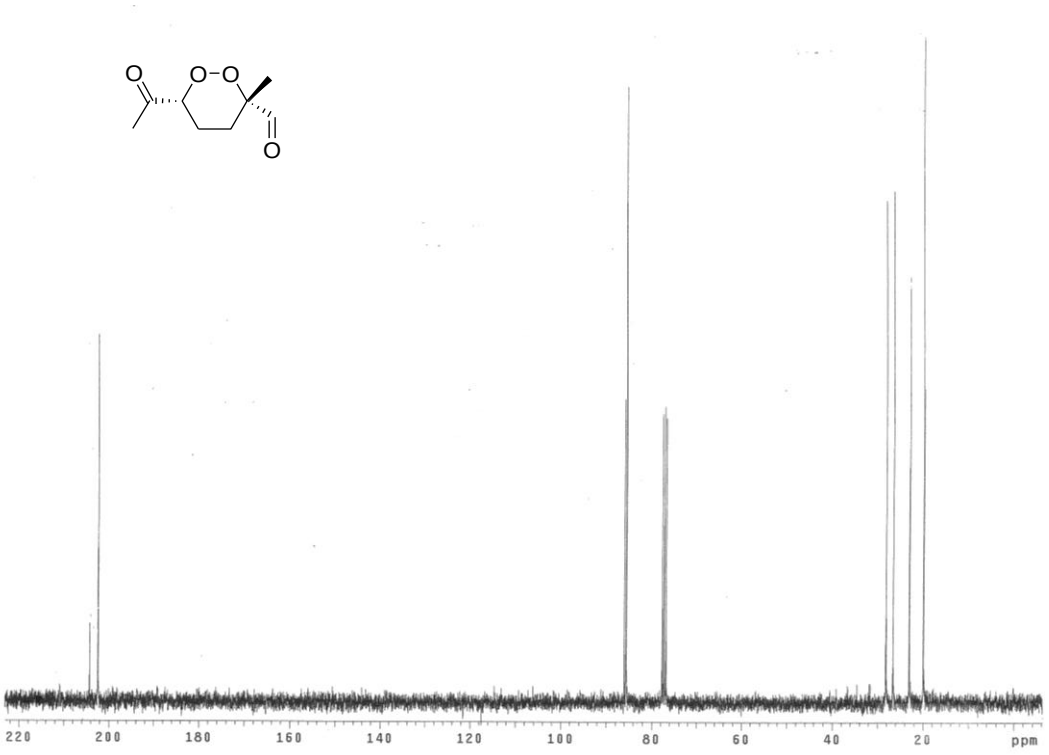

Figure 29: 300 MHz ^{13}C NMR Spectrum for Keto-Aldehyde **156**.

The next step towards the construction of furans **101** and **102** required ring-contraction into the furan **153**. With the presence of an acidic proton α to the peroxide, it was predicted that the dioxine would undergo a Kornblum DeLaMare rearrangement to give furan **153** upon treatment with base, *Scheme 62*. The mechanism of this reaction was discussed in Chapter 1 (*Scheme 6*) involving deprotonation followed by cleavage of the

peroxide linkage to give the ring-opened ketol **186** which exists in equilibrium with the ring-closed furanol, **153**.

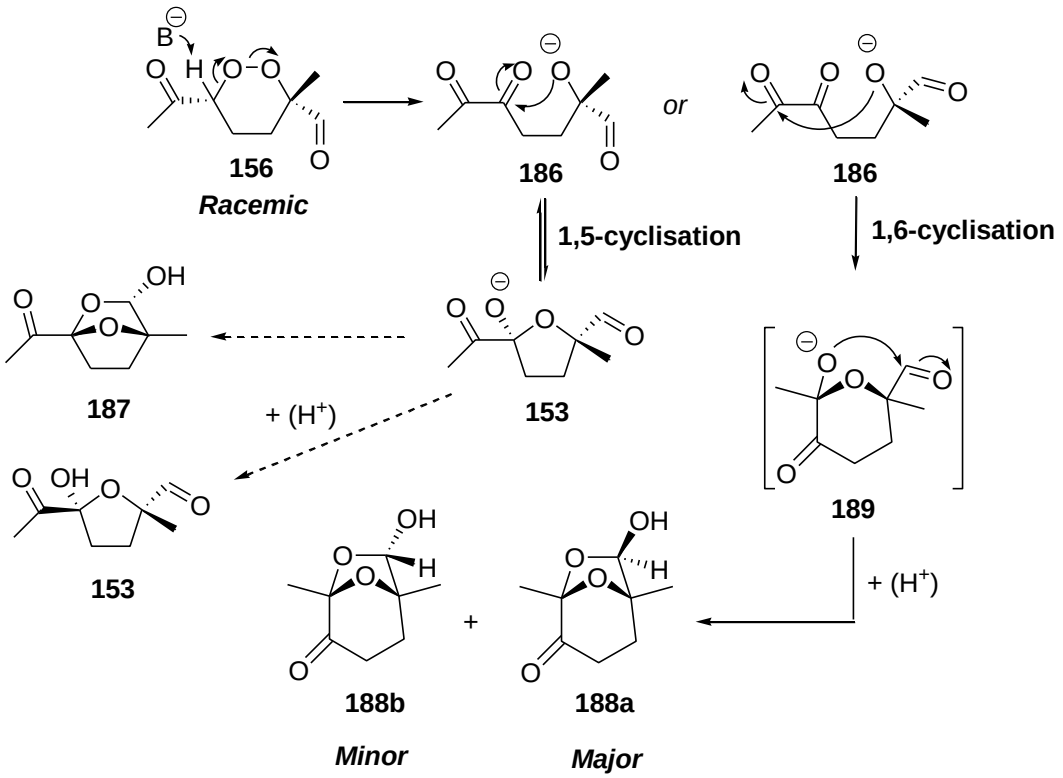

Scheme 62

Upon adding a catalytic amount of NEt_3 to pure **156** it was immediately evident from the lack of aldehyde peaks in the NMR spectra that the product formed was not the desired furan **153**. Examination revealed that the products formed were a mixture of two diastereomers, present in a 2.7 : 1 ratio, labelled as 'major' and 'minor' isomers. The two diastereomers were inseparable *via* column chromatography, and upon adding a further catalytic amount of base (NEt_3) to the diastereomeric mixture, the minor isomer could be readily converted into > 95% of the major isomer.

Bicyclic **187** was initially proposed as the likely product, postulated to occur *via* an intramolecular 1,5-cyclisation of furan **153** (*Scheme 62*), although it was soon evident that this was not the correct structure. The major isomer was a crystalline product, which enabled a crystal structure to be obtained, unambiguously determining the

structure to be that of bicyclic lactol **188a** (*Figure 30*) likely to result from a cascading reaction involving a 1,6-cyclisation of γ-hydroxydione **186**, to afford pyran intermediate precursor **189**, as shown in *Scheme* 62

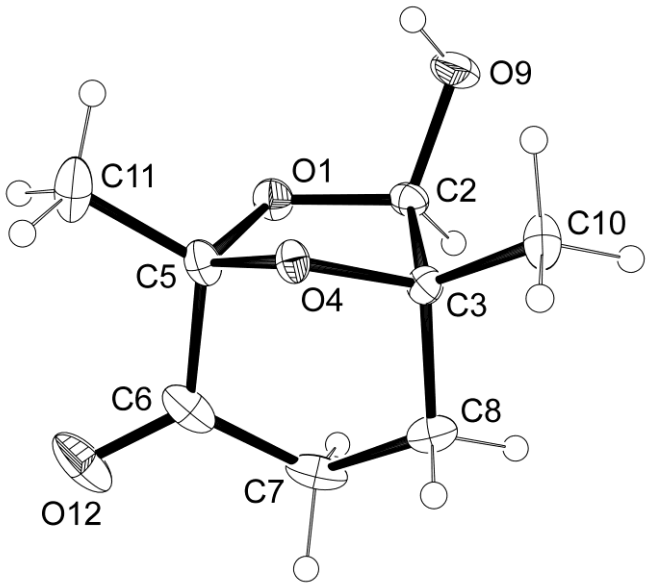

Figure 30: Crystal Structure of Bicyclic **188a** Showing the Crystallographic Numbering Employed.

No examples of this kind of 'competitive' cyclisation could be found within the literature, however our results clearly indicate that 1,6-cyclisation is preferred over 1,5 under the reaction conditions employed.

The major isomer, **188a**, was fully characterised, but the minor isomer, **188b**, was not able to be isolated and fully characterised in its own right due to difficulties in separation of **188b** from **188a**. Proton and carbon NMR data, along with 2D spectra of the isomeric mixture was obtained and this allowed us to clearly identify each isomer and confirm stereochemistry. Along with the crystallographic structure obtained for **188a**, ROESY correlations supported the H_2 proton facing 'down' relative to the ether bridge, with correlations seen between the H_2 and H_7 and H_8 protons, as depicted in *Figure 31*. An absence of any ROESY correlations in **188b** between these protons in the minor isomer confirms that the H_2 proton must be facing upwards.

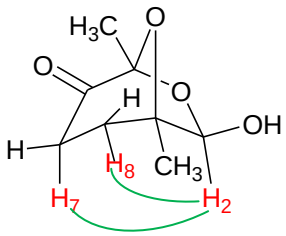

Figure 31: ROESY Correlations for Major Isomer of Bicyclic **188a**.

The overall yield for the catalytic conversion from keto-aldehyde **156** to bicyclic **188** was 74 % for both isomers. Additional experiments found that further addition of base to the isomeric mixture resulted in a conversion from 2.7 : 1 major : minor isomers to > 95 % major isomer. The mixture also isomerised to predominately the major isomer upon performing NMR in d_6-benzene, and the minor isomer also slowly isomerised to give > 95% major crystalline isomer upon being kept neat in the refrigerator overnight. This indicates that firstly, the major isomer **188a** is clearly the preferred isomer, likely to be the thermodynamic product, and secondly, that in order for the isomerisation of **188b** into **188a** to occur, the products must be in equilibrium with their ring-opened counterpart **189**.

As mentioned above, keto-aldehyde **156** was stable upon purification, although further experimentation found that if there was a delay of more than approximately two days between performing ozonolysis and subsequent PPh_3 reduction on dioxine **154** before purification of the resulting crude mixture, bicyclic compounds **188a** and **b** began to form, with full conversion from **156** to **188** within a week. This indicated that even upon being exposed to mildly basic conditions (eg PPh_3), removal of the most acidic proton to initiate ring-opening is possible. Under these conditions the reaction is much slower and resulted in a lower amount of the major isomer being formed (1.6 : 1 major : minor isomer).

Since it was apparent that the equilibrium for the bicyclic lactones **188a** and **188b** could easily be reversed upon addition of base, it was anticipated that a stabilised phosphorous ylide could be used to firstly act as a base to reverse the equilibrium back to the ring-opened *cis*-γ-hydroxyone **186** and then act in its capacity as an ylide to trap

the aldehyde and prevent any undesired intramolecular cyclisations from occurring. Formation of the desired furan was hoped to result *via* conventional ring-closure of the *cis*-γ-hydroxyenone **186**. Accordingly, upon adding benzyl-(triphenylphosphanylidene) (**190**) to the bicyclic lactone **188**, four products were formed, which after full characterisation were identified as being **191**, **192a**, **192b**, and **193**, *Scheme 63*. These products were each derived from Wittig reactions on the different products in the equilibrium series. Yields for the four products were dependent upon the amount of ylide used, which will be discussed in detail later in this chapter.

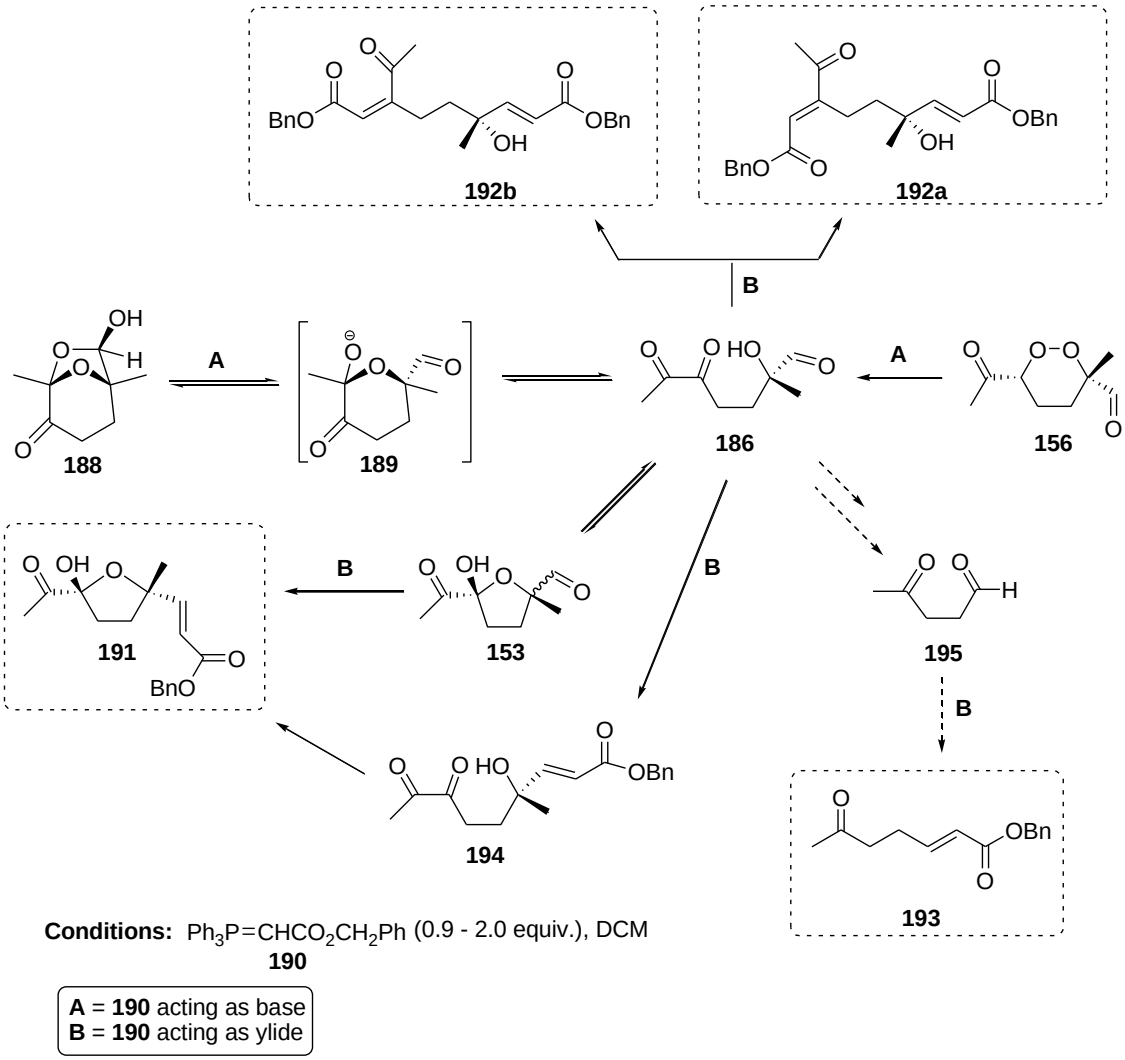

Scheme 63

Since we know that bicyclic **188** exists in equilibrium with the *cis*-γ-hydroxyone **186**, which in turn is derived from 1,2-dioxine **156**; it was envisioned that furan **153** could also be formed directly from **156** upon addition of ylide **190** which would firstly act as a base to give the ring-opened γ-hydroxyone **186**, and then follow the same reactions to yield **191**. It is also possible that furan **191** is formed *via* initial trapping of the aldehyde moiety in **186** to furnish **194** followed by subsequent ring-closure into **191**, thereby not forming furan **153** at all. The addition of ylide to **156** worked successfully, with the same four products (**191**, **192a** and **192b**, and **193**) formed, once again with yields dependent upon the amount of ylide used (to be discussed later).

The desired 'trapped' furan **191** existed as an inseparable mixture of *cis*- and *trans*-diastereomers. The ^{1}H NMR spectrum showed two separate sets of alkene peaks each with a coupling of J = 15.6 Hz, indicative of *E*-geometry. The methyl ketone protons resonated at δ = 2.30 and 2.31 ppm for each diastereomer, whilst the hydroxyl peaks were easily identified as singlets at δ = 4.38 and 4.37 ppm due to their disappearance upon addition of D_2O. The ^{1}H NMR spectrum is depicted in *Figure 32*, whilst a summary of key ^{13}C NMR shifts is shown in *Table 17*, with the resonances of the two bridgehead carbons (C_3 and C_6) being indicative of a furanol structure. Carbon peaks were assigned *via* HMQC and HMBC correlations. Individual NMR data and associated stereochemistry was unable to extracted from the 2D spectra for the individual diastereomers due to the peaks being too close to differentiate from each other.

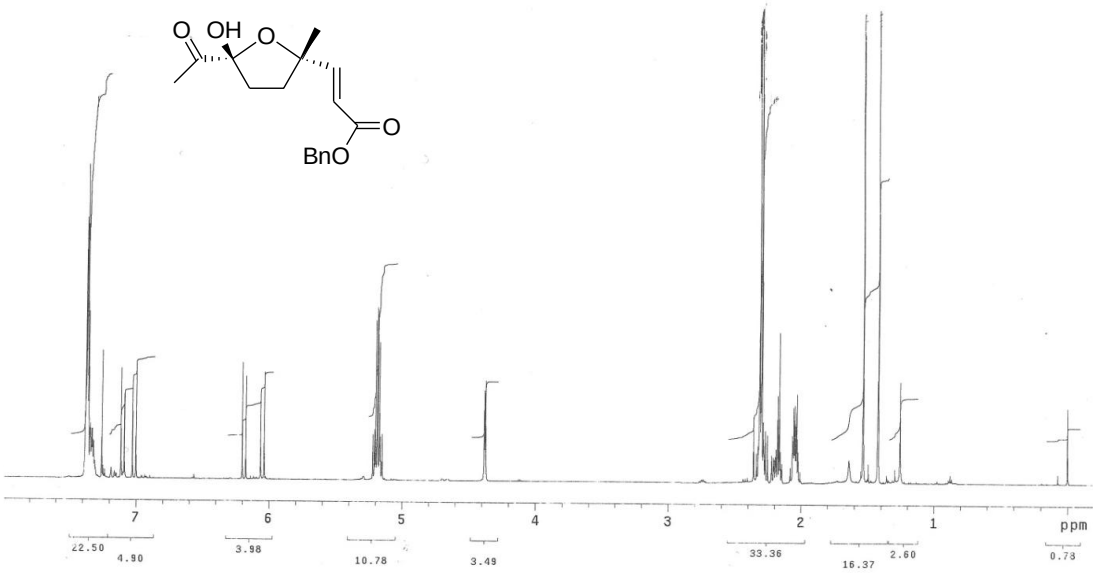

Figure 32: 600 MHz ^{1}H NMR Spectrum Trapped Furan **191**.

Table 17: Important ^{13}C NMR Resonances for Diastereomeric Furans **191**.

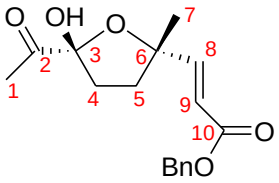

Carbon No.	δ (ppm)*
1	23.3, 22.7
2	205.2, 205.0
3	104.7, 104.6
4	35.2, 34.9
5	36.74, 36.66
6	85.2, 85.1
7	27.8, 26.0
8	152.4, 152.0
9	119.0, 118.5
10	166.5, 166.3

* 600 MHz Spectrum

Products **192a** and **192b** showed NMR data indicating that two carbonyl groups had been trapped by the ylide, with doubling up on both the benzyl and ester peaks. Each structure contained two doublets in the alkene region with coupling constants of J = 15.9 Hz and 15.3 Hz for products **192a** and **192b** respectively, indicating that the aldehyde had been trapped to give the alkene with *E*-geometry. Further singlet peaks at δ = 6.56 ppm and 5.71 ppm (**192a** and **192b** respectively) each integrating to one proton were seen in the ^{1}H NMR spectrum, indicating that a ketone group had likely been trapped. ^{13}C NMR for products **192a** and **192b** suggested that the methyl ketone group was still present. Structures **192a** and **192b** were therefore proposed, derived from protection of the central carbonyl in *cis*-γ-hydroxyone **188**. The signals at δ = 6.56 and 5.71 ppm were therefore assigned to the alkene peaks of **192a** and **192b** respectively. At ambient temperature, stabilised ylides usually only react with aldehydes, however as previous research within our group has found,[207] the presence of a hydroxyl group within the vicinity of a ketone promotes intramolecular hydrogen bonding thereby enhancing the electrophilicity of the carbon atom of the ketone enabling it to participate in Wittig type reactions.

ROESY correlations were used to define the geometry around the tri-substituted alkene in both **192a** and **192b**. For **192a** the ROESY correlation between the alkene proton and the methyl ketone protons (shown in red, *Figure 33*) was evident and therefore assigned *E*-geometry.

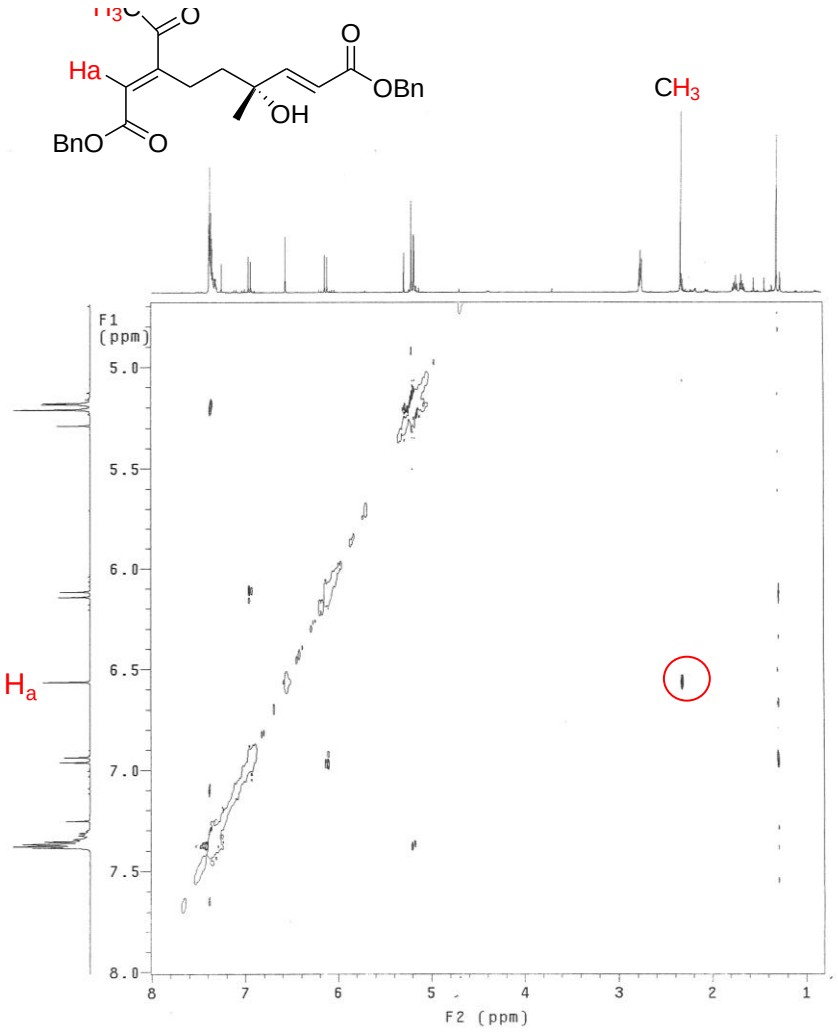

Figure 33: ROESY Spectrum of **192a**.

192b lacked any ROESY correlation between these protons, but rather showed ROESY correlations between the alkene proton and its adjacent methylene protons (shown in red, *Figure 34*), which would only be seen with *Z* geometry about the alkene.

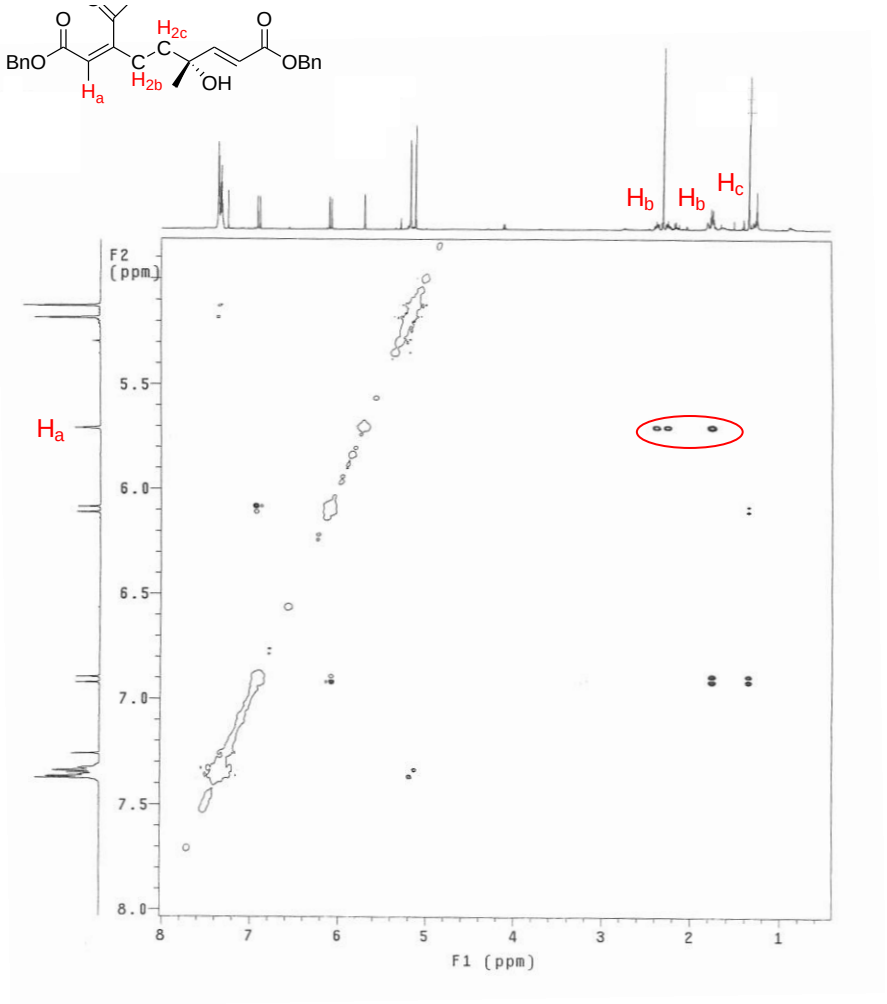

Figure 34: ROESY Spectrum of **192b**.

NMR data for the final unusual product **193** showed the alkene benzyl ester sub-unit had indeed formed, along with a methyl ketone, and IR spectra revealed an absence of any hydroxyl groups. After careful analysis of all data, including 2D NMR, this previously unknown compound was determined to be that of **193**. Similar esters, namely an *n*-butyl group replacing of the methyl in **193** and another example where a methyl group replaces the phenyl in **193** have previously been reported,[208,209] with these products showing similar resonances and coupling patterns to that of **193**. The proton NMR spectrum showed the alkene protons splitting into a dt, with major coupling of J = 15.6 Hz, evident of *E*-geometry. The alkene proton α to the ester (H_a) also showed long-range coupling of J = 1.6 Hz to its β-methylene protons, whilst H_b exhibited coupling of J = 6.6 Hz to its neighbouring methylene group (both evident through ROESY correlations), *Figure 35*.

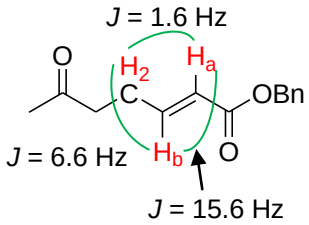

Figure 35: [1]H NMR ROESY Correlations and Coupling Constants for **193**.

With full characterisation data confirming the structure of product **193**, the question arose as to how this product was formed. Retro analysis from **193** back to starting materials **156** or **188** (*Scheme 64*) shows a likely pathway leading to the formation of **193**, with the most likely precursor being keto-aldehyde **195**, whereby the aldehyde portion is subsequently trapped *in-situ* by ylide **190** to ultimately yield **193**.

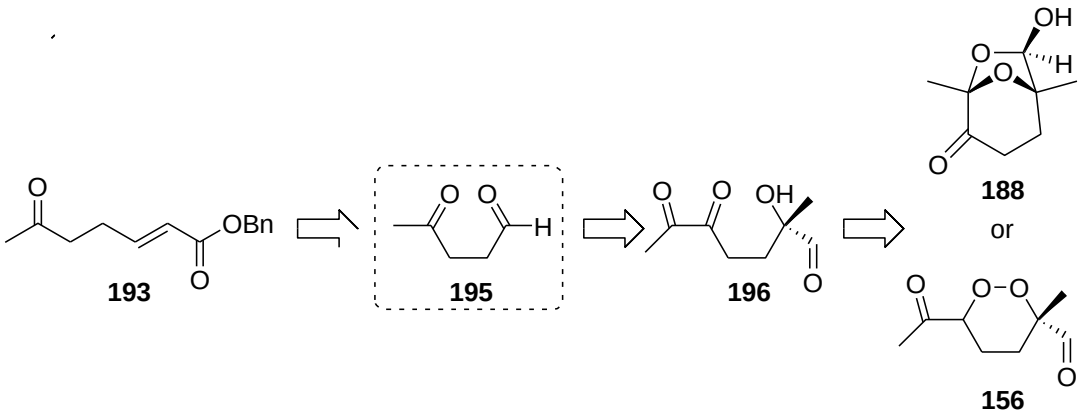

Scheme 64

The next logical question one would then ask is how was keto-aldehyde **195** formed? *Scheme 65* shows a potential pathway for the formation of **195** from **186**, involving the initial formation of a cyclopropanol **196** intermediate *via* the base-promoted breakdown of **186**, which could rearrange into aldehyde **195** *via* two plausible pathways.

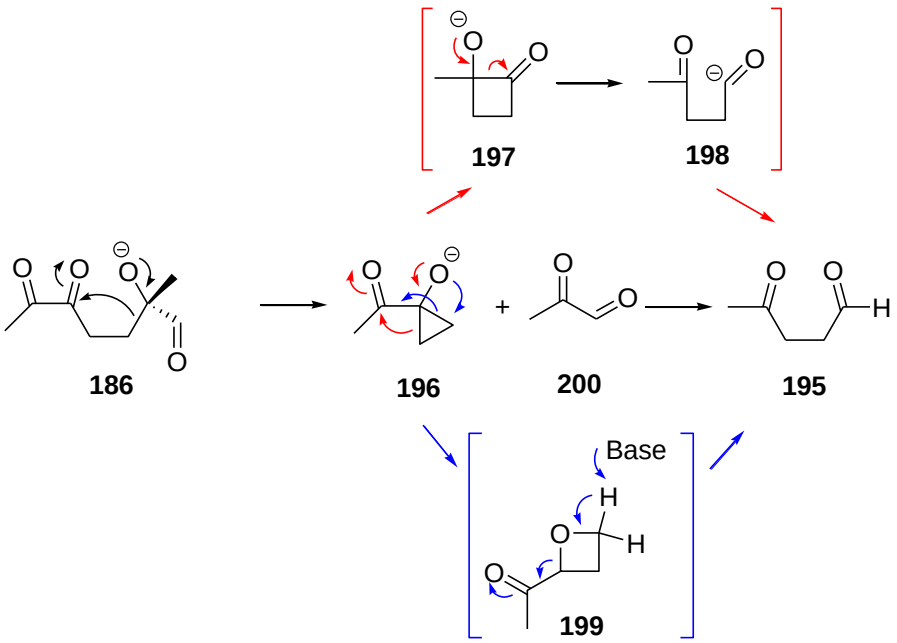

Scheme 65

The pathway in red involves a base-promoted *α*-ketol rearrangement of **196**, involving a 1,2-alkyl shift to give cyclobutanone **197**. This would likely proceed *via* an umpolong intermediate employing polarity inversion to give acyl anion **198** enabling the formation of keto-aldehyde **195** under basic conditions. Similar rearrangements have previously been reported, acting as precedents for this pathway.[210,211] The pathway in blue involves formation of an oxetane intermediate **199**, which is postulated to rearrange under basic conditions, in a step similar to the second step in the Kormblum DeLaMare rearrangement, to give the keto-aldehyde **195**. A search of the literature found no precedent for this type of rearrangement occurring. The keto-aldehyde **200** is commonly known as methylglyoxal, and is a highly toxic by-product of several metabolic pathways.[212] This product was not isolated, although if formed would likely be an unstable by-product and polymerise upon formation. The cyclopropane intermediate **196** is likely to exhibit ring strain, making strain release a driving force for its rearrangement and subsequent ring-opening.

Whilst the formation of the benzyl-ester-ketone **193** is of interest, it is difficult to postulate how this by-product formed without a more detailed investigation, and whilst some interesting mechanistic chemistry seems to be at play within this reaction, it was

only formed in minor quantities and was beyond the scope of this research to investigate this further.

The yields for the Wittig reactions on both the keto-aldehyde **156** and bicyclic **188** were highly variable and found to be dependent upon both the amount of ylide used and the rate of addition. The general trend seen was that the more equivalents of ylide added the lower the yields and the more complex the mixture of products that resulted, as collated in *Table 18*.

Table 18: Yields for Keto-Aldehyde **156** and Bicyclic **188** Wittig Reactions.

Entry	SM		Ylide	Products and Yields (%)					
			(equiv.) 190	191	192a	192b	193	188	Total
1	**156**	*Pure*	0.9	12	6	8	-	-	26
2			1.1	9	5	11	10	-	35
3			1.2	complex mixture products formed					
4		*Crude**	0.6	22	-	-	8	29	59
5	**188**	*Pure*	0.9	54	14	16	-	8	92
6			1.0	39	-	35	-	-	74

* Yield taken over three steps: ozonolysis and reduction of dioxine **154** and Wittig of crude **156**.

When 1.2 equivalents of ylide was added to the pure keto-aldehyde **156** (*Table 18, Entry 3*), a complex mixture with at least eight spots visible by TLC was observed. It is likely that the ylide was reacting with carbonyl groups within both the cyclic and ring-opened intermediates, producing a complex mixture of products.

Addition of ylide to the crude keto-aldehyde ozonolysis mixture was also found to be an effective way to obtain furan **191**, thereby eliminating an extra purification step, *Table 18, Entry 4*. It was found that upon adding 0.6 equivalents of ylide to the crude ozonolysis mixture (assuming 100 % conversion from dioxine **154** to keto-aldehyde **156**), furan **191** was isolated in 22% yield, along with **193** (8%) and bicyclic **188** (29%) (which could easily be recovered and recycled). Under these conditions, none of the double addition products **192a** or **192b** were seen. Upon examination of all entries in *Table 18*, it can be seen that by increasing the amount of ylide used, the yield of furan **191** decreased in favour of **192a** and **192b**, making it therefore favourable to add a

lower amount of ylide, recover the bicyclic starting material and treat this again with more ylide. Interestingly, none of **193** was seen upon using bicyclic **188** as the starting material, *Table 18*, *Entries 5* and *6*.

Since furan **191** could be formed from keto-aldehyde **156** it was therefore deemed unnecessary to incorporate bicyclic **188** into the synthetic pathway. As can be seen in *Scheme 66, Pathway (a)* this multi-step sequence requires two extra purification steps and an overall lower yield. If *Pathway (b)*, *Scheme 66* is followed, the ylide can be added directly to the crude ozonolysis mixture containing keto-aldehyde **156**, thereby making it possible to go straight from 1,2-dioxine **154** to furan **191** in a simple one pot procedure resulting in a slightly higher yield and requiring only a single purification step.

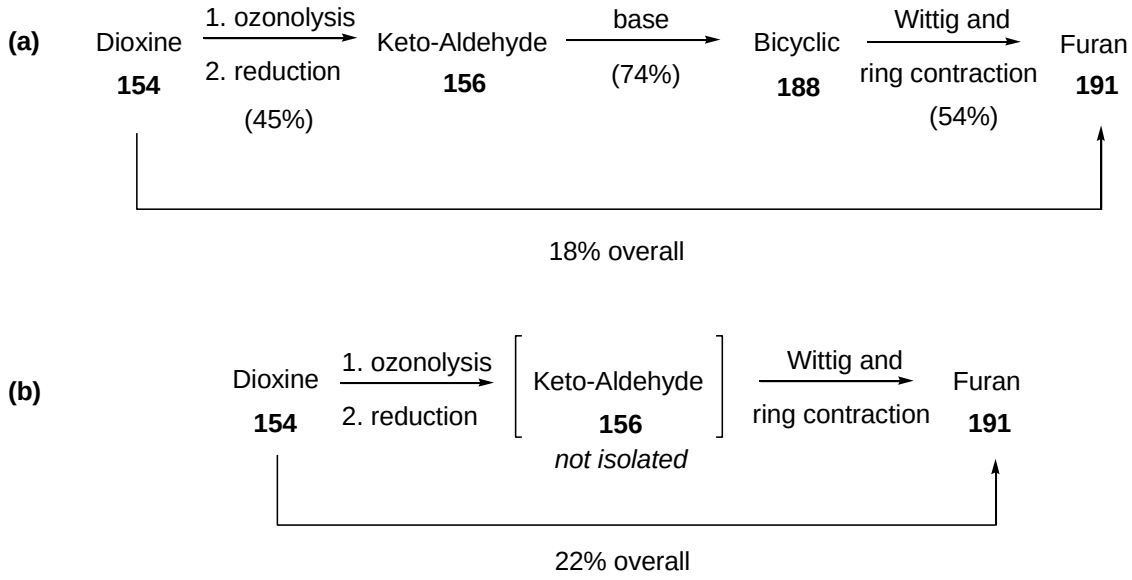

Scheme 66

5.3.3 Xanthation and Acetylation of 191.

With the core furan structure **191** in hand, there were three sections of the molecule left to structurally manipulate in order to give the desired functionalities required for the two wine compounds **101** and **102**.

It was initially proposed to reduce the hydroxyl moiety in **191** *via* a Barton-McCombie Deoxygenation[213] which firstly involves the conversion of the hydroxyl moiety into a xanthate to give **201**, followed by radical induced reduction to yield the desired furan **202** which bears the necessary proton α to the ketone moiety, *Scheme 67, Pathway A*. Upon following the standard literature procedure[214] in an attempt to make Xanthate **201** it was found that bicyclic ester **203** was formed in preference, *Scheme 67, pathway B*.

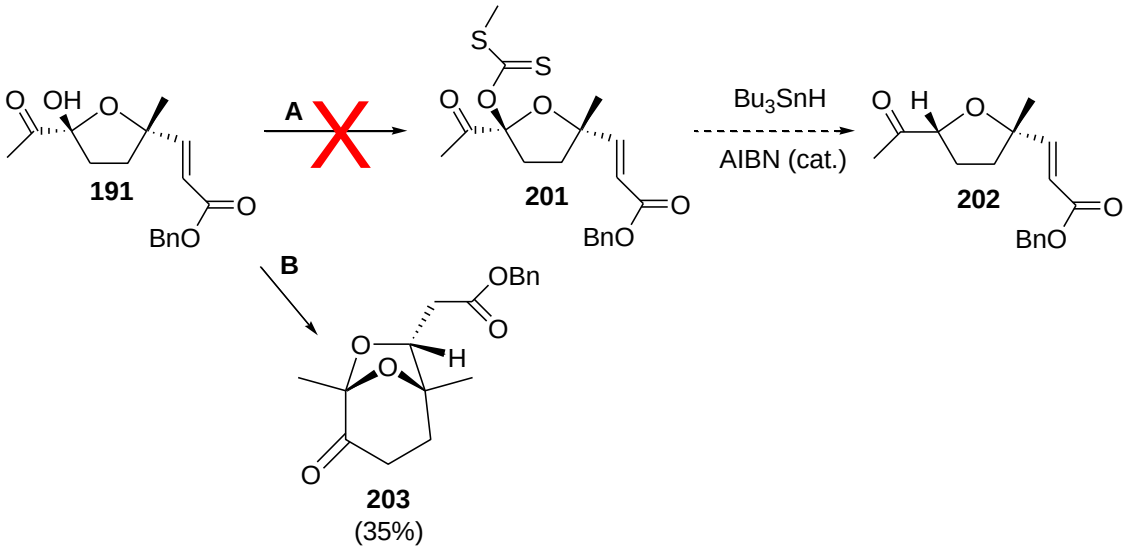

Conditions: NaH (1.5 equiv.), THF, 0 °C, CS_2 (70 equiv.), MeI (70 equiv.), 0 °C, 40 min.

Scheme 67

NMR spectra showed only a single diastereomer, with 2D ROESY correlations determining the stereochemistry to be that where the ester group is on the opposite face to the bridgehead ether group, as can be seen in *Table 19*.

Table 19: ROESY Peaks of Interest for Bicyclic **203**.

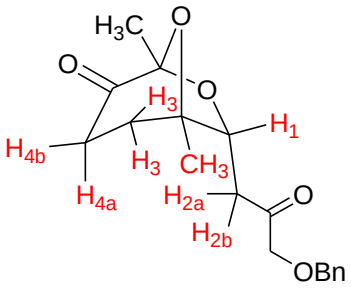

	^{1}H NMR δ (ppm)*	ROESY
H_1	4.27 (dd, 1H, *J* = 9.0, 4.6 Hz)	CH_3
H_{2a}	2.85 (dd, 1H, *J* = 15.3, 9.0 Hz)	H_3, H_{4a}, CH_3
H_{2b}	2.63 (dd, 1H, *J* = 15.3, 4.6 Hz)	H_3, H_{4a}, CH_3
H_3	2.14-2.11 (m, 2H)	H_{2a}, H_{2b}, CH_3
H_{4a}	2.76 (dt, 1H, *J* = 16.8, 10.2 Hz)	H_{2a}, H_{2b}
H_{4b}	2.34ddd, 1H, *J* = 16.8, 6.9, 2.7 Hz)	-

*600 MHz Spectra

Although the desired furan **202** was not formed in this instance, these unexpected results are of interest, as the formation of this bicyclic compound is likely to follow a similar pathway to that previously seen for the formation of bicyclic **188**, *Scheme 62*. Under basic conditions initially induced by the addition of NaH, alcohol **191** is likely to be in equilibrium with its ring-opened counterpart **204**, which readily undergoes intramolecular 1,6-cyclisation to yield pyran **205**. Intramolecular cyclisation then affords bicyclic ester **203**, *Scheme 68*, providing a further example of 1,6-cyclisation being favoured over 1,5-cyclisation.

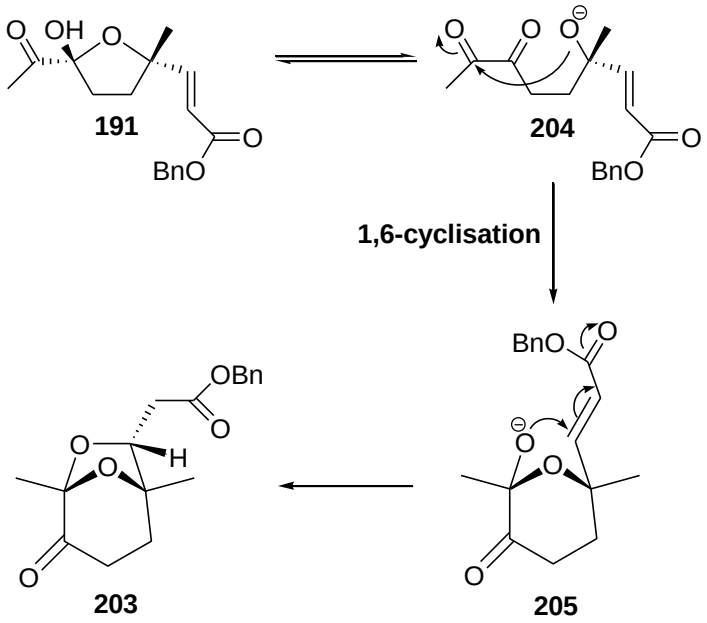

Scheme 68

A thorough search of the literature found numerous examples of various dioxa-substituted bicyclo[3.2.1]octanes, with some bearing various carbonyl, hydroxyl or methyl substrates,[103,215-218] although none had a skeletal structure exactly resembling that of either **188** or **203**, making the formation of these new core structures of synthetic interest. This could prove to be an interesting new area of chemistry worthy of future exploration.

It would appear that having a hydroxyl moiety α to the furan could lead to problematic ring-opening reactions. It was decided that the best approach would be to protect the hydroxyl to prevent any further ring-opening and potential cyclisations from occurring, and initially focus on converting the remaining groups into the necessary functionalities. Once this was achieved deprotection could take place as the final stage of the synthetic sequence to ultimately furnish the wine compounds **101** and **102**.

Furan **191** was successfully acetylated in an excellent 89% yield to furnish **204**, *Scheme 69*. Despite employing mildly basic conditions (pyridine), no rearrangements were seen. An inseparable mixture of diastereomers was produced, with individual NMR data for each isomer unable to be extracted due to diastereomeric resonances appearing too

close to one another. The acetate group was evident through singlet methyl peaks seen at $\delta = 2.33$ and 2.32 ppm for the two isomers in the ^{1}H NMR spectrum. ^{13}C signals showed two carbonyl peaks and quaternary bridgehead carbons in accord with that of the starting hydroxyl furan **191**, along with the additional acetate carbonyl, as summerised in *Table 20*.

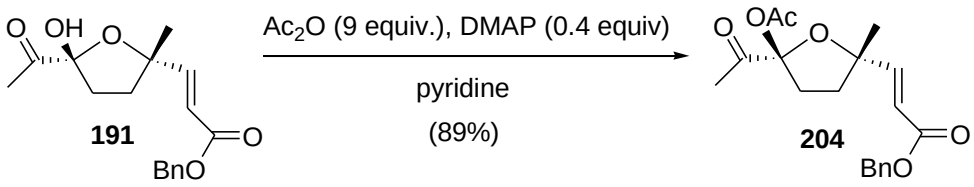

Scheme 69

Table 20: Characteristic ^{13}C NMR Data for Diastereomeric Acetate Furans **204**

Carbon	**^{13}C δ (ppm)***
Methyl ketone	202.6, 201.9
Acetate carbonyl	169.9, 169.8
Alkene-ester carbonyl	166.3, 166.2
Bridgehead carbon (α to acetate)	108.7, 108.3
Bridgehead carbon (α to methyl)	87.09, 87.07

*300 MHz Spectra

With the protecting acetate locking the furan structure into place, the remaining parts of the molecule could be manipulated to give their desired functionalities. It was decided that the next step would be formation of the terminal alkene common to both the furanoid linalool oxides (**101**) and anhydrofuran linalool oxides (**102**).

5.3.4 Attempted Formation of Terminal Alkene Subunit.

Scheme 70 below outlines a retrosynthetic scheme showing how terminal alkene **205** was to be synthesised from the acetate-protected furan **204**. The aim was to firstly convert **204** into acid **206** followed by a Barton-decarboxylation to yield the desired alkene **205**.

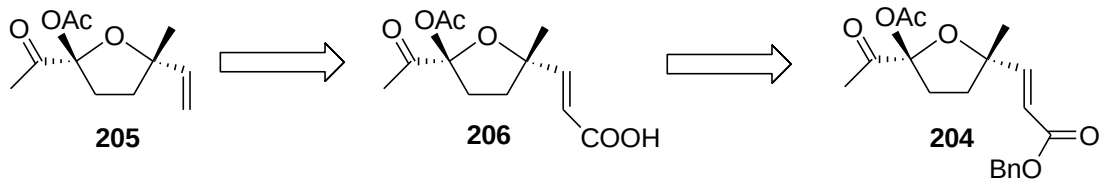

Scheme 70

Upon performing base-promoted hydrolysis of **204** in methanol, acid **207** was formed instead of **206**, *Scheme 71*. It is of no surprise that the acetate group did not survive treatment with base, although its presence did successfully prevent ring-opening and rearrangement of the furan. The formation of **207** over **206** has no bearing on the desired outcome of these reactions, and is therefore of no ill-consequence. Acid **207** was isolated as an inseparable mixture of diastereomers, evident through the absence of a benzyl group in the NMR spectra. The other interesting feature seen in the NMR spectra was the distinct absence of acetate peaks along with the appearance of a set of singlets at δ = 3.26 and 3.27 ppm in the proton spectrum, and δ = 51.1 and 50.7 ppm in the carbon spectrum, indicative of methoxy peaks, due to the acetate being replaced with methoxy at this position. All other spectral data were consistent with the proposed **207**. Although the hydrolysis reaction did indeed successfully furnish the desired acid **207**, the yields were disappointingly low (16 %), *Table 21*. It was suspected that some acid may have remained in the aqueous layer upon workup, although several attempts to improve the workup method were trialled without success. An alternative method was therefore sought for the formation of **207** in more reasonable quantities.

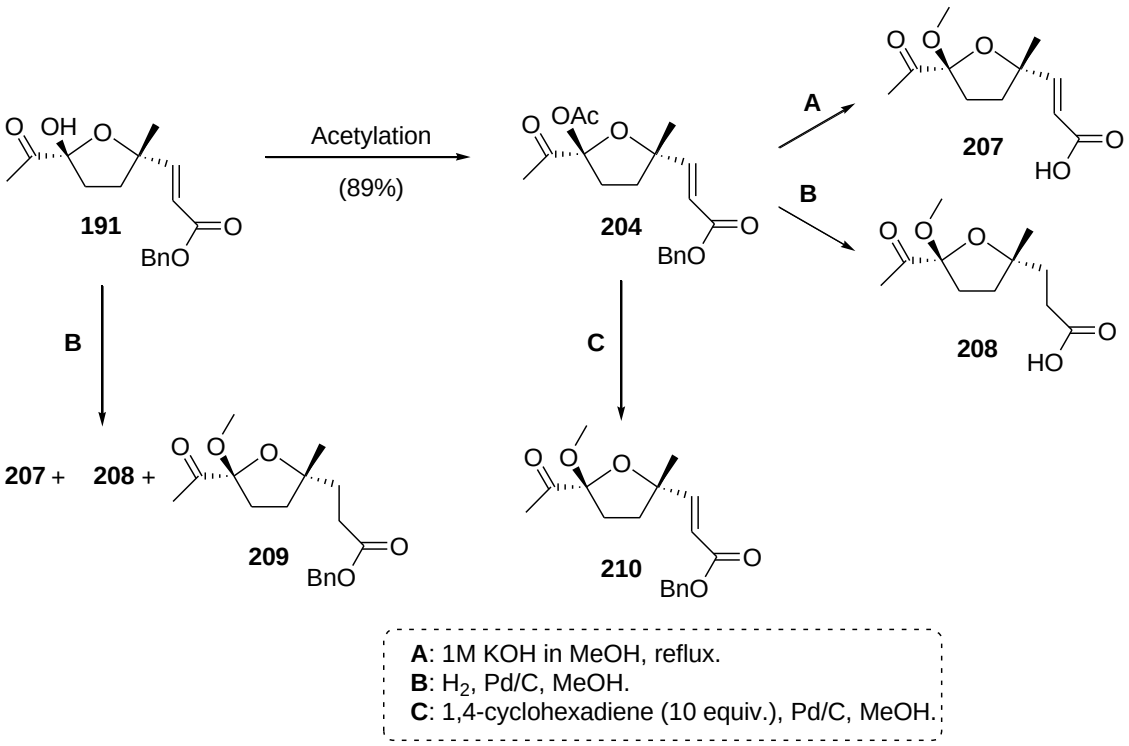

Scheme 71

Table 21: Yields for the Formation of Compounds **207-210**.

			Products (% yield recovered)			
SM	**Conditions**[#]	**Time**	**207**	**208**	**209**	**210**
204	A	15 hrs	16	-	-	-
	B	2 hrs	-	63	-	-
	B	1 hr	*			
	C	2 days	-	-	-	71
191	B	2 hrs	-	69	-	-
	B	1.5 hrs^	14	27	7	-

[#] See Scheme 71.
* complex mixture, see discussion.
^ 5% starting material also recovered.

Selective hydrogenolysis in the presence of alkenes has been reported in the literature,[219] and it was anticipated that upon treating acetate **204** with hydrogen and a metal catalyst that hydrogenolysis of the benzyl ester would occur faster than

hydrogenation of the alkene, thereby leaving the double bond intact. It was found that upon treating **204** with hydrogen and 10% w/w of 5% Pd/C in methanol, the resulting products were highly dependent upon reaction time, *Scheme 71* and *Table 21*. If the reaction was left for too long, both the alkene and ester groups were reduced resulting in alkane-acid **208**. By carefully monitoring the reaction *via* TLC and ceasing it upon consumption of starting material, a complex mixture of products was formed, including the desired alkene-acid **207**, although purification was difficult and yields were very low. The formation of alkane-acid **208** was evident through the distinct lack of alkene protons in the NMR spectra, along with the appearance of extra alkane peaks and distinct acid resonances. As with the alkene-acid **207**, NMR data for the alkane acid **208** also showed methoxy instead of acetate peaks.

It was apparent that substitution of the acetate by a methoxy must be due to the use of methanol as solvent, and as a result it seemed reasonable to trial the hydrogenolysis experiment directly on the hydroxy-furan **191** (*Scheme 71*), to see whether the hydroxyl would be substituted with a methoxy thereby eliminating the need to acetylate the alcohol. Upon full consumption of starting material **191** (2 hours), only the alkane-acid **208** was isolated in 69% yield. In a bid to maximise the alkene-acid yield (before the alkene was also reduced), the reaction was stopped before all starting material was consumed, although as can be seen in *Scheme 71* and *Table 21*, despite starting material still being present, three products were observed, **207**, **208** and **209**. A third product, determined to be **209** where the alkene acid had been reduced whilst leaving the ester functionality intact, was evident through the absence of alkene peaks along with the presence of the benzyl ester functionality in both the carbon and proton NMR spectra. Although the yield for **209** was low (7%), the isolation of all three products along with unreacted starting material indicates that the ester is not being reduced either before or in favour of the alkene, but rather it seems that both the alkene and ester reductions are competitive reactions occurring independently of each other. Previous instances where selective hydrogenation of alkenes without hydrogenolysis of benzyl esters have occurred,[220] along with reports of hydrogenation and concomitant hydrogenolysis of benzyl esters.[221]

Even though the desired alkene-acid **207** was isolated *via* this method, it was difficult to control the conditions to prevent unwanted reduction of the alkene moiety. Time constraints did not permit a lengthy investigation into the factors which control the chemoselectivity of the reaction to enhance the formation of **207** over **208** or **209**. Such factors would include reaction time along with reactant concentration and choice of solvent and catalyst. A more selective and reliable method of producing the desired alkene-acid was once again sought.

Catalytic transfer hydrogenolysis has previously been reported as a milder method for the successful removal of benzyl esters with no simultaneous reduction of alkenes present in the structure.[222] Upon reacting acetate **204** with 1,4-cyclohexadiene as a hydrogen donor in the presence of 5% Pd/C, methylation of the acetate occurred to furnish **210** in 71% yield, although no reduction of either the alkene or ester groups occurred, *Scheme 71*, *Table 21*. This reaction was also quite slow, taking two days for all starting material to be consumed.

All reactions outlined above involved replacement of the acetate moiety with a methoxy. This is likely to occur *via* the pathway outlined in *Scheme 72*, whereby solvolysis of the acetate generates carbocations **211a** and **211b** followed by trapping of the resultant carbocation by methanol to afford compounds **207**-**210**.

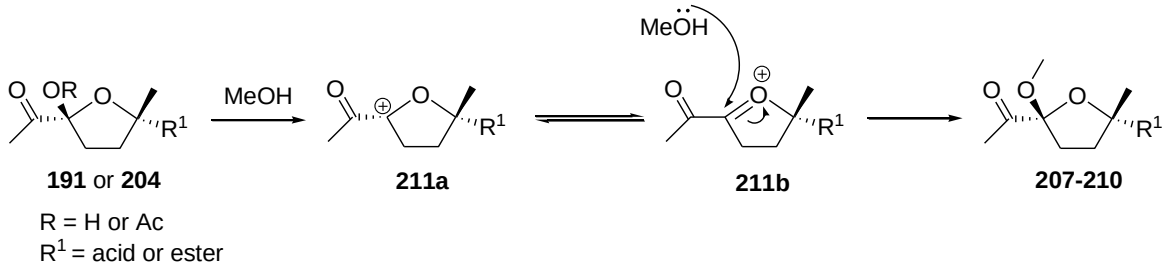

Scheme 72

To further investigate the methoxyl replacement of both the acetate and hydroxyl groups four experiments were set up to observe the outcome of reacting both **191** or **204** with (1) methanol only, and (2) methanol containing 10% w/w of 5% Pd/C. As can be seen in *Scheme 73*, methanol alone did not react with either the alcohol or acetate,

whereas upon reacting acetate **204** with methanol containing catalytic Pd/C, the acetate was substituted for the methoxy to give **210**. A pleasing 98% yield was obtained, although full conversion was quite slow, requiring 2 days. Interestingly, upon adding the hydroxyl-furan **191** to the metal catalyst in methanol, bicyclic **203** was formed, the same product seen upon attempted Xanthation of **191**. This suggests that the metal catalyst must be inducing ring-opening of the furan and subsequent intramolecular ring-closures, in the same manner as seen previously in *Scheme 68*. This further confirms the need to protect the hydroxyl, due to its instability and sensitivity towards ring-opening, leading to unwanted side-reactions.

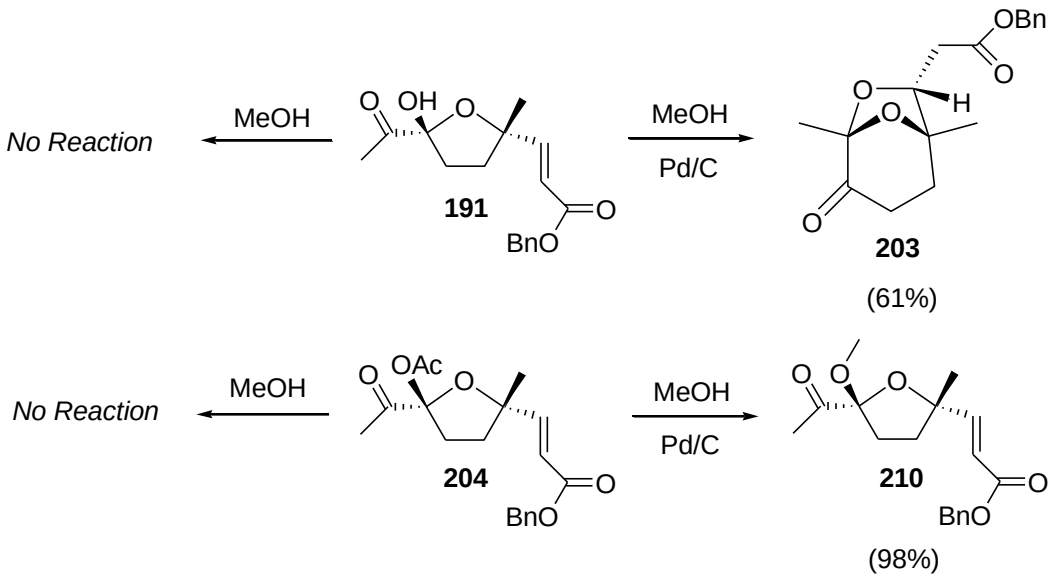

Scheme 73

Whilst the mechanistic details of these apparent metal-assisted solvolyses and ring-opening reactions are of interest, a study into how and why they are occurring was beyond the scope of this project. In spite of these results, the presence of a methoxy group over an acetate offers no hindrance to the aims of this synthesis, as the methoxy can also act as a protecting group.

Since the hydrogenolysis reactions proved rather unsuccessful, it seemed reasonable to trial using the methoxy-furan **210** (easily formed in high yield from the reaction of acetate **204** with Pd/C in methanol) to re-attempt hydrolysis of the benzyl-ester, in hope that the reaction would be more successful with the methoxy substituent already in

place. This approach did indeed prove successful, with the desired alkene-acid **207** isolated in 64% yield, *Scheme 74*.

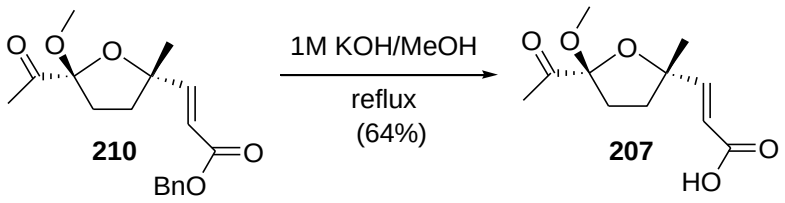

Scheme 74

With alkene-acid **207** in hand, referring back to the retro synthetic plan (*Scheme 70*), it was envisioned that the acid moiety could be removed *via* a Barton-decarboxylation,[213,223] as depicted in *Scheme 75* below.

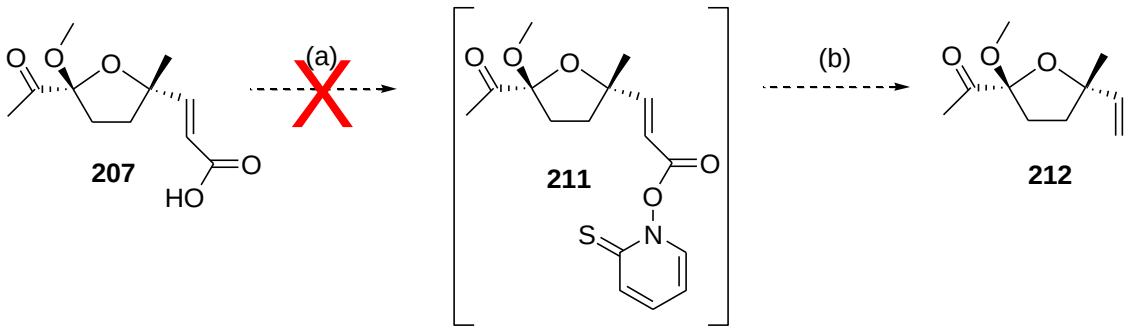

(a) 1-Hydroxy-pyridinethione (1 equiv.), DCC (1 equiv.) , DCM, 0 ^{o}C (2 hrs.) - r.t (2 hrs.)
(b) Bu_3SnH (2 equiv.), benzene, sun lamp (3 hrs.)

Scheme 75

This involves the conversion of acid **207** into the thiohydroxamate ester **211** followed by radical-induced cleavage of the nitrogen-oxygen bond and ultimate formation of a new C-H bond to yield **212**. The reaction was attempted several times, although only the expected by-products were isolated with no evidence of the desired product. Reaction conditions were carefully monitored to ensure no loss of product upon workup or concentration of the Barton ester. The crude Barton ester mixture was analysed *via* ^{1}H NMR, and an NMR experiment was performed to follow the deoxygenation step, although these processes gave no further insight into why the reaction was failing.

To further investigate where this reaction may be going wrong, two NMR experiments were set up whereby one equivalent of each of the reagents was added to acid **207** in order to monitor if the individual reagents were reacting in an unfavourable manner with the starting material. As can be seen in *Table 22*, upon adding one equivalent of 1-hydroxy pyridine-2-thione to the acid in $CDCl_3$ and leaving for 12 hours (protected from light) no reaction resulted, with the ^1H NMR spectrum revealing a clean mixture of starting materials. When one equivalent of DCC was added to the acid in $CDCl_3$ and left for 12 hours, ^1H NMR analysis showed a messy spectrum containing many alkene and alkane peaks, indicating that the starting material, **207** had broken down into a range of unidentifiable decomposition products.

Table 22: NMR Experiments of Alkene-Acid **207**.

Starting Material	Reagent	Outcome
207	1-Hydroxy-pyridinethione	No Rxn
207	DCC	Complex mixture products

These results indicate that **207** must be sensititve to DCC, resulting in product breakdown, thereby explaining why the Barton decarboxylation reaction had not been successful. No further investigation was conducted into this reaction, and another route to acquire the desired terminal alkene was sought.

5.3.5 Ozonolysis and Wittig of Methoxy-Furan 210.

With the above synthetic pathway proving unsuccessful, it was decided to perform ozonolysis on the diastereomeric mixture of methoxy-alkene-ester **210** to cleave the alkene to give a carbonyl product, which could subsequently undergo a Wittig reaction to yield the desired terminal alkene.

Ozonolysis was performed using the same standard conditions described in Chapter 3, once again using triphenylphosphine to reduce the ozonide. This worked successfully in a total yield of 78% for the two diastereomeric aldehydes, **213**, initially labelled diastereomers 1 and 2 in accordance with their elution order off the chromatography

column, *Scheme 76*. Key NMR data (*Table 23*) showed the quaternary carbon resonances as expected for the furan ring system remaining intact, along with the expected carbonyl peaks.

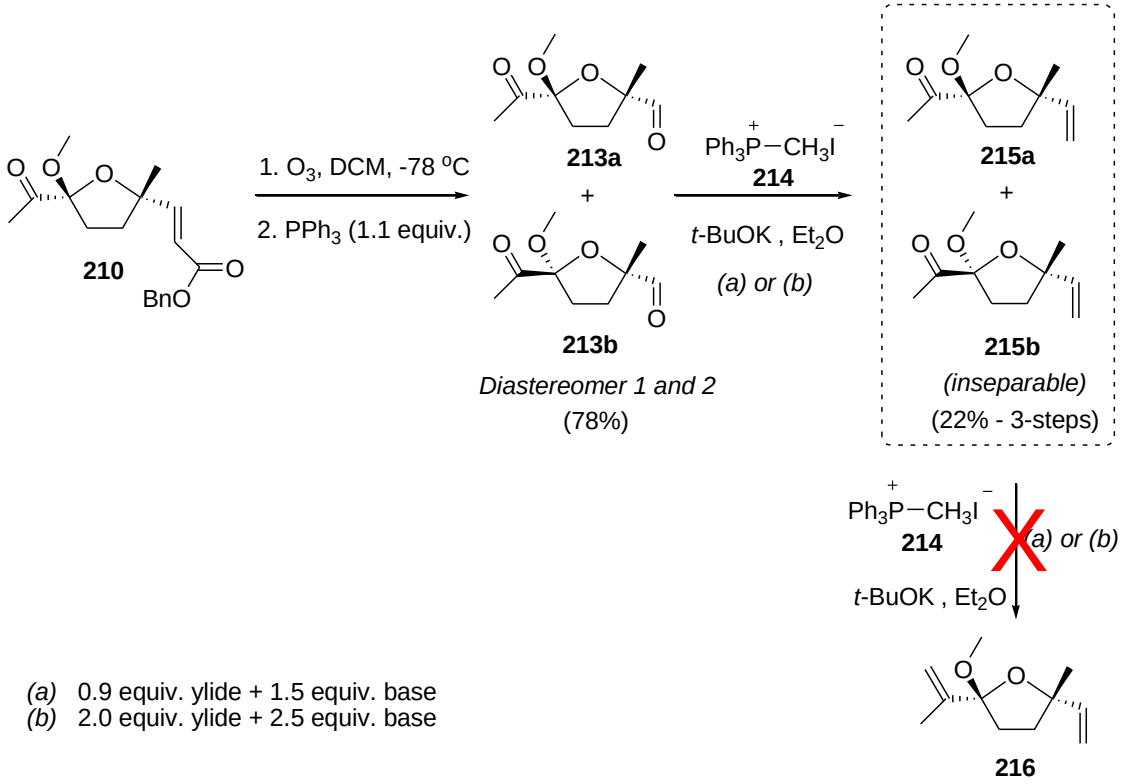

Scheme 76

Table 23: Key NMR Data for Aldehydes **213a** and **b**.

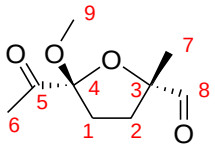

	δ (ppm)*			
	Diastereomer 1		Diastereomer 2	
Carbon	^{13}**C**	^{1}**H**	^{13}**C**	^{1}**H**
1	33.9	2.13-2.09 (m, 2H)	34.0	2.12 (m, 1H); 1.95 (m, 1H)
2	31.1	2.43 (m, 1H); 1.79 (m, 1H)	32.2	2.34 (m, 1H); 2.03 (m, 1H)
3	89.2	-	89.6	-
4	110.5	-	110.3	-
5	204.6	-	204.9	-
6	25.7	2.28 (s, 3H)	25.7	2.29 (s, 3H)
7	20.8	1.39 (s, 3H)	21.8	1.46 (s, 3H)
8	201.5	9.62 (s, 1H)	201.5	9.65 (s, 1H)
9	51.3	3.28 (s, 3H)	50.8	3.30s, 3H)

* 600 MHz Spectra.

Despite trialling extensive solvent systems the two diastereomers were only partially separable, as the two spots on the TLC plate and chromatography column always overlapped to a large degree. Samples containing varying ratios of diastereomers 1:2 were easily obtained without any by-products, and these combined pure mixtures of both isomers were used for yield determination (78%) along with IR and accurate mass analysis. Incomplete separation also made determination of the overall ratio of isomers formed difficult. A pure sample of diastereomer 1 was able to be obtained for NMR analysis, although NMR spectra of diastereomer 2 always contained some of diastereomer 1 due to the inability to fully separate 1 from 2. A fairly pure sample of diastereomer 2 (containing a small amount of diastereomer 1) was obtained for NMR analysis, which enabled NMR data for diastereomer 2 to be deduced. The structures were confirmed *via* COSY, HMBC and HMQC correlations. ROESY correlations were not helpful in determining the structure of either diastereomer 1 or 2.

As seen in *Table 24*, diastereomer 1 showed COSY correlations between all the methyl ketone, methoxy and methyl protons, whereas diastereomer 2 only showed COSY correlations between methoxy and methyl protons.

Table 24: COSY Correlations Seen for Selected Peaks of **213**.*

	C_4	**C_5**	**C_6**	**C_7**
C_4	-	1	1	1
C_5	1	-	1	1, 2
C_6	1	1	-	1
C_7	1	1, 2	1	-

* 1,2 = Diastereomers 1 & 2 respectively.

Based on these COSY correlations, and lack of ROESY correlations, the stereochemistry of diastereomers 1 and 2 could not be absolutely determined. Correlations between the methyl and methoxy protons in diastereomer 2 suggest that these two isomers are likely on the same side, giving **213a**, however due to conflicting correlations in diastereomer 1, this cannot be claimed with certainty.

With the desired isomers of furan keto-aldehyde **213a** and **213b** in hand, both diastereomers were together subjected to Wittig reaction, using unstabilised ylide **214** to convert the aldehydes into their respective terminal alkenes **215a** and **b**, *Scheme 76*. This worked successfully in 22% yield over three steps from ozonolysis and reduction of **210** and subsequent Wittig of the aldehyde **213**. The diastereomeric mixture of **215a** and **215b** was inseparable and the two isomers unable to be differentiated upon using 2D NMR techniques. Despite adding two equivalents of the ylide, only the aldehyde was converted into its corresponding alkene.

NMR analysis revealed that the carbon and proton shifts for the ^{13}C and ^{1}H NMR spectra of alkenes **215a** and **215b** were comparable to that given in *Table 23* for C_1-C_5 and C_7 for diastereomers 1 and 2 of **213a** and **213b**. The notable difference between the two spectra was the absence of aldehyde peaks along with the formation of alkene peaks. The alkene resonances for **215a** and **215b** are shown in *Figure 36*, where it can

be seen that for each diastereomer the H_1 alkene proton couple as a dd to both terminal protons H_{2a} and H_{2b}, which in turn each couple to H_1, but not to each other. H_{2a} and H_{2b} are designated in accordance to the expected coupling to H_1, with the larger coupling of J = 17.4 Hz corresponding to *trans* coupling and the smaller splitting of J = 10.8 Hz belonging to the *cis*.

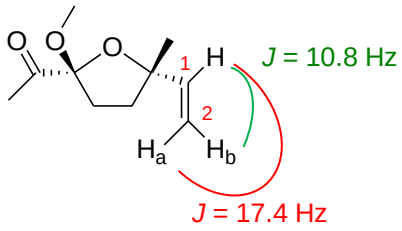

		δ (ppm)*
^{13}C	C_1	143.5, 142.6
	C_2	112.3, 112.1
^{1}H	H_1	6.04, 5.89
	H_{2a}	5.27, 5.25
	H_{2b}	5.07, 5.03

* 600 MHz Spectra

Figure 36: Alkene ^{1}H and ^{13}C NMR data for Diastereomers **215a** and **b.**

With the terminal alkene in hand, the right-hand side of the molecule is complete for both the wine compounds **101** and **102**. All that remains is to reduce off the methoxy and convert the ketone firstly into an alkene to give the anhydrofuran linalool oxide (**2**), and secondly a tertiary alcohol to yield the furanoid linalool oxide (**1**).

As seen above, upon reacting keto-aldehyde **213** with two equivalents of unstabilised ylide **214**, only the aldehyde group reacted. In an attempt to convert the ketone into the desired alkene which would give the diene precursor **216** to the anhydrofuran linalool oxide **102**, keto-alkene **215** was subjected to a second Wittig reaction (*Scheme 76*), although no reaction proceeded, and only starting material was recovered.

5.3.6 Attempted Wittig (unstabilised ylide) and Peterson Olefinations on 156.

A potentially simple way of making the desired furan ring system with terminal alkene moieties would involve ring-contracting the parent 1,2-dioxine **156** into its respective furan, followed by trapping of the aldehyde (and possibly ketone) with a methylene unit to give **217** or **218** in a one pot reaction. Two conventional ways of doing this would be

to perform either a Wittig or Peterson olefination, both of which employ basic conditions to firstly promote the base-catalysed removal of the acidic proton α to the dioxine linkage to initiate the Kornblum-DeLaMare rearrangement, followed by simultaneous trapping of the carbonyl group(s) to yield the desired alkene(s) and ring-closure to the furan, *Scheme 77*.

Upon treating keto-aldehyde **156** with unstabilised ylide **214** in the presence of base, a complex mixture of products was observed. Depending on the stoichiometric amount of ylide and base utilised in the reaction, the only identifiable products isolated were small amounts of either diene **219** or triene **220**, *Scheme 77* and *Table 25*. Attempts to isolate other products *via* column chromatography only resulted in mixtures of messy polymeric-like products *via* ^{1}H NMR.

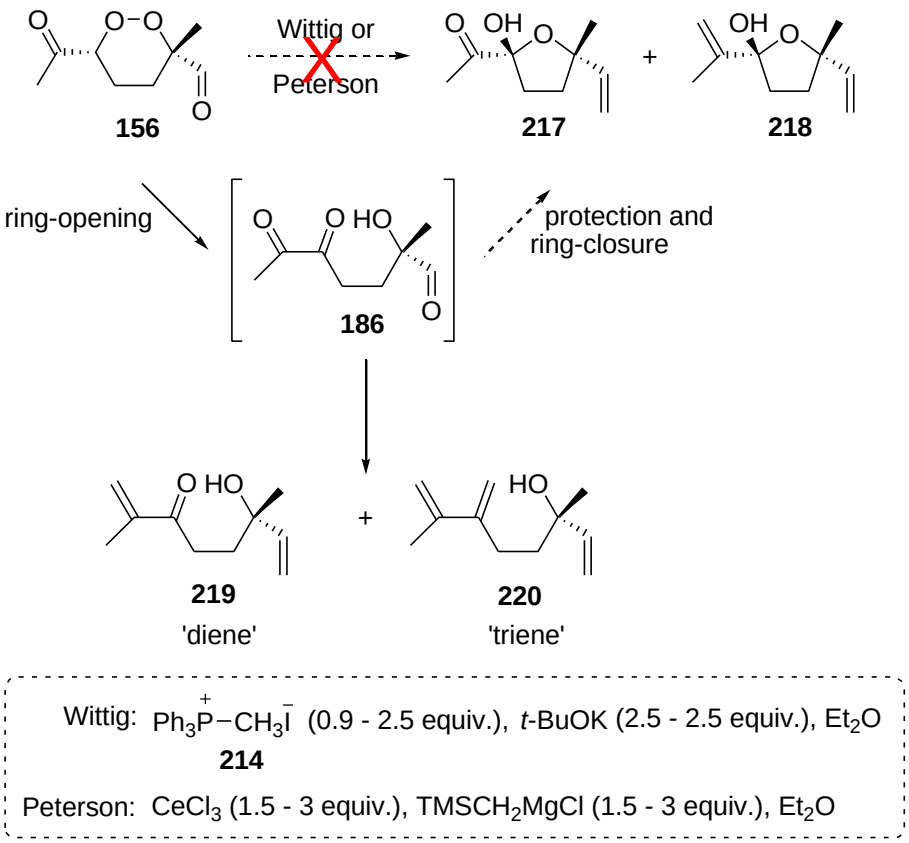

Scheme 77

Table 25: Conditions and Yields for Wittig Reaction on Keto-Aldehyde **156**.

Entry	No. Equiv.		Yield (%)	
	Ylide	Base	219	220
1	2.6	4.3	-	5
2	0.9	1.5	2	-

These results indicate that the 1,2-dioxine **156** did indeed ring-open to give the *cis*-γ-hydroxyone **186**, although the desired furan was not seen. When an excess of ylide and base were added, all three carbonyl groups were trapped to give **220**, thereby inhibiting the ability for furan **217** to form, and upon adding slightly less than one equivalent of ylide, both aldehyde and methyl ketone groups were trapped to give **219**, *Scheme 77* and *Table 25*. These results are similar to those seen earlier where the addition of stabilised benzyl-ester ylide **190** to either keto-aldehyde **156** or bicyclic lactone **188** resulted in the formation of **192a** and **192b**, (*Scheme 63*).

The diene, **219** matched data previously reported in the literature for this known compound.[224] Along with the expected alkene peaks, **219** was particularly evident by a carbonyl peak at δ = 202.6 ppm and quaternary carbon peak at δ = 72.7 ppm in the ^{13}C spectrum and hydroxyl peak at δ = 4.68 ppm in the ^{1}H NMR spectrum.

Triene **220**, a previously unknown compound showed no carbonyl peaks in the ^{13}C spectrum, although a peak at δ = 73.3 ppm was indicative of a quaternary carbon. No hydroxyl peak was detected in the ^{1}H NMR spectrum, although a large band at 3393 cm^{-1} in the IR spectra supported the presence of an alcohol. This indicated that the structure had indeed ring-opened, as per diene **209**, with additional alkene peaks and 2D NMR correlations pointing toward the structure being that of triene **220**. ^{1}H and ^{13}C NMR spectra are shown below in *Figure 37*. Upon attempting to acquire a mass spectrum and accurate mass data for **220**, no results were able to be obtained, presumably due to the instability of the product, and its likely potential for intermolecular Diels-Alder reactions to occur. This could account for why the yield for this reaction was so low, and why such a complex mixture of unidentifiable polymeric-

like products was observed. With an incomplete set of characterisation data, one cannot unequivocally say that the structure is indeed that of triene **220**.

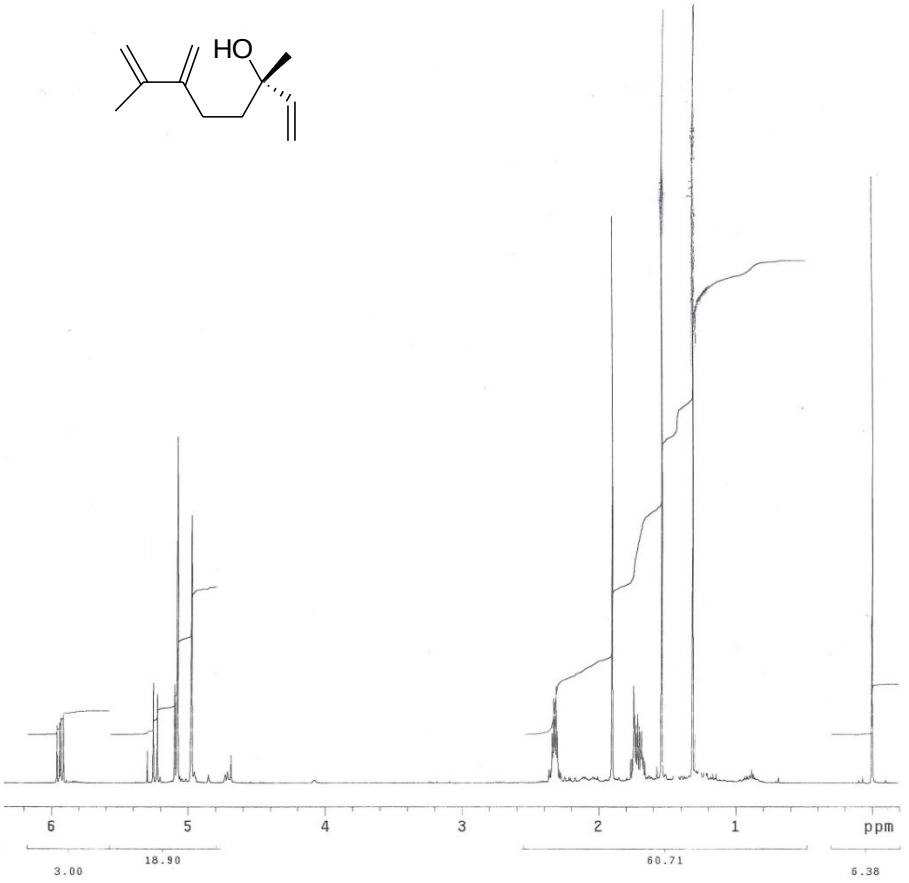

(a)

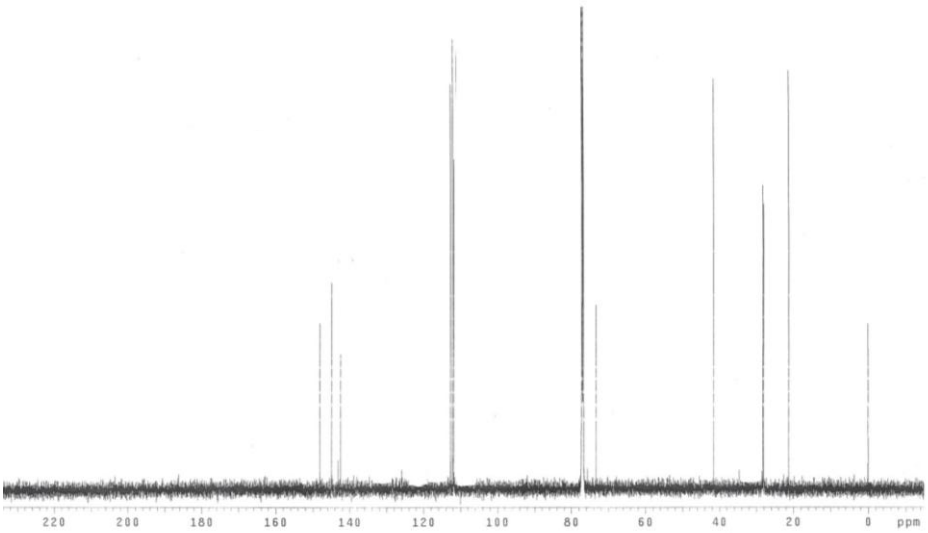

(b)

Figure 37: 600 MHz (a) ^{1}H and (b) ^{13}C NMR Spectra of Triene **220**.

It was hoped that by using a Peterson Olefination, a common alternative to the Wittig reaction, the desired trapped furan compounds could be formed in good yield. The Peterson reaction involves the formation of a *β*-silyl alkoxide intermediate which can be eliminated under either basic (*syn*-favoured) or acidic (*anti*-favoured) conditions to form the *Z* or *E*- alkene, respectively[225,226] (although alkene geometry was unimportant in our case, due to the formation of a terminal alkene). Two different sets of conditions utilising trimethylsilylmethylmagnesium chloride, cerium chloride and acidic elimination were trialled, although unfortunately, as per the Wittig reaction, this also resulted in a low amount (4 %) of triene **220** formed upon adding three equivalents of reagents at room temperature, and no identifiable products upon using 1.5 equivalents of the two reagents at -78 ^{o}C, *Scheme 77* and *Table 26* Crude ^{1}H NMR spectra of the eliminated products were very messy, with a large number of peaks in the 0-2 ppm range, indicative of a complex mixture of products, largely polymeric, as per the Wittig reaction.

Table 26: Conditions and Yields for Peterson Reaction of Keto-Adledhyde **156**.

Entry	**No. Equivalents**		**Temp (^{o}C)**	**Yield (%)**
	$CeCl_3$	**$TMSCH_2MgCl$**		**220**
1	3	3	25	4
2	1.5	1.5	-78	*

* no identifiable products isolated

As a result of these unsuccessful attempts to form the furan alkene directly from the 1,2-dioxine keto-aldehyde, this pathway was abandoned and no further exploration into the products obtained was conducted.

5.4 Conclusion and Future directions.

This chapter firstly saw the synthesis of the new bicyclic 1,2-dioxine **154** in good yield, followed by successful ozonolysis and ring-contraction into the core 2,2,5-trisubstituted THF. We saw that having a hydroxyl α to either the furan or dioxine ring systems could be problematic and lead to unwanted ring-opening and further rearrangements. Investigations revealed that this could be overcome upon protection of the alcohol with an acetate or methoxy substrate, thereby enabling structural manipulation of the other functional groups to proceed smoothly.

Research along the synthetic pathway did reveal a new potential route to dioxabicyclo[3.2.1]octanes, with two new bicyclic compounds **188** and **203** formed as a result of selective 1,6-cyclisation of a *cis*-γ-hydroxydione intermediate, a reaction previously unseen within the literature.

Time was a limiting factor in being able to complete the total synthesis of the desired compounds, but the major ground work has been achieved. The C_2 functionalisation of the THF ring has successfully been completed, and with a newfound understanding as to the nature and reactivity of these compounds, only minor structural manipulations to the C_5 positions are required to give the furanoid and anhydrofuran linalool oxides, (**101** and **102** respectively). There are many synthetic options at hand to achieve this, and incorporation of chiral reagents could prove useful for resolution of isomers, thereby enabling enantiomerically pure samples of the compounds to be isolated. This, for example, could prove useful for the sensory evaluation of all enantiomers in wine to determine their individual aroma thresholds.

Functionalised THF structures are an important skeleton structure, found in a variety of natural products that exhibit a broad range of biological activities.[102,103,227] New synthetic methodologies developed within this thesis, with particular emphasis on the ozonolysis of bicyclic 1,2-dioxines, have the potential to be useful tools in the synthesis of other natural products containing functionalised THF structures.

CHAPTER 6: Experimental

6.1 General Experimental.

Solvents were dried by appropriate methods as required.[228] THF and ether were distilled over sodium wire with benzophenone as indicator and freshly distilled prior to use. Methanol was dried and stored over 4 Å molecular sieves. All organic extracts were dried over anhydrous magnesium sulphate. Reactions employing moisture sensitive reagents were handled under nitrogen and performed in flame or oven dried glassware. *N*-Butyllithium was titrated against diphenylacetic acid prior to use. Cerium chloride heptahydrate was dried by heating to 140 ^{o}C under vacuum whilst rapidly stirring for 4 hours.

^{1}H and ^{13}C NMR spectra were recorded in $CDCl_3$ on either a Varian Gemini 2000 (300 MHz) or Varian INOVA (600 MHz) instrument. TMS (0.00 ppm) and $CDCl_3$ (77.00 ppm) were used as internal standards. All resonances are reported in parts per million (ppm). ^{1}H NMR multiplicities are abbreviated as follows: singlet (s), doublet (d), triplet (t), quartet (q), quintet (quin), septet (sept), multiplet (m), AB quartet (ABq), broad (br) denoting broadened signals and (apt) denoting 'apparent' coupling. All coupling constants are reported in hertz (Hz). ^{13}C NMR data is reported to two decimal places in the instance where two peaks are observed, but can only be differentiated *via* a second decimal place.

Flash chromatography was performed using *Merck* silica gel 60 (230-400 mesh ASTM). Thin-layer chromatography (TLC) was performed using aluminium sheets of silica gel 60 F_{254} from *Merck*, and visualised under 254 nm light or developed in either vanillin or potassium permanganate dip.

Melting Points were determined using a *Mel Temp* apparatus and are uncorrected.

Specific rotations were measured with a PolAAr 21 polarimeter and referenced to the D sodium line (589 nm) at 20 ^{o}C in a cell with 1dm path length. The concentration (*c*) is specified in g/100 mL and the solvent used as reported.

Accurate Mass determination was performed by the Central Science Laboratories, University of Tasmania.

X-ray crystallography was performed courtesy of Dr Edward R. T. Tiekink at the Department of Chemistry, University of Malaya, Malaysia.

Infrared spectra were recorded on a Lambda Scientific FTIR 7600 series spectrophotometer, either neat or as a nujol mull, as indicated.

Ozone was generated from oxygen *via* Corona discharge using an Ozone Industries Model 7230 Ozone generator. Flow rates and ozone concentration levels were not recorded, as reactions proceeded until solutions were saturated with ozone, however instrument recommendations are between 2 and 4 LPM of oxygen input.

All yields reported refer to isolated material judged to be homogeneous by NMR or TLC, unless otherwise stated.

The following compounds were purchased from *Sigma-Aldrich* Chemical Company Inc. and used without further purification: 7-dehydrocholesterol, α-terpinene, rose bengal, *bis*(triethylammonium) salt, triphenyl phosphine, dimethyl disulphide, bromobenzene, 2-cyclohexen-1-one, *n*-butyllithium, 1,4-cyclohexadione, triethyl phosphonoacetate, 1,4-cyclohexanedicarboxylic acid, 3-methyl-2-cyclohexen-1-one, methylmagnesium bromide, iodomethane, 1,4-cyclohexadiene and trimethylsilylmethylmagnesium chloride. Methyl triphenylphosphine iodide was kindly synthesised by Dr Peter Valente.

6.2 Compounds Described in Chapter 2.

(±)-1-Phenylcyclohex-2-en-1-ol (106).

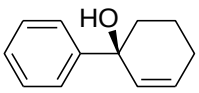

A solution of bromobenzene (**103**) (15.39 g, 98.7 mol) in dry THF (50 mL) was added dropwise over 1 hour to a mixture of magnesium turnings (2.40 g, 98.7 mmol) with a catalytic amount of iodine under a dry atmosphere of nitrogen with constant stirring. The resulting suspension was bought to reflux for 2 hours. The solution was cooled to room temperature and 2-cyclohexen-1-one (**105**) (9.42 g, 98.7 mmol) in dry THF (20 mL) was added dropwise over 30 minutes. The solution was heated under reflux for 1 hour and then cooled to room temperature before being quenched with saturated ammonium chloride (50 mL). The layers were separated, and the aqueous layer extracted with diethyl ether (3 x 50 mL). The combined organic extracts were washed with water (50 mL), brine (50 mL) and dried ($MgSO_4$). The solvent was removed *in vacuo* and the crude product purified by flash chromatography to afford a pale yellow solid (11.21 g, 66%) (**106**). Mp 44-45 ^oC (lit[229] 44-45 ^oC). R_f 0.47 (1 : 4 ethyl acetate : hexane). Physical and chemical properties were as reported in the literature.[229]

Cyclohexa-1,3-dien-1-ylbenzene (6b).

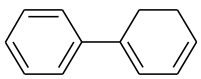

To a mixture of 1-phenyl-2-cyclohexen-1-ol (**106**) (4.02 g, 23.0 mmol) and triethylamine (5.84 g 57.8 mmol) in dichloromethane (50 mL) at 0 ^oC under nitrogen was added slowly 2,4-dinitrobenzenesulfenyl chloride (**107**) (10.83 g, 46.2 mmol) with stirring. The mixture was allowed to slowly warm to room temperature overnight. Hexane (150 mL) was added and the slurry filtered. The slurry was washed with a further portion of hexane (150 mL), and the filtrate concentrated *in vacuo* followed by purification by flash chromatography to furnish a white solid (2.12 g, 58%) (**6b**). Mp

39-40 °C (lit[118] 38-39 °C). R_f 0.80 (1 : 9 ethyl acetate : hexane). Physical and chemical properties were as reported in the literature.[118]

Isomeric mixture of 1,1'-Cyclohexa-1,3-diene-1,4-diyldibenzene (6c) and 1,1'-cyclohexa-1,4-diene-1,4-diyldibenzene (111).

n-Butyllithium (64 mL, 96.8 mmol, 1.5 M in cyclohexane) was added dropwise to a solution of bromobenzene (**103**) (15.19 g, 96.8 mmol) in dry diethyl ether (50 mL) with stirring at -5 °C under nitrogen. After the addition was complete the reaction mixture was warmed to room temperature and 1,4-cyclohexadione (**109**) (2.71 g, 24.1 mmol) in dry diethyl ether (50 mL) was added dropwise to the phenyllithium solution. The resulting mixture was heated under reflux for 1 hour, cooled to 0 °C and 50% sulphuric acid (100 mL) added slowly. The organic layer was separated and the aqueous layer was extracted with diethyl ether (3 x 100 mL). The combined organic extracts were washed with saturated sodium bicarbonate solution (100 mL) followed by water (100 mL). The extracts were then dried ($MgSO_4$), concentrated *in vacuo* and purified by flash chromatography to afford **6c** and **111** as a yellow solid (2.50 g, 44%). R_f 0.84 (1 : 4 ethyl acetate : hexane). The ratio of 1,3- to 1,4-isomers was 6:4. Physical and chemical properties were as reported in the literature.[119]

1,1'-Cyclohexa-1,3-diene-1,4-diyldibenzene (6c).

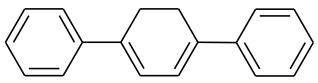

The isomeric mixture of 1,4-diphenylcyclohexadienes (**6c** and **111**) (1.29 g, 5.57 mmol) was heated under reflux for 4 hours in *t*-butanol (220 mL) containing potassium *t*-butoxide (10 g). The solution was cooled to room temperature and the majority of *t*-butanol was removed under reduced pressure. The mixture was diluted with diethyl ether (100 mL) followed by the addition of water (100 mL). The layers were separated

and the aqueous layer extracted with diethyl ether (3 x 50 mL). The combined organics were dried ($MgSO_4$) and concentrated *in vacuo* to afford yellow crystals (1.17 g, 91%) (**6c**). Mp 180-182 ^oC (lit[119] 179-180 ^oC). R_f 0.84 (1 : 4 ethyl acetate : hexane). Physical and chemical properties were as reported in the literature.[119]

Isomeric mixture of diethyl 2,2'-cyclohexa-1,3-diene-1,4-diyldiacetate (113); Diethyl (2*E*,2'*E*)-2,2'-cyclohexane-1,4-diylidenediethanoate (114a) and diethyl (2*Z*,2'*Z*)-2,2'-cyclohexane-1,4-diylidenediethanoate (114b).

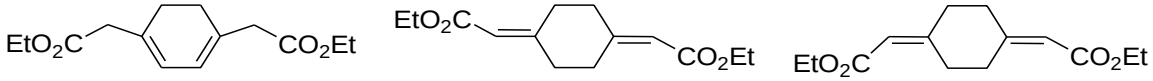

To a dry 250 mL, 3-necked round bottom flask, under nitrogen, was added 80% sodium hydride in mineral oil (2.30 g, 76.6 mmol). The mineral oil was removed with anhydrous benzene (3 x 20 mL) and a further portion of benzene (20 mL) added. The mixture was cooled in an ice-bath whilst triethyl phosphonate (**112**) (15.76 g, 70.3 mmol) was added dropwise over 40 minutes with stirring. The resulting mixture was maintained at 0 ^oC whilst being stirred for 1 hour after which hydrogen evolution had ceased. A solution of 1,4-cyclohexadione (**109**) (4.00 g, 35.7 mmol) in benzene (20 mL) was added dropwise over 30 minutes. A gummy brown precipitate (sodium diethyl phosphate) formed during the addition, making stirring difficult. The mixture was heated under reflux for 1 hour before being cooled to room temperature. The liquid was decanted and the residue washed with hot benzene (3 x 20 mL). The organics were combined and concentrated *in vacuo* and the crude product purified by flash chromatography to afford a 6:2:2 mixture of the 1,3-diene (**113**) and *E* and *Z*-isomers (**114a** and **114b**) respectively, as a white solid (7.62 g, 86%). R_f 0.62 (1 : 4 ethyl acetate : hexane). Physical and chemical properties were as reported in the literature.[120]

2,2'-Cyclohexa-1,3-diene-1,4-diylidacetic acid (115).

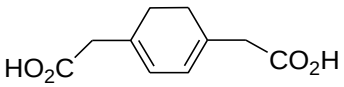

To a solution containing a 6:2:2 mixture of the 1,3-diene (**113**), *E* and *Z* isomers (**114a** and **114b**) (1.33 g, 5.26 mmol) in methanol (30 mL) was added potassium hydroxide (2.95 g, 52.6 mmol) and the solution stirred under reflux for 1 hour. The solvent was removed *in vacuo* and the residue taken up in water (50 mL) and acidified to pH = 1 with concentrated HCl. The aqueous solution was extracted with diethyl ether (3 x 30 mL), and the combined organic layers were dried ($MgSO_4$) and concentrated *in vacuo* to afford a pale cream solid (785 mg, 76%) (**115**). Mp 186-188 ^oC (lit[230] 184-188 ^oC). The product was used without further purification. Physical and chemical properties were as reported in the literature.[230]

Dimethyl 2,2'-cyclohexa-1,3-diene-1,4-diyldiacetate (6d).

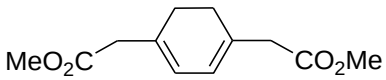

A mixture of 2,2'-cyclohexa-1,3-diene-1,4-diyldiacetic acid (**115**) (2.80 g, 14.3 mmol) in dry methanol (50 mL) containing concentrated sulphuric acid (3 mL) was heated under reflux overnight. The methanol was removed *in vacuo* and saturated sodium bicarbonate solution (30 mL) added. The solution was extracted with diethyl ether (3 x 30 mL), washed with brine (30 mL) and the combined organics concentrated *in vacuo* to furnish a yellow oil (2.28 g, 71%) (**6d**). Product was used without any further purification. R_f 0.43 (1 : 1 ethyl acetate : hexane). Physical and chemical properties were as reported in the literature.[60]

Dimethyl cyclohexa-1,3-diene-1,4-dicarboxylate (6e).

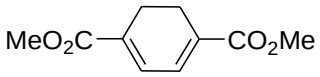

A mixture of 1,4-cyclohexanedicarboxylic acid (**116)** (4.15 g, 24.1 mmol) in thionyl chloride (20 mL) was heated under reflux with stirring for 2 hours. Bromine (8.50 g, 53.0 mmol) was slowly added and the solution was fitted with a drying tube and irradiated with a sun lamp for 4 hours. The volatiles were removed under reduced pressure and the resulting crude product dissolved in methanol (50 mL) and heated under reflux under an atmosphere of nitrogen overnight. The solution was cooled and the residual solid was filtered off to give 4.3 g of the *trans*-isomer **119a** as a white solid (mp = 142-144 ^{o}C) (lit[121] = 148-150 ^{o}C). The methanol solution was condensed *in vacuo* to give 4.0 g of crude *cis*-isomer **119b** as a yellow oil. The crude *cis*- and *trans*-isomers were combined and dissolved in pyridine (150 mL) and heated under reflux overnight, with stirring under nitrogen. The mixture was cooled, most of the pyridine removed under reduced pressure and the solution was diluted with dichloromethane (100 mL) followed by water (100 mL). The layers were separated and the aqueous layer was extracted with dichloromethane (3 x 50 mL). The combined organic extracts were washed with 10% HCl (100 mL) and brine (100 mL). The solution was dried ($MgSO_4$) and concentrated *in vacuo* to afford colourless crystals (3.78 g, 80%) (**6e**). Mp 70-73 ^{o}C (lit[121] 83-85 ^{o}C). R_f 0.67 (3 : 7 ethyl acetate : hexane). ^{1}H NMR (300 MHz, $CDCl_3$): 7.09 (s, 2H), 3.79 (s, 6H, 2.56 (s, 2H); ^{13}C NMR (75 MHz, $CDCl_3$): 167.3, 133.1, 132.0, 52.2, 21.9. Remaining physical and chemical properties were as reported in the literature. [121,231]

General Procedure for the Preparation of 1,2-Dioxines (3a-e, 82 and 154).

To a solution of 1,3-butadiene (**6a-e, 121** or **155**) in dichloromethane (30 mL / g of 1,3-butadiene), in a custom-made pyrex flask fitted with a cooling jacket, was added rose bengal, *bis*(triethylammonium) salt (100 mg). Ice water was pumped throughout the cooling jacket to maintain a temperature of *ca* 5-10 ^{o}C within the reaction mixture at all times. Oxygen was bubbled through the solution, and the reaction was irradiated with 3 x 500W tungsten halogen lamps until complete *via* TLC (1-8 hours). The mixture was then concentrated *in vacuo* and the residue purified by flash chromatography. Any unreacted diene was also recovered at this time.

(±)-1-Methyl-4-(propan-2-yl)-2,3-dioxabicyclo[2.2.2]oct-5-ene (3a) .

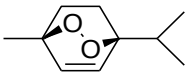

Pale yellow oil. Yield 94%. R_f 0.62 (1 : 4 ethyl acetate / hexane). Physical and chemical properties were as reported in the literature.[22]

(±)-(1*R*,4*S*)-1-Phenyl-2,3-dioxabicyclo[2.2.2]oct-5-ene (3b).

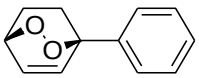

Colourless solid. Yield 36%. Mp 49-51 ^{o}C (lit[60] 50-52 ^{o}C). R_f 0.42 (1 : 4 ethyl acetate : hexane). Physical and chemical properties were as reported in the literature.[60]

(±)-(1*R*,4*S*)-1,4-Diphenyl-2,3-dioxabicyclo[2.2.2]oct-5-ene (3c).

White solid. Yield 83%. Mp 131-133 °C (lit[122] 131-132 °C). R_f 0.47 (1 : 4 ethyl acetate : hexane). Physical and chemical properties were as reported in the literature.[122]

(±)-Dimethyl 2,2'-[(1*R*, 4*S*)-2,3-dioxabicyclo[2.2.2]oct-5-ene-1,4-diyl]diacetate (3d).

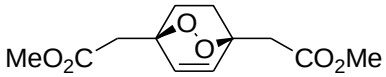

Crystalline pale yellow solid. Yield 63%. Mp 34-35 °C (lit[60] 32-34 °C). R_f 0.48 (2 : 3 ethyl acetate : hexane). Physical and chemical properties were as reported in the literature.[60]

(±)-Dimethyl (1*R*,4*S*)-2,3-dioxabicyclo[2.2.2]oct-5-ene-1,4-dicarboxylate (3e).

Colourless needles. Yield: 46%. Mp 66-68 °C. R_f 0.37 (3 : 7 ethyl acetate : hexane) ^{1}H NMR (300 MHz, $CDCl_3$): 6.88 (s, 2H), 3.86 (s, 6H), 2.56-2.49 (m, 2H), 1.83-1.77 (m, 2H); ^{13}C NMR (75 MHz, $CDCl_3$): 168.6, 132.5, 77.9, 53.1, 26.3; IR (nujol) 2927, 1745, 1306, 1119, 989, 702 cm^{-1}; HRMS calcd. for $(M)^+$ $C_{10}H_{12}O_6$: 228.0634; found 228.0630.

(3β)-Cholesta-5,7-dien-3-yl acetate (121).

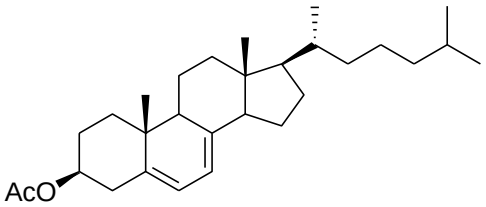

To a stirring solution of 7-dehydrocholesterol (**120**) (5.04 g, 13.1 mmol) in pyridine (40 mL) at ambient temperature under an atmosphere of nitrogen, was added, acetic anhydride (12.05 g, 118 mmol) and DMAP (481 mg, 3.94 mmol), and the mixture was stirred overnight. Most of the pyridine was removed *in vacuo*, and the remaining mixture was diluted with dichloromethane (30 mL) and washed with 10% HCl (30 mL). The organic layer was then removed, and the aqueous layer extracted with dichloromethane (3 x 30 mL). The organic layers were combined, washed with brine (30 mL), dried ($MgSO_4$) and concentrated *in vacuo*. The residue was purified *via* flash chromatography to afford a white solid (5.07 g, 91%) (**121**). Mp 128-130 ^oC (lit[232] 129-130 ^oC). R_f 0.56 (1 : 9 ethyl acetate : hexane). Physical and chemical properties were as reported in the literature.[233]

(3*S*,5*S*,8*S*,9*R*,10*R*,13*R*,14*R*,17*R*)-10,13-dimethyl-17-(6-methylheptan-2-yl)-1,3,4,9,10,11,12,13,14,15,16,17-dodecahydro-2*H*-5,8-epidioxycyclopenta[*a*]phenanthren-3-yl acetate (82).

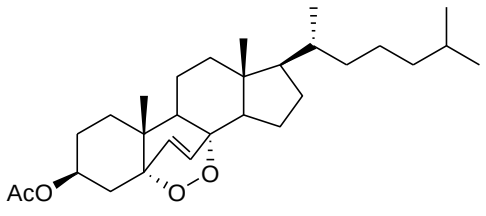

Amorphous white solid. Yield 72%. R_f 0.48 (3 : 17 ethyl acetate : hexane). Physical and chemical properties were as reported in the literature.[123]

6.3 Compounds Described in Chapter 3.

General Procedure for Ozonolysis of 1,2-Dioxines.

A solution of 1,2-dioxine (**3a-e**, **82** or **154**) (3 mmol) in dichloromethane (50 mL) was cooled to -78 ^{o}C under an atmosphere of argon. A stream of ozone was bubbled through the mixture until the solution turned pale blue. The mixture was bought back to room temperature, followed by the addition of triphenylphosphine (3.3 mmol). The resulting solution was stirred at room temperature overnight. The mixture was then concentrated *in vacuo* and the products purified by flash chromatography.

(1*R*,3a*R*,3b*S*,5a*R*,7*S*,9a*R*,9b*R*,11a*R*)-3b,5a-diformyl-9a,11a-dimethyl-1-(6-methylheptan-2-yl)tetradecahydro-1*H*-benzo[*c*]indeno[5,4-*e*][1,2]dioxin-7-yl acetate (85).

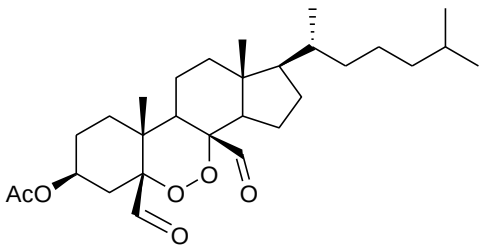

Colourless oil. Yield 92%. R_f 0.60 (3 : 7 ethyl acetate : hexane). ^{1}H NMR (300 MHz, $CDCl_3$): 10.01 (s, 1H), 9.62 (s, 1H), 5.28 (m, 1H), 2.83 (dd, 2H, J = 15.6, 3.6 Hz), 2.13 (m, 1H), 2.02 (s, 3H), 1.92-1.11 (m, 22H), 1.02 (s, 3H), 0.89 (d, 3H, J = 6.3 Hz), 0.87 (d, 3H, J = 1.2 Hz), 0.85 (d, 3H, J = 1.2 Hz), 0.74 (s, 3H); ^{13}C NMR (75 MHz, $CDCl_3$): 202.5, 196.8, 169.8, 88.5, 87.7, 69.2, 56.5, 55.8, 45.8, 45.5, 40.5, 39.4, 35.7, 35.4, 35.2, 31.0, 28.8, 28.01, 27.96, 24.0, 23.6, 22.7, 22.5, 21.2, 19.8, 19.3, 18.3, 18.1, 13.2. Dialdehyde **85** was unstable thus full characterisation was not possible.

Attempted Wittig Reaction on Steroid 85.

To a solution of dialdehyde (**85**) (95.0 mg, 0.19 mmol) in dichloromethane (5 mL) under an atmosphere of nitrogen was added ethyl 2-(triphenylphosphanylidene) acetate (**126**) (134 mg, 0.39 mmol). The mixture was stirred at ambient temperature and monitored *via* TLC for 2 days, with no change detected. The mixture was then heated under reflux for a further 2 days. Crude ^{1}H NMR of the resulting crude product showed only starting material **85**.

(1*R*,3a*R*,3b*S*,5a*R*,7*S*,9a*R*,9b*R*,11a*R*)-3b,5a-Bis(hydroxymethyl)-9a,11a-dimethyl-1-(6-methylheptan-2-yl)tetradecahydro-1*H*-benzo[*c*]indeno[5,4-*e*][1,2]dioxin-7-ol (127).

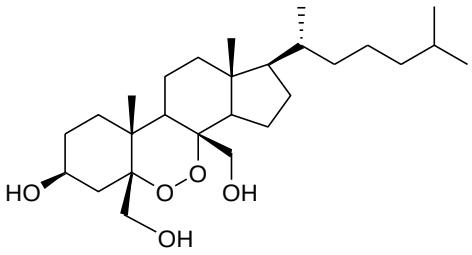

To a solution of dialdehyde (**85**) (927 mg, 1.89 mmol) in anhydrous THF (5 mL) at 0 ^{o}C under an atmosphere of nitrogen was added $LiAlH_4$ (215 mg, 5.67 mmol) in portions, with stirring. The mixture was kept at 0 ^{o}C until TLC showed the disappearance of the starting material (60 minutes). The mixture was quenched with saturated NH_4Cl (5 mL) and diluted with diethyl ether (10 mL). The mixture was then acidified to pH 1 with the addition of HCl (2M, few drops). The layers were separated and the aqueous layer extracted with diethyl ether (3 x 5 mL). The combined organic layers were washed with saturated aqueous $NaHCO_3$ (10 mL) brine, dried ($MgSO_4$) and concentrated *in vacuo*. The crude mixture was then purified by flash chromatography to furnish a white solid (106 mg, 55%) (**127**). Mp 174-175 ^{o}C. R_f 0.27 (6 : 4 ethyl acetate : hexane). $[\alpha]_D$ = +111.76 (*c* = 0.34, THF). ^{1}H NMR (300 MHz, $CDCl_3$): 4.61 (d, 1H, *J* = 12.3 Hz), 4.33 (s, 1H), 3.90 (d, 2H, *J* = 12.9 Hz), 3.48 (d, 1H, *J* = 12.3 Hz), 2.67 (dd, 1H, *J* = 15, 3 Hz), 2.41-1.06 (m, 27H), 1.01 (s, 3H), 0.93 (d, 3H, *J* = 10.8 Hz), 0.90 (s, 3H), 0.87 (d, 3H, *J* = 1.2Hz), 0.85 (d, 3H, *J* = 1.2 Hz); ^{13}C NMR (75 MHz, $CDCl_3$): 85.8, 85.2, 67.3,

64.6, 61.7, 57.8, 56.8, 45.5, 45.3, 41.6, 39.4, 35.8, 35.38, 35.35, 31.2, 29.0, 28.2, 28.0, 27.5, 23.7, 22.8, 22.5, 21.2, 18.9, 18.8, 18.4, 13.9; IR (nujol) 3313, 2927, 1464, 1379, 1059, 1034 cm^{-1}; HRMS calcd. for $(M+NH_4)^+$ $C_{27}H_{51}NO_5$: 470.3840; found 470.3835.

(±)-(3*R*,6*R*)-3-Methyl-6-(propan-2-yl)-1,2-dioxane-3,6-dicarbaldehyde (128a).

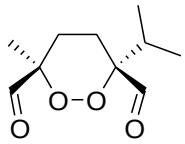

Colourless oil. Decomposes readily. Typically the crude sample was used immediately for Wittig protection and subsequent full characterisation. R_f 0.52 (3 : 7 ethyl acetate : hexane). A small amount was able to be isolated for NMR analysis before composition. ^{1}H NMR (300 MHz, $CDCl_3$): 9.69 (s, 1H), 9.42 (s, 1H), 2.12-2.03 (m, 2H), 1.85-1.78 (m, 2H), 1.59 (m, 1H), 1.44 (s, 3H), 0.98 (d, 3H, J = 7.2 Hz), 0.97 (d, 3H, J = 7.2 Hz); ^{13}C NMR (75 MHz, $CDCl_3$): 202.7, 199.1, 89.1, 84.4, 31.8, 24.4, 19.5, 17.3, 16.3, 15.9.

(±)-6-Methylheptane-2,5-dione (20a).

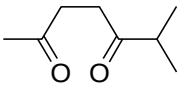

Colourless oil. R_f 0.24 (3 : 7 ethyl acetate : hexane). Physical and chemical properties were as reported in the literature.[234]

(±)- (3*R*,6*R*)-3-Phenyl-1,2-dioxane-3,6-dicarbaldehyde (128b).

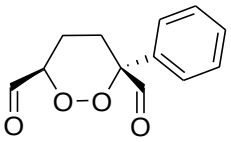

Colourless oil. Decomposes readily. Typically the crude sample was used immediately for Wittig protection and subsequent full characterisation. Yield 33 % isolated. R_f 0.38 (1 : 1 ethyl acetate : hexane). A small amount was able to be isolated for NMR analysis before decomposition. ^{1}H NMR (300 MHz, $CDCl_3$): 9.69 (d, 1H, J = 1.5 Hz), 9.61 (s,

1H), 7.52-7.30 (m, 5H), 4.69 (dd, 1H, *J* = 11.1, 3.0 Hz), 2.84 (m, 1H), 2.18-1.79 (m, 3H); ^{13}C NMR (75 MHz, $CDCl_3$): 197.7, 197.0, 129.2, 129.1, 129.0, 128.6, 125.4, 125.2, 89.0, 84.7, 26.6, 21.3.

(±)-Dimethyl 2,2'-[(3*R*,6*S*)-3,6-diformyl-1,2-dioxane-3,6-diyl]diacetate (128d)

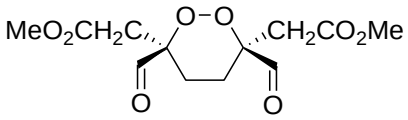

Purification and characterisation proved difficult, as the sample decomposed upon attempted column chromatography. Typically the crude sample was used immediately for Wittig protection and subsequent full characterisation. Crude NMR showed dialdehyde peaks present, see discussion. R_f 0.61 (7 : 3 ethyl acetate : hexane).

General procedure for Wittig Reaction of Ozonolysis Products.

To a solution of dialdehyde (**128a,b,** or **d**) (3 mmol) in dichloromethane (50 mL) under an atmosphere of nitrogen was added ethyl 2-(triphenylphosphanylidene) acetate (6 mmol) (**126**). The mixture was stirred at ambient temperature until complete by ^{1}H NMR or TLC. The mixture was then concentrated *in vacuo* and the products purified by flash chromatography.

(±)-Ethyl (2*E*)-3-[(3*R*,6*R*)-6-formyl-3-methyl-6-(propan-2-yl)-1,2-dioxan-3-yl]prop-2-enoate (129a).

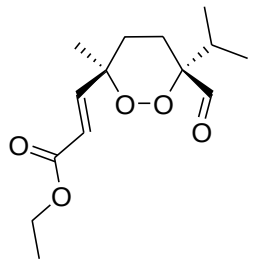

Colourless oil. Yield 44% (over three steps: ozonolysis, reduction and Wittig). R_f 0.55 (1 : 4 ethyl acetate : hexane). ^{1}H NMR (600 MHz, $CDCl_3$): 9.74 (br s, 1H), 6.72 (d, 1H, *J* = 16.2 Hz), 5.84 (d, 1H, *J* = 16.2 Hz), 4.19 (q, 2H, *J* = 7.2 Hz), 2.09 (ddd, 1H, *J* = 13.8, 5.4, 2.4 Hz), 1.93 (sept 1H, *J* = 7.2 Hz), 1.81 (m, 1H), 1.69 (apt dt, 1H, *J* = 13.2,

4.8 Hz), 1.63 (ddd, 1H, *J* = 13.8, 5.4, 3.0 Hz), 1.52 (s, 3H), 1.28 (t, 3H, *J* = 7.2 Hz), 0.97 (d, 3H, *J* = 7.2 Hz), 0.93 (d, 3H, *J* = 7.2 Hz); ^{13}C NMR (150 MHz, $CDCl_3$): 204.0, 166.1, 148.4, 120.3, 89.1, 79.0, 60.6, 32.3, 29.4, 20.8, 19.8, 16.3, 15.7, 14.1; IR (neat) 2976, 1723, 1655, 1369, 1309, 1184, 1036, 749 cm^{-1}; LRP (+LSIMS) *m/z* (*%*) 271 (M^+, 8), 258 (10), 242 (12), 225 (100), 195 (12), 179 (50); HRMS calcd. for $(M+H)^+$ $C_{14}H_{23}O_5$: 271.1545; found 271.1535.

(±)-Ethyl (2*E*)-3-[(3*R*,6*R*)-6-formyl-6-phenyl-1,2-dioxan-3-yl]prop-2-enoate (129b).

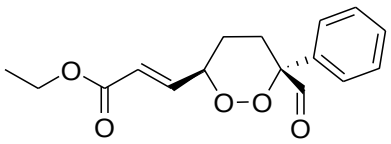

Colourless oil. Yield 10% over three steps (ozonolysis, reduction and Wittig). R_f 0.61 (dichloromethane). ^{1}H NMR (300 MHz, $CDCl_3$): 9.71 (d, 1H, *J* = 2.1 Hz), 7.43-7.30 (m, 5H), 6.74 (dd, 1H, *J* = 16.2, 5.1 Hz,), 5.98 (dd, 1H, *J* = 16.2, 1.6 Hz,), 4.88 (m, 1H), 4.21 (q, 2H, *J* = 7.2), 2.87 (m, 1H), 2.06-1.74 (m, 3H), 1.30 (t, 3H, *J* = 7.2 Hz); ^{13}C NMR (75 MHz, $CDCl_3$): 198.8, 165.7, 142.0, 134.9, 129.0, 125.1, 123.2, 88.6, 79.7, 60.8, 27.8, 26.5, 14.2 (3 aromatic C masked); IR (neat) 2987, 1724, 1658, 1452, 1309, 1275, 1193, 1036, 700 cm^{-1}; FTMS (+ESI) *m/z* (*%*): 291 (M^+, 4) 279 (5), 277 (12), 262 (16), 261 (100), 259 (2); HRMS calcd. for $(M+H)^+$ $C_{16}H_{19}O_5$: 291.1232; found 291.1229.

(±)-Diethyl (2*E*,2'*E*)-3,3'-[(3*R*,6*S*)-3,6-bis(2-methoxy-2-oxoethyl)-1,2-dioxane-3,6-diyl]bisprop-2-enoate (129d).

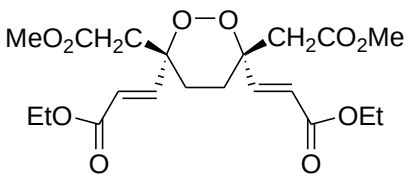

Colourless oil. Yield 21% (over three steps – ozonolysis, reduction and Wittig). R_f 0.51 (1 : 1 ethyl acetate : hexane). ^{1}H NMR (50 ^{o}C, 300 MHz, $CDCl_3$): 6.93 (d, 2H, *J* = 16.2 Hz), 6.00 (d, 2H, *J* = 16.2 Hz), 4.20 (q, 4H, *J* = 7.2 Hz), 3.67 (s, 6H), 2.92-2.63 (m, 4H),

2.23-2.15 (m, 2H), 1.95-1.88 (m, 2H), 1.29 (t, 6H, J = 7.2 Hz); ^{13}C NMR (50 ^{o}C, 75 MHz, $CDCl_3$): 169.1, 165.8, 146.4, 122.2, 80.3, 60.6, 51.7, 41.1, 27.1, 14.1; IR (neat) 2955, 1720, 1656, 1438, 1311, 1179, 1034, 865, 731 cm^{-1}; LRP (+LSIMS) *m/z* (*%*): 857 (10), 429 (M^+, 100), 412 (19), 337 (8), 235 (50); HRMS calcd. for $(M^+ + H)^+$ $C_{20}H_{29}O_{10}$: 429.1761; found 429.1752.

(±)-[(3*R*,6*R*)-3-Methyl-6-(propan-2-yl)-1,2-dioxane-3,6-diyl]dimethanediyl diacetate (131).

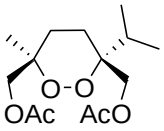

Ozonolysis was performed on ascaridole (**3a**) (260 mg, 1.55 mmol) and reduced with triphenylphosphine (407 mg, 1.55 mmol) *via* the general method to afford a crude oily solid. This was triturated with hexane to give a crude yellow oil (141 mg). To a stirred solution of this crude dialdehyde (141 mg, 0.70 mmol *(assuming 100% product)*) in anhydrous THF (5 mL) at 0 ^{o}C under an atmosphere of nitrogen was added $LiAlH_4$ (80 mg, 2.11 mmol) in portions, with stirring. The resulting mixture was stirred at 0 ^{o}C until TLC showed the disappearance of the starting material (30 minutes). The solution was quenched with saturated NH_4Cl (5 mL) and diluted with diethyl ether (10 mL). The mixture was acidified to pH 1 with the addition of conc. HCl (2M, 2 drops). The layers were separated and the aqueous layer extracted with diethyl ether (3 x 10 mL). The combined organic layers were washed with saturated aqueous $NaHCO_3$ (10 mL), water (10 mL), dried ($MgSO_4$) and concentrated *in vacuo*. To this crude mixture of diol **130** was added pyridine (1 mL), acetic anhydride (0.64 g, 6.34 mmol) and DMAP (17 mg, 0.14 mmol), and the resulting solution was stirred overnight. The mixture was diluted with dichloromethane (5 mL) and washed with 10% HCl (5 mL). The organic layer was then removed and the aqueous layer extracted with dichloromethane (3 x 5 mL). The organic layers were combined, washed with water (5 mL) and brine (5 mL), dried ($MgSO_4$) and concentrated *in vacuo*. The residue was purified *via* flash chromatography to afford a colourless oil (65 mg, 32%) (**131**). R_f 0.57 (3 : 7 ethyl acetate : hexane). ^{1}H NMR (+50 ^{o}C, 300 MHz, $CDCl_3$): 4.28 (d, 1H, J = 12.3 Hz), 4.16 (d, 1H, J = 12.3 Hz), 4.10 (br s, 2H), 2.23 (m, 1H), 2.08 (s, 3H), 2.07 (s, 3H), 1.82-1.54 (m, 4H), 1.27 (s, 3H),

0.97 (d, 6H, J = 6.9 Hz); ^{13}C NMR (+ 50 ^{o}C, 75 MHz, $CDCl_3$): 170.6 (x2 overlapping), 82.4, 78.8, 67.3, 63.1, 31.9, 26.5, 22.0, 20.8, 20.7, 19.9, 16.7, 16.6; IR (neat): 2974, 2364, 1747, 1458, 1377, 1246, 1049 cm^{-1}; LRP (+LSIMS) *m/z* (*%*): 530 (67), 475 (9), 338 (26), 289 (M^+, 35), 243 (24) (219 (100). HRMS calcd. for $(M+H)^+$ $C_{14}H_{25}O_6$: 289.1651; found 289.1639.

(±)- (2*S*)-2-Hydroxy-5-oxo-2,5-diphenylpentanal (132a)

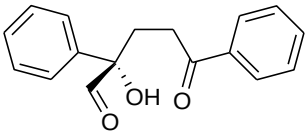

Method A: Reduction with PPh_3.

Following general procedure outline for the ozonolysis of 1,2-dioxines.

Method B: Reduction with Me_2S.

A solution of 1,2-dioxine (**3c**) (3 mmol) in dichloromethane (50 mL) was cooled to -78 ^{o}C under an atmosphere of argon. A stream of ozone was bubbled through the mixture until the solution turned pale blue. The mixture was bought back to room temperature and placed under an atmosphere of nitrogen. Dimethyl disulphide (3.3 mmol) was slowly added, and the resulting mixture was stirred at room temperature overnight. The mixture was then concentrated *in vacuo* and the products purified by flash chromatography.

Colourless needles. Yield 26%. Mp 82-84 ^{o}C. R_f 0.29 (1 : 4 ethyl acetate : hexane) ^{1}H NMR (300 MHz, $CDCl_3$): 9.64 (d, 1H, J = 1.2 Hz), 7.93-7.89 (m, 2H), 7.58-7.30 (m, 8H), 4.34 (d, OH, J = 1.2 Hz), 3.14 (dt, 1H, J = 18.2, 7.5 Hz), 3.02 (dt, 1H, J = 18.2, 6.6 Hz), 2.52 (dd, 2H, J = 7.5, 6.6 Hz); ^{13}C NMR (75 MHz, $CDCl_3$): 200.1, 199.7, 138.0, 136.4, 133.4, 128.9, 128.6, 128.1, 128.1, 125.8, 81.0, 32.2, 30.7; IR (nujol) 3448, 2927, 2859, 1722, 1676, 741 cm^{-1}; LRP (+LSIMS) *m/z* (*%*) 269 (M^+, < 1), 239 (100), 221 (24), 193 (9), 178 (7), 161 (43), 133 (18), 115 (23), 105 (87), 77 (48); HRMS calcd. for $(M)^+$ $C_{17}H_{16}O_3$: 268.1099; found 268.1105.

Details of crystal structure determination of $C_{17}H_{16}O_3$.

Crystal data for $C_{17}H_{16}O_3$: M = 268.30, T = 98(2) K, triclinic, P-1, a = 5.6262(15), b = 10.040(3), c = 12.165(3) Å, α = 95.510(4), β = 90.569(6), γ = 100.990(7)º, V = 671.2(3) Å^3, Z = 2, D_x = 1.328, $F(000)$ = 284, μ = 0.090 mm^{-1}, no. of unique data (Rigaku AFC12κ/SATURN724 CCD using Mo Kα radiation so that θ_{max} = 26.5°) = 2741, no. of parameters = 184, R (2418 data with $I \geq 2\sigma(I)$) = 0.054, wR (all data) = 0.153. The structure was solved by direct-methods (SHELXS-97) and refined (anisotropic displacement parameters, H atoms in the riding model approximation, and a weighting scheme $w = 1/[\sigma^2(F_o^2) + (0.071P)^2 + 0.33P]$ where $P = (F_o^2 + 2F_c^2)/3$) with SHELXL-97 on F^2. CCDC deposition number: 743807.

1,1':4',1''-Terphenyl (133).

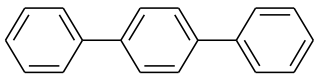

White solid. Yield 21%. Mp 210-212 °C (lit[235] 212-213 °C). R_f 0.88 (2 : 8 ethyl acetate : hexane). Physical and chemical properties were as reported in the literature.[235]

1,4-Diphenylbutane-1,4-dione (20b).

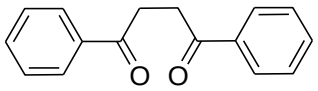

White solid. Yield 7%. Mp 146-148 °C (lit[236] 142-146 °C). R_f 0.20 (2 : 8 ethyl acetate : hexane). Physical and chemical properties were as reported in the literature.[236]

(±)-Dimethyl (3*R*, 6*S*)-3,6-diformyl-1,2-dioxane-3,6-dicarboxylate (128e); (±)-dimethyl (2*S*)-2-formyl-2-hydroxy-5-oxohexanedioate (132b) and (±)-1,6-dimethyl 3,4-dideoxy-2,5-di-*C*-formyl-D-*erythro*-hexarate (137)

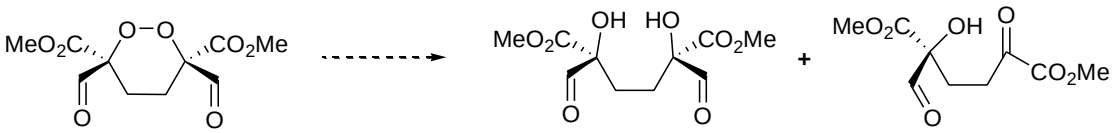

Following general procedure outline for the ozonolysis of 1,2-dioxines. Multiple attempts were made to isolate and purify the compounds resulting from the ozonolysis of 1,2-dioxine **3e**, but all were unsuccessful. Crude and impure ^{1}H NMR's were obtained that showed distinctive dialdehyde peaks, athough products could not be separated out and no further data could be extracted from this. See discussion for further details. The crude sample was immediately subjected to Wittig reaction.

Compounds **134**, **135** and **136** were synthesised following the general procedure for the Wittig reaction of ozonolysis products using the crude products from the ozonolysis of **3e**.

(±)-1,7-Diethyl 3-methyl (1*E*,3*S*)-3-hydroxy-6-propanoylhepta-1,6-diene-1,3,7-tricarboxylate (134).

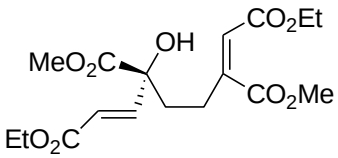

Colourless oil. Yield 15% (over three steps: ozonolysis and Wittig). R_f 0.69 (1 : 1 ethyl acetate : hexane) ^{1}H NMR (600 MHz, $CDCl_3$): 6.99 (d, 1H J = 15.3 Hz), 6.77 (s, 1H), 6.27 (d, 1H J = 15.3 Hz), 4.24 (q, 2H, J = 7.2 Hz), 4.19 (q, 2H, J = 7.2 Hz), 3.82 (s, 3H), 3.81 (s, 3H), 2.89-2.80 (m, 2H), 2.10 (ddd, 1H, J = 15.9, 9.9, 6.6 Hz), 1.96 (ddd, 1H, J = 15.9, 9.9, 6.6 Hz), 1.31 (t, 3H, J = 7.2 Hz), 1.29 (t, 3H, J = 7.2 Hz) (hydroxl proton not detected); ^{13}C NMR (150 MHz, $CDCl_3$): 174.0, 166.8, 166.1, 165.5, 146.7, 146.1, 127.7, 121.8, 76.8, 60.9, 60.5, 53.3, 52.5, 37.4, 22.3, 14.1, 14.0; IR (neat) 3497, 2956, 1711, 1647, 1438, 1263, 1176, 1028, 983, 732 cm^{-1}; LRP (+LSIMS) *m/z* (%) 373

(M^+, 100), 355 (19), 327 (30), 309 (34), 295 (32), 281 (74), 267 (36), 249 (28), 235 (25), 221 (60), 207 (68); HRMS calcd. for $(M+H)^+$ $C_{17}H_{25}O_9$: 373.1499; found 373.1499.

(±)-1,7-Diethyl 3-methyl (1*E*,3*S*,5*E*)-3-hydroxy-6-propanoylhepta-1,5-diene-1,3,7-tricarboxylate (135).

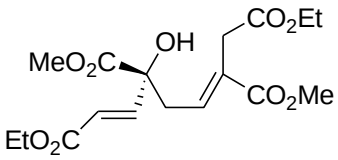

Colourless oil. Yield 31% (over three steps: ozonolysis and Wittig). R_f 0.57 (1 : 1 ethyl acetate : hexane) ^{1}H NMR (600 MHz, $CDCl_3$): 6.94 (d, 1H, *J* = 15.6 Hz), 6.25 (d, 1H, *J* = 15.6 Hz), 5.83 (t, 1H, *J* = 1.5 Hz), 4.21 (q, 2H, *J* = 7.2 Hz), 4.18 (q, 2H, *J* = 7.2 Hz), 3.84 (s, 3H), 3.82 (s, 3H) 3.51 (s, 1OH), 2.46 (m, 1H), 2.31 (m, 1H), 2.05 (m, 1H), 1.97 (m, 1H), 1.30 (t, 3H, *J* = 7.2 Hz), 1.27 (t, 3H, *J* = 7.2 Hz); ^{13}C NMR (150 MHz, $CDCl_3$): 173.8, 168.7, 165.9, 164.7, 148.0, 146.1, 122.5, 120.9, 76.4, 60.8, 60.7, 53.8, 52.4, 35.9, 28.2, 14.2, 14.1; IR (neat) 3484, 2957, 1717, 1437, 1259, 1173, 1030, 983, 735 cm^{-1}; LRP (+LSIMS) *m/z* (%) 373 (M^+, 100), 341 (17), 327 (32), 309 (5), 295 (44), 281 (26), 263 (12), 249 (18), 235 (12), 221 (13), 207 (14); HRMS calcd. for $(M+H)^+$ $C_{17}H_{25}O_9$: 373.1499; found 373.1502.

(±)-1,6-Dimethyl 3,4-dideoxy-2,5-bis-*C*-[(1*E*)-3-ethoxy-3-oxoprop-1-en-1-yl]-D-*erythro*-hexarate (136).

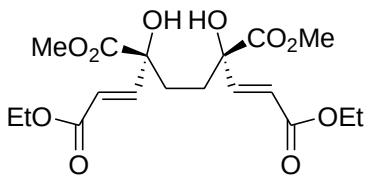

Colourless oil. Yield: 7% (over three steps: ozonolysis and Wittig). R_f 0.48 (1 : 1 ethyl acetate : hexane). ^{1}H NMR (600 MHz, $CDCl_3$): 6.93 (d, 2H, *J* = 15.3 Hz), 6.23 (d, 2H, *J* = 15.3 Hz), 4.21 (q, 4H, *J* = 7.2 Hz), 3.83 (s, 6H), 3.52 (s, 2H), 1.95 (dd, 2H, *J* = 13.8, 4.8 Hz), 1.72 (dd, 2H, *J* = 13.8, 4.8 Hz), 1.30 (t, 6H, *J* = 7.2 Hz); ^{13}C NMR (150 MHz,

$CDCl_3$): 174.0, 166.0, 146.4, 122.3, 76.5, 60.7, 53.7, 32.4, 14.2; IR (neat) 3458, 2958, 1710, 1437, 1231, 1105, 996 cm^{-1}; LRP (+LSIMS) *m/z* (%) 403 (M+, 100), 369 (18), 327 (32), 311 (21), 281 (28), 251 (15), 235 (20), 219 (27), 191 (23); HRMS calcd. for $(M+H)^+$ $C_{18}H_{27}O_{10}$: 403.1604; found 403.1602.

Attempted Isomerisation of 134 and 135.

Method A: Heat

An NMR tube containing **134** (10 mg) or **135** (27 mg) in $CDCl_3$ was heated to 60 ^oC, and the temperature was maintained for 7 hours. No change was detected for either sample *via* TLC or ^1H NMR.

Method B: Heat and Acidic Conditions

An NMR tube containing **134** (10 mg) or **135** (27 mg) in $CDCl_3$ with a catalytic amount (10 mol %) of PTSA was heated to 60 ^oC, and the temperature was maintained for 6 hours. No change was detected for either sample *via* TLC or ^1H NMR.

See Table 5 and discussion for further details.

General Procedure for Unsymmetrical Ozonolysis of 1,2-Dioxines.

An ozone stream was bubbled through a stirred suspension of 1,2-dioxine **3a** or **3e** (1 mmol) and $NaHCO_3$ (0.5 mmol) in a 5 : 1 mixture of CH_2Cl_2 : MeOH (10 mL) at -78 ^oC under an atmosphere of argon, until the solution turned pale blue. The solution was bought back to room temperature. The $NaHCO_3$ was filtered off and the mother liqueur concentrated *in vacuo*. The residue was taken up in CH_2Cl_2 (10 mL) and cooled to 0 ^oC. Triethylamine (1.5 mmol) and acetic anhydride (3 mmol) were then added, and the solution brought to room temperature and stirred for 1 hour. This mixture was treated with methanol (1 mL) (to destroy the excess acetic anhydride), stirred for 15 minutes and then diluted with diethyl ether (5 mL) and washed with 5% H_2SO_4 (3 x 10 mL), saturated $NaHCO_3$ (10 mL), brine (10 mL), dried ($MgSO_4$) and concentrated *in vacuo*. The crude mixture was purified by flash chromatography.

(±)-Methyl [(3*R*,6*R*)-6-formyl-3-methyl-6-(propan-2-yl)-1,2-dioxan-3-yl]acetate (145a).

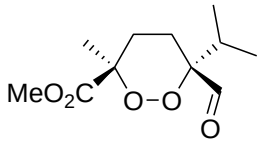

Colourless crystals. Yield 13 %. R_f 0.70 (3 : 7 ethyl acetate : hexane). Mp 64-66 °C. ^{1}H NMR (300 MHz, $CDCl_3$): 9.71 (br d, 1H, J = 1.5 Hz), 3.71 (s, 3H), 2.10-1.74 (m, 5H), 1.58 (s, 3H), 0.94 (d, 3H, J = 6.9 Hz), 0.92 (d, 3H, J = 6.9 Hz); ^{13}C NMR (75 MHz, $CDCl_3$): 203.5, 171.7, 89.2, 81.2, 52.5, 32.1, 27.3, 19.9, 19.8, 16.3, 15.8; IR (neat) 2971, 1738, 1456, 1374, 1288, 1248, 1123, 748 cm^{-1}; LRP (+LSIMS) *m/z* (*%*): 483 (22), 304 (30), 269 (16), 248 (100), 231 (5), 186 (23); HRMS calcd. for $(M+H)^+$ $C_{11}H_{19}O_5$: 231.1232; found 231.1227.

Details of crystal structure determination of $C_{11}H_{18}O_5$.

Crystal data for $C_{11}H_{18}O_5$: M = 230.25, T = 98(2) K, monoclinic, $P2_1/c$, a = 10.686(3), b = 7.0118(19), c = 16.046(5) Å, β = 107.784(3)º, V = 1144.9(6) Å^3, Z = 4, D_x = 1.336, F(000) = 496, μ = 0.105 mm^{-1}, no. of unique data (Rigaku AFC12κ/SATURN724 CCD using Mo Kα radiation so that θ_{max} = 26.5°) = 2352, no. of parameters = 146, R (2203 data with $I \geq 2\sigma(I)$) = 0.044, wR (all data) = 0.115. The structure was solved by direct-methods (SHELXS-97) and refined (anisotropic displacement parameters, H atoms in the riding model approximation, and a weighting scheme $w = 1/[\sigma^2(F_o^2) + (0.053P)^2+0.748P]$ where $P = (F_o^2 + 2F_c^2)/3$) with SHELXL-97 on F^2. CCDC deposition number: 743808.

(±)-Methyl [(3*S*,6*R*)-6-formyl-6-methyl-3-(propan-2-yl)-1,2-dioxan-3-yl]acetate (145b).

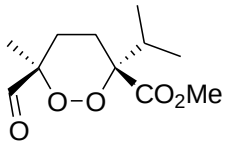

Colourless oil. Yield 11%. R_f 0.53 (3 : 7 ethyl acetate : hexane). ^{1}H NMR (600 MHz, $CDCl_3$): 9.58 (s, 1H), 3.78 (s, 3H), 2.41-2.32 (m, 1H), 2.14-1.98 (m, 4H), 1.32 (s, 3H), 0.99 (d, 3H, J = 7.2) 0.97 (d, 3H, J = 7.2 Hz); ^{13}C NMR (75 MHz, $CDCl_3$): 200.9, 170.8, 87.4, 84.6, 52.1, 31.9, 24.9, 22.7, 18.2, 16.9, 16.8; IR (neat) 2972, 1737, 1444, 1372, 1243, 1043, 754 cm^{-1}; LRP (+LSIMS) *m/z* (*%*): 231 (M+, 10), 201 (5), 185 (21), 171 (8), 155 (100), 143 (19); HRMS calcd. for $(M+H)^+$ $C_{11}H_{19}O_5$: 231.1232; found 231.1240.

(±)-Trimethyl (5*S*)-5-hydroxydihydrofuran-2,2,5(3*H*)-tricarboxylate (148).

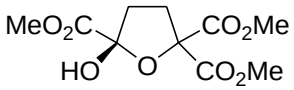

Colourless waxy oil. Yield: 25%. R_f 0.52 (3 : 7 ethyl acetate : hexane). ^{1}H NMR (600MHz, $CDCl_3$): 4.26 (s, OH), 3.84 (s, 3H), 3.82 (s, 3H), 3.80 (s, 3H), 2.74-2.68 (m, 2H), 2.54 (dt, 1H, J = 13.2, 9 Hz), 2.17 (m, 1H); ^{13}C NMR (150 MHz, $CDCl_3$): 169.4, 169.2, 168.4, 104.1, 87.3, 53.4, 53.3, 53.2, 34.4, 32.2; IR (neat) 3471, 2964, 2364, 1749, 1441, 1288, 1209, 1076, 1016, 669 cm^{-1}; LRP (+LSIMS) *m/z* (*%*): 295 (18), 267 (30), 245 ($(M - OH)^-$, 33), 221 (100), 204 (33), 193 (33), 185 (34); HRMS calcd. for $(M - OH)^-$ $C_{10}H_{13}O_7$: 245.0661; found 245.0666.

6.4 Compounds Described in Chapter 5.

(±)-1,5-Dimethylcyclohexa-1,4-diene (182).

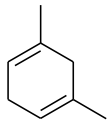

Ammonia (100 mL) was condensed in a 500 mL flask at -78 ^{o}C under an atmosphere of nitrogen. *m*-xylene (**181**) (11.48 g, 0.108 mol) in dry THF (20 mL) was added slowly with stirring. Lithium pieces (3.00 g, 0.43 mol) were added in small portions over 30 minutes. The solution was kept at -78 ^{o}C for a further 30 minutes after which the temperature was raised to -35 ^{o}C and stirred for a further 45 minutes. Ethanol (15 mL) was added dropwise over a period of 1 hour followed by a further portion of ethanol (15 mL) slowly added over 30 minutes. The resulting mixture was allowed to heat up to room temperature and any remaining ammonia was evaporated off by bubbling nitrogen through the mixture for 1 hour. Water (50 mL) was added slowly and the resulting mixture was extracted with hexane (3 x 50 mL). The combined organics were dried ($MgSO_4$) and concentrated *in vacuo* to afford a pale yellow oil (6.89 g, 59%) (**182**). Physical and chemical properties were as reported in the literature.[237]

Attempted isomerisation of 182 to 155.

The following methods were trialled in an attempt to isomerise **182** into **155**.
10% HCl (aq) heated under reflux overnight; 10 : 1 MeOH : H_2SO_4 heated under reflux overnight; *t*-BuOH/*t*-BuOK heated under reflux overnight; 1 : 1 THF : 2.5 M $LiOH.H_2O$ stirred at room temperature overnight. Each attempt resulted in the apparent polymerisation of **182**. See discussion for further details.

(±)-1,3-Dimethylcyclohex-2-en-1-ol (183).

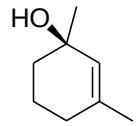

3-Methyl-2-cyclohexen-1-one (**185**) (12.71 g, 0.115 mol) in dry diethyl ether (50 mL) was added over 30 minutes to a solution of methylmagnesium bromide (50 mL, 0.150 mol, 3M solution in diethyl ether) at 0 ^{o}C under a dry atmosphere of nitrogen with stirring. The mixture was bought to reflux for 3 hours, after which it was cooled to 0 ^{o}C and icy water (100 mL) slowly added. The aqueous layer was separated and extracted with diethyl ether (4 x 50 mL). The combined organic extracts were washed with water (100 mL), brine (100 mL) and then dried ($MgSO_4$) and concentrated *in vacuo* to give a yellow oil (12.80 g 88%) (**183**). R_f 0.56 (3 : 7 ethyl acetate : hexane). Physical and chemical properties were as reported in the literature.[205]

1,3-Dimethylcyclohexa-1,3-diene (184) and 1-methyl-3-methylidenecyclohexene (155).

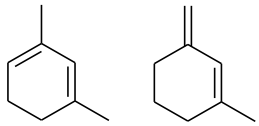

A solution of 1,3-dimethyl-2-cyclohexen-1-ol (**183**) (9.15 g, 72.6 mmol) in diethyl ether (80 mL) and 5% perchloric acid (80 mL) was stirred vigorously at 0 ^{o}C for 2 hours. The aqueous layer was separated and extracted with diethyl ether (2 x 50 mL). The combined organic extracts were washed with water (50 mL), dried ($MgSO_4$) and *carefully* concentrated *in vacuo* to yield a pale yellow oil (6.59 g, 84%) (**188** and **155**). R_f 0.83 (1 : 9 ethyl acetate : hexane). NMR confirmed a 1:1 mixture of dienes. ^{1}H NMR (300 MHz, $CDCl_3$): 5.93 (m, 1H), 5.54 (apt. quin, 1H, J = 1.5 Hz), 5.32 (m, 1H), 4.66-4.63 (m, 2H), 2.71 (m, 1H), 2.15-2.09 (m, 2H), 2.05-1.97 (m, 5H), 1.78 (s, 3H), 1.76 (3, 3H), 1.72-1.66 (m, 2H), 1.70 (s, 3H); ^{13}C NMR (75 MHz, $CDCl_3$): 114.0, 139.0, 136.0, 131.9, 125.0, 122.9, 117.2, 107.9, 30.4, 30.3, 28.1, 23.8, 23.2, 23.13, 23.10, 21.4. Remaining physical and chemical properties were as reported in the literature.[205,206] The

mixture was used without delay for photolysis, due to polymerisation of products with time.

(±)-(1*R*,4*S*)-1,5-Dimethyl-2,3-dioxabicyclo[2.2.2]oct-5-ene (154).

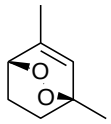

An 1:1 isomeric mixture of **188** and **155** was subjected to the general photolysis conditions to afford **154** as a colourless oil. Yield 76%. R_f 0.27 (1 : 9 ethyl acetate : hexane). ^{1}H NMR (300 MHz, $CDCl_3$): 6.03 (s, 1H), 4.42 (m, 1H), 2.29 (m, 1H), 2.02 (m, 1H), 1.95 (s, 3H), 1.56-1.40 (m, 2H), 1.35 (s, 3H); ^{13}C NMR (75 MHz, $CDCl_3$): 141.5, 128.9, 75.4, 75.2, 29.1, 23.1, 21.8, 18.5; IR (neat) 2932, 2360, 1660, 1444, 1374, 1224, 1158, 886, 764 cm^{-1}; LRP (+LSIMS) *m/z* (*%*) 190 (4), 173 (2), 158 (36), 155 (13), 141 (95), 125 (M+, 13), 123 (100), 113 (9); HRMS calcd. for $(M+H)^+$ $C_8H_{13}O_2$: 141.0916; found 141.0910.

(±)-(3*R*,6*S*)-6-Acetyl-3-methyl-1,2-dioxane-3-carbaldehyde (156).

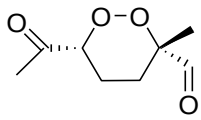

1,2-Dioxine **154** was subjected to the standard ozonolysis conditions outlined for 1,2-dioxines **3a-e**. to afford **156** as a pale yellow oil. Yield 45%. R_f 0.46 (3 : 7 ethyl acetate : hexane). ^{1}H NMR (300 MHz, $CDCl_3$): 9.75 (d, 1H, J = 1.8 Hz), 4.55 (dd, 1H, J = 11.7, 3.0 Hz), 2.39 (m, 1H), 2.14 (s, 3H), 1.95 (m, 1H), 1.75-1.51 (m, 2H), 1.19 (s, 3H); ^{13}C NMR (75 MHz, $CDCl_3$): 204.0 202.2, 85.8, 85.3, 27.9, 26.4, 22.8, 19.8; IR (neat) 2934, 2360, 1724, 1446, 1363, 1115, 935, 749 cm^{-1}; LRP (+LSIMS) *m/z* (*%*) 295 (20), 279 (33), 255 (9), 215 (12), 211 (97), 195 (100), 181 (22), 173 (M+, 2), 139 (36), 123 (19) HRMS calcd. for $(M+H)^+$ $C_8H_{13}O_4$: 173.0814; found 173.0808.

Kornblum-DeLaMare Rearrangement of Dioxine Ketal (156).

To a solution of dioxine (**156**) (31 mg, 0.18 mmol) in dichloromethane (2 mL) at room temperature under an atmosphere of nitrogen was added four drops of a mixture of triethylamine in dichloromethane (0.069 M). The mixture was stirred at room temperature until complete *via* TLC (*ca* 8-10 hrs). The volatiles were removed *in vacuo* and the crude product was purified by flash chromatography to give a 2.7 : 1 ratio of diastereomers (**188a** and **188b**) (23 mg, 74%). R_f 0.27 (3 : 7 ethyl acetate : hexane).

Major Isomer **(±)-(1*S*,5*S*,7*R*)-7-Hydroxy-1,5-dimethyl-6,8-dioxabicyclo[3.2.1]octan-4-one (188a).**

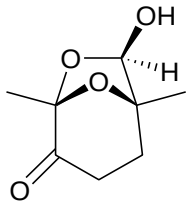

Colourless crystalline needles. Mp 77-78 ^{o}C. ^{1}H NMR (600 MHz, $CDCl_3$): 5.36 (d, 1H, J = 6.6 Hz), 2.96 (d, OH, J = 7.8 Hz), 2.73 (ddd, 1H, J = 16.5, 12.0, 9.0 Hz), 2.37 (ddd, 1H, J = 16.5, 7.8, 1.2 Hz), 2.17 (ddd, 1H, J = 13.8, 12.0, 7.8 Hz), 2.09 (ddd, 1H, J = 13.8, 9.0, 1.2 Hz), 1.51 (s, 3H), 1.41 (s, 3H); ^{13}C NMR (150 MHz, $CDCl_3$): 201.0, 105.7, 98.3, 83.7, 34.3, 31.3, 19.5, 17.5; IR (neat) 3449, 2942, 1732, 1456, 1383, 1226, 1097, 982, 866 cm^{-1}; LRP (+LSIMS) *m/z* (*%*) 463 (12), 431 (82), 338 (21), 295 (11), 259 (14), 227 (100), 190 (13), 173 (M+, 5) 155 (66), 137 (19); HRMS calcd. for $(M+H)^+$ $C_8H_{13}O_4$: 173.0814; found 173.0808.

Details of crystal structure determination of $C_8H_{12}O_4$.

Crystal data for $C_8H_{12}O_4$: M = 172.18, T = 100(1) K, monoclinic, $P2_1/n$, a = 12.5116(3), b = 5.1731(1), c = 13.8903(3) Å, β = 111.523(1)º, V = 836.34(3) Å^3, Z = 4, D_x = 1.367, F(000) = 368, μ = 0.110 mm^{-1}, no. of unique data (Bruker SMART APEX II using Mo Kα radiation so that θ_{max} = 27.5°) = 1923, no. of parameters = 115, R (1750 data with $I \geq 2\sigma(I)$) = 0.046, wR (all data) = 0.104. The structure was solved by direct-methods (SHELXS-97) and refined (anisotropic displacement parameters, H atoms in the riding

model approximation, and a weighting scheme $w = 1/[\sigma^2(F_o^2) + (0.027P)^2+0.631P]$ where $P = (F_o^2 + 2F_c^2)/3)$ with SHELXL-97 on F^2. The hydroxyl-H9 atom was disordered over two sites of equal weight. This arrangement allows for cohesive hydrogen bonding interactions leading to a supramolecular chain motif. CCDC deposition number: 743809.

Minor Isomer **(±)-(1*S*,5*S*,7*S*)-7-Hydroxy-1,5-dimethyl-6,8-dioxabicyclo[3.2.1]octan-4-one (188b).**

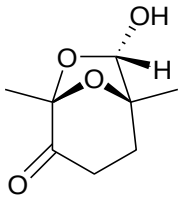

Colourless oil. ^{1}H NMR (600 MHz, $CDCl_3$): 5.31 (d, 1H, J = 3.0 Hz), 3.88 (d, OH, J = 3.6 Hz), 3.16 (ddd, 1H, J = 17.1, 11.4, 9.0 Hz), 2.42-2.33 (m, 2H), 2.01 (ddd, 1H, J = 13.8, 11.4, 7.5 Hz), 2.00 (m, 1H), 1.42 (s, 3H), 1.40 (s, 3H); ^{13}C NMR (150 MHz, $CDCl_3$): 202.4, 104.9, 101.4, 81.8, 32.4, 31.5, 21.3, 17.6. ^{1}H and ^{13}C NMR data was extracted from a diastereomeric mixture of **188a** and **188b** utilising 2D NMR. See discussion for full details.

Wittig Reaction on 156 and 188.

<u>*Method A:*</u> *(Using pure bicyclic or keto-aldehyde).*

To a solution of keto-aldehyde **156** or bicyclic **188a** and **188b** (1 mmol) in dichloromethane (30 mL) under an atmosphere of nitrogen was added slowly benzyl-(triphenylphosphanylidene) acetate (**190**) (0.9 to 2 mmol) in dichloromethane (20 mL) *via* a dropping funnel with stirring. The mixture was stirred overnight at ambient temperature. The mixture was then concentrated *in vacuo* and the products purified by flash chromatography.

Method B: (Using crude keto-aldehyde-directly from ozonolysis).

A solution of 1,2-dioxine **156** (1 mmol) in dichloromethane (30 mL) was cooled to -78 ^{o}C under an atmosphere of argon. A stream of ozone was bubbled through until the solution turned pale blue. The solution was bought back to room temperature and put under an atmosphere of nitrogen. Triphenylphosphine (1.1 mmol) in a minimum amount of dichloromethane was slowly added *via* a dropping funnel and the resulting mixture was stirred under an atmosphere of nitrogen at room temperature overnight. To this crude mixture was added slowly benzyl-(triphenylphosphanylidene) acetate (**190**) (0.9 to 2 mmol) in dichloromethane (20 mL) *via* a dropping funnel and the resulting mixture was stirred at room temperature overnight. The mixture was then concentrated *in vacuo* and the products purified by column chromatography.

(±)-Benzyl (2*E*)-3-[(2*R*,5*R*)-5-acetyl-5-hydroxy-2-methyltetrahydrofuran-2-yl]prop-2-enoate and (±)-Benzyl (2*E*)-3-[(2*R*,5*S*)-5-acetyl-5-hydroxy-2-methyltetrahydrofuran-2-yl]prop-2-enoate (191).

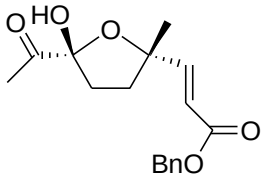

Mixture of inseparable diastereomers. Colourless oil. R_f 0.39 (1 : 9 ethyl acetate : dichloromethane). ^{1}H NMR (600 MHz, $CDCl_3$): 7.38-7.31 (m, 10H), 7.10 (d, 1H, *J* = 15.6 Hz), 7.02 (d, 1H, *J* = 15.6 Hz), 6.19 (d, 1H, *J* = 15.6 Hz), 6.05 (d, 1H, *J* = 15.6 Hz), 5.22-5.15, 5.21 and 5.18 (ABq, 2H, *J* = 12.0 Hz), 5.20 and 5.16 (ABq, 2H, *J* = 12.0 Hz), 4.38 (s, OH), 4.37 (s, OH), 2.31 (s, 3H), 2.30 (s, 3H), 2.36-2.25 (m, 4H), 2.22-2.14 (m, 2H), 2.08-2.01 (m, 2H), 1.54 (s, 3H), 1.42 (s, 3H); ^{13}C NMR (150 MHz, $CDCl_3$): 205.2, 205.0, 166.5, 166.3, 152.4, 152.0, 135.9, 135.8, 128.6, 128.5, 128.3, 128.3, 128.2, 119.0, 118.5, 104.7, 104.6, 85.2, 85.1, 66.4, 66.3, 36.74, 36.66, 35.2, 34.9, 27.8, 26.0, 23.3, 22.7; IR (neat) 3461, 2982, 1718, 1658, 1457, 1286, 1160, 982, 741, 698 cm^{-1}; LRP (+LSIMS) *m/z* (%) 573 (13), 523 (10), 447 (21), 391 (19), 338 (11), 322 ($M+NH_4^+$), 313 (16), 287 (100), 235 (22), 198 (88) 179 (98); HRMS calcd. for $(M+NH_4)^+$ $C_{17}H_{20}O_5NH_4$: 322.1649; found 322.1642.

(±)-Diphenyl (2*E*,6*R*,7*E*)-3-acetyl-6-hydroxy-6-methylnona-2,7-dienedioate (192a).

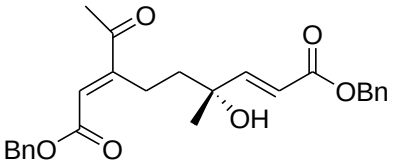

Colourless oil. R_f 0.31 (1 : 9 ethyl acetate : dichloromethane). ^{1}H NMR (600 MHz, $CDCl_3$): 7.99-7.30 (m, 10H), 6.95 (d, 1H, *J* = 15.9 Hz), 6.56 (s, 1H), 6.13 (d, 1H, *J* = 15.9 Hz), 5.21 (s, 2H), 5.18 (d, 2H, *J* = 3 Hz), 2.75 (t, 2H, *J* = 7.8 Hz), 2.32 (s, 3H), 1.74 (dt, 1H, *J* = 13.8, 8.0 Hz), 1.66 (dt, 1H, *J* = 14.7, 7.0 Hz), 1.30 (s, 3H) (hydroxyl peak not detected) ; ^{13}C NMR (150 MHz, $CDCl_3$): 199.5, 166.5, 165.9, 155.2, 154.4, 136.0, 135.1, 128.7, 128.6, 128.6, 128.5, 128.2, 128.1, 118.8, 72.7, 67.1, 66.1, 40.7, 27.6, 26.2, 21.3; IR (neat) 3464, 2952, 1718, 1456, 1374, 1285, 1165, 984, 738, 697 cm^{-1}; FTMS (+ESI) *m/z* (*%*) 475 (7), 459 (9), 454 ($M+NH_4^+$,100), 437 (8), 419 (6); HRMS calcd. for $(M+NH_4)^+$ $C_{26}H_{28}O_6NH_4$: 454.2224; found 454.2214.

(±)-Dibenzyl (2*Z*,6*R*,7*E*)-3-acetyl-6-hydroxy-6-methylnona-2,7-dienedioate (192b).

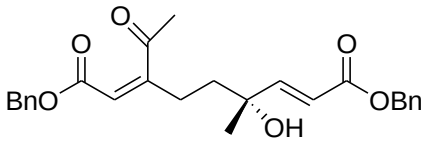

Colourless oil. R_f 0.21 (1 : 9 ethyl acetate : dichloromethane). ^{1}H NMR (600 MHz, $CDCl_3$): 7.39-7.31 (m, 10H), 6.91 (d, 1H, *J* = 15.3 Hz), 6.10 (d, 1H, *J* = 15.3 Hz), 5.71 (s, 1H), 5.18 (s, 2H), 5. 13 (s, 2H), 2.41-2.36 (m, 1H), 2.31 (s, 3H), 2.28-2.23 (m, 1H), 1.80-1.71 (m, 2H), 1.35 (s, 3H) (hydroxyl peak not detected); ^{13}C NMR (150 MHz, $CDCl_3$): 206.2, 166.2, 164.9, 161.4, 153.2, 135.8, 135.3, 128.58, 128.57, 128.4, 128.3, 119.4, 116, 72.4, 66.7, 66.4, 38.5, 29.4, 28.4, 28.3 (overlapping aromatic peaks); IR (neat) 3473, 2926, 1712, 1644, 1457, 1380, 1240, 1160, 983, 738, 697 cm^{-1}; FTMS (+ESI) *m/z* (*%*) 510 (30), 475 (32), 468 (11), 460 (33), 459 ($M+Na^+$, 100), 454 ($M+NH_4^+$,54), 437 (M^+, 9); HRMS calcd. for $(M+NH_4)^+$ $C_{26}H_{28}O_6NH_4$: 454.2224; found 454.2219.

Benzyl (2*E*)-6-oxohept-2-enoate (193).

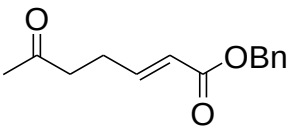

Colourless oil. R_f 0.67 (1 : 9 ethyl acetate : dichloromethane). ^{1}H NMR (600 MHz, $CDCl_3$): 7.37-7.31 (m, 5H), 6.97 (dt, 1H, *J* = 15.6, 6.6 Hz), 5.88 (dt, 1H, *J* = 15.6, 1.6 Hz), 5.16 (s, 2H), 2.59 (t, 2H, *J* = 6.9 Hz), 2.47 (q, 2H, *J* = 6.9 Hz), 2.15 (s, 3H); ^{13}C NMR (150 MHz, $CDCl_3$): 206.6, 166.1, 147.8, 136.0, 128.5, 128.2, 128.1, 121.7, 66.1, 41.4, 29.9, 25.9; IR (neat) 2955, 2360, 1714, 1658, 1457, 1375, 1261, 1151, 980, 740, 697 cm^{-1}; MS (+ESI) *m/z* (*%*) 255 ($M+Na^+$, 100), 245 (97), 233 ($M+H^+$,19), 223 (6), 177 (31), 149 (12), 91 (19); HRMS calcd. for $(M+Na)^+$ $C_{14}H_{16}O_3Na$: 255.0997; found 255.0995.

(±)-Benzyl [(1*S*,5*R*,7*S*)-1,5-dimethyl-4-oxo-6,8-dioxabicyclo[3.2.1]oct-7-yl]acetate (203).

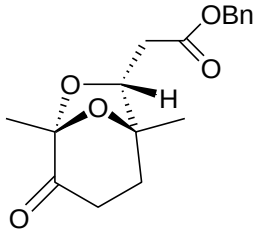

Method A:

To a solution of hydroxy ester (**191**) (94.0 mg, 0.31 mmol) in THF (20 mL) was added carbon disulfide (1.69 g, 22 mmol) and iodomethane (3.07 g, 22 mmol) at 0 ^{o}C under an atmosphere of nitrogen with stirring. The mixture was kept at the same temperature for 15 minutes before sodium hydride (80% suspension in mineral oil, 18.5 mg, 0.62 mmol) was added. After 25 minutes at 0 ^{o}C the reaction was quenched by the slow addition of crushed ice (*ca* 60 g). The resulting mixture was raised to room temperature and the layers were separated. The aqueous layer was extracted with dichloromethane (3 x 20 mL) and the combined organic extracts were washed with brine (40 mL), dried

($MgSO_4$) and concentrated *in vacuo*. The crude product was purified by flash chromatography to afford a pale yellow oil (33 mg, 35%) (**203**).

Method B:

To a stirring solution of hydroxy ester (**191**) (220 mg, 0.072 mmol) in methanol (5 mL) was added 5% palladium on carbon (22 mg, 10% w/w), and the mixture was stirred at room temperature until all starting material had disappeared by TLC (48 hours). The reaction mixture was filtered through a bed of celite, washed with methanol and concentrated *in vacuo* to yield pure (**203**) as a pale yellow oil (133 mg, 61%).

R_f 0.33 (3 : 7 ethyl acetate : hexane). ^{1}H NMR (600 MHz, $CDCl_3$): 7.38-7.33 (m, 5H), 5.21 (d, 1H, *J* = 11.7 Hz), 5.16 (d, 1H, *J* = 11.7 Hz), 4.27 (dd, 1H, *J* = 9.0, 4.6 Hz), 2.85 (dd, 1H, *J* = 15.3, 9.0 Hz), 2.76 (dt, 1H, *J* = 16.8, 10.2 Hz), 2.63 (dd, 1H, *J* = 15.3, 4.6 Hz), 2.34 (ddd, 1H, *J* = 16.8, 6.9, 2.7 Hz), 2.14-2.11 (m, 2H), 1.45 (s, 3H), 1.33 (s, 3H); ^{13}C NMR (150 MHz, $CDCl_3$): 200.6, 169.9, 135.3, 128.6, 128.5, 128.4, 104.8, 81.9, 80.2, 66.9, 35.2, 32.3, 31.6, 21.6, 17.1; IR (neat) 2943, 1734, 1457, 1381, 1166, 1093, 737, 697 cm^{-1}; MS (+ESI) *m/z* (*%*) 695 (40), 681 (20), 663 (5), 359 (100), 345 (40), 327 ($M+Na^+$, 50), 305 ($M+H^+$, 3), 277 (11), 197 (10), 91 (8); HRMS calcd. for $(M+Na)^+$ $C_{17}H_{20}O_5Na$: 327.1208; found 327.1203.

(±)-(2*E*)-3-[(2*R*,5*S*)-5-Acetyl-5-(acetyloxy)-2-methyltetrahydrofuran-2-yl]prop-2-enoate and (±)-(2*E*)-3-[(2*R*,5*R*)-5-acetyl-5-(acetyloxy)-2-methyltetrahydrofuran-2-yl]prop-2-enoate (204).

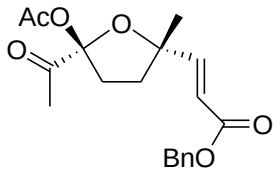

To a solution of alcohol (**191**) (2.16 g, 7.09 mmol) in pyridine (50 mL) at ambient temperature under an atmosphere of nitrogen, was added, acetic anhydride (6.51 g, 63.8 mmol), DMAP (356 mg, 2.83 mmol) and the resulting solution stirred overnight. Most of the pyridine was removed *in vacuo*, and the remaining mixture was taken up in

dichloromethane (50 mL) and washed with 10% HCl (50 mL). The organic layer was then removed, and the aqueous layer extracted with dichloromethane (3 x 50 mL). The organic layers were combined, washed with water (50 mL) and brine (50 mL), dried ($MgSO_4$) and concentrated *in vacuo*. The residue was purified *via* flash chromatography to yield a yellow oil (2.17 g, 89%) (**204**) as an inseparable mixture of diastereomers. R_f 0.57 (1 : 9 ethyl acetate : dichloromethane). ^{1}H NMR (300 MHz, $CDCl_3$): 7.39-7.35 (m, 10H), 7.04 (d, 1H, *J* = 15.6 Hz), 6.96 (d, 1H, *J* = 15.6 Hz), 6.13 (d, 1H, *J* = 15.6 Hz), 6.02 (d, 1H, *J* = 15.6 Hz), 5.19 (apt t, 4H, *J* = 2.1 Hz), 2.33 (s, 3H), 2.32 (s, 3H), 2.28-2.22 (m, 4H), 2.20-2.16 (m, 2H), 2.14-2.09 (m, 2H), 2.08 (s, 3H), 2.01 (s, 3H), 1.51 (s, 3H), 1.44 (s, 3H); ^{13}C NMR (75 MHz, $CDCl_3$): 202.6, 201.9, 169.9, 169.8, 166.3, 166.2, 151.8, 150.8, 135.8, 135.7, 128.6, 128.32, 128.29, 128.27, 128.21, 119.2, 118.4, 108.7, 108.3, 87.09, 87.07, 66.5, 66.4, 35.5, 35.1, 33.9, 33.7, 27.8, 26.0, 25.4, 25.0,20.9, 20.8; IR (neat) 2979, 1726, 1659, 1457, 1374, 1246, 1163, 1079, 978, 885, 741, 699 cm^{-1}; LRP (+LSIMS) *m/z* (*%*) 269 (100), 270 (18), 287 (43), 288 (8), 304 (13), 319 (63), 320 (12), 347 ($M+H^+$, 9), 364 (20), 376 (11); HRMS calcd. for $(M+H)^+$ $C_{19}H_{23}O_6$: 347.1495; found 347.1489.

General Procedure for Hydrolysis of Alkene-Esters 204 and 210.

Ester (**204** or **210**) (1.0 mmol) was heated under reflux overnight in a solution of 1M KOH in methanol (10 mL) overnight. The solution was concentrated *in vacuo*, diluted with H_2O (10 mL) and acidified to pH 1 (conc HCl). The solution was extracted with ethyl acetate (3 x 10 mL) and the combined organic layers were washed with brine (10 mL), dried ($MgSO_4$) and concentrated *in vacuo*. The crude product was purified *via* flash chromatography.

General Procedure for Hydrogenolysis of Alkene-Esters 204 or 191.

To a solution of ester (**204** or **191**) (1.0 mmol) in methanol (10 mL) was added 10% w/w of 5% palladium on carbon and the mixture was stirred under an atmosphere of hydrogen until complete *via* TLC. The reaction mixture was filtered through a bed of celite, washed with methanol and concentrated *in vacuo*. The crude product was purified by flash chromatography.

(±)-(2*E*)-3-[(2*R*,5*S*)-5-Acetyl-5-methoxy-2-methyltetrahydrofuran-2-yl]prop-2-enoic acid and (±)-(2*E*)-3-[(2*R*,5*R*)-5-acetyl-5-methoxy-2-methyltetrahydrofuran-2-yl]prop-2-enoic acid (207).

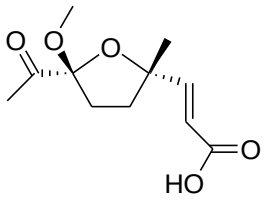

Inseparable mixture of diastereomers. Colourless oil. R_f 0.37 (1 : 9 methanol : ethyl acetate). ^{1}H NMR (600 MHz, $CDCl_3$): 10.48 (br s, 2 x OH), 7.15 (d, 1H, *J* = 15.6 Hz), 7.01 (d, 1H, *J* = 15.6 Hz), 6.15 (d, 1H, *J* = 15.6 Hz), 6.07 (d, 1H, *J* = 15.6 Hz), 3.27 (s, 3H), 3.26 (s, 3H), 2.27 (s, 6H), 2.22-2.16 (m 2H), 2.15-2.09 (m, 2H), 2.08-2.04 (m, 2H), 2.01-1.92 (m, 2H), 1.53 (s, 3H), 1.42 (s, 3H); ^{13}C NMR (150 MHz, $CDCl_3$): 205.5, 204.7, 171.8, 171.7, 154.4, 153.9, 118.5, 118.1, 109.9, 109.7, 85.4, 85.2, 51.1, 50.7, 35.9, 35.6, 33.8, 33.2, 27.3, 25.9, 25.8, 25.5; IR (neat) 3370, 2982, 2362, 1701, 1658, 1417, 1050, 909, 731 cm^{-1}; HRMS calcd. for $(M+H)^+$ $C_{11}H_{16}O_5$: 229.1076; found 229.1074.

(±)-3-[(2*R*,5*S*)-5-Acetyl-5-methoxy-2-methyltetrahydrofuran-2-yl]propanoic acid and (±)-3-[(2*R*,5*R*)-5-acetyl-5-methoxy-2-methyltetrahydrofuran-2-yl]propanoic acid (208).

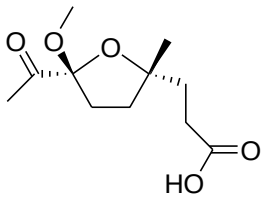

Inseparable mixture of diastereomers. Colourless oil; R_f 0.37 (1 : 9 methanol : ethyl acetate); ^{1}H NMR (600 MHz, $CDCl_3$): 10.67 (br s, OH), 10.48 (br s, OH), 3.22 (s, 3H), 3.21 (s, 3H), 2.58-2.45 (m, 4H), 2.23 (s, 3H), 2.22 (s, 3H), 2.15-2.08 (m 4H), 2.07-1.97 (m, 2H), 1.94-1.85 (m, 2H), 1.82-1.78 (m, 4H), 1.38 (s, 3H), 1.26 (s, 3H); ^{13}C NMR (150 MHz, $CDCl_3$): 206.2, 205.6, 179.6, 179.5, 109.42, 109.36, 86.2, 85.8, 50.6, 50.5,

36.5, 35.7, 35.6, 35.4, 34.2, 34.0, 29.7, 29.3, 26.8, 25.6 (1C masked), 25.3; IR (neat) 3371, 2978, 2362, 1725, 1046, 880, 669 cm^{-1}; HRMS calcd. for $(M+Na)^+$ $C_{11}H_{18}O_5Na$: 253.1052; found 253.1049.

(±)-Benzyl (2*E*)-3-[(2*R*,5*S*)-5-acetyl-5-methoxy-2-methyltetrahydrofuran-2-yl]propanoate and (±)-benzyl (2*E*)-3-[(2*R*,5*R*)-5-acetyl-5-methoxy-2-methyltetrahydrofuran-2-yl]propanoate (209).

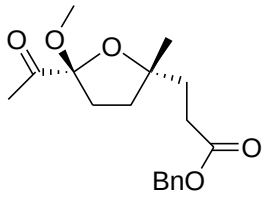

Inseparable mixture of diastereomers. Colourless oil. R_f 0.74 (1 : 9 methanol : ethyl acetate). ^{1}H NMR (300 MHz, $CDCl_3$): 7.37-7.34 (m, 10H), 5.13 (apt d, 4H, J = 1.8 Hz), 3.20 (s, 3H), 3.19 (s, 3H), 2.54-2.46 (m, 4H), 2.22 (s, 3H), 2.20 (s, 3H), 2.13-1.73 (m, 12H), 1.36 (s, 3H), 1.24 (s, 3H). ^{13}C NMR (75 MHz, $CDCl_3$): 206.3, 205.8, 173.4 (1 C Masked), 135.9 (1 C Masked), 128.6, 128.3, 128.2 (1 aromatic C masked), 109.4, 109.3, 86.4, 86.0, 66.4 (1 C Masked), 50.7, 50.5, 36.8, 36.0, 35.5, 35.4, 34.4, 34.1, 30.0, 29.6, 26.9, 25.7, 25.6, 25.4; IR (neat) 2931, 2362, 1729, 1457, 1357, 1158, 1053, 909 cm^{-1}; HRMS calcd. for $(M+Na)^+$ $C_{18}H_{24}O_5Na$: 343.1521; found 343.1518.

(±)-Benzyl (2*E*)-3-[(2*R*,5*S*)-5-acetyl-5-methoxy-2-methyltetrahydrofuran-2-yl]prop-2-enoate and (±)-benzyl (2*E*)-3-[(2*R*,5*R*)-5-acetyl-5-methoxy-2-methyltetrahydrofuran-2-yl]prop-2-enoate (210).

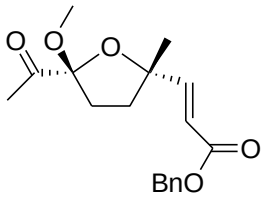

Method A: Transfer Hydrogenation.

To a solution of acetate ester (**204**) (98.0 mg, 0.26 mmol) in methanol (4 mL) was added 1,4-cyclohexadiene (208 mg, 2.60 mmol) and 5% palladium on carbon (9.8 mg, 10% w/w). The reaction mixture was stirred and room temperature and monitored by TLC until complete (4 days). The mixture was filtered through a bed of celite, washed with methanol (10 mL) and concentrated *in vacuo* to give a pale yellow oil (**210**) (58.7 mg, 71 %).

Method B: MeOH with Pd/C.

To a solution of acetate ester (**204**) (2.28 g, 6.59 mmol) in methanol (25 mL) was added 5% palladium on carbon (228 mg, 10% w/w), and the mixture was stirred at room temperature until complete *via* TLC (2 days). The reaction mixture was filtered through a bed of celite, washed with methanol and concentrated *in vacuo* to afford (**210**) as a yellow oil (2.05 g, 98%). Products were an inseparable mixture of diastereomers. R_f 0.34 (3 : 7 ethyl acetate : hexane). ^{1}H NMR (600 MHz, $CDCl_3$): 7.38-7.30 (m, 10H), 7.09 (d, 1H, J = 15.6 Hz), 6.95 (d, 1H, J = 15.6 Hz), 6.18 (d, 1H, J = 15.6 Hz), 6.10 (d, 1H, J = 15.6 Hz), 5.22-5.15 (m, 4H), 3.248 (s, 3H), 3.246 (s, 3H), 2.25 (s, 6H), 2.22-1.88 (m, 8H), 1.39 (s, 3H).; ^{13}C NMR (150 MHz, $CDCl_3$): 205.5, 204.7, 166.4, 166.3, 152.3, 151.8, 135.9, 135.8, 128.51, 128.48, 128.3, 128.2, 128.1, 118.8, 118.5, 109.9, 109.6, 85.4, 85.2, 66.3, 66.2, 51.0, 50.6, 35.9, 35.7, 33.8, 33.1, 27.4, 25.9, 25.8, 24.4; IR (neat) 2974, 2363, 1723, 1659, 1457, 1377, 1290, 1163, 1050, 741, 699 cm^{-1}; HRMS calcd. for $(M+Na)^+$ $C_{18}H_{22}O_5Na$: 341.1365; found 341.1364.

Attempted Barton-Decarboxylation of Acid 207.

1-Hydroxy-pyridinethione (60 mg, 0.47 mmol) was added to a solution of acid **207** (108 mg, 0.47 mmol) in dry dichloromethane (20 mL) under an atmosphere of nitrogen at 0 ^{o}C. The mixture was protected from light and 1,3-dicyclohexylcarbodiimide (98mg, 0.47 mmol) was added and the reaction kept at 0 ^{o}C for 4 hours with stirring. The suspension was filtered and washed with cold dichloromethane (20 mL), followed by removal of volatiles *in vacuo* (without heat). The resulting green oil was taken up in benzene (25 mL) under an atmosphere of nitrogen and 2-methyl-2-propanthiol (251 μL, 0.95 mmol) was added. The resulting mixture was irradiated with 1 sun lamp (approximately 30 cm distance, with a condenser fitted to the reaction flask) for 3 hours. The mixture was then concentrated *in vacuo* to give a brown oil. NMR analysis of both crude and attempted flash chromatography products showed no evidence of the desired products.

(±)-(2*R*,5*S*)-5-Acetyl-5-methoxy-2-methyltetrahydrofuran-2-carbaldehyde and (±)-(2*R*,5*R*)-5-acetyl-5-methoxy-2-methyltetrahydrofuran-2-carbaldehyde (213).

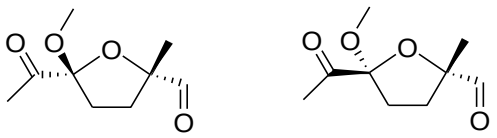

Alkene-ester **210** was subjected to the standard ozonolysis conditions outlined for 1,2-dioxines **3a-e** to afford a mixture of **213a** and **213b**. Combined yield 78%. IR (neat, mixture diast.) 2984, 2361, 1732, 1457, 1359, 1268, 1048, 910, 734 cm^{-1}; HRMS calcd. for $(M+H)^+$ $C_9H_{15}O_4$: 187.0970; found 187.0965. Stereochemistry could not be assigned for each isomer with certainty, see discussion.

Diastereomer 1

Pale yellow oil. R_f 0.57 (1 : 4 diethyl ether : dichloromethane). ^{1}H NMR (600 MHz, $CDCl_3$): 9.62 (s, 1H), 3.28 (s, 3H), 2.43 (m, 1H), 2.28 (s, 3H), 2.13-2.09 (m, 2H), 1.79 (m, 1H), 1.39 (s, 3H); ^{13}C NMR (150 MHz, $CDCl_3$): 204.6, 201.5, 110.5, 89.2, 51.3, 33.9, 31.1, 25.7, 20.8.

Diastereomer 2

Pale yellow oil. R_f 0.38 (1 : 4 diethyl ether : dichloromethane). ^{1}H NMR (600 MHz, $CDCl_3$): 9.65 (s, 1H), 3.30(s, 3H), 2.34 (m, 1H), 2.29 (s, 3H), 2.12 (m, 1H), 2.03 (m, 1H), 1.95 (m 1H), 1.46 (s, 3H); ^{13}C NMR (150 MHz, $CDCl_3$): 204.9, 201.5, 110.3, 89.6, 50.8, 34.0, 32.2, 25.7, 21.8. ^{1}H and ^{13}C NMR data was extracted from a diastereomeric mixture of 1 and 2 utilising 2D NMR.

(±)-1-[(2*R*,5*R*)-5-Ethenyl-2-methoxy-5-methyltetrahydrofuran-2-yl]ethanone (215).

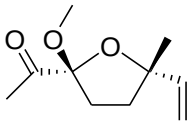

To a suspension of vigorously stirring methyl triphenylphosphine iodide (**214**) (0.9-2.0 mmol) in diethyl ether (10 mL) at 0 ^{o}C was added potassium *tert*-butoxide (1.5-2.5 mmol) under an atmosphere of nitrogen. The mixture was stirred for 30 minutes after which keto-aldehyde **213** (1 mmol) in diethyl ether (1 mL) was slowly added. The resulting solution was stirred for 2 hours, concentrated *in vacuo* and the crude products purified by flash chromatography to furnish a pale yellow oil, **215** as an inseparable mixture of diastereomers. R_f 0.56 (1 : 9 diethyl ether:dichloromethane). ^{1}H NMR (600 MHz, $CDCl_3$): 6.04 (dd, 1H, J = 17.4, 10.8 Hz), 5.89 (dd, 1H, J = 17.4, 10.8 Hz), 5.27 (d, 1H, J = 17.4 Hz), 5.25 (d, 1H, J = 17.4 Hz), 5.07 (d, 1H, J = 10.8 Hz), 5.03 (d, 1H, J = 10.8 Hz), 3.25 (s, 3H), 3.24 (s, 3H), 2.254 (s, 3H), 2.252 (s, 3H) 2.19-1.97 (m, 8H), 1.47 (s, 3H), 1.37 (s, 3H); ^{13}C NMR (150 MHz, $CDCl_3$): 206.1, 205.5, 143.5, 142.6, 112.3, 112.1, 109.5, 109.4, 86.4, 86.3, 50.8, 50.5, 35.9, 35.8, 33.8, 33.7, 27.5, 25.75, 25.73, 25.5; IR (neat) 2979, 2362, 1730, 1458, 1358, 1218, 1051, 916, 735 cm^{-1}; HRMS calcd. for $(M+Na)^+$ $C_{10}H_{16}O_3Na$: 207.0997; found 207.1021.

Attempted Wittig reaction on keto-alkene 215.

To a suspension of vigorously stirring methyl triphenylphosphine iodide (**214**) (0.9-2.0 mmol) in diethyl ether (10 mL) at 0 ^{o}C was added potassium *tert*-butoxide (1.5-2.5 mmol) under an atmosphere of nitrogen. The mixture was stirred for 30 minutes after which keto-alkene **215** (1 mmol) in diethyl ether (1 mL) was slowly added. The resulting solution was monitored *via* TLC for 2 days, with no change detected.

Attempted Wittig and Peterson Olefinations on 156

Method A: Wittig with Unstabilised ylide:
To a suspension of vigorously stirring methyl triphenylphosphine iodide (**214**) (0.9-2.5 mmol) in diethyl ether (10 mL) at 0 ^{o}C was added potassium *tert*-butoxide (2.5-4.5 mmol) under an atmosphere of nitrogen. The mixture was stirred for 30 minutes after which keto-aldehyde **156** (1 mmol) in diethyl ether (1 mL) was slowly added. The resulting solution was stirred for 2 hours, concentrated *in vacuo* and the crude products purified by flash chromatography.

Method B: Peterson 1:
A solution of anhydrous cerium (III) chloride (439 mg, 1.78 mmol) in dry diethyl ether (5 mL) was stirred under nitrogen for 2 hours at room temperature to form a uniform white suspension. Trimethylsilylmethylmagnesium chloride (1.78 mL, 1.78 mmol, 1M in ether) was slowly added and the solution was stirred for 1 hour. Keto-aldehyde **156** (102 mg, 0.59 mmol) was added and the resulting solution was stirred at room temperature until all starting material had disappeared *via* TLC (*ca* 45-90 minutes). Saturated NH_4Cl (5 mL) was added, the layers were separated and the aqueous layer was extracted with diethyl ether (3 x 5 mL). The combined organic layers were washed with brine (10 mL), dried ($MgSO_4$) and concentrated *in vacuo*. The crude product was dissolved in dry diethyl ether (5 mL) and five drops of concentrated sulphuric acid was added. The reaction was stirred at room temperature for 1 hour before saturated $NaHCO_3$ (5 mL) was added. The layers were separated and the aqueous layer was extracted with diethyl ether (2 x 5 mL). Combined organic layers were washed with

brine (10 mL), dried ($MgSO_4$) and concentrated *in vacuo*. The crude mixture was purified by flash chromatography.

Method C: Peterson 2:

A solution of anhydrous cerium (III) chloride (232 mg, 0.94 mmol) in dry diethyl ether (5 mL) was stirred under nitrogen for 2 hours at room temperature to form a uniform white suspension. The suspension was cooled to -78 ^oC and stirred for a further 15 minutes after which trimethylsilylmethylmagnesium chloride (941 μL, 0.94 mmol, 1M in ether) was slowly added and the solution was stirred for 15 minutes. Keto-aldehyde **156** (108 mg, 0.63 mmol) was added and the resulting solution was warmed to room temperature and stirred until all starting material had disappeared *via* TLC (*ca* 60 minutes). The mixture was cooled to 0 ^oC and quenched with HCl (1M, *ca* 2 mL) The aqueous layer was extracted with diethyl ether (3 x 3 mL) and the combined organics were washed with $NaHCO_3$ (10 mL), bine (10 mL) and dried ($MgSO_4$). The volatiles were removed *in vacuo* and the crude product was dissolved in dry diethyl ether (5 mL) and five drops of concentrated sulphuric acid was added. The reaction was stirred at room temperature for 1 hour before saturated $NaHCO_3$ (5 mL) was added. The layers were separated and the aqueous layer was extracted with diethyl ether (3 x 5 mL). Combined organic layers were washed with brine (10 mL), dried ($MgSO_4$) and concentrated *in vacuo*. The crude mixture was purified by flash chromatography.

(±)-(6*R*)-6-Hydroxy-2,6-dimethylocta-1,7-dien-3-one (219).

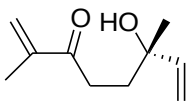

Colourless oil. Yield 2%. R_f 0.40 (1 : 4 diethyl ether : dichloromethane). ^1H NMR (600 MHz, $CDCl_3$): 5.98 (s, 1H), 5.86 (dd, 1H, J = 17.4, 10.8 Hz), 5.76 (s, 1H), 5.24 (dd, 1H, J = 17.4, 1.5 Hz), 5.08 (dd, 1H, J = 10.8, 1.5 Hz), 4.68 (s, OH), 2.84-2.74 (m, 2H), 1.87 (s, 3H), 1.93-1.80 (m, 2H), 1.31 (s, 3H); ^{13}C NMR (150 MHz, $CDCl_3$): 202.6, 144.3 (x2), 124.7, 112.2, 72.7, 35.7, 32.3, 28.7, 17.7; IR (neat) 3354, 2977, 2362, 1671, 1376, 1088, 1049, 924 cm^{-1}. Remaining physical and chemical properties were as reported in the literature.[224]

(±)-(3*R*)-3,7-Dimethyl-6-methylideneocta-1,7-dien-3-ol (220).

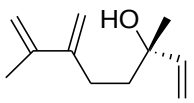

Pale yellow oil. R_f 0.47 (3 : 7 ethyl acetate : hexane). ^{1}H NMR (600 MHz, $CDCl_3$): 5.94 (dd, 1H, *J* = 17.4, 10.8 Hz), 5.24 (dd, 1H, *J* = 17.4, 1.5 Hz), 5.09 (dd, 1H, *J* = 10.8, 1.5 Hz), 5.08 (s, 2H), 4.98 (s, 2H), 2.36-2.28 (m, 2H), 1.90 (s, 3H), 1.77-1.66 (m, 2H), 1.31 (s, 3H); ^{13}C NMR (150 MHz, $CDCl_3$): 148.1, 144.9, 142.5, 112.7, 112.1, 111.9, 73.3, 41.5, 28.1, 28.0, 21.2; IR (neat) 3393, 2925, 2361, 1599, 1440, 1371, 1184, 999, 890, 721 cm^{-1}. No results were obtained for accurate mass or mass spectrum data, see discussion

APPENDIX 1: Semi Empirical Data for the Ozonolysis Mechanism of 1,2-Dioxines

Table 29: AM1 Energy Values for the Ozonolysis Mechanism (kJ/mol).

	exo-endo	***exo-exo***	***endo-endo***	***endo-exo***
SM (Ozone)*	157.96			
SM (Dioxine)*	39.87			
SM (Total)*	197.83			
TS1	266.48	275.16	275.41	272.86
I1	20.21	26.36	18.57	23.38
TS2	92.17	89.18	86.28	85.95
TS3[#]	-7.81		-6.57	
P[#]	-239.37		-237.80	

* Single set of values (*endo*/*exo* does not apply for SM).

[#] Only two conformations for TS3 and P (*exo* and *endo*).

APPENDIX 2: *Ab Initio* Data for the Ozonolysis Mechanism of 1,2-Dioxines

Table 27: HF/3-21G* (Gas) Energy Values for the Ozonolysis Mechanism (Hartree, E_h).

	exo-endo	***exo-exo***	***endo-endo***	***endo-exo***
SM (Ozone)*	-222.989218			
SM (Dioxine)*	-379.349884			
SM (Total)*	-602.339102			
TS1	-602.341067	-602.337099	-602.340768	-602.341790
I1	-602.538302	-602.536814	-602.548548	-602.548474
TS2	-602.437197	-602.440405	-602.454656	-602.455580
TS3[#]	-602.503281		-602.510537	
P[#]	-602.602160		-602.603408	

Table 28: HF/3-21G* (Dichloromethane) Energy Values for the Ozonolysis Mechanism (Hartree, E_h).

	exo-endo	***exo-exo***	***endo-endo***	***endo-exo***
SM (Ozone)*	-222.991969			
SM (Dioxine)*	-379.358805			
SM (Total)*	-602.350774			
TS1	-602.346599	-602.350049	-602.350289	-602.351181
I1	-602.549863	-602.548409	-602.558245	-602.558159
TS2	-602.449827	-602.452890	-602.464916	-602.466656
TS3[#]	-602.516280		-602.522356	
P[#]	-602.612579		-602.612987	

* Single set of values (*endo*/*exo* does not apply for SM).

[#] Only two conformations for TS3 and P (*exo* and *endo*).

REFERENCES

(1) Jin, H.-X.; Liu, H.-H.; Zhang, Q.; Wu, Y. *Journal of Organic Chemistry* **2005**, *70*, 4240-4247.

(2) Yadav, J. S.; Babu, R. S.; Sabitha, G. *ARKIVOC* **2003**, 125-139.

(3) Macreadie, P.; Avery, T.; Greatrex, B.; Taylor, D.; Macreadie, I. *Bioorganic Medicinal Chemistry Letters* **2006**, *16*, 920-922.

(4) Avery, T. D.; Macreadie, P. I.; Greatrex, B. W.; Robinson, T. V.; Taylor, D. K.; Macreadie, I. G. *Bioorganic & Medicinal Chemistry* **2007**, *15*, 36-42.

(5) Ann Casteel, D. *Natural Product Reports* **1999**, *16*, 55-73.

(6) Robert, A.; Meunier, B. *Chemical Society Reviews* **1998**, *27*, 273-274.

(7) Lai, H.; Singh, N. P. *Cancer Letters* **1995**, *91*, 41-46.

(8) Singh, N. P.; Lai, H. *Life Sciences* **2001**, *70*, 49-56.

(9) Gochfeld, D. J.; Hamann, M. T. *Journal of Natural Products* **2001**, *64*, 1477-1479.

(10) Patil, A. D.; Freyer, A. J.; Carte, B.; Johnson, R. K.; Lahouratate, P. *Journal of Natural Products* **1996**, *59*, 219-223.

(11) MacDonald, D.; VanCrey, K.; Harrison, P.; Rangachari, P. K.; Rosenfeld, J.; Warren, C.; Sorger, G. *Journal of Ethnopharmacology* **2004**, *92*, 215-221.

(12) Boche, J.; Runquist, O. *Journal of Organic Chemistry* **1968**, *33*, 4285-4286.

(13) Casteel, D. A. *Natural Product Reports* **1992**, *9*, 289-312.

(14) Kahlos, K.; Kangas, L.; Hiltunen, R. *Planta Medica* **1989**, *55*, 389-390.

(15) Lindequist, U.; Lesnau, A.; Teuscher, E.; Pilgrim, H. *Pharmazie* **1989**, *44*, 579-580.

(16) Matsumoto, M.; Dobashi, S.; Kuroda, K.; Kondo, K. *Tetrahedron* **1985**, *41*, 2147-2154.

(17) Clennan, E. L. *Tetrahedron* **1991**, *47*, 1343-1382.

(18) Adam, W.; Prein, M. *Accounts of Chemical Research* **1996**, *29*, 275-283.

(19) Balci, M. *Chemical Reviews* **1981**, *81*, 91-108.

(20) Ensley, H. E.; Balakrishnan, P.; Ugarkar, B. *Tetrahedron Letters* **1983**, *24*, 5189-5192.

(21) Aubry, J.-M.; Bouttemy, S. *Journal of the American Chemical Society* **1997**, *119*, 5286-5294.

(22) Fuchter, M. J.; Hoffman, B. M.; Barrett, A. G. M. *Journal of Organic Chemistry* **2006**, *71*, 724-729.

(23) Lamberts, J. J. M.; Schumacher, D. R.; Neckers, D. C. *Journal of the American Chemical Society* **1984**, *106*, 5879-5883.

(24) Hewton, C. E.; Kimber, M. C.; Taylor, D. K. *Tetrahedron Letters* **2002**, *43*, 3199-3201.

(25) Boger, D. L.; Boyce, C. W.; Labroli, M. A.; Sehon, C. A.; Jin, Q. *Journal of the American Chemical Society* **1999**, *121*, 54-62.

(26) Bohlmann, F.; Zdero, C. *Chemistry of Heterocyclic Compounds* **1985**, *44*, 261-323.

(27) Kondo, K.; Matsumoto, M. *Chemistry Letters* **1974**, 701-704.

(28) O'Shea, K. E.; Foote, C. S. *Journal of Organic Chemistry* **1989**, *54*, 3475-3477.

(29) Dervan, P. B.; Jones, C. R. *Journal of Organic Chemistry* **1979**, *44*, 2116-2122.

(30) Adam, W.; Albert, R.; Dachs Grau, N.; Hasemann, L.; Nestler, B.; Peters, E. M.; Peters, K.; Prechtl, F.; Von Schnering, H. G. *Journal of Organic Chemistry* **1991**, *56*, 5778-5781.

(31) Adam, W.; Szendrey, L. *Chemical Communications* **1971**, 1299-1300.

(32) Greatrex, B. W.; Taylor, D. K. *Journal of Organic Chemistry* **2004**, *69*, 2577-2579.

(33) Clennan, E. L.; Heah, P. C. *Journal of Organic Chemistry* **1981**, *46*, 4105-4107.

(34) Zhang, X.; Lin, F.; Foote, C. S. *Journal of Organic Chemistry* **1995**, *60*, 1333-1338.

(35) Adam, W.; Balci, M. *Journal of the American Chemical Society* **1979**, *101*, 7542-7547.

(36) Kornblum, N.; DeLaMare, H. E. *Journal of the American Chemical Society* **1951**, *73*, 880-881.

(37) Avery, T. D.; Taylor, D. K.; Tiekink, E. R. T. *Journal of Organic Chemistry* **2000**, *65*, 5531-5546.

(38) Mete, E.; Altundas, R.; Secen, H.; Balci, M. *Turkish Journal of Chemistry* **2003**, *27*, 145-153.

(39) Avery, T. D.; Jenkins, N. F.; Kimber, M. C.; Lupton, D. W.; Taylor, D. K. *Chemical Communications* **2002**, 28-29.

(40) Herz, W.; Ligon, R. C.; Turner, J. A.; Blount, J. F. *Journal of Organic Chemistry* **1977**, *42*, 1885-1895.

(41) Hagenbuch, J. P.; Vogel, P. *Chemical Communications* **1980**, 1062-1063.

(42) Suzuki, M.; Oda, Y.; Hamanaka, N.; Noyori, R. *Heterocycles* **1990**, *30*, 517-535.

(43) Greatrex, B. W.; Jenkins, N. F.; Taylor, D. K.; Tiekink, E. R. T. *Journal of Organic Chemistry* **2003**, *68*, 5205-5210.

(44) Avery, T. D.; Fallon, G.; Greatrex, B. W.; Pyke, S. M.; Taylor, D. K.; Tiekink, E. R. T. *Journal of Organic Chemistry* **2001**, *66*, 7955-7966.

(45) Avery, T. D.; Haselgrove, T. D.; Rathbone, T. J.; Taylor, D. K.; Tiekink, E. R. T. *Chemical Communications* **1998**, 333-334.

(46) Avery, T. D.; Greatrex, B. W.; Taylor, D. K.; Tiekink, E. R. T. *Perkin 1* **2000**, 1319-1321.

(47) Kimber, M. C.; Taylor, D. K. *Journal of Organic Chemistry* **2002**, *67*, 3142-3144.

(48) Palmer, F. N.; Taylor, D. K. *Perkin 1* **2000**, 1323-1325.

(49) Stanley, N. J.; Hutchinson, M. R.; Kvist, T.; Nielsen, B.; Mathiesen, J. M.; Braeuner-Osborne, H.; Avery, T. D.; Tiekink, E. R. T.; Pedersen, D. S.; Irvine, R. J.; Abell, A. D.; Taylor, D. K. *Bioorganic & Medicinal Chemistry* **2010**, *18*, 6089-6098.

(50) Taylor, D. K. *Chemistry in Australia* **2001**, *68*, 15-16.

(51) Greatrex, B.; Jevric, M.; Kimber, M. C.; Krivickas, S. J.; Taylor, D. K.; Tiekink, E. R. T. *Synthesis* **2003**, 668-672.

(52) Greatrex, B. W.; Kimber, M. C.; Taylor, D. K.; Fallon, G.; Tiekink, E. R. T. *Journal of Organic Chemistry* **2002**, *67*, 5307-5314.

(53) Brown, R. C.; Taylor, D. K.; Elsey, G. M. *Organic Letters* **2006**, *8*, 463-466.

(54) Brown, R. C.; Sefton, M. A.; Taylor, D. K.; Elsey, G. M. *Australian Journal of Grape and Wine Research* **2006**, *12*, 115-118.

(55) Avery, T. D.; Caiazza, D.; Culbert, J. A.; Taylor, D. K.; Tiekink, E. R. T. *Journal of Organic Chemistry* **2005**, *70*, 8344-8351.

(56) Adam, W.; Bloodworth, A. J.; Eggelte, H. J.; Loveitt, M. E. *Angewandte Chemie (International ed. in English)* **1978**, *17*, 209.

(57) Bascetta, E.; Gunstone, F. D.; Scrimgeour, C. M. *Journal of the Chemical Society, Perkin Transactions 1: Organic and Bio-Organic Chemistry* **1984**, 2199-2205.

(58) Foster, C. H.; Berchtold, G. A. *Journal of Organic Chemistry* **1975**, *40*, 3743-3746.

(59) Robinson, T. V.; Taylor, D. K.; Tiekink, E. R. T. *Journal of Organic Chemistry* **2006**, *71*, 7236-7244.

(60) Valente, P.; Avery, T. D.; Taylor, D. K.; Tiekink, E. R. T. *Journal of Organic Chemistry* **2009**, *74*, 274-282.

(61) Zvarec, O.; Avery, T. D.; Taylor, D. K.; Tiekink, E. R. T. *Tetrahedron* **2010**, *66*, 1007-1013.

(62) Clayden, J.; Greeves, N.; Warren, S.; Wothers, P. *Organic Chemistry*; Oxford University Press: New York, **2001**, p 938-939.

(63) Cotton, F. A.; Wilkinson, G.; Murillo, C., A; Bochmann, M. *Advanced Inorganic Chemistry*; 6th ed.; John Wiley & Sons, Inc: New York, **1999**, p 453.

(64) Razumovskii, S. D.; Zaikov, G. E. *Ozone and its Reactions with Organic Compounds*; Elsevier Science Publishers: Amsterdam, **1984**, p 36.

(65) Schwartz, C.; Raible, J.; Mott, K.; Dussault, P. H. *Tetrahedron* **2006**, *62*, 10747-10752.

(66) Criegee, R. *Ann.* **1953**, *583*, 1-2.

(67) Criegee, R. *Angewandte Chemie* **1975**, *87*, 765-771.

(68) Jung, I. C. *European Journal of Organic Chemistry* **2001**, 1899-1901.

(69) Geletneky, C.; Berger, S. *European Journal of Organic Chemistry* **1998**, 1625-1627.

(70) Griesbaum, K.; Volpp, W.; Greinert, R.; Greunig, H. J.; Schmid, J.; Henke, H. *Journal of Organic Chemistry* **1989**, *54*, 383-389.

(71) Smith, M.; March, J. *March's Advanced Organic Chemistry*; 5 ed.; John Wiley & Sons, Inc., **2001**, 1736-1742.

(72) Schank, K. *Helvetica Chimica Acta* **2004**, *87*, 2074-2084.

(73) Bailey, P. S.; Ferrell, T. M. *Journal of the American Chemical Society* **1978**, *100*, 899-905.

(74) Carroll, F. A. *Perspectives on Structure and Mechanism in Organic Chemistry*; Brooks/Cole Publishing Company: California, **1998**, 760-762.

(75) Van Ornum, S. G.; Champeau, R. M.; Pariza, R. *Chemical Reviews* **2006**, *106*, 2990-3001.

(76) Chen, L.; Wiemer, D. F. *Journal of Organic Chemistry* **2002**, *67*, 7561-7564.

(77) Story, P. R.; Morrison, W. H., III; Hall, T. K.; Farine, J. C.; Bishop, C. E. *Tetrahedron Letters* **1968**, 3291-3294.

(78) Griesbaum, K.; Hilss, M.; Bosch, J. *Tetrahedron* **1996**, *52*, 14813-14826.

(79) Miura, M.; Nagase, S.; Nojima, M.; Kusabayashi, S. *Journal of Organic Chemistry* **1983**, *48*, 2366-2370.

(80) Vennerstrom, J. L.; Arbe-Barnes, S.; Brun, R.; Charman, S. A.; Chiu, F. C. K.; Chollet, J.; Dong, Y.; Dorn, A.; Hunziker, D.; Matile, H.; McIntosh, K.; Padmanilayam, M.; Santo Tomas, J.; Scheurer, C.; Scorneaux, B.; Tang, Y.; Urwyler, H.; Wittlin, S.; Charman, W. N. *Nature* **2004**, *430*, 900-904.

(81) Muraleedharan, K. M.; Avery, M. A. *Drug Discovery Today* **2009**, *14*, 793-803.

(82) Olliaro, P.; Wells, T. N. C. *Clinical Pharmacology & Therapeutics* **2009**, *85*, 584-595.

(83) Dong, Y.; Wittlin, S.; Sriraghavan, K.; Chollet, J.; Charman, S. A.; Charman, W. N.; Scheurer, C.; Urwyler, H.; Santo Tomas, J.; Snyder, C.; Creek, D. J.; Morizzi, J.; Koltun, M.; Matile, H.; Wang, X.; Padmanilayam, M.; Tang, Y.; Dorn, A.; Brun, R.; Vennerstrom, J. L. *Journal of Medicinal Chemistry* **2010**, *53*, 481-491.

(84) Griesbaum, K.; Liu, X.; Kassiaris, A.; Scherer, M. *Liebigs Annalen/Recueil* **1997**, 1381-1390.

(85) Pappas, J. J.; Keaveney, W. P.; Gancher, E.; Berger, M. *Tetrahedron Letters* **1966**, 4273-4278.

(86) O'Murchu, C. *Synthesis* **1989**, 880-882.

(87) Wrobleski, A.; Sahasrabudhe, K.; Aube, J. *Journal of the American Chemical Society* **2004**, *126*, 5475-5481.

(88) Flippin, L. A.; Gallagher, D. W.; Jalali-Araghi, K. *Journal of Organic Chemistry* **1989**, *54*, 1430-1432.

(89) White, R. W.; King, S. W.; O'Brien, J. L. *Tetrahedron Letters* **1971**, 3591-3593.

(90) Neumeister, J.; Keul, H.; Saxena, M. P.; Griesbaum, K. *Angewandte Chemie* **1978**, *90*, 999.

(91) Higley, D. P.; Murray, R. W. *Journal of the American Chemical Society* **1976**, *98*, 4526-4533.

(92) Hon, Y.-S.; Wong, Y.-C. *Tetrahedron Letters* **2005**, *46*, 1365-1368.

(93) Ferraboschi, P.; Gambero, C.; Azadani, M. N.; Santaniello, E. *Synthetic Communications* **1986**, *16*, 667-672.

(94) Lorenz, O. *Analytical Chemistry* **1965**, *37*, 101-102.

(95) Lorenz, O.; Parks, C. R. *Journal of Organic Chemistry* **1965**, *30*, 1976-1981.

(96) Gallaher, K. L.; Kuczkowski, R. L. *Journal of Organic Chemistry* **1976**, *41*, 892-893.

(97) Ornstein, P. L.; Schoepp, D. D.; Arnold, M. B.; Augenstein, N. K.; Lodge, D.; Millar, J. D.; Chambers, J.; Campbell, J.; Paschal, J. W. *Journal of Medicinal Chemistry* **1992**, *35*, 3547-3560.

(98) Ornstein, P. L.; Arnold, M. B.; Augenstein, N. K.; Deeter, J. B.; Leander, J. D.; Lodge, D.; Calligaro, D. O.; Schoepp, D. D. *Bioorganic & Medicinal Chemistry Letters* **1993**, *3*, 2067-2072.

(99) Hansen, M. M.; Bertsch, C. F.; Harkness, A. R.; Huff, B. E.; Hutchison, D. R.; Khau, V. V.; LeTourneau, M. E.; Martinelli, M. J.; Misner, J. W.; Peterson, B. C.; Rieck, J. A.; Sullivan, K. A.; Wright, I. G. *Journal of Organic Chemistry* **1998**, *63*, 775-785.

(100) Macias, F. A.; Varela, R. M.; Torres, A.; Oliva, R. M.; Molinillo, J. M. G. *Phytochemistry* **1998**, *48*, 631-636.

(101) Macias, F. A.; Lopez, A.; Varela, R. M.; Torres, A.; Molinillo, J. M. G. *Phytochemistry* **2004**, *65*, 3057-3063.

(102) Phommart, S.; Sutthivaiyakit, P.; Chimnoi, N.; Ruchirawat, S.; Sutthivaiyakit, S. *Journal of Natural Products* **2005**, *68*, 927-930.

(103) Shiao, H.-Y.; Hsieh, H.-P.; Liao, C.-C. *Organic Letters* **2008**, *10*, 449-452.

(104) Mehta, G.; Vidya, R. *Journal of Organic Chemistry* **2000**, *65*, 3497-3502.

(105) Ragan, J. A.; am Ende, D. J.; Brenek, S. J.; Eisenbeis, S. A.; Singer, R. A.; Tickner, D. L.; Teixeira, J. J., Jr.; Vanderplas, B. C.; Weston, N. *Organic Process Research & Development* **2003**, *7*, 155-160.

(106) Cabaj, J. E.; Kairys, D.; Benson, T. R. *Organic Process Research & Development* **2007**, *11*, 378-388.

(107) Yoshioka, M. *Pure and Applied Chemistry* **1987**, *59*, 1041-1046.

(108) Avery, M. A.; Chong, W. K. M.; Jennings-White, C. *Journal of the American Chemical Society* **1992**, *114*, 974-979.

(109) Gumulka, J.; Szczepek, W. J.; Wielogorski, Z. A. *Polish Journal of Chemistry* **1983**, *57*, 403-411.

(110) Gumulka, J.; Szczepek, W. J.; Wielogorski, Z. *Tetrahedron Letters* **1979**, 4847-4850.

(111) del Sol Jimenez, M.; Garzon, S. P.; Rodriguez, A. D. *Journal of Natural Products* **2003**, *66*, 655-661.

(112) Stierle, D. B.; Faulkner, D. J. *Journal of Organic Chemistry* **1980**, *45*, 3396-3401.

(113) Rudi, A.; Kashman, Y. *Journal of Natural Products* **1993**, *56*, 1827-1830.

(114) Yanai, M.; Ohta, S.; Ohta, E.; Hirata, T.; Ikegami, S. *Bioorganic & Medicinal Chemistry* **2003**, *11*, 1715-1721.

(115) Fontana, A.; Ishibashi, M.; Shigemori, H.; Kobayashi, J. i. *Journal of Natural Products* **1998**, *61*, 1427-1429.

(116) Ayer, W. A.; Talamas, F. X. *Canadian Journal of Chemistry* **1988**, *66*, 1675-1685.

(117) Adam, W.; Erden, I. *Angewandte Chemie International Edition English* **1978**, *17*, 210.

(118) Reich, H. J.; Wollowitz, S. *Journal of the American Chemical Society* **1982**, *104*, 7051-7059.

(119) Dale, J.; Kristiansen, P. O. *Acta Chemica Scandinavica* **1971**, *25*, 359-360.

(120) Engel, P. S.; Allgren, R. L.; Chae, W.-K.; Leckonby, R. A.; Marron, N. A. *Journal of Organic Chemistry* **1979**, *44*, 4233-4239.

(121) Chapman, N. B.; Sotheeswaran, S.; Toyne, K. J. *Journal of Organic Chemistry* **1970**, *35*, 917-923.

(122) Suzuki, M.; Ohtake, H.; Kameya, Y.; Hamanaka, N.; Noyori, R. *Journal of Organic Chemistry* **1989**, *54*, 5292-5302.

(123) Ramesh, P.; Reddy, V. L. N.; Reddy, N. S.; Venkateswarlu, Y. *Journal of Natural Products* **2000**, *63*, 1420-1421.

(124) Minh, C. V.; Kiem, P. V.; Huong, L. M.; Kim, Y. H. *Archives of Pharmacal Research* **2004**, *27*, 734-737.

(125) Ponce, M. A.; Ramirez, J. A.; Galagovsky, L. R.; Gros, E. G.; Erra-Balsells, R. *Photochemical & Photobiological Sciences* **2002**, *1*, 749-756.

(126) Takahashi, K.; Yamaguchi, Y.; Hayashi, A. *Acta Crystallographica, Section C: Crystal Structure Communications* **1991**, *C47*, 2581-2583.

(127) Campagnole, M.; Bourgeois, M.-J.; Montaudon, E. *Tetrahedron* **2002**, *58*, 1165-1171.

(128) Schreiber, S. L.; Claus, R. E.; Reagan, J. *Tetrahedron Letters* **1982**, *23*, 3867-3870.

(129) Kawamura, S.-i.; Yamakoshi, H.; Nojima, M. *Journal of Organic Chemistry* **1996**, *61*, 5953-5958.

(130) Bunnelle, W. H.; Isbell, T. A. *Journal of Organic Chemistry* **1992**, *57*, 729-740.

(131) Taber, D. F.; Nakajima, K. *Journal of Organic Chemistry* **2001**, *66*, 2515-2517.

(132) Pryor, W. A.; Giamalva, D.; Church, D. F. *Journal of the American Chemical Society* **1985**, *107*, 2793-2797.

(133) Pryor, W. A.; Giamalva, D.; Church, D. F. *Journal of the American Chemical Society* **1983**, *105*, 6858-6861.

(134) Munaf Kharbuli, A.; Duncan Lyngdoh, R. H. *Theochem* **2008**, *860*, 150-160.

(135) Iwai, T.; Fujihara, T.; Tsuji, Y. *Chemical Communications* **2008**, 6215-6217.

(136) Fristrup, P.; Kreis, M.; Palmelund, A.; Norrby, P.-O.; Madsen, R. *Journal of the American Chemical Society* **2008**, *130*, 5206-5215.

(137) Doughty, D. H.; Pignolet, L. H. *Journal of the American Chemical Society* **1978**, *100*, 7083-7085.

(138) Curtin, D. Y.; Kauer, J. C. *Journal of Organic Chemistry* **1960**, *25*, 880-885.

(139) Berman, J. D.; Stanley, J. H.; Sherman, W. V.; Cohen, S. G. *Journal of the American Chemical Society* **1963**, *85*, 4010-4013.

(140) Li, Y.; Liu, H.-l.; Huang, X.-r.; Li, Z.; Sun, Y.-b.; Sun, C.-c. *Theochem* **2010**, *945*, 120-128.

(141) Yoshioka, Y.; Yamaki, D.; Kubo, S.; Nishino, M.; Yamaguchi, K.; Mizuno, K.; Saito, I. *Electronic Journal of Theoretical Chemistry* **1997**, *2*, 236-252.

(142) Ponec, R.; Yuzhakov, G.; Haas, Y.; Samuni, U. *Journal of Organic Chemistry* **1997**, *62*, 2757-2762.

(143) McKee, M. L.; Rohlfing, C. M. *Journal of the American Chemical Society* **1989**, *111*, 2497-2500.

(144) Spartan '08; Wavefunction, Inc: Irvine, CA.

(145) Cremer, D. *Journal of the American Chemical Society* **1981**, *103*, 3627-3633.

(146) Rapp, A.; Mandery, H. *Experientia* **1986**, *42*, 873-884.

(147) Askari, C.; Hener, U.; Schmarr, H. G.; Rapp, A.; Mosandl, A. *Fresenius' Journal of Analytical Chemistry* **1991**, *340*, 768-772.

(148) Demyttenaere, J. C. R.; Adams, A.; Vanoverschelde, J.; De Kimpe, N. *Journal of Agricultural and Food Chemistry* **2001**, *49*, 5895-5901.

(149) Du, X.; Finn, C. E.; Qian, M. C. *Journal of Agricultural and Food Chemistry* **2010**, *58*, 3694-3699.

(150) Alissandrakis, E.; Tarantilis, P. A.; Harizanis, P. C.; Polissiou, M. *Food Chemistry* **2006**, *100*, 396-404.

(151) Mestres, M.; Busto, O.; Guasch, J. *Journal of Chromatography, A* **2000**, *881*, 569-581.

(152) Ebeler, S. E. *Food Reviews International* **2001**, *17*, 45-64.

(153) Rapp, A. *Nahrung* **1998**, *42*, 351-363.

(154) Bayer, E.; Kupfer, G.; Reuther, K.-H. *Fresenius' Zeitschrift fuer Analytische Chemie* **1958**, *164*, 1-10.

(155) Misra, G.; Pavlostathis, S. G.; Perdue, E. M.; Araujo, R. *Applied Microbiology and Biotechnology* **1996**, *45*, 831-838.

(156) Simmonds, J.; Robinson, G. K. *Enzyme and Microbial Technology* **1997**, *21*, 367-374.

(157) Boelens, M. H.; van Gemert, L. J. *Perfumer & Flavorist* **1993**, *18*, 2-16.

(158) Mateo, J. J.; Jimenez, M. *Journal of Chromatography, A* **2000**, *881*, 557-567.

(159) Strauss, C. R.; Wilson, B.; Gooley, P. R.; Williams, P. J. *ACS Symposium Series* **1986**, *317*, 222-242.

(160) Margalit, Y. *Concepts in Wine Chemistry* San Francisco, **1997**, 150-153.

(161) Marais, J. *South African Journal for Enology and Viticulture* **1983**, *4*, 49-58.

(162) Cordonnier, R. *Ann. inst. natl. recherche agron., Ser. E, Ann. technol. agr.* **1956**, *5*, 75-110.

(163) Williams, P. J.; Strauss, C. R.; Wilson, B.; Massy-Westropp, R. A. *Phytochemistry* **1982**, *21*, 2013-2020.

(164) Maicas, S.; Mateo, J. J. *Applied Microbiology and Biotechnology* **2005**, *67*, 322-335.

(165) Williams, P. J.; Strauss, C. R.; Wilson, B. *American Journal of Enology and Viticulture* **1981**, *32*, 230-235.

(166) Gunata, Y. Z.; Bayonove, C. L.; Baumes, R. L.; Cordonnier, R. E. *American Journal of Enology and Viticulture* **1986**, *37*, 112-114.

(167) Wust, M.; Mosandl, A. *Zeitschrift fuer Lebensmittel-Untersuchung und -Forschung A: Food Research and Technology* **1999**, *209*, 3-11.

(168) Felix, D.; Malera, A.; Seibl, J.; Kovats, E. s. *Helvetica Chimica Acta* **1963**, *46*, 1513-1536.

(169) Williams, P. J.; Strauss, C. R.; Wilson, B. *Journal of Agricultural and Food Chemistry* **1980**, *28*, 766-771.

(170) Engel, K. H.; Tressl, R. *Journal of Agricultural and Food Chemistry* **1983**, *31*, 998-1002.

(171) Luan, F.; Hampel, D.; Mosandl, A.; Wuest, M. *Journal of Agricultural and Food Chemistry* **2004**, *52*, 2036-2041.

(172) Corma, A.; Iglesias, M.; Sanchez, F. *Chemical Communications* **1995**, 1635-1636.

(173) Demyttenaere, J. C. R.; Willemen, H. M. *Phytochemistry* **1998**, *47*, 1029-1036.

(174) Simpson, R. F. *Vitis* **1979**, *18*, 148-154.

(175) Simpson, R. F.; Miller, G. C. *Vitis* **1983**, *22*, 51-63.

(176) Wilson, B.; Strauss, C. R.; Williams, P. J. *Journal of Agricultural and Food Chemistry* **1984**, *32*, 919-924.

(177) Marais, J.; Van Wyk, C. J. *South African Journal for Enology and Viticulture* **1986**, *7*, 26-35.

(178) Werkhoff, P.; Guentert, M.; Krammer, G.; Sommer, H.; Kaulen, J. *Journal of Agricultural and Food Chemistry* **1998**, *46*, 1076-1093.

(179) Ribereau-Gayon, P.; Boidron, J. N.; Terrier, A. *Journal of Agricultural and Food Chemistry* **1975**, *23*, 1042-1047.

(180) Georgilopoulos, D. N.; Gallois, A. N. *Food Chemistry* **1988**, *28*, 141-148.

(181) Wang, D.; Ando, K.; Morita, K.; Kubota, K.; Kobayshi, A. *Bioscience, Biotechnology, and Biochemistry* **1994**, *58*, 2050-2053.

(182) Ito, Y.; Sugimoto, A.; Kakuda, T.; Kubota, K. *Journal of Agricultural and Food Chemistry* **2002**, *50*, 4878-4884.

(183) Ghasemi, Y.; Mohagheghzadeh, A.; Moshavash, M.; Ostovan, Z.; Rasoul-Amini, S.; Morowvat, M. H.; Ghoshoon, M. B.; Raee, M. J.; Mosavi-Azam, S. B. *World Journal of Microbiology & Biotechnology* **2009**, *25*, 1301-1304.

(184) Mischitz, M.; Faber, K. *Synlett* **1996**, 978-980.

(185) David, L.; Veschambre, H. *Tetrahedron Letters* **1984**, *25*, 543-546.

(186) Mirata, M.-A.; Wuest, M.; Mosandl, A.; Schrader, J. *Journal of Agricultural and Food Chemistry* **2008**, *56*, 3287-3296.

(187) Hartung, J.; Drees, S.; Geiss, B.; Schmidt, P. *Synlett* **2003**, 223-226.

(188) Meou, A.; Bouanah, N.; Archelas, A.; Zhang, X. M.; Guglielmetti, R.; Furstoss, R. *Synthesis* **1990**, 752-753.

(189) Borg-Karlson, A.-K.; Unelius, C. R.; Valterova, I.; Nilsson, L. A. *Phytochemistry* **1996**, *41*, 1477-1483.

(190) Sakaguchi, S.; Nishiyama, Y.; Ishii, Y. *Journal of Organic Chemistry* **1996**, *61*, 5307-5311.

(191) Konstantinovic, S.; Bugarcic, Z.; Marjanovic, L.; Gojkovic, S.; Mihailovic, M. L. *Journal of the Serbian Chemical Society* **1997**, *62*, 1151-1156.

(192) Lattanzi, A.; Della Sala, G.; Russo, M.; Scettri, A. *Synlett* **2001**, 1479-1481.

(193) Hartung, J.; Drees, S.; Greb, M.; Schmidt, P.; Svoboda, I.; Fuess, H.; Murso, A.; Stalke, D. *European Journal of Organic Chemistry* **2003**, 2388-2408.

(194) Askari, C.; Mosandl, A. *Phytochemical Analysis* **1991**, *2*, 211-214.

(195) Wu, G.; Ma, Y.; Ge, M.; Li, Z.; Liu, Z. *Chinese Science Bulletin* **1989**, *34*, 305-308.

(196) Rychnovsky, S. D.; Bartlett, P. A. *Journal of the American Chemical Society* **1981**, *103*, 3963-3964.

(197) Fournier-Nguefack, C.; Lhoste, P.; Sinou, D. *Tetrahedron* **1997**, *53*, 4353-4362.

(198) Howell, A. R.; Pattenden, G. *Journal of the Chemical Society, Perkin Transactions 1: Organic and Bio-Organic Chemistry* **1990**, 2715-2720.

(199) Howell, A. R.; Pettenden, G. *Chemical Communications* **1990**, 103-104.

(200) Volz, F.; Wadman, S. H.; Hoffmann-Roeder, A.; Krause, N. *Tetrahedron* **2009**, *65*, 1902-1910.

(201) Epling, G. A.; Florio, E. *Tetrahedron Letters* **1986**, *27*, 1469-1472.

(202) Birch, A. J. *Journal of the Chemical Society* **1947**, 1642-1648.

(203) Kinsman, A. C.; Kerr, M. A. *Journal of the American Chemical Society* **2003**, *125*, 14120-14125.

(204) Ingham, S. L.; Johnson, B. F. G.; Sadler, I. H.; Nairn, J. G. M. *Journal of Organometallic Chemistry* **1997**, *531*, 237-242.

(205) Mirrington, R. N.; Schmalzl, K. J. *Journal of Organic Chemistry* **1969**, *34*, 2358-2363.

(206) Eilbracht, P.; Jelitte, R.; Trabold, P. *Chemische Berichte* **1986**, *119*, 169-181.

(207) Haselgrove, T. D.; Jevric, M.; Taylor, D. K.; Tiekink, E. R. T. *Tetrahedron* **1999**, *55*, 14739-14762.

(208) Liu, H.-H.; Zhang, Q.; Jin, H.-X.; Shen, X.; Wu, Y.-K. *Chinese Journal of Chemistry* **2006**, *24*, 1180-1189.

(209) Lory, P. M. J.; Jones, R. C. F.; Iley, J. N.; Coles, S. J.; Hursthouse, M. B. *Organic & Biomolecular Chemistry* **2006**, *4*, 3155-3165.

(210) Denis, J. M.; Conia, J. M. *Tetrahedron Letters* **1972**, 4593-4596.

(211) Paquette, L. A.; Hofferberth, J. E. *Organic Reactions* **2003**, *62*, 477-567.

(212) Greig, N.; Wyllie, S.; Patterson, S.; Fairlamb, A. H. *FEBS Journal* **2009**, *276*, 376-386.

(213) Zard, S. Z. *Australian Journal of Chemistry* **2006**, *59*, 663-668.

(214) Calter, M. A.; Liao, W.; Struss, J. A. *Journal of Organic Chemistry* **2001**, *66*, 7500-7504.

(215) Jun, J.-G.; Lee, D. W. *Tetrahedron Letters* **1997**, *38*, 8207-8210.

(216) Jun, J.-G.; Kim, A.-R.; Kim, S. H. *Synthetic Communications* **2002**, *32*, 45-52.

(217) DeBergh John, R.; Spivey Kathleen, M.; Ready Joseph, M. *Journal of the American Chemical Society* **2008**, *130*, 7828-7829.

(218) Grubbs, E. J.; Froehlich, R. A.; Lathrop, H. *Journal of Organic Chemistry* **1971**, *36*, 504-509.

(219) Katkevichs, M.; Korchagova, E.; Ivanova, T.; Slavinska, V.; Lukevics, E. *Chemistry of Heterocyclic Compounds* **2006**, *42*, 872-874.

(220) Maki, S.; Harada, Y.; Matsui, R.; Okawa, M.; Hirano, T.; Niwa, H.; Koizumi, M.; Nishiki, Y.; Furuta, T.; Inoue, H.; Iwakura, C. *Tetrahedron Letters* **2001**, *42*, 8323-8327.

(221) Fuwa, H.; Ebine, M.; Bourdelais, A. J.; Baden, D. G.; Sasaki, M. *Journal of the American Chemical Society* **2006**, *128*, 16989-16999.

(222) Biftu, T.; Acton, J. J.; Berger, G. D.; Bergstrom, J. D.; Dufresne, C.; Kurtz, M. M.; Marquis, R. W.; Parsons, W. H.; Rew, D. R.; Wilson, K. E. *Journal of Medicinal Chemistry* **1994**, *37*, 421-424.

(223) Saraiva, M. F.; Couri, M. R. C.; Le Hyaric, M.; de Almeida, M. V. *Tetrahedron* **2009**, *65*, 3563-3572.

(224) Bezard, M.; Gimenez-Arnau, E.; Meurer, B.; Grossi, L.; Lepoittevin, J.-P. *Bioorganic & Medicinal Chemistry* **2005**, *13*, 3977-3986.

(225) Pulido, F. J.; Barbero, A. *Nature Protocols* **2006**, *1*, 2068-2074.

(226) van Staden, L. F.; Gravestock, D.; Ager, D. J. *Chemical Society Reviews* **2002**, *31*, 195-200.

(227) Anjum, T.; Bajwa, R. *Phytochemistry* **2005**, *66*, 1919-1921.

(228) Armarego, W. F.; Chai, C. L. *Purification of Laboratory Chemicals*; 5th ed.; Butterworth-Heinermann: Bath, **2003**.

(229) Shibuya, M.; Ito, S.; Takahashi, M.; Iwabuchi, Y. *Organic Letters* **2004**, *6*, 4303-4306.

(230) Bryce, M. R.; Coates, H. M.; Cooper, J.; Murphy, L. C. *Journal of Organic Chemistry* **1984**, *49*, 3399-3401.

(231) Bandara, B. M. R.; Birch, A. J.; Raverty, W. D. *Journal of the Chemical Society, Perkin Transactions 1: Organic and Bio-Organic Chemistry* **1982**, 1763-1769.

(232) Hercsel, I.; Ecsery, Z.; Laurencsik, Z.; Sumegi, J.; Komlos, F.; (Chinoin Gyogyszer es Vegyeszeti Termekek Gyara Rt.). HU, **1964**, p 7.

(233) Wilson, W. K.; Sumpter, R. M.; Warren, J. J.; Rogers, P. S.; Ruan, B.; Schroepfer, G. J., Jr. *Journal of Lipid Research* **1996**, *37*, 1529-1555.

(234) Moreau, J. L.; Couffignal, R. *Journal of Organometallic Chemistry* **1985**, *294*, 139-144.

(235) Petrova, O. V.; Mikhaleva, A. I.; Sobenina, L. N.; Trofimov, B. A. *Russian Journal of Organic Chemistry* **2010**, *46*, 452-454.

(236) Huang, J. T.; Su, T. L.; Watanabe, K. A. *Journal of Organic Chemistry* **1991**, *56*, 4811-4815.

(237) Mohan, S. K.; Mereyala, H. B. *Synthetic Communications* **2001**, *31*, 3851-3858.